Université catholique de Louvain
Faculté d'Ingénierie Biologique, Agronomique et Environnementale
Département des Sciences du Milieu et de l'Aménagement du Territoire

Agricultural and climatic impacts on the groundwater resources of a small island: measuring and modelling water and solute transport in soil and groundwater on Tongatapu

Marijn van der Velde

May 2006

Thèse présentée en vue de l'obtention
du grade de docteur en Sciences Agronomiques
et Ingénierie Biologique

Jury members:

President:	Prof. B. Delvaux (UCL, Belgium)
Promotor:	Prof. M. Vanclooster (UCL, Belgium)
Co-promotor:	Dr. B.E. Clothier (HortResearch, Palmerston North, New Zealand)
Readers:	Prof. C. Bielders (UCL, Belgium)
	Dr. C. Ritsema (Alterra, Wageningen, the Netherlands)
	Prof. H. Savenije (TU Delft, the Netherlands)
	Prof. V. Hallet (FUNDP, Namur, Belgium)

After a still winter night I awoke with the impression that some question had been put to me, which I had been endeavoring in vain to answer in my sleep, as what – how – when – where? But there was dawning Nature, in whom all creatures live, looking in at my broad windows with serene and satisfied face, and no question on her lips. I awoke to an answered question, to Nature and daylight. The snow lying deep on the earth dotted with young pines, and the very slope of the hill on which my house is placed, seemed to say, Forward! Nature puts no question and answers none which we mortals ask. She has long ago taken her resolution.

— Henry David Thoreau - Walden or Life in the Forest - 1854

Preface

Fellow Dutchmen Abel Tasman was the first explorer to add the island of Tongatapu to the European knowledge of the world in 1643. A mere 359 years later I set sail to the South Seas for an endeavour on the island that, to me, he so fittingly had named the 'Island of Amsterdam' (150 years later James Cook wisely renamed it Tongataboo as it was being referred to by its inhabitants). The ship the 'Zeehaen' landed with one main reason; to obtain fresh water for it's crew and to replenish the Zeehaen's water barrels. The friendly Tongans were most willing to provide the ship with their precious water. The ship's painter drew this scene (see below) and we can see Tasman (with flag) and his crew taking the barrels towards the ships' boats. Tasman's journal reports on the 22^{th} of January, 1643 'after our boats had rowed a considerable distance along the northeast side of this land they were finally led to three small wells from which the water had to be scooped up by means of a cocoanut shell'. Later the wells were enlarged and the water 'quite green and dirty of colour' was stored in barrels. Prior to getting the water they had participated in a so-called water ceremony 'these people who had shown this place to our men led them inland to a kind Plaisance and elegant Baleye where our men were placed on fine little mats. These people did not bring there anything but two cocoanut shells full of water one for the chief and the other for our skipper' (excerpts from *Anderson* [2001]).

Figure 1. Detail from a drawing from Tasman's journal (1643) shows the Tongan chief seated in front of his welcoming party, with Tasman standing in front of him, and the filling of the water barrels and floating them out to the ships' boats (from *Anderson* [2001]).

So, in a humble return of favours, I dedicate this thesis to Tongatapu and it's inhabitants. In the hope that its contents may become usefull, and that the knowledge contained in the following pages will find it's way to the Tongan people that can ensure that the water resources of this tiny dot in the Pacific Ocean will continue to be available for future generations of Tongans, and their guests.

Acknowledgements

In a moment of time
When the fruit becomes wine
And the thought becomes the memory
— Goldenhorse (New Zealand rockband)

Many are the thoughts and the memories from these past four years. The memories that are now stored in the cellar of my mind will ripe into wines of many flavours and colours. Wines of premium quality! This has been an enriching experience, and I thank this mainly to the many people I got to know over these last four years. Working in the three different countries of Tonga, Belgium and New Zealand meant a lot of travelling and also meeting a lot of new people.

Professor Marnik Vanclooster and Brent Clothier were the co-promoters of this PhD research. Marnik's rigour and diligence was exemplary and much appreciated. Brent's guidance and commentary was always to the point and inspirational. And on a different note, I very much enjoyed the discussions with Penny and Brent at the dinner table. A special thank you goes to Steve Green who set me on the scientific track in Tonga and continued to do so back in New Zealand. Thanks Steve!

It was of course in Tonga where the most important work was done. A key role was played here by all the Tongan people I met while I was over there. I gratefully acknowledge the field staff of the Vaini Research Station of the Ministry of Agriculture, Food and Forestry, for their help and support, including the installation of the equipment, the sampling of the groundwater around the island, but especially the enjoyable moments in the field talking about topics as diverse as Tonga's political system, Jonah Lomu and even religion. Vuni, Printer, Samueala, Taniella, Siua.. Thanks! Those were great days in the field with fresh coconut juice and popoa for lunch! The supervision of the field activities by the head of the soil unit, Viliami Manu, was exemplary. Gregoire Pochet is thanked for the nice times we had together when he joined me on Tonga for his MSc research.

Steve, Carlo van den Dijssel, Brett Robinson, Philip Charlesworth and Glendon Gee are gratefully acknowledged for their assistance in the installation of the field equipment in Tonga. Thanks to their fire-fighting talents protecting the research equipment from a fire turned into a great story. Glendon is especially acknowledged for proposing us to use and test some of his newly designed fluxmeters. Decagon Devices, Inc, Pullman, Washington, USA, and Sledge Products, Dayton, Oregon, USA, are thanked for supplying these fluxmeters (Chapters 5 and 7).

I would also like to express my appreciation to the following institutes in Tonga: the World Health Organisation at the Vai'ola Hospital, the Environmental Health Unit at the Vai'ola Hospital, the Vaini Research Station

of the Ministry of Agriculture, the headquarters of the Ministry of Agriculture, the South Pacific Geosciences Commission, the Tongan Waterboard, the Hydrogeological Unit at the Ministry of Lands and Survey and Natural Resources, the Department of Environment and the library at the 'Atenisi University. Special thanks go to Malakai Vakasiuola of the Tongan waterboards, Nils from WHO, and the eminent Professor Futu Helu from the 'Atenisi University.

Back in New Zealand many people helped me with conducting the laboratory analysis. The advice from Valerie Snow and Don McNaughton was much appreciated. At Massey's Soil and Fertiliser Lab Ian Furkert and Bob Toes helped me out many a time.

A note of thanks is also reserved for Professor Willem Bouten from the University of Amsterdam with whose support I first went to the other side of the world. At that time I joined Brent's group for a 6-month internship at the final stages of my MSc.

I hope to be able to continue working on modelling the freshwater lens of Tongatapu during my postdoc. A big thanks goes to Dr. Gualbert P. Oude-Essink from TNO who introduced me to this subject with much enthusiasm.

All the reviewers that have commented the papers presented in this thesis are kindly acknowledged for their valuable comments. I gratefully acknowledge A.C. Falkland for his comments on Figure 12.5 and Professor J. Kirchner for his comments on Chapter 10.

The members of the jury are kindly acknowledged for their critical comments on the prelimary version of this final manuscript.

Although these acknowledgements are written in haste and just as the final seconds to hand in the thesis pass away, I wonder, don't these acknowledgements deserve more time, aren't they not expressing an essential part that led to the thesis? Yes, of course! Nevertheless, it is nearly impossible to thank personally all the wonderful people I got to know over these last years. Everybody I shared a house with: it was great living with you! All the people I played football with: that was a great match! The people I played football with came from all over the place, I regularly played with people from Tonga, New Zealand, Brazil, Argentina, Paraguay, Germany, Italy, Spain, USA, Belgium (both Vlaanderen and Wallonie!), the Netherlands, Cote d'Ivoire, Japan, South Korea, China, Australia, Ireland, Scotland, Chili, and so on...

Back in Tonga. Living at the farm was sometimes a bit of a solitary exercise, where it not for my Tongan and Japanese neighbours with whom I often enjoyed a traditional Tongan 'umu breakfast. Excellent! Thank you Neeli and Barbara Tuipulotu and their family as well as Tevita and his family! Special thanks also go to Hans and Tesi Jensen. I promise you will get a copy of this thesis in your hands! The nicest coffee on Tongatapu is drunk at Friends café. Paul Johansson and the staff at the Friends café: malo 'aupito!

Back in Belgium. The technical and administrative staff at the Génie Rural of the UCl, Carine, Guido and Benjamin have always been very supportive. Une grande merci! I would like to thank all my colleagues at the Génie Rural for the pleasant conversations and lunches we had together. Personally, I always enjoy walking around in libraries, so to all the librarians: thank you!

Financial support for this work was provided by the European Commission under the INCO-DEV Programme (ICFP500A4PRO2) and the New Zealand Agency for International Development as part of the Pacific Initiative for the Environment.

Finally and foremost I am very grateful that my friends and family have been friends and family over these last four years. Only when you go away you can see where you came from!

Nature, assisted by a little art, no were appears in a more flourishing state than at this isle.

— *James Cook, 1787*

Contents

Chapter 1

Introduction and objectives

Of all water on earth, only 1% is liquid fresh water. Even then, almost all of this is groundwater being more than 97%. The remaining 3% occurs in lakes and streams, which are often fed by groundwater [*Bouwer*, 2000]. During the second part of last century, groundwater pollution was recognised as a serious problem, posing a threat to both drinking water supplies and environment. Globally an increased number of groundwater bodies are reported to be contaminated [*Sampat*, 2000; *Foster and Chilton*, 2003]. One of the main contributors to the non-point source pollution of groundwater is agriculture. Other causes result from demographic pressures and include urbanisation, sewage water disposal, industrial activities and land clearance. Sustaining the quantity and quality of the world's groundwater resources is essential for all life on earth, as well as sustaining economic growth.

Groundwater is a precious resource, and especially so in small island developing states (SIDS). One of the key challenges facing SIDS now, and in the future, is the need to ensure the ability to enjoy sufficient water resources of high quality. Two of the main issues that have to be dealt with by SIDS that wish to sustain their water resources are 1) intensification of agriculture and 2) climate change and variability.

Sustainable management of water resources must increasingly incorporate the human demands and pressures, and the climatic influences upon these water resources. Sustainable water resource systems have been defined as 'those designed and managed to fully contribute to the objectives of society, now and in the future, while maintaining their ecological, environmental and hydrological integrity' *UNESCO* [1999].

On small islands, especially those of volcanic and limestone origin, freshwater occurs as lenses that float on the denser seawater underneath the island (Figure 1.1). All SIDS rely partly on the freshwater lenses for their water needs, and it is the primary water source on several of these islands. After rainfall, drainage water filters through the protective skin of the soil and the vadose zone, and then mixes with the freshwater of the lens.

The size and shape of these lenses are determined by the hydrogeological characteristics of the aquifer as well as the rainfall recharge rate and its temporal variation, plus abstractions for domestic, industrial or agricultural uses. The quantity of drainage water is determined by the prevailing climatic

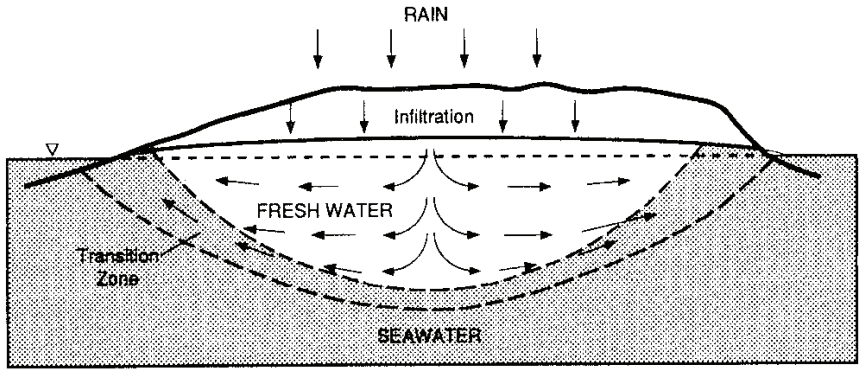

Figure 1.1. Schematic cross section of an island showing freshwater lens and transition zone (from *Griggs and Peterson* [1993].

conditions that determine the amount and temporal and spatial distribution of rainfall. The quality of the drainage water is largely determined by the effects of human activities occurring at the surface. Withdrawals in excess of natural recharge can cause intrusion of salt water into the aquifer. Also, the groundwater lenses of SIDS are often inter-connected to a lagoon and the coastal areas. These are important interfaces where (often endemic) flora and fauna live, including fish and coral species.

Currently, there is no generally accepted definition of a small island developing state. Small island developing states cannot be regarded as a uniform, undifferentiated group [*UNCTAD*, 2004]. However, SIDS have been recognised as a political identity since the establishment in 1990 of the Alliance of Small Island States that currently compromises 39 members *. Nevertheless, SIDS share several characteristics. They are recognised as being geographically disadvantaged, small in both economic and ecological sense, and consequently vulnerable. The concept of vulnerability is hotly debated, but relates to ecological fragility, proneness to natural disasters and the concentration of exports on a limited range of products and markets [*UNCTAD*, 2004].

Agriculture has been the cornerstone of many SIDS [*FAO*, 1999]. Subsistence agriculture has for long sustained populations, and nowadays agriculture is one of the main export earners. In the search for a diversification of economical exports, SIDS have introduced new crops, often a monoculture, for export to international markets. This has consequently led many SIDS to intensify their agricultural practises. The effect of the increased usage of agricultural chemicals on the environment of SIDS is still poorly quantified.

*Including four low-lying coastal states: Belize, Guinea-Bissau, Guyana and Suriname, but excluding two SIDS: Bahrain and the Dominican Republic. Eleven of these states are defined as 'least developed countries' by the UN.

Nevertheless, several SIDS have increasingly voiced their concerns since the first signs of environmental deterioration became apparent. Agriculture does not only influence the quality of the water resources, but through the need for irrigation in these tropical climates, also the quantity of the fresh groundwater resources below the island. Many governments of SIDS struggle with the notion that short-term economic benefits may lead to long-term environmental deterioration. Costa Rica's environmental minister was quoted in *The Economist* [2005] as saying: 'We need to learn the language of finance and economics, and demonstrate the economic benefits of the environment.'

Although minimally responsible, SIDS will be among the first to be struck by climate change and increased climatic variability, related, for example, to the El Niño-Southern Oscillation. Recently, effects of climate change have led to the first climate–change refugees from the Pacific's Carteret Islands. Climate change was the most controversial item on the agenda of the 10-year review of the Barbados Programme of Action for the sustainable development of small island developing states (SIDS), recently held in Mauritius. The 10-year review resulted in the Mauritius Declaration [*United Nations*, 2005]. These islands need 1) sound evidence to illustrate their needs and special position in front of the international community 2) a scientific understanding of the relationships between climatic variations and the quality and availability of freshwater and 3) a sustainable development framework that accounts for the natural capital of these remote biodiversity 'hot spots' [*Myers et al.*, 2000].

Small islands are also on the receiving end of other effects related to a warming climate, especially sea water level rise. Sea–level rise will lead to an increased risk of inundation and coastal flooding, marked increases of erosion, saltwater intrusion of a smaller freshwater lens, and changes in sediment deposition patterns. Small islands also have to deal with the damages induced by tropical cyclones that appear to be occurring with increasing intensity. Other natural disturbances of the system include earthquakes (such as those associated with the 'Pacific Ring of Fire'), and associated tsunamis [*Sawkins*, 1856]. In summary, current and continuing pressures upon the freshwater lenses of SIDS are either of anthropogenic or of climatic origin (Table 1.1).

1.1 Objectives of the research

This PhD research was performed within the context of an applied research project. Within the project (*www.croppro.alterra.nl*) we wished to develop sustainable strategies for managing agrichemicals on the island of Tongatapu (175^o12'W, 21^o08'S), the main island of the Kingdom of Tonga. Tongatapu is a raised coral atoll. It turned out that Tongatapu provided a good opportunity to study both the agricultural and climatic influences on its

Table 1.1. Some anthropogenic and climatic influence on the water resources of a SIDS.
(1) Anthropogenic influences
  (1.1) Sewerage system (leaking septic systems);
  (1.2) Solid waste problems;
  (1.3) Leaching of (residues of) chemicals used in agriculture;
  (1.4) Salt water intrusion due to overpumping;
(2) Climatic influences
  (2.1) Rising sea–levels (salt water intrusion, coastal erosion);
  (2.2) Increased frequency of cyclone induced impacts;
  (2.3) Increased frequency of El Niño related droughts;

water resources. In 1987, a squash (*Cucurbita maxima Duchesne*) industry emerged on Tongatapu that solely exports to the Japanese market during an off-season period in November. At a national level, the squash industry has accounted for about 40% of the total export revenue and about 80% of export revenue derived from agriculture during the last 10 years. With the export of the squash, a significant increase in the import and use of agrichemicals has occurred (see Chapter 12). Knowledge on the flux of water and solutes is needed to develop better application strategies for fertilisers and pesticides. This can be both economically and ecologically beneficial. At the same time, an increasing population exerts a stress on the fresh groundwater resources of the island. There is no surface water on Tongatapu. Both pollution and an increase in pumping leads to deterioration of the water resource. This, coupled with expected sea–level rise and an increase in the frequency of El Niño episodes, puts additional pressures on the water resources and the environment.

This thesis deals with the broad dimensions of sustainability in a fragile environment. The general aim of this PhD research was to quantify the impacts of agriculture and climatic variations on groundwater of small islands and to provide a scientific basis for the management of their water resources by studying the specific case study area of Tongatapu. This knowledge should provide means for SIDS to increase their resilience in both environmental and economical senses. In this study, solute transport processes are examined at two different spatial scales: the scale of a field soil using in-situ observations and at the island-scale using in-situ observations from wells and boreholes, with accompanying modelling strategies. The general aim is targeted with specific research objectives listed below (Table 1.2).

Table 1.2. Specific PhD research objectives.

(1) To assess the current environmental state of Tongatapu and collate the information currently available on Tongatapu's environmental resources;
(2) To quantify the impact of land–use intensification on soil quality, namely soil aggregation and associated hydraulic properties;
(3) To provide a physical understanding of Tongan soils
(4) To characterize water and solute transport using models and tools that are easy to operate in the field;
(5) To quantify the transpiration of a squash in the field used for agricultural production;
(6) To investigate climatic (El Niño-Southern Oscillation) and hydrogeological controls on the quality and quantity of the freshwater lens;
(7) To provide means that allow agricultural workers, well-field managers, and governmental planners to evaluate agricultural and climatic impacts on the environment;
(8) To identify a framework for sustainable development in a SIDS that takes account of economical development through agricultural export in relation to environmental integrity;

These objectives provide means to achieve an understanding of the impacts of agriculture and climate variability on the environmental and economic welfare of small island developing states.

1.2 Outline of the thesis

The thesis is organised in four parts. Each part discusses several of the specific objectives highlighted above. The first part is introductory, the second part deals specifically with agriculture, while the third part deals specifically with climate–change and its impacts. The fourth part focuses on aspects of management and sketches a framework for sustainable development of SIDS.

The biophysical characteristics of the island, including its geology, hydrology, and a physico-chemical description of the soil, are described in Chapter 2. Chapter 2 also provides a description of the experimental site at the Vaini Research Station. The current quality of the soil and water resources of the island, including a summary of past environmental analyses and a survey of pesticide contamination of Tongatapu's environment, is presented in Chapter 3. The impact of land use intensification on Tongatapu's soil resources is described in Chapter 4.

The second part describes the (potential) impact of agriculture on Tongatapu's water resources using measurements of the field water balance com-

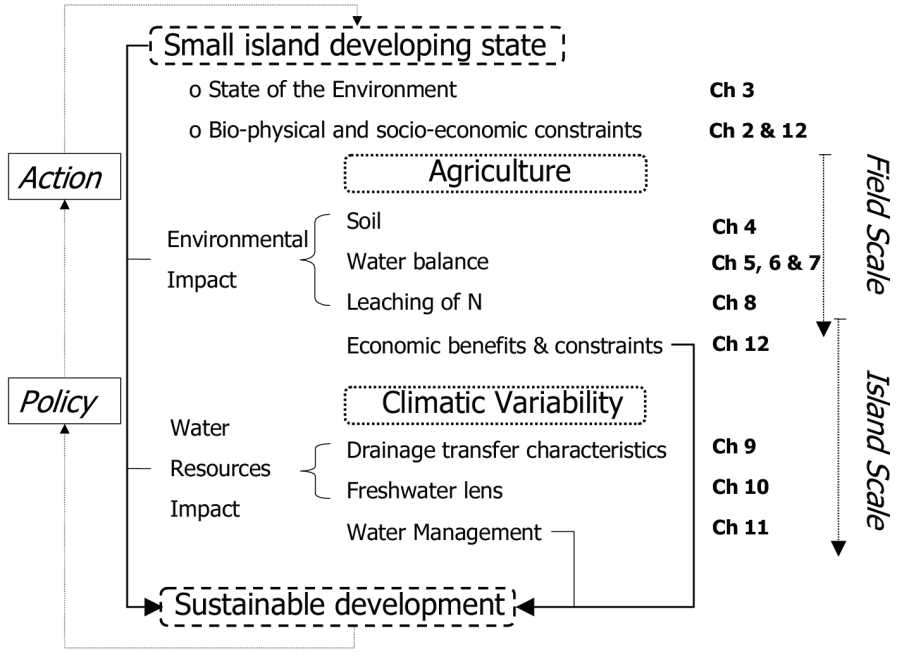

Figure 1.2. Flow diagram depicting the outline of this thesis.

ponents. Chapter 5 describes the modelling and measurement with specifically designed heat-pulse equipment of transpiration in squash. Chapter 6 analyses the performance of three types of fluxmeters to measure the drainage-flux in Tongatapu's soil during the 2003 experimental season. Integration of the water balance components is provided in Chapter 7. Measurements in the field of nitrate and ammonium leaching from the rootzone with the fluxmeters, and subsequent modelling involving preferential flow phenomena in the soil, is presented in Chapter 8.

The third part deals with the hydrogeological and anthropogenic controls (Chapter 9), and the impact of climatic variations (Chapter 10), on the quality (salinity) and availability of the freshwater lens at the larger temporal, and spatial scale of the island. Transfer functions were used to characterise the conductivity of the limestones, and to show a lagged control of the El Niño-Southern Oscillation on the quality of the freshwater lens.

The fourth part begins by describing options to manage the water resources by illustrating the dependence of freshwater lens quality on climatic variability (Chapter 11). Agricultural exports are put in a context of a sustainable development scenario that respects socio-economic, as well as the environmental constraints of this SIDS (Chapter 12). This is done through an evaluation of the interactions between the biophysical and socio-economic domains. This understanding is necessary to govern and manage the island's

ecological and economical resources in a sustainable way.

The thesis concludes with a synthesis of the results and sketches some perspectives for future research aimed to harness Tongatapu's water resources against agricultural intensification and processes influenced by climate change and variability (Chapter 13). This could, with local variation, be applied to other SIDS.

Part I

Tongatapu: The Biophysical Setting

Chapter 2

Description of the Biophysical Characteristics of Tongatapu

2.1 Introduction

This Chapter presents the main biophysical characteristics of the island of Tongatapu. Since the research presented in this thesis focuses both on the field scale, including the experimental site, and also on the island scale, both are discussed separately.

2.2 Location

The island archipelago of the Kingdom of Tonga consists of about 170 islands and lies between the latitudes from 15^o S to 23.5^o S and between the longitudes from 173^o W to 177^o W. Tonga lies approximately 700 km to the southeast of Fiji and approximately 900 km to the southwest of Samoa. New Zealand is the closest larger country and lies 2000 km south of Tonga (see Figure 2.1). The total surface of Tonga equals to about 0.7 x 10^6 km^2 of which only 747 km^2 is land area. Tonga stretches over 1000 km from the northernmost island of Niuafo'ou to the southernmost point of Tonga, the Minerva Reef.

Tonga consists of four main island groups (see Figure 2.2): the southern Tongatapu group, the Ha'apai group, the northern Vava'u group and the northernmost Niues. About 36 of the islands are inhabited. Tongatapu is the main island of the Kingdom of Tonga where the capital Nuku'alofa is located. About 100,000 people live in Tonga, of which 60,000 live on Tongatapu, of these, 40,000 live in Nuku'alofa. It is estimated that another 100,000 Tongans live overseas.

2.3 Climate

Tonga is a tropical country, being north of the Tropic of Capricorn. The climate is characterised by hot humid summers and warm winters. The South Pacific Convergence Zone (SPCZ) is an important feature of the tropical South Pacific. Long-term rainfall distribution can be directly related to

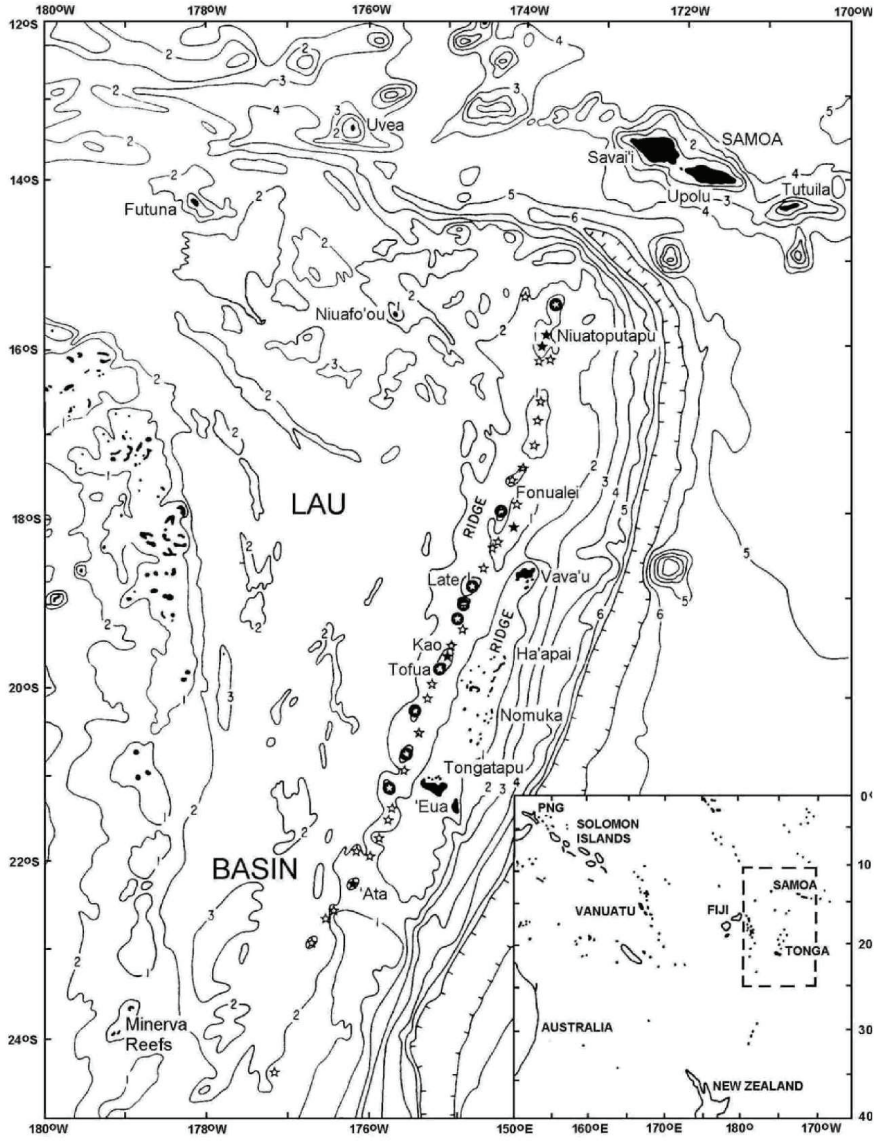

Figure 2.1. Bathymatric and locality map for the Tofua Volcanic Arc and the Tonga Ridge and the location of the island archipelago of the Kingdom of Tonga. The ridge of volcanoes can be recognised. Lines with numbers indicate x 1000 m of depth (e.g. 1 = 1000 m, 6 =6000 m). The Tonga Trench is indicated by the line with ticks indicating a depth deeper than 7500 m. Symbols - (Circle) volcanoes with a record of historic eruptions, (Closed Star, ⋆) volcanic islands with no record of historic eruptions, assumed to be either dormant or extinct; (Open Star) submarine highs, many of which may be of volcanic origin.The map was obtained from *Cronin* [2005].

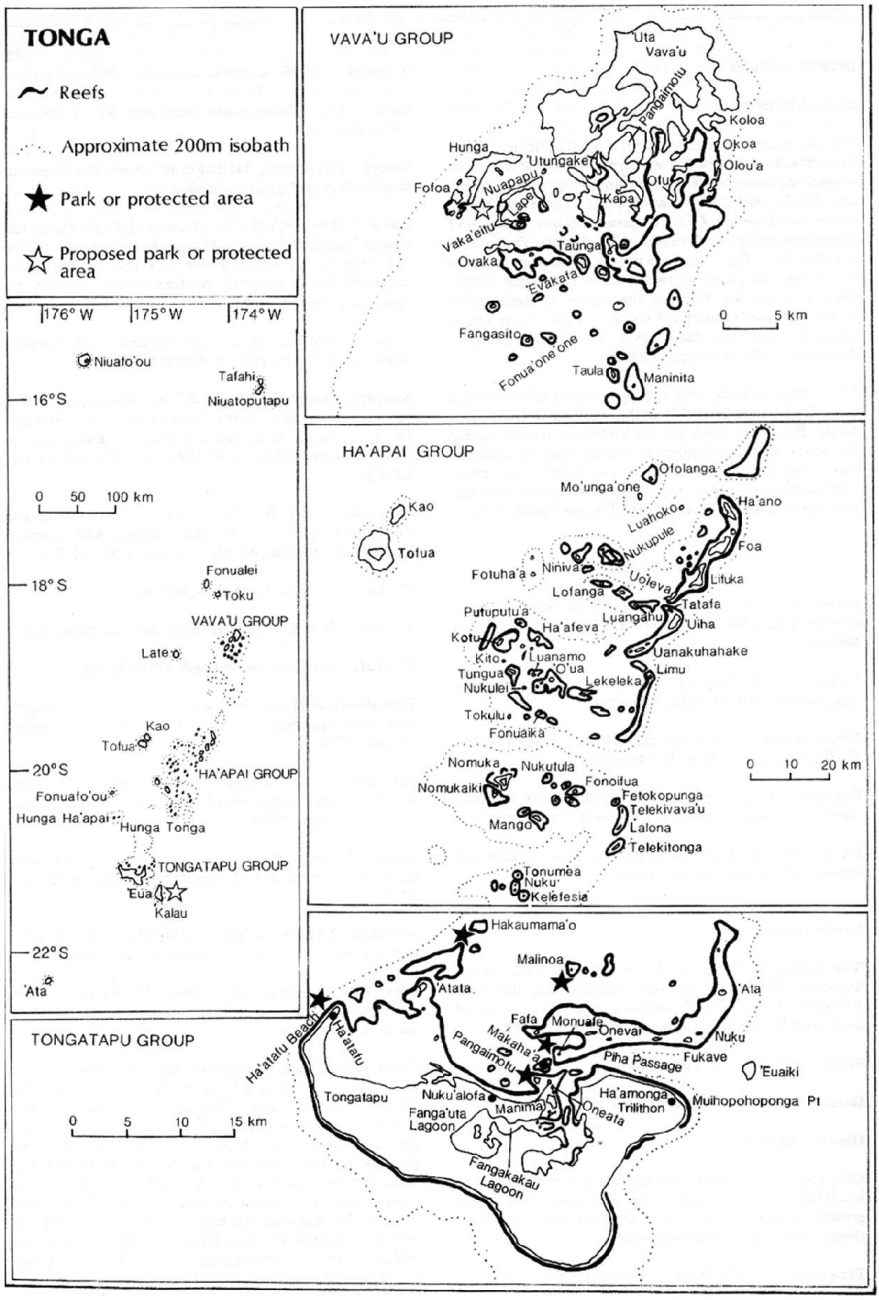

Figure 2.2. The island archipelago of the Kingdom of Tonga. The location of the island groups are indicated at the left, while the individual island groups are depicted in more details on the right. Coral reefs and parks or protected areas are also indicated. The map was obtained from *www.coral.noaa.gov*.

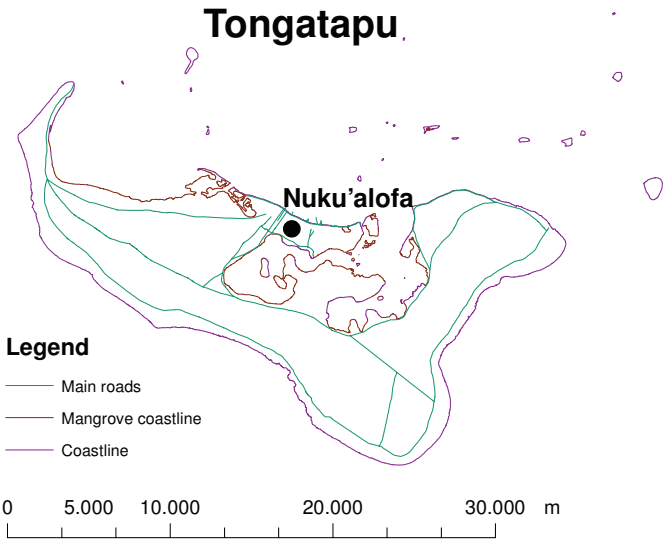

Figure 2.3. The island of Tongatapu. Most of the northern shore consists of swamp area and mangrove forest.

the SPCZ. The SPCZ is a low-level convergence extending from the west–Pacific warm pool, southeastwards towards French Polynesia [*Ropelewski and Halpert*, 1987]. The zone is where the low latitude easterly trade winds and the higher latitude southeasterly trade winds meet. The rainfall intensity associated with the SPCZ can vary considerably. The location of the SPCZ is affected by the El Niño-Southern Oscillation and the Interdecadal Pacific Oscillation.

In Tongatapu, precipitation results from convective processes, from tropical cyclones, and from rain associated with the cloud sheets of the subtropical jet-stream [*Thompson*, 1986]. Annual rainfall was reported to equal 1888 mm year^{-1} for the 1951-1980 period and is highly variable (*Thompson* [1986] and see Figure 2.4 and Table 2.1). From measurements between 1972 and 2001 provided by Tonga's Meterological Bureau, we calculated an average annual rainfall of 1670 mm. Nevertheless, it can be seen in Figure 2.4 and Table 2.1 that rainfall is seasonal with a wet period from November to April and a dry period from May to October. Rainfall varies considerable within each month from year to year as indicated by the large coefficients of variation (CV).

There is a slight orographic effect on the rainfall distribution over Tongatapu, which leads to a 9% gradient from west to east across island [*Thompson*, 1986]. The rainfall regime shows a pronounced wet season from November

to April, and a dry season from May to October. Heavy rains fall throughout the year, but occur mainly in the hurricane season between December and January. Droughts are also common and regularly occur in the period between June and November. A high humidity throughout the year is also characteristic for this climate. The annual mean relative humidity for Tongatapu is 77 %.

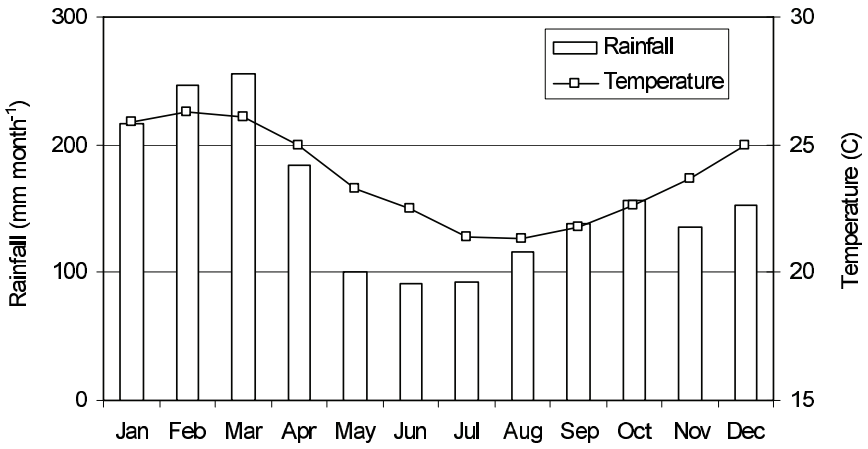

Figure 2.4. The mean monthly rainfall (mm month^{-1} in Tongatapu calculated for 1951-1980, and the mean monthly temperature (C, defined as the average of maximum and minimum monthly temperature) calculated for 1949-1984 from *Thompson* [1986].

Table 2.1. Monthly rainfall extremes and coefficient of variation (CV) for Tongatapu (Nuku'alofa).

	Jan	Feb	Mar	Apr	May	Jun	Jul	Aug	Sep	Oct	Nov	Dec
Maximum	582	564	469	458	241	243	259	273	341	452	368	783
Lowest	10	61	71	9	17	7	18	17	11	17	6	3
CV (%)	65	51	37	63	62	72	60	58	63	81	87	109

Tonga is also regularly struck by tropical cyclones. From satellite data available since 1969, it has been determined that Southern Tonga is hit by an average of 1.3 cyclones per year [*Thompson*, 1986]. Tropical cyclones may occur all year around, but they are principally confined to the wet season from November to April. Fittingly, this is called the cyclone season [*Thompson*, 1986]. *Woodroffe* [1983] reported on the devastating effects of Cyclone Isaac on the Ha'apai and Tongatapu islands on the 3^{rd} of March 1982. Extensive damage was caused to buildings and crops, as well as coastlines and vegetation.

2.4 Geology

Tonga lies next to the Tonga Trench that reaches a depth of 10,882 m below sea level. It is situated on the Tonga Ridge, an active fore-arc [*Roy*, 1990; *Pfeifer and Stach*, 1972]. Here the Pacific tectonic plate is being subducted underneath the Indo-Australian plate. The Kingdom of Tonga therefore lies in a geologically active area and earthquakes occur regularly. Most recently, there was a 8.0 magnitude earthquake on the 4^{ht} May 2006, some 160 km northeast of the coast of Nuku'alofa. The highest point of Tonga is Kao, an active volcano with an elevation of 1000 m (see Hapa'ai box of Figure 2.2).

The islands of Tonga are recognised as either volcanic islands, uplifted coral limestone islands, or low coral islands. The low coral islands are newly formed, being flat or gently undulated islands of sand that rise to 15 m above sea level. On the western side of Tonga a linear chain of volcanoes can be recognised stretching from Hunga Ha'apei towards Tofoa, an active volcano, and Fonualei in the north (see left box of Figure 2.1 and 2.2). On the eastern side of Tonga, a similar chain consisting mainly of uplifted or raised coral atolls can be recognised stretching from Tongatapu to Vava'u. The research presented in this thesis deals with the main island of Tongatapu. The geology, geomorphology, hydrology, soils, and the vegetation of Tongatapu are now discussed.

Tongatapu is an uplifted coral atoll (256 km^2). Tongatapu is composed of emerged and tilted coral limestones of Pliocene and Pleistocene age overlying a base of Pliocene and older volcanic rocks. From borehole-data it has been shown that the limestone has a thickness of about 134 m around Nuku'alofa and 247 m near Fua'amotu in the southeast [*Lowe and Gunn*, 1986]. The groundwater aquifer is thus entirely composed of limestone.

In 1842, Charles Darwin is credited to have been the first to propose a theory that links volcanic islands with coral atolls and reefs through a process of geological 'evolution' [*Darwin*, 1842]. The evolution of a coral atoll starts with the growth of a volcano from the ocean floor and its emergence above the sea. If the volcanic and tectonic activity is not too high, coral can grow in warm tropical oceans in the shallow water around the volcano, thereby forming a fringing reef. As the volcano subsides (see *Summerfield* [1996]) the coral is able to build the reef upward to maintain its upper surface close to sea level. In this process, a barrier reef is formed that is separated from the volcanic cone by a lagoon. If the volcano subsides completely below sea level a classical coral atoll will be formed. In the case of Tongatapu, the whole ensemble of thick coral limestone, with its volcanic base, was subsequently uplifted and tilted forming a raised coral atoll with a relatively sheltered lagoon.

2.5 Geomorphology

The geomorphology of Tongatapu is described in detail by *Roy* [1990]. The land surface is typically flat to gently undulating with occasional steep-sided hills 10-25 m high [*Roy*, 1990]. These hills are relict patch reefs that rise above the old lagoon bed. Primary depositional features such as the reef rim, 'patch–reefs' and a lagoon bed are evident on Tongatapu. Elevation decreases from the highest elevation of 60 m in the southeast to sea level to the northern side of the island. The high point is part of a narrow and irregular ridge, some 0.5 to 1.25 km wide and mostly rising more than 20 m above sea level, that extends to the northeast and northwest [*Roy*, 1990]. The ridge encompasses a low area in the central and northern part of the island that rises gently to the south. It is thought that the ridge corresponds to a former reef and the central low area is part of an original lagoon bed [*Roy*, 1990]. The morphology and surface geology are mainly the result of subaerial and marine erosion [*Roy*, 1990]. *Roy* [1990] notes that a marine dissolution process, termed solution cliffing, is thought to be responsible for excavating depressions and channel–ways below present sea level in the interiors of the island. The presence of solution channels and big caves are apparent in several places. A detailed description of the caves on Tongatapu was made during several visits by the British Geological Survey [*Lowe and Gunn*, 1986; *Harrison*, 1993]. *Lowe and Gunn* [1986] made detailed descriptions of 3 caves that were explored for the first time. They reported on the large dimensions of the caves, being up to 50 m wide and 20 m high. Similar to *Roy* [1990], they proposed that several of the caves were formed by phreatic solution when the land was lower, and that elevation of the land has rendered the caves relict.

The limestones are of karst-type with open cracks, and they are generally very porous, except where the spaces between the individual coral masses have been infilled with fine-grained detrital material [*Pfeifer and Stach*, 1972]. The limestone is an aquifer wherein freshwater lenses float on denser salt water. More details on the freshwater lens can be found in Chapters 9, 10 and 11.

2.6 Hydrology

Tongatapu's characteristic shape is due to its internal lagoon. The relatively enclosed lagoon consists of two connected parts, the Fanga'uta and Fanga Kakau lagoons that extends inland from the north-central coast. The lagoon is brackish and it was reported to have a salinity of approximately 25.7 to 32.9 ppt dissolved solids compared to open ocean water with approximately 35.4 ppt dissolved solids [*Zann et al.*, 1982].The lagoon has a surface area of about 27 km^2. It is shallow with an average depth of 1.4 m, and maximum

of 6 m. *Zann et al.* [1982] provide an overview of the fish, coral and shell species living in the lagoon, calculated values for primary production and related variables. As well, they designed a water circulation model of the lagoon. Based on the occurrence of many dead 'micro–atolls', and living coral being found 20 to 40 cm below the upper level of the dead coral, *Zann et al.* [1982] concluded that this difference indicates a sudden change in the elevation of the land, possibly corresponding to an earthquake in 1914.

Circulation in the lagoon is mainly driven by tides. *Zann et al.* [1982] write 'The ocean tidal range of about 1 m drives a current of up to 2.6 knots (corresponding to 1.34 m s^{-1}) in the main channel, producing a tide within the Mu'a branch that is smaller than and which lags behind the oceans tide. This tide causes the current to flow through the side pass to and from the Nuku'alofa sector, producing a tidal range at Nuku'alofa of only 0.13 m. This tide lags behind the ocean tide by 3 to 4 hours. Thus, the small cross-section of the passes allows relatively little tidal exchange between ocean and lagoon.' Evaporation rates for the open water are high and were estimated to be between 4.9 mm day^{-1} to 6.2 mm day^{-1} for different sectors of the lagoon by [*Zann et al.*, 1982]. *Zann et al.* [1982] calculated an average freshwater input of about 26,6000 m^3 day^{-1}, by calibrating a model against measured rainfall inputs and evaporation rates. Several approaches to calculate water flows in the estuarian system exist [*Seabergh*, 2006]. We opted for a simple approach to estimate the exchange between lagoon and ocean. The freshwater replacement time F (days) can be calculated so that [*Waring et al.*, 2003]:

$$F = \frac{V}{Q_f} \tag{2.1}$$

where V is the average volume of the estuary througout the tidal cycle, and Q_f the freshwater inflow into the lagoon. V equals the average lagoon depth (1.4 m) times the lagoon surface (2.7 * 10^7 m^2) and equals 3.78 * 10^7 m^3. We take Q_f to equal 26,6000 m^3 day^{-1} and find that F equals 142 days. The number of days it takes for exchange with the ocean to replace the water in the estuary, T_r equals [*Waring et al.*, 2003]:

$$T_r = F * \frac{S_O - S_L}{S_L} \tag{2.2}$$

where S_O is the ocean's salinity (ppt) which equals 35 ppt, and S_L the average salinity (ppt) of the lagoon measured by *Zann et al.* [1982], which equaled 30 ppt. This yields a T_r of 24 days. It is thus estimated that tidal mixing of ocean and lagoon waters results in only about 4% of the lagoon's volume being exchanged with ocean water each day.

Zann et al. [1982] argued that, except from heavy rains, freshwater input to the lagoon comes from springs connected to the groundwater lens. *Zann et al.* [1982] estimated that 85 % enters through subsurface springs and 15 %

from solution channels on the shore. Groundwater input into the lagoon can be approximated to be proportional to watershed area. The total watershed area of the lagoon was estimated to be 80 * 10^6 m^2 by *Zann et al.* [1982]. The derived freshwater flow into the lagoon was estimated to be 26,6000 m^3 day^{-1}, or some 65% of rain that fall over the estimated watershed area. This seems unrealistic. Alternatively, we calculated the direct average daily recharge of the lagoon by rainfall that fell over the lagoon surface area. We used data from 1972 to 2001. Rainfall recharged the lagoon if daily rainfall exceed a a daily average evaporation rate of 5.3 mm day^{-1} (derived from measurements by *Zann et al.* [1982]). We then find an average daily direct recharge by rainfall of 3.3 mm day^{-1}. If we substract this amount from the freshwater inflow derived by *Zann et al.* [1982] and calculate the percentage of rainfall that fell on the watershed area and subsequently recharged the lens and the lagoon, we find a more realistic recharge of 43%.

There are no perennial surface streams on Tongatapu. It is however reported, and confirmed by my observations, that in the northern part after heavy rainfall some intermittent surface flow may occur [*Pfeifer and Stach*, 1972]. *Lowe and Gunn* [1986] reported the presence of talus cones and soil material around the entrances of several caves, indicating that intermittent surface flow had caused soil erosion.

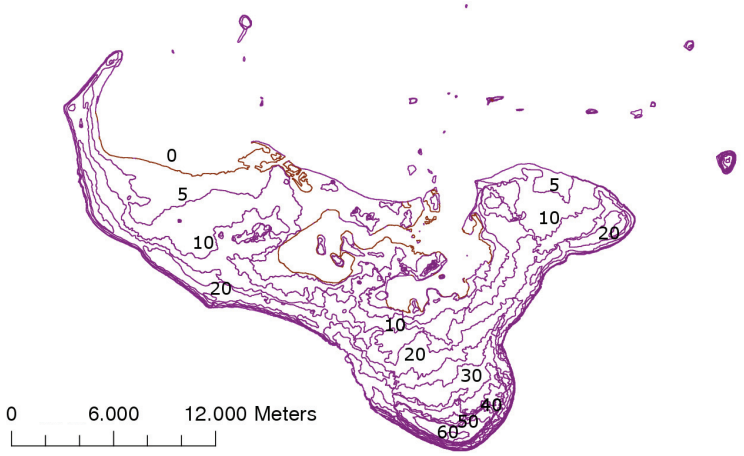

Figure 2.5. The elevation map of Tongatapu. Contours are drawn every 5 m.

The lagoon is in direct contact with freshwater lenses that float on denser salt water. At low tide, a mix of groundwater, lagoon and sea water from the transition zone underneath the freshwater lens can be seen seeping into the lagoon at specific points. A total of six of these points where identified

along the lagoon edge. The tilting of the limestone causes subsurface and occasional surface flow towards the lagoon. The main flow direction can also be derived from the elevation map provided by Figure 2.5. Other evidence of groundwater discharge along the coastline is found in the occurrence of 'beachrock'. Beachrock forms in the intertidal zone. This formation is not related to the discharge of groundwater as as postulated by *Lao* [1978]. An explanation for the formation of beachrock can be found in *Dickinson et al.* [1999] who describe a theory by *Ginsburg* [1953]. Here precipitation of calcium carbonate rich 'interstitial cement is caused by warming of seawater trapped in the pores between sand grains near the surfaces of wet beaches that are heated by sunshine during exposure at low tide'. The slope of the beachrock formations follows the beach gradient, and the thickness of the deposition varies between several centimetres to several meters.

The freshwater lenses are the islands main source of potable water which is used for domestic and farm purposes. There are a number of small public water supplies. Maintaining the quality of this freshwater resource is essential to the health and economic well being of the island community.

2.7 Soils

Tongatapu has a relatively flat terrain comprising shallow, free-draining clay soils overlying the permeable limestone aquifer. A detailed survey was carried out by *Cowie* [1980] and *Cowie et al.* [1991]. The soils on Tongatapu are derived from several deposits of volcanic ash derived from the volcanoes in the west. A distinction can be made between two main phases of deposition resulting in a younger-reddish brown tephra overlying an older browner and fine textured tephra. The deposition of the older and younger ashes is reported to have occurred respectively 20,000 and 5,000 years ago. These dates have not actually been confirmed. *Cronin* [2005] reports on the occurrence of a recent ash layer on Tongatapu, and attributes this to a 'moderate to large magnitude volcanic eruption [which] has probably occurred at one of the volcanoes to the W or NW of Tongatapu, at least once during the past 1-2,000 years.' The location of the volcanoes resulted in the ash being deposited so that the thickest depositions occur in the western part of Tongatapu. *Thompson* [1986] has shown that low-level wind flow around Tongatapu is generally from the southeast under the influence of the southeast Trade Winds. During the wet season as the inter-tropical convergence zone moves southward, the winds tend to be more variable in direction. *Cronin* [2005] thus concludes that 'ash from a small magnitude event would be dispersed dominantly to the northwest. Ash ejected to heights of > 3 kms, i.e. above the trade wind shear zone, would then be dispersed in an opposite direction toward the southeast, i.e. in the direction of Tongatapu.'

The soil on the island was generally classified as typic argiudoll, very-

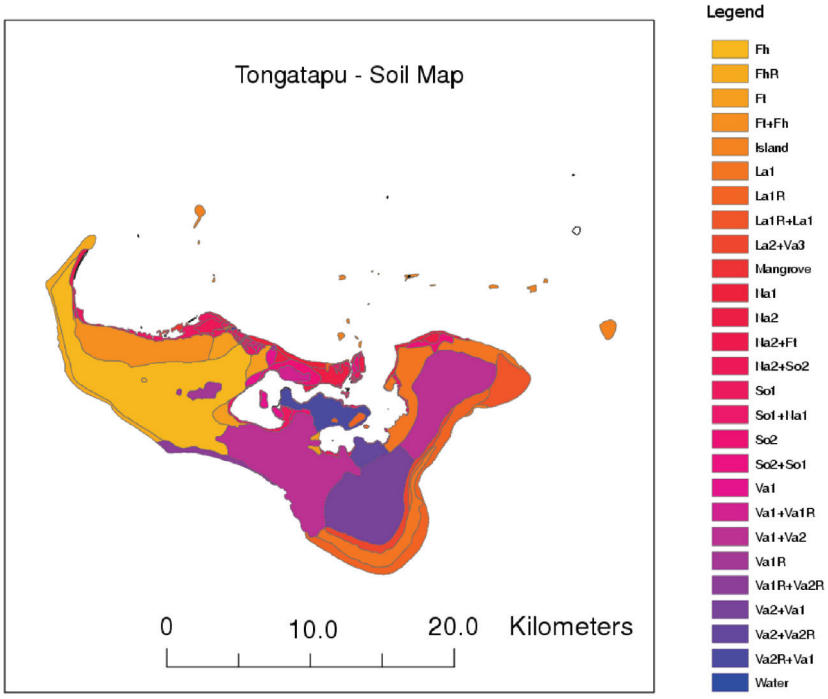

Figure 2.6. The soil map of Tongatapu. For definitions of soil codes see Appendix A.1.

fine, halloysitic and isohyperthermic [*Cowie et al.*, 1991]. Halloysite is the dominant clay mineral ($> 90\%$). Between the two characteristic soil layers, associated with different volcanic deposits, often a thin (< 50 mm) buried soil can be found. Perched water tables may occur at the transition between the young and old ash deposits. The soil types on Tongatapu are mainly differentiated by the thickness of soil developed in the young ash. The young ash has a thickness of > 2 m in the west, ranging to < 0.5 m in the east (see Figure 2.6). Total soil thickness ranges from about 5 m in the west, to 0.5 m in the east. The soils in the west of the island are generally less weathered and coarser in texture, while the soils in the east are most weathered and finer textured. The younger ash soils have higher amounts of 0.5 M H_2S0_4 soluble P, acid oxalate extractable Fe, Al, Si, and a higher CEC. This indicates that these soils are less weathered (see *Manu* [2000]). The iron-oxides give the rusty colour to the soil, and cause the high retention of P, and aid in soil aggregation. These clay soils have high to very high clay contents dominated by halloysite. Hallosytic soils are characterised by a specific hydrodynamic behaviour. *Dorel et al.* [2000] measured large water retention at -1500 kPa

and high saturated hydraulic conductivity in a clayey soil rich in halloysite (70-90%) and iron oxides, derived from volcanic ash. The soils in Tongatapu show a similar behaviour. A detailed physicochemical description of the soils on Tongatapu is provided in *Pochet et al.* [2006]. Differences in structure and properties of the soils are closely related to the nature and content of the iron–oxides, and their interaction with the halloysite minerals. This process also contributes to the micro-aggregation observed in the soil [*Pochet et al.*, 2006].

2.8 Vegetation

Vegetation along the coast consists of small areas of swamp vegetation, mangrove forests, with creeping grass and bush vegetation at the beach. Further inland, this is gradually replaced by coastal forest, especially along the limestone cliffs. The interior of Tongatapu used to be covered by tropical lowland rainforest with high species diversity. However, because of an increasing human population and a consequent increased demand for land this has mostly disappeared. On Tongatapu, a very large proportion of the land has been cleared for farming, and other purposes. Only 3.2% of the island is now covered by native forest, and most of it is on the coast [*Wiser et al.*, 2002]. A small patch of natural forest is preserved in the Toloa Rainforest Reserve [*Ball*, 2001]. *Wiser et al.* [2002] carried out a detailed analysis of the vegetation cover of Tongatapu using aerial photographs from 1990, and they sampled forest fragments and selected regenerating stands for analysis. They concluded that: 'forest fragments occupy 3.2% of the land area; regenerating 'bush fallow' stands occupy 7.9%'. *Wiser et al.* [2002] recorded 209 vascular plant species, of which 8% were ancient introductions while 33% were modern introductions. *Wiser et al.* [2002] also reported that 'late bush fallow stands support the highest alien cover.' The influence of an extinct pigeon species on seed dispersal of several trees is discussed in *Meehan et al.* [2002]. *Meehan et al.* [2002] concluded that 'species that once relied on the large extinct pigeons for dispersal may have become reduced in abundance in their absence'. A large part of the land has been transformed into an area of coconut (*Cocos nucifera L.*) plantations that are mixed with other crops. Secondary fallow vegetation mainly consists of large Guinea grass (*Panicum maximum J*). *Manu* [2000] wrote that the 'gradual disappearance of these forests has resulted in a shortage of wood for fuel, coastal and slope erosion, and an increase in the impact of strong winds, floods and salt spray on plantations'.

Agricultural crops may suffer from water stress. The evaporative demand of vegetation and crops, and the variable nature of the rainfall, can create soil moisture deficits at any time of the year *Thompson* [1986].

2.9 Demography

Archaeological findings indicate that Tonga was settled about 3000 years BP. The archaeological 'Lapita' sites typically lie inland from the present coastline [*Dickinson et al.*, 1999]. The Lapita settlements overlap in time with the latter part of a regional mid-Holocene glacio–hydro–isostatic rebound in relative sea level that affected essentially all Pacific islands [*Dickinson et al.*, 1999; *Mitrovica and Peltier*, 1991].

The population has increased enormously during the 20^{th} Century. Total population was around 20,000 at the beginning of the 20^{th} Century and at present has passed a total of 100,000. This number does not include the number of people that have moved overseas which is also estimated at 100,000. Increase in population has lead to large migrations to the larger cities in New Zealand, Australia and the United States of America. An internal migration to the capital of Nuku'alofa in Tongatapu means that it hosts over 40% of the total population.

2.10 Land Use

Agriculture in Tonga was largely subsistence based and traditionally consisted of a shifting cultivation. The traditional cropping system is described in detail by *Manu* [2000]. Secondary fallow vegetation was partly cleared by cutting the undergrowth, shrubs and small tree vegetation, while the bigger trees were burned at the base to die slowly during the cropping phase. *Manu* [2000] reported that 'the cropping phase is initiated by planting a mixed crop of yam (*Dioscorea alata L.*), giant taro (*Alocasia sp.*), and plantain (*Colocasia esculenta L.*). This is followed by sequential harvesting and planting of tannia (*Xanthosoma saggitarius*) as the second crop, followed by sweet potatoes (*Ipomoea batatas*) and then cassava (*Manihot esculenta*). The order of the crops in the cropping sequence matches their respective nutritional demand from the soil as the soil fertility decreases from yam towards cassava'. Traditionally, according to *Manu* [2000], 'farmers in Tonga have always chosen prime land for cultivation (...) using the species composition of the bush fallow vegetation as an indicator for ranking land capability and soil fertility'. Over the last three decades it has been increasingly attractive for Tongan farmers to grow cash crops. These include indigenous crops such as vanilla (*Vanilla fragrans*) and kava (*Piper methysticum*), as well as non–indigious crops, most notably squash pumpkin (*Cucurbita maxima L.*).

2.11 Main Field Site - Vaini Research Station

The main field site for this research was located at flat terrain at the Vaini Research station of the Research and Extension Division of the Ministry of

Agriculture of Tonga. A photograph of the experimental field site is shown in Figure 2.7.

Figure 2.7. The experimental field site at the Vaini Research Station before crop emergence (23/07/2002).

2.11.1 Soil - Experimental Site

The soil at the experimental station is part of the Vaini soil series ([*Cowie et al.*, 1991], Figure 2.6). The transition from the younger to the older ash layer occurs at around 90 to 100 cm (Figure 2.8). The beginning of the limestone layer occurs at around 280 cm. The groundwater is found at a depth of about 20 meters. We distinguished an A_p horizon until 9 cm and an A_h layer from 9 to 38 cm. For a detailed soil description see Appendix D.1. The soil had a clay content from about 70% at the top of the profile, to 90% at 1 m depth. Soft, weathered lapilli occur throughout the whole soil profile. The dry bulk density of the soil ranged from 0.5 to 1.2 * 10^3 kg m^{-3} and the pH ranged between 6 and 7.2. The organic carbon content in the top 18 cm was about 3.4%, and decreased to 0.8% at a depth between 28 and 43 cm [*Cowie et al.*, 1991]. Water retention properties [*van der Velde et al.*,

2005] indicated that for the top soil, both high saturated ($\sim$0.6 m^3 m^{-3}) and residual water contents, as measured at 1.5 10^3 kPa, ($>$ 0.2 m^3 m^{-3}) occur. The topsoil is very free draining with high values for saturated hydraulic conductivity ($>$ 5 m day^{-1}). These were extrapolated from measurements done with tension disc infiltrometers (see *van der Velde et al.* [2005] and Chapter 5).

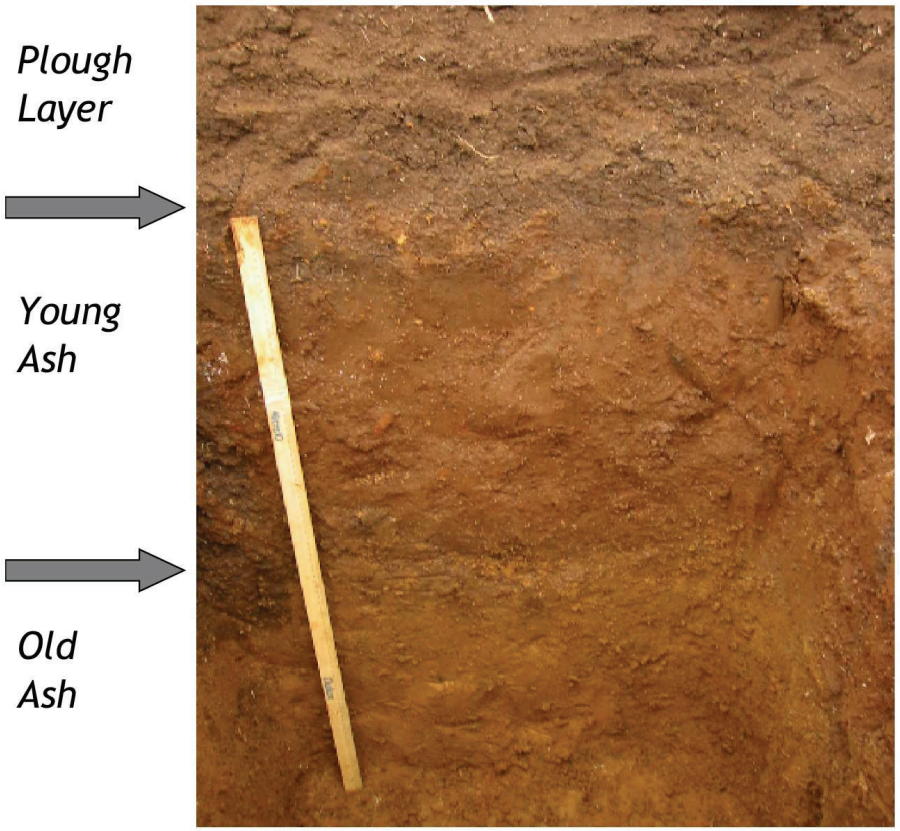

Figure 2.8. Picture of the main soil horizons at the Vaini Research Station

2.11.2 Land use - Experimental Site

This site had been under Guinea grass (*Panicum Maximum L.*) fallow for the last 20 years and was cultivated during the 2002 and 2003 growing season using the method prescribed by MAF for the growing of squash on small agricultural fields. Guinea grass has deep penetrating roots ($>$ 1 m). The grass was slashed three months before planting of the squash, and burned two months before planting. The field was ploughed one month before planting and then ploughed and disked a couple of days before planting of squash. It

was last ploughed 2 months before the period of the measurements of the soil's hydraulic properties.

2.11.3 Meteorological Station and Soil Instrumentation

At the experimental site, a weather station and soil instrumentation were installed. The weather station measured incoming global radiation, relative humidity, air temperature, wind speed and rainfall. These data were collected for the purpose of modelling the water balance of the site. Measurements were taken every 15 seconds and half hour averages were stored on a data logger (CR10X, Campbell Scientific, Logan, Utah, USA). Global radiation was measured with a silicon cell pyranometer (SKS 1110, Skye, Powys, UK), air temperature and relative humidity were measured with a HMP45A probe (Vaisala, Helsinki, Finland) wind speed was measured with a sensitive 3-cup anemometer (R30, Vector Instruments, Rhyl, UK), and a tipping-bucket rain gauge (Rain-O-Matic, Pronamic Co., Silkeborg, Denmark) was used to monitor rainfall. These instruments were mounted on a mast in the middle of the field, at a height of about 2 m above the ground. The vapour pressure deficit of the air, D_A, was calculated using the average air temperature and the relative humidity. A 20 W solar panel was used to recharge the 12V power supply.

The data logger also recorded the output from a number of drainage flux meters [*Gee et al.*, 2002; *van der Velde et al.*, 2005] that were used to monitor water draining through the root–zone soil. Also, the output from several arrays of soil moisture and soil temperature probes that were installed in the root-zone soil to a depth of 1.2 m were logged. Soil moisture content (SMC) was measured using a number of reflectometer probes (CS616, Campbell Scientific, Logan, Utah, USA). Measurements of SMC were done once every half hour. Two horizontal sets (30–, 60–, 90– and 120– cm) and two vertical probe sets (0–30, 30–60, 60–90 and 90–120 cm) were installed in the volcanic ash soil. Soil temperature was measured with one set of Campbell temperature probes installed at 15, 45, 75 and 105 cm.

Other field sites were investigated, and these are reported on in detail in Chapter 4.

Chapter 3

Survey and Inventory of the Soil and Water Quality of Tongatapu

3.1 Introduction

Since background data on the quality of Tongatapu's natural resources are scarce, and not well documented, a survey of the quality of the soil and water resources of Tongatapu was carried out. The aim of this survey was two-fold. First, it was meant to collect all the readily available measurements of the quality of Tongatapu's soil and water resources. Second, actual measurements were carried out of agrichemical residues in groundwater obtained from wells, agricultural fields, seepage into the lagoon, and lagoon sediment.

3.2 Materials and Methods

3.2.1 Previous measurements

All relevant governmental and non-governmental agencies were visited and key persons were contacted. These included the World Health Organisation at the Vai'ola Hospital, the Environmental Health Unit at the Vai'ola Hospital, the Vaini Research Station of the Ministry of Agriculture, the headquarters of the Ministry of Agriculture, the South Pacific Geosciences Commission, the Tongan Water Board, the Hydrogeological Unit at the Ministry of Lands and Survey and Natural Resources, the Department of Environment, the library of the University of the South Pacific Campus, the library at the 'Atenisi University, as well as several private persons. If measurements had been carried out it was kindly requested if these measurements could be made publicly available. After obtaining all the measurements, they were organised to provide a picture of the past environmental quality assessments. Most results where obtained through a literature search including several reports, as well as scientific publications [*Fuavao et al.*, 1996; *Harrison et al.*, 1996; *Morrison and Brown*, 2003]. The references that were obtained, and the information these contain are listed in Table 3.1. Many of the reports mentioned in Table 3.1 also report on salinity measurements of well water.

Table 3.1. Survey of references that report on chemical analysis for pollution in Tongatapu.

Reports	Year	Analysed for	Analysed
Ministry of Health Tonga [1998]		pesticides, nutrients	well water
Lao [1978]	1978	nutrients	well water
Chesher [1984]	1980	pollution sources survey, solide waste, pesticides	well water vegetables, milk human tissue
Zann et al. [1982]	1982	nutrients	lagoon
Falkland [1992]	1991	pesticides, nutrients copper, arsenic chromium	well water
Furness and Helu [1993]	1991	pesticides, nutrients copper, arsenic chromium	well water sludge soil
Falkland [1995]		pesticides, nutrients	
Douglas Partners [1996], WHO	1995	pesticides, nutrients	well water
Morrison [2000]	1994-1997	pesticides, nutrients	soil, well water, lagoon sediment, shellfish
van der Velde [2006]	2002-2003	pesticides, nutrients	soil, well water, lagoon
Scientific Articles			
Fuavao et al. [1996]	1996	basic data	drinking water
Harrison et al. [1996]	1991	pesticides	lagoon sediment, shellfish
Morrison and Brown [2003]	1999	metals	lagoon

3.2.2 Field survey

The field survey focused on measurement of pesticides, nitrates and ammonium in soil, groundwater, and groundwater seepage. Possible occurrence of insecticides, fungicides and herbicides were analysed in three agricultural fields, ten wells, one groundwater seepage point, and one lagoon sediment sample collected directly under a groundwater seepage point. Samples were collected at the sites on the 11^{th} of November 2002 and then frozen. A drop of toluene was added to the water samples to minimize vapour loss during transport. Samples were flown to New Zealand and analysed at HortResearch's Ruakura laboratory. The limits of detection are reported in Appendix B.1. The approximate locations of soil and water analysis for pesticide analyis are of the sites are shown on the map in Figure 3.1.

Soil samples for pesticide analysis were taken at three different sites on the 14^{th} of November, 2002. The tree sites included the field of Manu Latu, next to the crown prince's recidence, a field located next to the airport, and the field of Lafulatu. The locations of the field sites that were used for soil sampling are indicated by their UTM coordinates in Appendix C.1.

Ten groundwater samples were taken from wells and one sample of groundwater seepage for pesticide analysis. The locations of the wells that were used for sampling are indicated by their UTM coordinates in Appendix C.1.

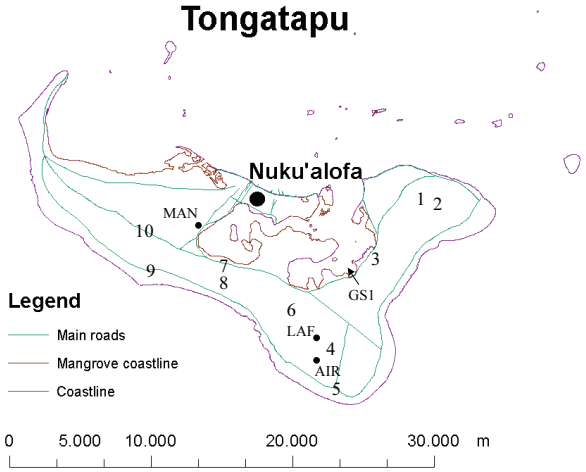

Figure 3.1. The location of well and soil samples for pesticide analysis. The UTM coordinates of the sampling sites are indicated in Appendix C.1.

During the field survey, groundwater was also monitored for nitrate and ammonium. In total, 27 groundwater samples were taken. The UTM coordinates of these wells can be found in Appendix C.1. These samples were taken on the 10^{th} and the 11^{th} of November 2002. Along the southern internal coastline of the lagoon, 6 groundwater seepage points were identified during the 2002 growing season. These points were monitored approximately biweekly for nitrate and ammonium during the 2003 season (not reported here). The samples were frozen after adding a drop of toluene, flown over to New Zealand, and analysed at the Soil and Fertilizer Laboratory of Massey University, Palmerston North.

3.3 Results

3.3.1 Previous research

A full inventory of pollution sources was made by *Chesher* [1984]. Instructively, *Chesher* [1984] used photographs to show the pollution sources. Problems identified included septic discharges from hotels and public buildings, destructive fishing techniques, including the use of poisons, as well as an emerging solid waste problem. One of the recommendations from *Chesher* [1984] was the establishment of a central library containing all reports, studies and documents related to pollution and environment conducted within the Kingdom of Tonga. We reaffirm this statement. The collection of the documents that are, for example, listed in this thesis should preferably be held at the library of the Department of Environment, which was estab-

lished in 2001. Another recommendation by *Chesher* [1984], that has been followed up recently, is that any major project in Tonga legally requires an Environmental Impact Study.

3.3.2 Soil resources

Intensifying agriculture may lead to soil degradation. Staff of the Ministry of Agriculture expressed concerns about soil erosion occurring during intense rainstorms and consequent pollution of the lagoon. In fields subjected to intensive cultivation, slaking (Dr. S. Halevatau, pers. comm.) was shown to occur. Tongatapu's soil is generally permeable and the island is generally flat. But, the fields gently slope towards the main lagoon. Runoff and ponding were observed at the site, and it was thought that this was related to the structural degradation of the topsoil. Concerns of soil degradation by pesticides usage were expressed by *Chesher* [1984].

3.3.3 Water resources

A good indicator for the environmental health of Tongatapu may be provided by the state of Tongatapu's internal lagoon. This is especially so since the lagoon is relatively sheltered from oceanic influences (see previous Chapter). The tilting of the highly porous limestone aquifer and the associated flow of groundwater towards the lagoon in the north makes the lagoon susceptible to contamination by agrichemicals that have leached through the soil profile. The quality of the lagoon integrates and reflects a multitude of effects, some of which may be related to human influences. Others may be related to 'natural' influences, such as earthquakes and cyclones. Care thus has to be taken when drawing conclusions on the information presented in this section.

There are several ways by which ground– and lagoon water can become contaminated. Agrichemicals in solution may drain out of the rootzone towards the freshwater lenses (Chapter 8). Spray drift of applied chemicals could contaminate the lagoon water directly. Heavy rains can detach soil particles with adsorbed agrichemicals and subsequently transport these through preferential flow channels towards the freshwater lens.

The Fanga'uta Lagoon had for many centuries supported an important mullet fishery. Declines in catches from 1960 onwards led to the lagoon being temporarily closed for commercial fishing in 1975. It was subsequently reopened in 1981, but unsuccessfully. Currently, the mullet industry has disappeared. The research by *Zann et al.* [1982] was carried out because Tongan planners needed information on Fanga'uta Lagoon for proper management. At the time of the research of *Zann et al.* [1982], other reported environmental changes in Fanga'uta Lagoon included shoaling, mangrove encroachment, and a decline in the number of formerly prolific edible mussels. Based on studies since 1981, *Kaly et al.* [2000] concluded that a general trend

in decreasing water clarity of the lagoon occurred and that generally nutrient concentrations had increased. Degradation of coral communities in the lagoon were attributed in some part to urban nutrient-runoff [*Zann*, 1994]. Other pressures associated with increases in the human population that were then identified, included dredging for building aggregate and increased land reclamation. Nowadays, coastal construction works, and especially uncontrolled solid waste dumping, as well as the waste dump being located next to and in part in the lagoon, places further pressures on the lagoon.

Changes in land use, and a general intensification of agriculture related to cropping of cash crops, will also negatively affect the lagoon and coastal marine environment. Increased clearance of fallow land and the cutting of coconut trees to allow tractors to work the land, will lead to erosion and consequent increased sediment inputs into the lagoon.

3.3.4 Pesticides in the environment

Agricultural chemicals pose another threat to the lagoon environment and groundwater resources of Tongatapu. Several pesticide analyses have been carried out on Tongatapu. *Chesher* [1984] provided pesticide analyses, from a survey done in 1980 by MAFF. These were analysed by the Pesticide Analytical Laboratory, in Manila, Philippines (Table 3.2), and indicate the occurrence of traces of pesticides in well water. These findings of agrichemical residues in the groundwater occur quite fast with respect to the agrichemical usage in Tongatapu, which may indicate the occurence of preferential flow of water and solutes [*Kladivko et al.*, 1991]. The data also show DDT accumulating in human tissue. However, there is possibly a problem with the units reported by *Chesher* [1984], as indicated in Table 3.2. The units are given as mg kg^{-1}, and this results in the values being a factor 1000 larger compared to the other values reported in this Chapter. Possibly, mg kg^{-1} in Table 3.2 should be replaced by μg kg^{-1}, and mg $liter^{-1}$ by μg $liter^{-1}$. This remains however unresolved.

The World Health Organisation in Tonga, in cooperation with the Ministry of Land Survey and Natural Resources, had 24 wells analysed by DSIR in New Zealand in 1991. *Furness and Helu* [1993] reported these analysis. Of the 24 samples collected, most wells had no residues except for the three listed in Table 3.3. In 1995, the World Health Organisation hired Douglas Partners [*Douglas Partners*, 1996] to test 20 samples for the presence of residues of organochlorine and organophosphate compounds. These included the wells analysed in 1991. No residues were found. In 1998 the Ministry of Health [*Ministry of Health Tonga*, 1998] hired Ecowise Environmental Ltd. to test 18 water samples taken from community water supplies. While testing for 33 active ingredients, including those being detected earlier, no residues were detected.

While there is some uncertainty about the units used in Table 3.2, the

Table 3.2. Pesticide analysis reported by *Chesher* [1984]. Vegetables, milk, human tissues as mg kg^{-1}. Water as mg l^{-1}. Possibly, the units reported in *Chesher* [1984] are not correct, and rather correspond to μg kg^{-1} and μg l^{-1}.

Sample	T Lindane	Heptachlor	T Aldrin	Endosulfan	T DDT
Cabbage	0.08	0.01			
Banana	0.05		0.09		0.02
Cucumber	0.02		0.03		
Tomato	0.01				
Water 101	0.21	0.16	0.09	0.06	0.04
Water 102	0.15	0.23	0.08		
Water 103	0.23	0.18	0.11	0.01	0.05
Water 104	0.07	0.03			0.02
Water 105	0.4	0.23	0.13	0.09	0.07
Water 106	0.06	0.01	0.04	0.04	0.02
Water 107	0.3	0.17	0.08	0.1	0.04
Water 108	0.06	0.01			
Water 109	0.14	0.01			
Milk	0.02-0.1	0.03-0.05	0.01-0.07		0.09-0.43
Human Fat					1.4-4.2

Table 3.3. Pesticide analysis from *Furness and Helu* [1993] made in 1991. Reported as μg l^{-1}.

Sample	p,p-DDE	Hexachlorobenzene
Well 21	0.04	
Well 220	0.06	
Well 170	0.08	0.02

Table 3.4. Organochlorine and PCB concentrations in sediments from Tongatapu, Tonga (μg kg^{-1} dry wt, detection limits in brackets) analysis from *Harrison et al.* [1996] carried out in 1991.

Organochlorine	**TGN/02**	**TNG/03**	**TNG/07**
a-BHC	<0.07	<0.05	<0.05
HCB	<0.02	<0.01	<0.01
b-BHC	<0.16	<0.11	<0.11
g-BHC	<0.11	<0.08	<0.08
Heptachlor	0.07 (0.03)	<0.08	<0.07
Aldrin	<0.03	<0.02	<0.02
Oxychlordane	<0.08	<0.05	<0.05
trans-Chlordane	0.24 (0.04)	2.22 (0.03)	<0.03
cis-Chlordane	<0.04	<0.02	<0.02
trans-Nonachlor	<0.01	<0.02	<0.02
cis-Nonachlor	<0.04	<0.03	<0.03
o,p'-DDE	0.11 (0.06)	0.95 (0.04)	<0.04
p,p'-DDE	2.20 (0.02)	17.1 (0.01)	0.04 (0.01)
o,p'-DDD	1.24 (0.14)	12.8 (0.09)	<0.09
p,p'-DDD	3.08 (0.09)	142 (0.06)	0.09 (0.06)
p,p'-DDT	0.59 (0.22)	854 (0.15)	<0.16
Mirex	<0.05	<0.03	<0.03
Hept. Epoxide	<0.01	0.13 (0.06)	<0.07
a-Endosulphan	<0.08	<0.06	<0.06
Dieldrin	<0.01	0.43 (0.08)	<0.09
Endrin	<0.34	<0.23	<0.24
Methoxychlor	<0.98	<0.66	<0.69
Aroclor 1242	<0.66	0.85 (0.30)	<0.46
Aroclor 1254	<0.20	12.1 (0.08)	<0.13
Aroclor 1260	2.64 (0.21)	5.33 (0.14)	<0.23

Table 3.5. Organochlorine and PCB concentrations in shellfish from Tongatapu, Tonga (μg kg^{-1} dry wt, detection limits in brackets) analysis from *Harrison et al.* [1996], carried out in 1991.

Organochlorine	**TNG/10**	**TNG/11**
a-BHC	<0.01	<0.16
HCB	<0.20	<0.42
b-BHC	<0.22	<0.35
g-BHC	<0.16	<0.26
Heptachlor	1.00 (0.15)	2.30 (0.24)
Aldrin	<0.04	<0.07
Oxychlordane	<0.18	<0.29
trans-Chlordane	<0.09	<0.14
cis-Chlordane	0.14 (0.08)	<0.13
trans-Nonachlor	<0.08	<0.13
cis-Nonachlor	<0.08	<0.14
o,p'-DDE	<0.16	<0.25
p,p'-DDE	0.23 (0.05)	1.00 (0.08)
o,p'-DDD	0.47 (0.31)	0.85 (0.17)
p,p'-DDD	0.80 (0.20)	<0.02
p,p'-DDT	0.48 (0.27)	<0.43
Mirex	<0.06	<0.10
Hept. Epoxide	<0.10	0.61 (0.15)
a-Endosulphan	<0.08	<0.13
Dieldrin	<0.12	0.96 (0.19)
Endrin	<0.33	<0.53
Methoxychlor	<1.24	<1.96
Aroclor 1242	<0.71	<0.65
Aroclor 1254	<0.17	<0.15
Aroclor 1260	<0.26	<0.23

result reported in Tables 3.2 and 3.3 suggest that some movement of agrichemicals has occurred towards the groundwater. Other studies focused on analysing the sediment and shellfish of the lagoon. Shellfish are known to accumulate pesticide residues in their tissues. They are popular for consumption. *Harrison et al.* [1996] found the occurrence of organochlorines in sediment (Table 3.4) and shellfish (Table 3.5) from the Fanga'uta lagoon. The low concentrations found were considered to have a minimal direct impact on human health. *Morrison* [2000] provided analyses of five lagoon sediment samples, plus two water samples derived from the sediment samples, and three soil samples from agricultural fields. The samples were tested for carbaryl (detection limit 0.1 mg kg^{-1}), chlorfluazuron (detection limit 0.2 mg kg^{-1}), dimethoate and flusilazole (detection limit 1 μg kg^{-1}). No residues of dimethoate were found. One soil sample (S1) tested positive for carbaryl (1.3 mg kg^{-1}). Three lagoon sediment samples (L2, L3, L5) and one soil sample (S2) tested positive for chlorfluazuron (respectively 8.8, 4.0, 5.0 and 1.0 mg kg^{-1}). Two lagoon sediment samples (L1 and L3), and one soil sample (S2) tested positive for flusilazole (2.0, 7.2 and 6.4 μg kg^{-1}). *Morrison and Brown* [2003] studied the occurrence of trace metals in sediment and shellfish of Fanga'uta Lagoon. Over 80 shellfish samples from the lagoon and nearby water were analysed. *Morrison and Brown* [2003] reported that no evidence of anthropogenic sources of metal where found and that no major health risks would arise from the metals in the shellfish.

All reported occurrences of pesticide residues in Tongatapu's environment, including soil, groundwater, lagoon sediment and shellfish, were very low and posed no health threat. We can, however, conclude that some migration of more persistent pesticides residues into the groundwater and into Fanga'uta lagoon has occurred.

3.3.5 Nutrients

Another concern related to agriculture, and possibly posing a bigger problem, is the leaching of nutrients from fertiliser usage. Indication of a nutrient enrichment in the lagoon is found in the algae blooms that can be observed around seepage points at the lagoon shore. One such point, located in the village of Vaini, had been a traditional bathing place for many centuries (V. Minoneti, pers. comm.). Bathing at this seepage point has been discontinued over the last 10–15 years since the algae blooms occurred. It is however difficult to determine the exact cause of these algae blooms. Although agriculture may be a part of the problem, it is likely that septic tank problems, as reported on by *Chesher* [1984], are also an important factor. Nevertheless, all analyses reported in Table 3.1 indicate low nitrogen and phosphorus levels in the groundwater, although some elevated levels of nitrogen and phosphorus have been found in the lagoon. During the so–called TEMPP project, *Morrison* [2000] found elevated levels of nitrogen and phosphorus

Table 3.6. Insecticides, fungicides and herbicides found in soil (mg kg^{-1}) of 3 agricultural fields **A, L and M**, in each field 3 samples were taken, and 1 sediment sample **GS** from the lagoon. No detectible residue was found for **M S1**. The limits of detection can be found in Appendix B.1, 't' indicates 'trace'.

Sample ID	**A S1**	**A S2**	**A S3**	**L S1**	**L S2**	**L S3**	**M S2**	**M S3**	**GS**
pp DDT				0.01	0.01	t	t	0.03	0.04
myclobutanil	t	t		0.01	0.01	0.01			
dichloran			0	t		0.01	0.01		
op DDT	t	t	t						0.07
deltamethrin		t			t	t			
terbufos				0.01		0.05			
pp DDE								t	0.04
cyfluthrin				0.02					
cyanazine						0.01			
op DDD								t	
pp DDD								t	
permethrin				t					
terbumenton					t				
tetradifon						t			

in the lagoon water. The sudden change in the lagoon from a phosphorus limited system in February 1999, to a nitrogen limited system with higher concentrations of phosphorus in July 1999, led *Morrison* [2000] to suggest a relation to fertilizer use. *Morrison* [2000] hypothesised a relation to the advent of the squash production. However the soil posses a large retention capacity for P, which would restrict P mobility *Cowie et al.* [1991]. Another explanation may relate to the use of P containing detergents that enter the lagoon through the reticulation system.

3.3.6 Field survey

3.3.7 Pesticides in the environment

The results of the pesticides analysed for our soil survey are presented in Table 3.6. The results in Table 3.6 indicate that there is a wide range of agrichemical residues found in Tongatapu's agricultural soils. The accumulation of agrichemical residues in the sediment of Tongatapu's lagoon suggests, and confirms the results from previous research, that there is a transport of contaminated water into the lagoon. However, cleaning of spray equipment directly in the lagoon cannot be ruled out. But it is highly unlikely at this specific seepage point which is not easily accessible. The concentrations are low, and most of these residues are 'old' agrichemicals. Some of them are currently on the 'Dirty Dozen' list of persistent organic pollutants and forbidden in international trade (DDT, aldrien, dieldrin). However, old stocks are still available on the island and possibly being used.

The analysis of ten groundwater samples for the occurrence of pesticides revealed three samples to have traces of either dieldrin, diazinon or carbaryl

Table 3.7. Insecticides, fungicides and herbicides found in groundwater (μg l^{-1}) as measured in 3 out of 10 monitored wells. No pesticides were detected in the other 7 sampled wells. The limits of detection can be found in B.1.

Sample ID	**2**	**3**	**14**
carbaryl	**t**	<0.02	<0.02
diazinon	<0.02	**t**	<0.02
dieldrin	<0.01	<0.01	**0.01**

(Table 3.7). Two of those samples (wells 2 and 3 on the map of Figure 3.1) came from hand–dug wells with a depth to the water table of 7 and 3.7 meters, and a soil depth of respectively 1.55 and 0.7 meters. Contamination of the hand–dug wells by the cleaning of spray equipment cannot be ruled out. The third sample came from water pumped up in the centre of the western part of Tongatapu (well 10 on the map of Figure 3.1). The occurrence of the pesticides in the groundwater shows that indeed there is transport of the applied chemicals through the soil. None of the six samples that were analysed for organochlorines were positive.

The seepage collected is a mix of lagoon and groundwater, and the samples had an average EC of 6.5 mS cm^{-1}, ranging from 2.15 to 10.08 mS cm^{-1}. At the entry of the lagoon in the north we have measured an EC of 49.1 mS cm^{-1}. Deeper into the lagoon, just above the small peninsula, an EC of 39.3 mS cm^{-1} was recorded. In the sheltered parts of the lagoon in the west, and east, we measured EC's of respectively 28.2 and 21.8 mS cm^{-1}. If we assume an EC of 30 mS cm^{-1} of the lagoon water and an EC of 0.8 mS cm^{-1} for the groundwater, we calculate a mixing ratio of ground- and lagoon water for the seepage. We find a ratio of about 4 to 1 respectively. So, this implies that the contaminants and nutrients that are occuring in the groundwater, will cause pollution of the lagoon.

3.3.8 Nutrients

Results of the organic N analysis show relative low concentrations in the groundwater (Table 3.8). The concentration of NO3–N in the seepage, similar to the groundwater NO3–N concentration, of about 1.5 mg l^{-1} does pose a threat to the local fragile ecosystem at those seepage points. The temporal variation in the N loading on the lagoon is not known. However, as mentioned above, algae blooms have also been observed around those seepage points, this may be related to the N input at those points. However, this would need to be investigated with more detail. The EC of the groundwater samples ranged from 362 μS cm^{-1} to 1316 μS cm^{-1} with an average of 762 μS cm^{-1}.

Table 3.8. Nitrate and ammonium analysis of groundwater, seepage and lagoon water.

2002	$NH4^+$ (N mg l^{-1})		$NO3^-$ (N mg l^{-1})		
	average	stdev	average	stdev	n
groundwater	0.07	0.06	1.45	1.05	39
seepage	0.49	0.25	1.54	0.64	6
lagoon	0.53	0.18	0.08	0.12	4

3.4 Conclusions

Observations on the quality of soil and water resources of Tongatapu indicate that the environment has degraded. The occurrence of agrichemicals in Tongatapu's environment provides one measure of this overall degradation. Thankfully, the currently measured quantities of agrichemicals in Tongatapu's environment are still very low. This should allow time for appropriate development of strategies to ensure that water quality does not degrade further.

Previous analyses of pesticides have indicated occasional occurrence of agrichemical contamination of Tongatapu's water resources. Other monitoring programs have failed to detect any agrichemical contamination. This may be related to the low values that have been reported but also to analytical difficulties. The earlies report analysing agrichemcial contamiation was found to be the highest with about a factor 1000. Possibly, this may be to eroneous reporting of the units of that analysis. But this remains unclear. We identified traces of pesticides in groundwater and agricultural soils. None of the values found for pesticides indicate a risk to human health. The concentrations of nitrate and ammonium in soil, lagoon, and groundwater are also low. However, the observations of algae blooms at seepage points in the lagoon indicate that an enrichment of nutrients is occurring. Also, as we will see in Chapter 7, the drainage water out of the rootzone contains high concentrations of nitrates.

The behaviour of agrichemicals in tropical ecosystems can be different from that which is experienced in the temperate regions [*Naidu et al.*, 1996]. This highlights the need for specific testing of the behaviour of agrichemicals in tropical soils and climatic conditions. Another issue relates to the lack of generally accepted 'good practice' protocols while working with agrichemicals. This includes the safe disposal of empty containers, which is a problem in several countries [*Espinosa-Gonzalez*, 1997]. This poses a threat to both the environment, as well as the health of agricultural workers. Also important, especially since 'good practice' protocols are lacking, is that the legislation of Tonga allows for the import of certain active ingredients, such as paraquat, that have been banned in several other countries because of its mobility and acute toxicity (Austria, Denmark, Finland, Hungary and Sweden).

Other pressures on Tongatapu's water environment may be more pressing, and relate to the overall degradation of the lagoon. These include coastal construction works, erosion of fallow land cleared for agricultural production, and over-fishing. Further attention to these issues will briefly be given in Chapter 12. The main scope of this thesis focuses on the impacts of agriculture and climatic variations on Tongatapu's environment.

Part II

Agricultural Impacts - Field scale

Chapter 4

Impact of Land Use Intensification on Soil Characteristics *

Abstract Soil structure is governed by the aggregate size–distribution and aggregate stability. Aggregate size distribution and stability affect both the water retention and the hydraulic conductivity of soil. Agricultural practices influence soil structure. The small islands located in the Pacific Ocean are increasingly intensifying their agricultural practices. On Tongatapu, agricultural practices have intensified since 1987 when a niche period for the export of squash into the lucrative Japanese market was identified. The soil in Tongatapu is a structured clay soil derived from weathered volcanic ash. We combine several measurements reflecting soil structure of the surface soil to study the impact of this intensification. These measurements are completed by infiltration measurements deeper down the profile. Five land–use types were identified; ranging from undisturbed tropical forest to the most intensively used field on the island. Aggregate stability of the topsoil was measured using the 'water drop test' and the 'modified Emerson water dispersion test'. Infiltration was characterised by means of disc permeameter measurements, done in triplicate at 5 depths. From these infiltrations measurements an 'effective' characteristic mean pore radius was derived. The weathered volcanic soil has high saturated and residual soil moisture contents (at pF 4.2) and thus low available water. Saturated hydraulic conductivities are generally high (> 1 m day^{-1}). The hydraulic conductivities, measured at 15 cm soil depth with heads of -120 and -80 mm, increased with more intense agricultural practices. The soil aggregate stability of the topsoil decreased with intensification of agricultural practice. The latter was confirmed by the slaking of aggregates observed solely at the most intensively cropped field. It is proposed that the increase of hydraulic conductivity is related to structural breakdown of the soil aggregates into smaller stable micro–aggregates which conduct water at more unsaturated heads. The characteristic mean pore radius is directly derived from the slope of the hydraulic conductivity curve and care has to be taken with its interpretation because of measurement protocols and errors–of–observation. Deeper down the profile, the calculated characteristic mean pore radius highlighted the occurrence of large pores indicating the possibility of macroporous preferential flow. A possible explanation is the capacity of the soil to swell and shrink. However, while the surface soil layer considerably dries out resulting in a shallow layer of loose aggregates, the deeper soil will retain a considerably amount of water even at very negative soil tension heads, as shown by the water retention curves.

In conclusion, intensification of agricultural practises on Tongatapu leads to

*van der Velde, M., Pochet, G., Delvaux, B., Vanclooster, M. and Clothier, B.E. To be submitted.

deterioration of the topsoil's aggregate structure. Consequently, at the field scale, this will likely lead to increased rates of runoff and erosion.

4.1 Introduction

Recently, the word 'hydropedology' has been coined to highlight a research field that aims to derive synergy from combining classical pedological observations with the quantitative approach of soil physicists and hydrologists (see for example *Bouma* [2006]). Similarly the research field of 'hydromorphology', which aims to combine further geomorphologic observations and hydrological modelling, was proposed by *Lall* [2006]. The wish to integrate further research fields originates from the notion that much information remains to be distilled from readily available pedological and geomorphologic datasets. Also, it is likely that progress in understanding hydrological processes may be achieved at the interface of classically different scientific domains. However, this insight has been around for a longer time, and already earlier morphological information has been used to explicitly account for soil hydrological behaviour (see for example *Anderson and Bouma* [1973]).

Aggregate size–distribution and stability affect both the water retention (see for example *Guber et al.* [2003]) and the hydraulic conductivity characteristics of soil (see for example *Nemati et al.* [2002]). *Guber et al.* [2003] studied the effect of aggregate size distributions and texture on soil water retention using regression trees to determine the functional relation of water retention with particle size distribution and aggregate size distribution. They stated that 'water retention reflects a complex interaction of texture and structure jointly affecting soil water retention'. *Guber et al.* [2003] observed no effect of aggregate composition on the water content at -10 kPa. For both water contents at -10 kPa and -33 kPa, samples with extremely low sand content formed a group with highest retention [*Guber et al.*, 2003]. However, at -33 kPa, *Guber et al.* [2003] found a marked effect of aggregate composition on water retention. On the basis of the percentage content of aggregates smaller than 3 mm, samples could be grouped in water retention being either dependent on particle size distribution, or on aggregate size distribution. The latter generally have a lower average water content. *Guber et al.* [2003] also showed that the shape of the aggregate size distribution modifies water retention at -33 kPa, regardless of textural composition.

Nemati et al. [2002] used a model based on the 'decrease in mean weight diameter of aggregates exposed to different rates of wetting' to predict changes in hydraulic conductivity. The model was able to predict the changes in measured hydraulic conductivities for two laboratory soils, and *Nemati et al.* [2002] suggested that information on aggregate size and stability would be useful for improving the prediction of changes in hydraulic conductivity. These two recent studies illustrate the use of morphological information to predict and understand the porous medium of soil that is seldom isotropic. In a soil with macroporous characteristics, the hydraulic conductivity was found to increase over three orders of magnitude across a small pressure head range (100 mm - 0 mm) [*Clothier and Smettem*, 1990].

Agricultural practices influence soil structure. Tillage enhances the breakdown of aggregates by 1) disrupting the biogeochemical gradients and microbial communities that promote the stabilisation of aggregates [*Park and Smucker*, 2005]; by 2) increasingly exposing the aggregates to raindrop impact; 3) mechanical impacts; and 4) increasing mineralisation of organic matter. *Park and Smucker* [2005] studied the saturated hydraulic conductivity and porosity within macroaggregates modified by tillage using measurements made with a specially designed microflow cell. They concluded that conventional tillage reduced the intra–aggregate properties and K_S within the macroaggregates.

In the topsoil, the role of organic matter is of great importance to structural stability. *Wittmuss* [1958] concluded that 'small aggregates ($<$ 0.3 mm) behave in the same way as soil particles in regard to water retention, whereas larger aggregates behave differently in regard to water retention compared with particles of the same size' [*Guber et al.*, 2003]. *Buytaert et al.* [2002] studied the effect of land use changes on the hydrological properties of volcanic ash soils in South Ecuador. They concluded that organic matter content was more important for the water retention of the topsoil compared to the allophane content. They also concluded that cultivation induced a decrease of 21% in water retention at a depth of 15 cm, but only 10% at 40 cm depth. *Armas-Espinel et al.* [2003] concluded that the aggregating effect of allophanes could not counterbalance soil structural degradation while studying a volcanic soil from Tenerife.

Small island developing states in the Pacific Ocean are undergoing an increasing intensification of agriculture. The intensification of agriculture on the islands has led to increasing pressures on their soil and water resources. In a study carried out in New Caledonia, for instance, *Duwig et al.* [1998] found that a substantial amount of nitrates leached down to the groundwater. *Motavalli and Mcconnell* [1998] compared the soil–N status at several land use sites in Micronesia and concluded that 'long-term tillage has a significant impact on soil properties in this tropical island environment, including reducing active and stable N pools'. They also remarked that 'the significance of these changes on NO_3^- leaching is unclear because alteration in soil properties affect both soil water movement and other N processes'.

The well–known phenomenon of soil structural degradation with increasing agricultural practices has not yet received much attention in this region. In this Chapter we analyse the impact of agricultural intensification on the soil structural properties of the weathered volcanic ash soil of Tongatapu. The principle objective is to elucidate the impact of land use on strong micro-aggregation and its consequences on the hydrological functioning of Tongatapu's soils. Agriculture has intensified on Tongatapu since the 1950's, but especially since 1987. At this time, a niche period for the export of squash into the lucrative Japanese market had been identified [*van der Velde et al.*, 2006b]. The initial reason to carry out this research was the

observations done by staff of the Ministry of Agriculture. In fields subjected to intensive cultivation, slaking was shown to occur (Dr. S. Halevatau, pers. comm.). Tongatapu's soil is generally permeable and the island is generally flat. But, the considered fields were gently sloping towards the main lagoon. Runoff and ponding were observed at this intensively cultivated site and it was thought that this was related to the structural degradation of the topsoil. Concerns of soil erosion occurring during intense rainstorms, and consequent pollution of the lagoon were expressed. Indeed, we have observed slaking and runoff in Tonga's most intensively used fields. Another reason to understand the impact of agriculture on soil structural degradation relates to the agrichemicals that might be more easily transported to the lagoon (see Chapter 3).

The objectives of this study were to identify the effects of tillage on aggregate distribution and stability, and to determine changes in the hydraulic conductivity of the topsoil along a gradient of intensifying land use. First, we focus on the effect of agricultural intensification on the structure of the topsoil, especially in relation to the topsoil's aggregates. Second, we focus on the effect of land use intensification on the infiltration characteristics of Tongatapu's weathered volcanic ash soil. Finally, we combine these results in a 'hydropedological' context to assess the relation between aggregates–size distribution and stability, and the hydraulic properties of the soil.

4.2 Materials

Before human settlement (around 3000 BP, *Dickinson et al.* [1999]) Tongatapu used to be covered with tropical forest. Nowadays only about 3 % of the native forest is still intact [*Wiser et al.*, 2002]. Most of the land has at one time been under cultivation. At the moment about 10% of the land's surface is regenerating 'bush fallow'. Traditional cropping involved long periods of fallow up to several years. However, the fallow periods have now generally been severely shortened to a couple of months, or have altogether been discarded due to shortage of available land and demands of food supply. Yet, some of the land still remains unused, so as to comply with Tonga's specific land tenure system [*Crawford*, 2001].

The soil of Tongatapu is derived from weathered volcanic ash and two distinct periods of ash deposition can be recognised on the island [*Cowie*, 1980; *Cowie et al.*, 1991]. Total soil thickness is highly variable but generally decreases from about 5 m in the west to about 0.5 m in the east of the island. At the interface, a buried soil layer of several centimetres thickness, sometimes partly rewashed, can often be recognised. Within the younger ash, several individual depositional events can be recognised and recent dating of the ash layers showed that Tongatapu was covered several times with ash, the last time being about 800 years ago (Dr. S. Cronin, pers. comm.).

4.3 Experimental Sites

The five experimental sites we have chosen are along a land–use gradient that ranged from native forest to a field under a long period of intensive agriculture.

4.3.1 Undisturbed Rain Forest

In one of the remnant patches of small and discontinuous undisturbed forest, measurements were made to obtain the soil properties under 'natural' conditions. These are considered as reference values. The same family has owned the forest for at least 4 generations (approximately 80 years). Clay contents are very high and increase with depth (see Table 4.1). Organic carbon is high in the topsoil and gradually decreases with depth. The litter layer is very thin ($<$ 1 cm, comprising detritus from just one season) which indicates a fast humification. The thickness of the A_h was measured to be 38 cm. The bulk density is below 1000 kg m^{-3}, except for the deepest layer that corresponds to the start of the older volcanic ash.

4.3.2 Agricultural Field After Fallow

This was the main field site and located at the Vaini research station. This site had been under Guinea grass (Panicum Maximum L.) fallow for the last 20 years and was then cultivated using the method prescribed by MAF for the growing of squash on small agricultural fields [*Manu et al.*, 1998]. Guinea grass has deep penetrating roots ($>$ 1 m). The grass was slashed three months before planting and burned two months before planting. The field was ploughed one month prior to planting, and then ploughed and disked again a couple of days before squash planting. It was last ploughed 2 months before the period of the measurements. We distinguished an A_p horizon until 9 cm and a A_h from 9 to 38 cm.

4.3.3 Low Intensity Agricultural Practice

Between 1970 and 1993 this field was an undisturbed plantation of coconut trees, Guineau grass and banana. Since 1993, a rotation of crops has been planted on the land; including traditional crops as well as non–traditional crops. In between cropping cycles, the field was under fallow for about 1 to 3 months. Application of fertilisers and fungicides was done manually. At the time of measurement, some re–growth of weeds had occurred and the field had been undisturbed for 2 months. We distinguished an A_p horizon until 15 cm and an A_h from 15 to 25 cm. Bulk densities were around 1000 kg m^{-3} and clay content increased with depth up to 95%.

4.3.4 Medium Intensity Agricultural Practise

This field had been under cultivation of squash for about 3 years. Before that, the field was cultivated by MAF for a couple of years to evaluate the effects of intensive agricultural use. During a single year the farmer ploughs the field three to five times, then lines the field and plants the seeds. The first year, the farmer ploughed five times. Over the last two years it was ploughed only three times. Machinery was also used to apply fertilisers and fungicides. The field is left fallow during the off–season. The land preparation had just finished at the time of the measurement.

4.3.5 High Intensity Agricultural Practice

This field was the most intensively used agricultural field on Tongatapu. The royal family who owns the land have had people working on the land for at least a hundred years. The current farmer had cropped the field for about 30 years with irregular fallow of a few months every couple of years. The field has alternated with traditional and non–traditional crops, as well as squash. During any year the field will characteristically be ploughed three times, and once with a disc or a rotary device. Harvesting is done manually as well as the application of fertilisers and fungicides. We distinguished an A_p horizon until 12 cm and an A_h from 12 to 30 cm. The land preparation had just finished at the time of the measurement.

4.3.6 Soil

The types of clay minerals that are present in a soil are an important factor determining the stability of soils. *Pochet et al.* [2006] made a detailed study on the soil physicochemical properties and the observed micro-aggregation in relation to the specific hydric properties of the soil on Tongatapu. The soil is a brown halloysitic soil (see *Pochet et al.* [2006]) and it is part of a weathering sequence that can generally be observed in volcanic soils occurring in the humid tropical region. This sequence ranges from young allophonic soils (Andosols) towards highly weathered clay soils (Ferralsols) (*Pochet et al.* [2006]). The soil is classified as typic Argiudoll in the Soil Taxonomy systems [*Soil Survey Staff*, 1999], and it is classified as a Nitisol in the WRB system [*ISSS Working Group Reference Base*, 1998]. A strong micro-aggregation was observed in the soil and this was explained by *Trangmar* [1992] to result from interactions of the halloysitic clay minerals, organic components and iron oxides. *Pochet et al.* [2006] considered that micro-aggregation involves interactions between high charge halloysite and high surface area ferrihydrite. Ferryhydrite and allophane content was generally low in the soil, and lower for the old ash layer (see *Pochet et al.* [2006]).

4.4 Methods

The water retention properties of the topsoil were determined at four sites using Haines' apparatus [*Haines*, 1930] and a pressure plate [*Richards*, 1941]. Particle size distribution, bulk density and organic carbon content [*Walkley and Black*, 1934] were determined at three sites (see *Pochet et al.* [2006]). Sodium adsorption ratio (SAR = $Na^+/ (Ca^{2+}+Mg^{2+})^{0.5}$), where the cation concentration is expressed in mmol L^{-1}) was calculated from determinations of Na^+, Ca^{2+} and Mg^{2+} by *Pochet et al.* [2006].

4.4.1 Aggregate stability and distribution

In the selected fields, 3 samples were taken from the top soil (0-15 cm) and these were bulked together and totalled approximately 0.5 kg. The samples were air dried and then sieved with a range of sieves to determine the aggregate–size distribution.

The stability of aggregates from the topsoil is used as a measure to characterise the structure of the topsoil. We used a procedure similar to *Cerda* [2000]. Aggregate stability tests were performed for initially air-dried aggregates. The mean and standard deviation of the values, as well as the Student's t Test [*Neter et al.*, 1996] were used to differentiate between sites. The modified Emerson water dispersion test (MEWDT) was applied to 10 aggregates (4-4.8 mm). The procedure used was to immerse the aggregates in 40 mL of distilled water at time intervals of 5, 120 and 1440 minutes and visually determine the degree (on a scale of 0-4) of aggregate dispersion:

0. No dispersion. Aggregate completely entire.
1. Dispersion of some particles. Milkiness close to the aggregate.
2. Aggregate partly dispersed or divided into different smaller aggregates.
3. Considerable dispersion. Most of the aggregates were dispersed and the milkiness is large.
4. Total dispersion. The aggregate ceases to exist.

The 'water-drop test', following the procedure of Imeson and Vis (1984) was used with air-dried aggregates (4-4.8 mm). A burette nozzle with silicon tubing was used, together with a constant head–supply system. The drops of distilled water produced had a weight of 0.1 g at 1 s intervals. They fell through a polythene pipe (15 cm diameter) from 1 m height onto the aggregates that rested on a 2.8 mm metal sieve. Ten aggregates were selected from the soil sample.

4.4.2 Infiltration measurements

Measurement of the soil's hydraulic conductivity was done with a disc permeameter at 4 unsaturated heads (-120, -80, -40 and -10 mm) at the 5 sites at 5 depths with 3 replicates per depth. At these depths, samples were also taken at 4 of the sites to construct water retention curves using Haines' apparatus and pressure plates.

Wooding's equation was solved simultaneously for the different heads to derive hydraulic conductivities from the disc permeametry data (see *Clothier* [2000]). *White and Sully* [1987] defined a characteristic mean microscopic pore radius λ_m following [*Philip*, 1987] by using Laplace's capillary–rise formula:

$$\lambda_m = \frac{\sigma}{\rho g}\lambda_c^{-1} \tag{4.1}$$

Here σ is the surface tension, ρ is water density, g the acceleration due to gravity, and λ_c is the capillary length. *White and Sully* [1987] described λ_m as a 'physically plausible estimate of flow-weighted mean pore dimensions'.

If the soil's K(h) is exponential then $\lambda_c = \alpha^{-1}$ [*Clothier*, 2000], where α is the slope of the exponential K(h), so that,

$$\alpha = \frac{ln\left(\frac{K_{h_1}}{K_{h_0}}\right)}{h_1 - h_0} \tag{4.2}$$

where K_{h_1} and K_{h_0} are pairs of hydraulic conductivity measurements, where h_0 is more negative than h1 (e.g. h_0 = -120 mm and h_1 = -80 mm). So from a combination of measurements of hydraulic conductivity at different heads we can derive α and thus λ_m.

4.4.3 Statistical tests

To test if the aggregated means of the measured aggregate stability and hydraulic conductivities of the five samples differ significantly from each other we performed Student t tests [*Neter et al.*, 1996].

4.5 Results

Soil chemical and physical characterisation were carried out for the three sites, 'Forest', 'Low' and 'High' (see *Pochet et al.* [2006]: 'Forest', 'After Fallow', 'Low', 'Medium', and 'High' correspond respectively to 'Fo', 'C', 'Pa', 'Mi' and 'Ma' in *Pochet et al.* [2006]). The location of the soil samples, from depth 135 cm, in the textural triangle (Figure 4.1, see *Gerakis and Bear* [1999]) indicates soil textural composition. The soil samples obtained from the forest reach maximum clay contents of 82%, while the 'Medium' and 'High' respectively reach 94 and 95%. The largest range in clay content

was observed in the 'High' site. The clay content increases with depth from about 65 to 80% in the topsoil while values generally above 90% are obtained beyond 50 cm. No difference in the clay contents of sites is observed in the topsoil and this indicates that there is no relation between land use and soil textural composition. 'Forest', 'Low', and 'High' respectively reach a clay content of, for respectively 0–10, 10–20 and 20–30 cm, 67.3, 80.9 and 73.4; 73.1, 84.7 and 83.9; 74.2, 64.6 and 73%.

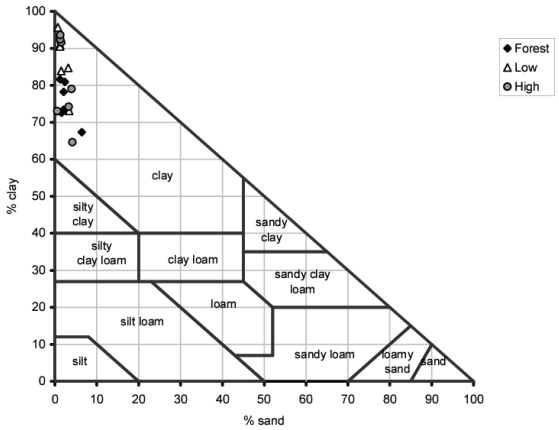

Figure 4.1. Particle size distribution for soils under three land uses. Textural triangle created with *Gerakis and Bear* [1999].

Some of the results of the soil physical and chemical characterisation for the soil at the three sites are presented in Table 4.1. More detailed physicochemical analysis is presented in *Pochet et al.* [2006]. The pH and the total nitrogen content of the soil samples are presented as well. The organic carbon content of the top 10 cm of soil is higher in the forest than at the cultivated sites (Table 4.1). Loss of organic matter is generally thought to lead to a deterioration of soil structure since organic matter compounds bind to charged clay particles to form micro–aggregates of soil particles. Lower organic matter contents characteristically lead to an increase in bulk density and a decrease in water holding capacity, macro porosity, hydraulic conductivity and aggregation.

Fertiliser applications have decreased the pH in the 'Medium' and 'High' soils. A lower pH in soils is generally thought to promote flocculation [*Haynes and Naidu*, 1998]. Higher activity of Al^{3+} and H^{+} promotes compression of the double layer and flocculation of clays. This is further enhanced by the attraction between negatively charged clay surfaces and positively charged Al and Fe hydrous oxides, and bridging between organic matter and clay surfaces [*Haynes and Naidu*, 1998]. Changes in the pH are likely to lead to changes in the soil's hydraulic and chemical properties.

Despite the fertilizer application at the cultivated soils, the total nitrogen content is higher in the forest soil. The effects of the application of fertiliser on soil–N status and soil structure are complex. Applications of fertiliser that contains or forms NH_4^+ has sometimes been shown to have an adverse effect on soil aggregation [*Haynes and Naidu*, 1998] for 'when the monovalent NH_4^+ ion accumulates in soils in large amounts it can become a dominant exchangeable cation favouring dispersion of soil colloids'. Several examples of a reduction in infiltration rate following application of compounds containing NH_4^+ are presented in *Haynes and Naidu* [1998]. In this tropical environment it is thought that ammonium will rapidly be nitrified to nitrate and the dispersing effect of ammonium might thus only be temporary.

The physical and chemical factors that govern soil structural stability and hydraulic conductivity are interrelated through a complex array of interactions. We investigate the effects of a lower organic carbon content, a lowered pH and fertiliser additions on the soil's structural properties and infiltration characteristics. The slaking and runoff that we observed at the most intensively used agricultural field, and possible erosion, may be related to increased dispersion and lower aggregate stability.

	Depth (cm)	Org. C (g kg^{-1})	N (g kg^{-1})	pH H_2O	SAR
Forest	0-10	8.0	6.0	7.1	0.01
	10-20	27.0	2.8	7.0	0.01
	20-30	13.0	1.7	6.3	0.02
Medium	0-10	32.5	3.0	5.5	0.01
	10-20	22.1	2.3	5.5	0.01
	20-30	10.5	1.7	5.9	0.01
High	0-10	25.4	2.4	5.9	0.01
	10-20	21.8	2.1	5.9	0.02
	20-30	14.6	2.0	5.9	0.05

Table 4.1. Soil Physical and chemical properties adapted from *Pochet et al.* [2006].

4.5.1 Aggregate size distribution and stability

The aggregate size distribution shows some marked differences with increasing land use intensification (Figure 4.2). Aggregates are most homogenously distributed in the forest soil. The cultivated soils have a large fraction of aggregates smaller than 1 mm and a considerable lower fraction of aggregates larger than 4.75 mm. A larger fraction of large aggregates may indicate the presence of larger intra–aggregate pore space. The soil from the 'After Fallow' site most closely resembles the Forest soil. The fields that have been under cultivation for a longer time do not show a clear relation between the intensity of land use (e.g. 'Low', 'Medium' and 'High') and aggregate distri-

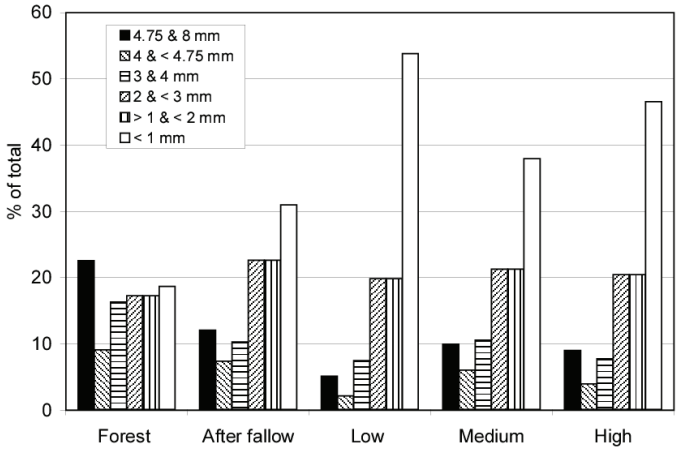

Figure 4.2. Aggregate size distribution under intensifying land use.

bution. It is however clear that land use affects aggregate size distribution: with intensifying land use the number of larger aggregates decrease, while the number of very small aggregates increases.

In comparison, the relation between the intensity of land use and aggregate stability is more pronounced (Figure 4.3). For the natural forest soil, of a total of 10 aggregates (4–4.75 mm) none passed through a 3 mm sieve after more than 100 drops had fallen on the aggregate. The number of drops it took to disintegrate the aggregate so that it passed through the sieve decreased from Forest to After Fallow, and then to the group comprising the Low, Medium and High intensity of land use. However, a note of caution is merrited here. The effects observed may partly be due to the time between the last land–use action, and the sampling of the aggregates.

The mean aggregate stability in the Forest soil differs significantly from the 'After Fallow' site at a p level of 0.05, and significantly differs from the other sites at a p level beyond 0.01. The 'After Fallow' site significantly differs from all the other cultivated soils (beyond a p level of 0.01) while the 'Low', 'Medium', and 'High' sites do not show a significant difference between themselves.

A similar observation can be made looking at the results of the Emmerson aggregate water dispersion test (Figure 4.4). The aggregates in the forest soil did not show any dispersion after 48 hours. The aggregates of the 'After Fallow' site mildly dispersed, while the dispersion was much greater for the 'Low', 'Medium', and 'High' intensity land use. We can conclude that the aggregates distribution is more homogeneous in the natural 'reference soil' of the forest, while the fraction of large aggregates decreases and the fraction of very small aggregates increases with intensifying land use. Therefore, aggregate stability decreases with intensifying land use.

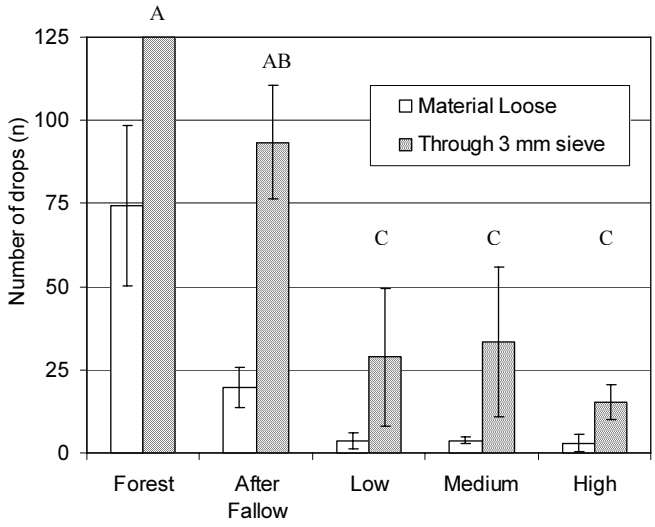

Figure 4.3. Aggregate stability. Water–Drop Test. The number of drops it takes to destroy the aggregate partly (loose material is observed) and total disaggregation of the aggregate through a 3 mm sieve (through 3 mm sieve) with 10 replicates. Error bars indicate the standard deviation around the mean.

These results are in agreement with several other studies on the impact of tillage on aggregates size distribution and stability [*Cerda*, 2000]. The exact cause of the structural breakdown may be related to the loss of organic carbon in the soil, the mechanical impact of tillage, as well as the disrupting effect of tillage on natural biogeochemical processes, and microbial community dynamics. In the topsoil of these soils, anthropogenic factors influence aggregation. Elsewhere, we [*Pochet et al.*, 2006] have shown how the micro–aggregation in this soil probably depends on the interaction between highly charged halloysite, and the high surface area of the ferrihydrite. The pedogenic factors involved in soil aggregation are complex. These results show that for the topsoil of this soil 1) anthropogenic factors negatively affect soil aggregation, and 2) this may be exacerbated through a loss of soil organic carbon.

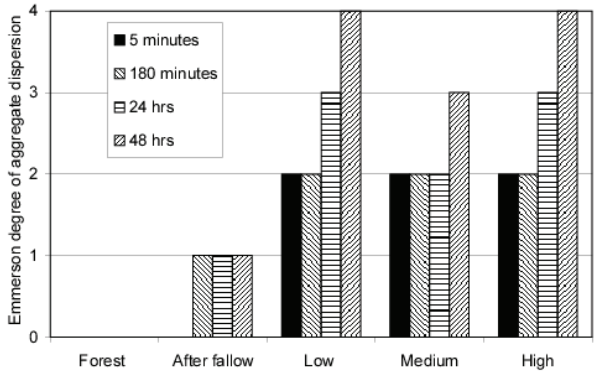

Figure 4.4. Aggregate stability. Emmerson aggregate water dispersion test.

4.5.2 Hydraulic conductivity and characteristic mean pore radius

Using in–situ infiltration experiments we were able to calculate the hydraulic conductivity at the unsaturated heads of -10, -40, -80 and -120 mm for soil depths at 15 and 30 cm. At the 15 cm depth K (-10 mm) ranged between 50 and 300 cm hr^{-1}. Hydraulic conductivities measured at a tension head of -10, -40, -80 and -120 mm at 15 and 30 cm have a similar magnitude and decrease at more negative heads. At 15 cm depth the hydraulic conductivities measured at -40 and -10 mm show no consistent pattern. Hydraulic conductivities measured at -120 and -80 mm show a similar pattern for the range of land uses. They increase with intensifying agricultural practices. It can be observed that the average hydraulic conductivities measured at different heads within the 'High' land use site are most similar comparer to the other land uses (Figure 4.5. The hydraulic conductivities measured at 30 cm show a more homogenous behaviour for the range of land uses over all tension heads. Hydraulic conductivities decrease with more negative heads. No observation on the relation between hydraulic conductivity measured at 30 cm and land use can directly be made.

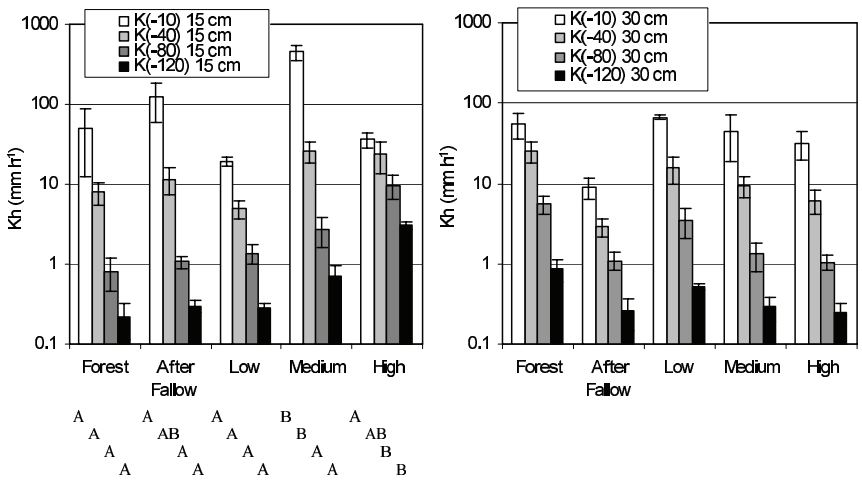

Figure 4.5. Hydraulic conductivity measurements (3) with standard deviation at tensions ranging from -10 to -120 mm for 15 and 30 cm of soil depth under intensifying agricultural land use.

To test if there are significant differences between the different land uses we used the Student's t Test. The differences in the means aggregated over tension heads between different land uses are indicated in Figure 4.5. The differences between conductivities measured at different land uses that are statistical significant differences at the p levels of 0.05 are indicated in Figure

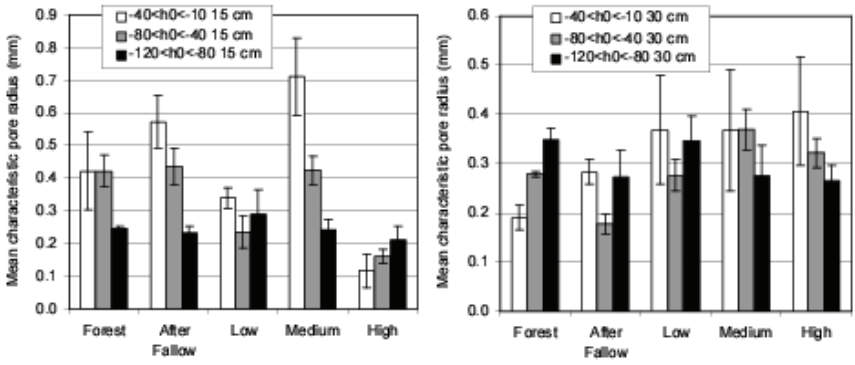

Figure 4.6. Characteristic mean pore radius with standard deviation calculated for 3 suction pairs at 15 and 30 cm soil depth under intensifying agricultural land use.

4.5. It shows that at 15 cm the hydraulic conductiivty at the 'High' landuse site is significantly different from the other land uses at the 0.05 level. This does however not reveal anything about the trend that can be observed at 15 cm with h = -80 mm and -120 mm.

The characteristic microscopic mean pore radii (λ_m) are plotted in Figure 4.6. The λ_m's reflect the slope between the hydraulic conductivities measured at different heads. The pore radii are large and range between 0.1 and 0.75 mm, and even at depth large pore radii where found, indicating the strong possibility of preferential flow.

The λ_m's measured at 15 cm in the 'High' site are, compared to the other land uses, the lowest measured over all heads, and strangely enough, increase with more negative heads. So this would 1) suggest that the pores functioning at the 'High' site are generally smaller than for the other land uses, and 2) that a larger volume of water is transported through smaller pores during the same time unit (α is the slope of K(h)). So, while the conductivities measured at low heads at 15 cm are the highest at the 'High' site (see Figure 4.5), these are in fact obtained by a larger fraction of small aggregates contributing to water transport. Also, the slaking of the soil, and the larger fraction of small aggregates would likely cause less preferential flow. This would make this field more susceptible to flooding and soil erosion.

At 30 cm the λ_m's are quite similar. It is interesting to note that here we observe a reversed pattern; at the 'Forest' site, λ_m increases with more negative heads, while at the 'High' site, λ_m decreases with increasing heads.

Measurements at -10 mm through to -120 mm would correspond, by directly calculating a corresponding pore diameter, again using Laplace's capillary-rise formula, to pores involved in the water movement with a diameter of respectively 3 through to 0.25 mm. The λ_m's we obtained from the slope of K(h) had a similar magnitude and ranged between 0.1 and 0.75

mm. These results are in agreement with our field observations of the slaking of the soil at the 'High' site, and our characterisation of aggregate size distribution and stability, indicating a larger fraction of smaller aggregates with intensifying land–use.

4.6 Discussion

Aggregate stability tests similar to these used here have been used successfully earlier [*Cerda*, 2000]. Nevertheless we concur with *Lebron et al.* [2002] who note that results from laboratory experiments using disturbed soil samples may overpredict the instability of aggregates, which is mainly caused by the destruction of the natural structure of the soil in the sample handling process.

Lebron et al. [2002] showed that the average diameter of pores and aggregates decreases as a function of sodium adsorption ratio (SAR), as well as pH. [*Lebron et al.*, 2002] hypothesized that 'the decrease in the aggregate stability is caused by the weakening of the binding capacity of the cementing agents bonding the domains that form the aggregates'. In our case, the values of SAR for the different soils were very similar and did not seem to be related to aggregate size distribution, or stability.

Considerable differences were observed in the hydraulic conductivities (h = -10 mm) measured at depth (see Figure 4.7 and *Pochet et al.* [2006]). The 'Forest' site shows a gradual decrease in K_{10mm}. The high conductivities in the 'After Fallow' and 'Medium' site could be explained by the recent ploughing of the fields (and no slaking of aggregates). Apart from the measurement at 15 cm, the K_{10mm} measurements at the 'After Fallow' site are all below 20 mm h^{-1}. Measurements of K_{10mm} in the 'Low' and the 'High' site indicate the occurence of preferential flow at depth. It is as yet unclear if this change at depth could have be related to a cultiviation of the ground. Possibly, decaying root channels after the original vegetation was removed may contribute to this preferential flow.

4.7 Conclusion

We can represent our results in the form of an imaginary catena along an intensifying land use gradient. The parentmaterial of all soils is characterised by a heavy clay soil that exhibits micro–aggregation resulting from the interaction between halloysitic clay minerals and ferrihydrite [*Pochet et al.*, 2006], and there is a considerable shrink and swell capacity. The soil in the undisturbed rainforest has the thickest A horizon, a A_h of about 38 cm. The 'Low' and 'High' sites had A_p's of 25 and 30 cm respectively. The horizons of the topsoils from the 'Forest', 'Low' and 'High' sites all, but one, contained

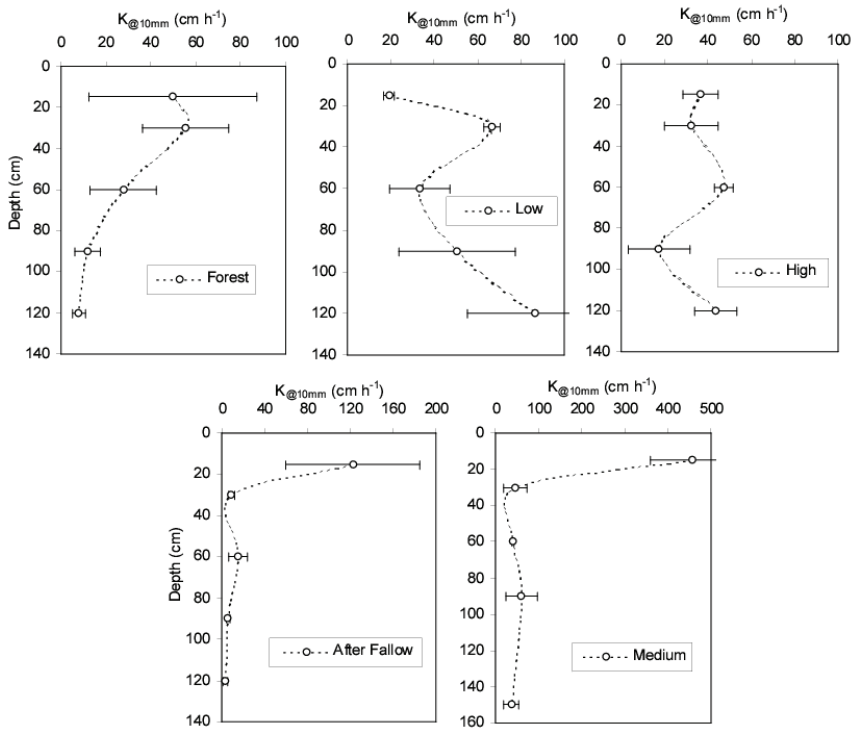

Figure 4.7. K (-10 mm) as measured through the profile of the 'Forest', 'After Fallow', 'Low', 'Medium' and 'High' soils.

many fine roots. The only exception was the A_h of the 'High' site, where only a few fine roots were found.

In comparing between the cultivated soils, the long–term application of fertiliser was proposed by *Haynes and Naidu* [1998] to have a positive effect on the organic matter content of the topsoil through an increased production of plant matter [*Haynes and Naidu*, 1998]. However, this is in contrast to our results presented in Table 4.1. We conclude that an increased intensification will lead to a lower organic matter content, a lower fraction of large aggregates and a decrease in aggregate stability of Tongatapu's soils. This translates into a higher fraction of smaller aggregates and an increase in conductivity at more negative heads.

The continuation of intensive agricultural practices well have negative impact on the structure of cultivated topsoils. Slaking leads to higher conductivities at unsaturated heads, but will diminish the occurence of preferential flow in Tongatapu's soil. This makes these fields more susceptible to runoff and erosion.

Chapter 5

Transpiration of Squash under a Tropical Climate *

Abstract We present the measurement and modelling of transpiration from squash (*Cucurbita maxima Duchesne*) growing in the field under a tropical maritime climate. Measurements were carried out on Tongatapu (175^{o}12'W 21^{o}08'S), a coral atoll located in the Pacific Ocean. Transpiration was determined from heat-pulse measurements of sap flow in the vine stem using the T-max method. Steady–state porometry was used to monitor stomatal conductance (g_S, mm s^{-1}). The data were used to derive parameters for a functional model of conductance that includes response functions for light, air temperature and vapour pressure deficit of the air, and a novel response function for soil moisture. Leaf area development was monitored through the growing season using a point quadrant approach. The maximum leaf area was about 2.7 m^2 per plant and the effective ground area was about 1 m^2 for each plant. Transpiration losses were calculated using a 2-layer big-leaf model in combination with modelled stomatal response and measured leaf area. In general, the sap flow measurements were in good agreement with the calculations of plant water use. Peak water use was between 3 to 5 l per plant per day. Daily transpiration measurements from heat-pulse were used to derive a crop factor, K$_C$, for squash in this tropical maritime climate. The derived seasonal pattern of K$_C$ was similar to the FAO recommended crop factor for squash. However, the growing season was a little shorter. Measured sap flow also revealed periods of short-term drought and leaf fungal disease that reduced the actual transpiration, and there was often a rapid recovery from water stress following rainfall events.

*Adapted from van der Velde, M., S.R. Green, M. Vanclooster and B.E. Clothier, Transpiration of squash under a tropical climate. *Plant and Soil*, 280 (1-2), 323-337, 2006

5.1 Introduction

A detailed estimate of the different components of the waterbalance of an agricultural field of Tongatapu is presented in the following three Chapters. We will first discuss the contribution of plant transpiration to the evapotranspirative losses of the field water balance.

Squash (*Cucurbita maxima Duchesne*) are widely grown in the Kingdom of Tonga. The bulk of the squash ($> 90\%$) is on the main island of Tongatapu (175^o12'W 21^o08'S) and takes advantage of a niche period for the export into the lucrative Japanese market. The Tongan squash 'industry' was first established in about 1987. Squash now accounts for about 40% of the national GDP, and represents about 80 % of GDP derived from agriculture. A rapid increase in cultivated area to support squash production has lead to a 10-fold increase in the import and usage of agricultural chemicals (data from Tonga's Statistical Bureau, Kingdom of Tonga). Concerns have been raised about the possible impact on Tongatapu's freshwater resources and fragile soil environment caused by increased agrichemical use (see Chapter 2). The research described here has been conducted to support a leaching risk assessment of the surface-applied agrichemicals.

Understanding the movement of water from the soil through the plants to the atmosphere is an essential part of understanding and interpreting the dynamics and movement of water through the soil profile. This requires an understanding of the seasonal crop development and its response to changes in soil moisture and climatic conditions. During full crop cover about 80 to 90% of the total evapotranspirational loss from a squash field is expected to be a direct result of plant transpiration [*Allen et al.*, 1998]. Transpiration and soil evaporation will have a large influence on the soil's antecedent moisture content prior to rain and subsequently affect the soil's infiltration response following rain. An accurate determination of crop ET is vital for a leaching risk-assessment.

Several measurement techniques currently exist to monitor transpiration from individual plants using heat to trace sap flow through the plant stem. Popular methods include both heat balance [*Sakuratani*, 1981] and heat-pulse [*Swanson and Whitfield*, 1981] that have been developed following the pioneering work by *Huber* [1932] and *Marshall* [1958]. Heat-pulse has been used successfully in a variety of woody tree species. Examples include walnut, olive, kiwifruit, grape, pear, apricot, and apple (see *Green et al.* [2003]). Heat-pulse has also been used successfully in a number of field crops including soybean, maize, sunflower, corn, and cotton (see *Cohen and Li* [1996]). In many cases the measurements of sap flow have been verified by independent calculations of plant water use using a water balance approach and by lysimetry. Heat-pulse measurements of sap flow in non-woody herbaceous species are still quite rare.

Here we quantify the transpiration of squash grown under a tropical

climate using the T-max heat-pulse method supported by modelling using a simple 2-layer big-leaf model.

5.2 Materials and Methods

5.2.1 Experimental site and agricultural practices

The experiment was carried out on the Vaini Agricultural Research Station, Tongatapu, during the 2003 growing season of squash. The soil is a structured halloysitic clay soil derived from volcanic ash [*Cowie*, 1980]. Two recent ash deposits of about 3 m depth sit on top of an underlying coral layer. The topsoil is very free draining with high values for saturated hydraulic conductivity (> 5 m day^{-1}) extrapolated from measurements done with tension disc infiltrometers [*van der Velde et al.*, 2005]. The dry bulk density of the soil ranged from 0.5 to 1.2 * 10^3 kg m^{-3} and the pH ranged between 6 and 7.2 [*Cowie et al.*, 1991]. Water retention properties [*van der Velde et al.*, 2005] indicated that for the topsoil both high saturated (0.6 m^3 m^{-3}) as well as residual, as measured at 1.5 10^3 kPa, (> 0.2 m^3 m^{-3}) soil moisture contents occur. Low water availability likely leads to soil moisture stress during droughts [*Cowie et al.*, 1991]. *Cowie et al.* [1991] also report, as indicated by low nitrogen and carbon contents, a generally low to medium organic matter content in the top soils. Furthermore, very low topsoil extractable phosphorus values indicate that phosphorus deficiencies may occur [*Cowie et al.*, 1991]. The potential nutrient deficiency is compensated by fertiliser addition.

The experimental site of 0.2 ha was prepared about 4 weeks before planting. Prior to planting, the field was typical of many neighbouring farms, having been in fallow for about 6 months and covered in 1.0-1.5 m tall Guinea grass. The preparation consisted of slashing following by disking and then ploughing to a depth of 0.3 m. The field was then mounded by hand, at a spacing of 1.5 to 1.5 m, and 120 grams of NPK fertiliser was added and mixed into each mound. The mounds had a height of about 10-15 cm and a diameter of about 30 cm. Squash seeds were planted on the 25^{th} of July (day of year, DOY 206) 2003 using a sequence of consecutive rows planted with 2 seeds per mound and the next row planted with 3 seeds per mound. Just before emergence the field was treated with Gramaxone herbicide, at a rate of 2.5 kg ha^{-1}, to kill off any residual weeds.

Many squash plants emerged about 10 days after planting (i.e. DOY 216). However, not all of the seeds were viable and some of the emerging plants showed signs of a fertiliser burn. Therefore some mounds were replanted two weeks after the plants emerged in an effort to increase the final yield. A side dressing of 15 grams of Urea was applied to each mound about 6 weeks after emergence. Hand weeding was carried out during the first two months when it was deemed necessary. A total of 5 fungicide sprays were applied

using a mist sprayer at approximately 2 weekly intervals from mid season until harvest. A range of compounds (e.g. Punch) was used for the control of powdery mildew. The fruits were harvested on the 28th of October (DOY 301). The field was then left in fallow until the following season.

5.2.2 Micrometeorology

A weather station was installed on site to measure incoming global radiation, relative humidity, air temperature, wind speed and rainfall. These data were collected for the purpose of modelling the water balance of the site. Measurements were taken every 15 seconds and half hour averages were stored on a data logger (CR10X, Campbell Scientific, Logan, Utah, USA). Global radiation was measured with a silicon cell pyranometer (SKS 1110, Skye, Powys, UK), air temperature and relative humidity were measured with a HMP45A probe (Vaisala, Helsinki, Finland) wind speed was measured with a sensitive 3-cup anemometer (R30, Vector Instruments, Rhyl, UK), and a tipping-bucket rain gauge (Rain-O-Matic, Pronamic Co., Silkeborg, Denmark) was used to monitor rainfall. These instruments were mounted on a mast in the middle of the field, at a height of about 2 m above the ground. Vapour pressure deficit of the air, D_A, was calculated using the average air temperature and the relative humidity. A 20 W solar panel was used to recharge the 12V power supply.

The data logger also recorded the output from a number of drainage flux meters [*Gee et al.*, 2002; *van der Velde et al.*, 2005] used to monitor water draining through the root-zone soil, as well as the output from several arrays of TDR and soil temperature probes that were installed in the root-zone soil to a depth of 1.2 m. Data from those instruments are presented elsewhere [*Gee et al.*, 2002; *van der Velde et al.*, 2005]. Here we include data from just two of the surface TDR probes (CS616, Campbell Scientific, Logan, Utah, USA) that were inserted vertically into the top 0.3 m of soil and located close to the taproot of a squash plant. These data are used to examine how changes in soil moisture influence transpiration losses from the squash plants.

5.2.3 Transpiration and sap flow

Transpiration from the squash plants was deduced from regular measurements of sap flow in the vine's main stem. We used the so–called 'T-max' heat-pulse method [*Marshall*, 1958; *Cohen et al.*, 1981]. This method is based on a measurement of the time delay, t_M (s), between the firing of a brief pulse of heat and the measurement of the maximum temperature rise at a distance x_D (m) downstream from a linear heat source. The corresponding heat pulse velocity, v (m s^{-1}), is calculated from [*Cohen et al.*, 1981]:

$$v = \sqrt{x_D - 4\kappa t_M}/t_M \tag{5.1}$$

and relies on a measurement of the thermal diffusivity of the sapwood, κ ($m^2\ s^{-1}$). This can be practically determined at a time when negligible sap flow occurs, using the equation [*Cohen et al.*, 1981],

$$\kappa = x_D^2/4t_M \tag{5.2}$$

During the night, sap flow is often very low or ceases so that no convective heat transport takes place and a determination of κ is possible [*Cohen et al.*, 1981]. Here, measurements of t_M between the hours of 0:00 and 4:30 were used to determine the thermal diffusivity.

The heat-pulse measurements were made using specially designed miniature probes similar to those of *Green et al.* [2003]. The heater was made from a length of stainless steel tube containing a central nichrome resistance wire (5 ohm m^{-1}) that was insulated using a fine (28 g) Teflon tube. The temperature sensor comprised a pair of copper-constantan thermo-couples (0.1 mm diameter wire) inside a 1.2 mm diameter Teflon tube filled with epoxy resin. Each set of probes was carefully inserted into the main stem using a jig designed to accurately place the temperature probe at a distance 10 mm downstream from the heater probe. A second reference temperature probe was placed a distance of 30 mm upstream of the heater to account for any drifts in stem temperature.

A datalogger (Model CR10X, Campbell Scientific, Logan, Utah, USA) was used to fire the heaters and record the temperature signals at 1 Hz for a period of 5 minutes following each heat-pulse. The recorded temperature signals were then smoothed and the time for a peak temperature rise (t_M) was calculated using the convoluted least squares procedure of Savitzky and Golay (1964), as described by *Green et al.* [2003]. Measurements were repeated once every half–hour and values of t_M were recorded for later analysis. Each measurement represents the average sap velocity over the sampled cross-section of plant stem and is computed using data from two thermocouples at radial depths of 5 mm and 10 mm.

Three and later (see below) four other squash plants were selected from the middle of the field and each had a single set of heat–pulse probes installed in the main stem about 0.1 m above the ground. These squash plants comprise the first dataset and they were monitored intensively between the 2nd until the 22^{nd} of September (DOY 245 - 265). Later heat pulse probes were reinstalled in four new plants for the period between the 23^{rd} until the 27^{th} of October (DOY 266 - 300). Squash is a non–woody herbaceous species with large xylem vessels that may affect the transmission and measurement of the heat-pulse. We were not able to quantify the magnitude of this effect on the convection of the heat-pulse, but it would appear to be small compared to the effect of the presence of the heater and the temperature probes, and the disruption of the xylem tissue following the insertion of the heat-pulse probes. To correct for this and calculate the corrected heat pulse

velocity V from the raw heat pulse velocity V_H, correction factors (a_0, a_1 and a_2) based on a numerical solution of the two-dimensional heat flow equation were applied to the T-max measurements following *Green et al.* [2003] so that,

$$V = a_0 + a_1 V_H + a_2 V_H^2 \tag{5.3}$$

The correction factors correspond to a wound width of 1.6 mm which equals the diameter of our sensors plus an additional 0.4 mm to allow for extra disruption of the xylem tissue due to probe insertion. The correction factors a_0, a_1 and a_2 respectively equal 7.53, 1.32 and 5.56E-03 (see Table 4 in *Green et al.* [2003]).

The working equation that relates the heat pulse velocity V to the actual sap velocity, J_S, is given by

$$J_S = (k_M F_M + F_L)\, V \tag{5.4}$$

where F_M and F_L are the volume fractions of sapwood and water, respectively. The k_M factor of 0.441 is related to the thermal properties of the sapwood [*Becker and Edwards*, 1999]. A gravimetric moisture content of about 90 % was measured in the 'woody part' of the stem towards the end of the experiments. This translates to a volumetric water content of $F_L = 0.75$ and a sapwood content of $F_W = 0.20$ assuming the bulk density of sapwood is similar to that of cellulose. The remaining air fraction was estimated to be around 5%.

5.2.4 Leaf area development

The seasonal development of leaf area was measured in two ways. Firstly, when the vines were just developing and before canopy closure occurred, the total leaf surface of individual vines was estimated using a simple relationship between the length and width of single leaves combined with a count of total leaf number. Three plants were monitored in this way and they were also equipped with heat-pulse sensors beginning on the 1^{st} of September. These squash plants comprise the first dataset and they were monitored intensively between the 2^{nd} until the 22^{nd} of September 2003 (DOY 245 - 265).

The canopy began to close around the 22^{nd} of September (DOY 265) and individual vines became intertwined. At that stage a determination of the leaf surface of single plants became almost impossible by counting single leaves. So, a point quadrant (PQ) method was subsequently used to track the leaf area development using a 0.15 x 0.15 m sample grid spanning an area of 0.9 x 2.3 m. The PQ measurements were taken bi-weekly between 12^{th} of September (DOY 255) until the 28^{th} of October (DOY 301) using at least five replicates each time. A sharpened steel rod (3 mm diameter) was pushed vertically through the leaf canopy and the total number of leaf

contacts, as well as the number of non-contacts (gaps) was recorded. This information was used to calculate the leaf area index (LAI) of the field and to estimate the fraction of sunlit and shaded leaves. We considered that the canopy consisted of a sunlit and a shaded leaf layer. This assumes a random leaf angle distribution and takes account of the gap fraction determined by the PQ measurements. The sunlit leaf surface was than taken to be twice the LAI of the 'first-contact' leaves using the PQ. The surface area of shaded leaves was determined as the combination of the second, third and fourth leaf contacts.

Heat–pulse probes were then re-installed into four new plants to minimise any long-term disturbance on the functioning of the squash plant and/or the sensitivity of the heat-pulse. These new plants thus comprise the second dataset and they were monitored intensively for the period between the 23rd until the 27^{th} of October (DOY 266 - 300). The total number of leaves on each plant was counted on a number of occasions (i.e. 2^{nd}, 15^{th} and 28^{th} of October, respectively DOY 275, 288 and 301) and the leaf surface area of each plant was estimated by assuming an average leaf size of 200 cm^2. This was done in order to compare the measured daily water use with the vines total leaf surface area. On the last day before harvest a distinction was made between dead leaves, leaves severely affected with powdery mildew (PMD) and those leaves that were only mildly affected with PMD.

5.2.5 Modelling plant transpiration

The FAO approach of *Allen et al.* [1998] is used here to calculate a daily value for crop reference evapotranspiration ET_0 (mm d^{-1}). ET_0 is used as a basis to model plant transpiration and water uptake in a number of integrated soil-plant-atmosphere system models. It is used here in combination with corresponding daily values of sap flow to derive a crop factor KC for squash in this tropical maritime climate. The modelling approach here was used to support the heat-pulse measurements but cannot provide a full validation. The squash develops long vines in the field (> 10 m) and therefore alternative water balance methods using a lysimeter to measure transpiration were not an option.

For half-hourly periods, plant transpiration was modelled using a more prescriptive 2-layer big leaf model [*Green*, 1993]. The total leaf canopy area, A_T (m^2), is divided into a sunlit leaf surface exposed to full sunlight and a complementary surface of leaves in the shade. Crop transpiration is then calculated using the following equation:

$$\lambda E_P = \sum_i a_i \left[\frac{s f_1 R_{N,i} + \rho c_P D_A g_{B,i}}{s + \gamma \left(2 + g_{B,i}/gS, i\right)} \right] + \sum_i b_i \left[\frac{s f_2 R_{N,i} + \rho c_P D_A g_{B,i}}{s + \gamma \left(2 + g_{B,i}/gS, i\right)} \right] \tag{5.5}$$

This equation assumes the squash leaves are hypostomatous and exposed to air with a common ambient saturation deficit. E_P represents the total transpiration flux (kg m^{-2} s^{-1}) from all the leaves and λ is the latent heat of vaporisation of water (J kg^{-1}). The above summation is made over a set of i uniform leaves with a fraction of the total leaf area A_T (m^2) either in the sun, a_i, or in the shade, b_i as determined from the PQ measurements. $R_{N,i}$ is the net radiation flux density (W m^{-2}) of the i-th set of leaves, D_A is the ambient vapour pressure deficit of the air (Pa), s is the slope of the saturation vapour pressure curve (Pa K^{-1}), ρ is the air density (kg m^{-3}), c_P is the specific heat capacity of air (J kg^{-1} K^{-1}) and γ is the psychrometric constant (Pa K^{-1}). Each class of leaves has an associated leaf stomatal and boundary-layer conductance equal to $g_{S,i}$ and $g_{B,i}$ (s m^{-1}), respectively (discussed later, see equation 8).

The net radiation flux on each leaf surface, R_N (W m^{-2}), is set equal to the sum of the amount of global short-wave radiation striking the leaf minus the fraction of light that is reflected upwards from the upper leaf surfaces (a_L=0.2), minus the fraction of light transmitted through the leaves (t_L=0.10). The average net quantum flux for the sunlit leaves is than set equal to half (f_1=0.5) of RN because we have assumed a random leaf angle distribution. Furthermore, the shaded leaves are assumed to capture the remaining 10% (f_2=0.1) of the net radiation flux that gets transmitted through the sunlit leaves. This value of f_2 was determined from the average amount of global PAR radiation actually striking the shaded leaves, as measured by the quantum sensor on our porometer (model Li 1600, Licor, Lincoln, Nebraska, USA).

Transpiration is controlled by leaf stomata that open to a lesser degree under levels of low light and/or increasing temperature and vapour pressure deficit [*Jarvis*, 1976]. Leaf stomata also partially close in dry soils. This action helps reduce evaporative losses and may even curtail productivity. At night the stomata are normally closed and nocturnal transpiration losses are often negligible. A semi-empirical model was used here to describe the leaf response to microclimate conditions [*Winkel and Rambal*, 1990].

Calculated stomatal conductance is used to model transpiration from the squash using Eq 5.6. Stomatal conductance (g_S, mm s^{-1}) is expressed as a function of quantum flux density (Q, umol m^{-2} s^{-1}), and the vapour pressure deficit (D_A, kPa) and the temperature (T_A, ^{o}C) of the air using a general multiplicative function of the form

$$g_S = g_{SM} g(Q) g(D_A) g(T_A) \tag{5.6}$$

Here g_{SM} is the maximum stomatal conductance and each $g()$ represents a partial function for the indicated independent variable ($0 \leq g \leq 1$). In their model, *Winkel and Rambal* [1990] included a 4^{th} term to account for the soil's matric potential, ϕ. Their 4^{th} term was not used here because we

Table 5.1. Model parameters for stomatal conductance derived from porometer measurements.

g_{SM} (mm s^{-1})	11.5
K_1 (μmol m^{-2} s^{-1})	265
K_3 (C^{-1})	0.003
K_2 (kPa^{-1})	0.10 – 0.42
T_0 (C)	30

had no direct measurements of ϕ from which to formulate the g(ϕ) factor. An alternative approach was applied as the soil became drier, as discussed below. The expanded form of the g_S model is written as

$$g_S = g_{SM}(1 - e^{Q/K_1})(1 - K_2 D_A)(1 - K_3(T_A - T_0)^2) \tag{5.7}$$

Average values of air temperature and vapour pressure deficit are used to simulate the combined T_A and D_A effects. The parameter T_0 was set equal to 30 C following *Winkel and Rambal* [1990]. Data to parameterise the model came from leaf measurements taken at hourly intervals on four full days using a steady state porometer (model Li 1600, Licor, Lincoln, Nebraska., USA). Measurements were made on at least six sunlit and six shaded leaves. Model parameters (g_{SM} and K_1-K_3) were derived from the porometer data using the least-squares regression and are given in Table 5.1.

The leaf boundary-layer conductance $g_{B,i}$, is calculated using the empirical relation of *Landsberg and Powell* [1973] that accounts for the mutual sheltering of clustered leaves:

$$g_{B,i} = 0.0172p - 0.56(u/d)^{0.5} \tag{5.8}$$

The parameter d represents the characteristic leaf dimension (0.2 m), and u is the mean wind speed (m s^{-1}) at canopy height (0.3 m). This has been derived using the measured wind speed at 2.0 m and assuming a lognormal wind profile that extends to the top of the leaf canopy [*Campbell and Norman*, 1998]. The parameter p strictly represents the projected foliage density in the direction of the mean wind flow. For simplicity, and because we have no data to show otherwise, the value of p was set equal to the LAI. This approximation is appropriate for a canopy of leaves that have a random leaf angle distribution.

5.3 Results

The daily climate during the experimental period is illustrated in Figure 5.1. Global radiation ranged between 5 and 30 MJ m^{-2} day^{-1}. The rainfall distribution was quite favourable during the growing season in what is normally a quite dry period of the year. The highest rainfall intensity was measured

at 6.6 mm hr^{-1}. The daily maximum air temperature ranged between 21 to 28 C, the daily minimum was between 11 and 22 C, and the maximum vapour pressure deficit ranged between 0.1 and 2.6 kPa. Soil moisture in the top 0.3 m showed considerable change over the season, reflecting inputs from rain and losses due to soil evaporation, plant water uptake and deep drainage (Figure 5.1). There was a period of very dry soil moisture conditions during the middle part of the season that was relieved by a rainfall of about 30 mm following a storm on the 30^{th} of September (DOY 273).

Figure 5.2 illustrates the seasonal development of leaf area for the 'average' squash plant along with the corresponding fraction of sunlit and shaded leaves estimated from the point quadrant measurements. The average ground area for each plant equals the available ground area for each mound (2.25 m^2) divided by the average number of plants per mound (2.33). This gives an effective ground area of about 1 m^2 per plant. Thus, the FAO estimate of crop water use (mm day^{-1}) is numerically equal to the daily water use per plant (L day^{-1}). The maximum leaf area peaked at about 2.7 m^2 per plant, which equates to a maximum LAI of around 2.7 m^2 m^{-2}. The maximum plant height was about 0.4 m. The root system was not measured in detail but it consisted of a well-developed taproot with a dense network of fibrous roots confined mostly to the top 0.3 m of the soil. The total length of these roots is argued to be comparable to vine length [*Weaver and Bruner*, 1927]. The squash also developed several adventitious roots at stem nodes. They remained small (< 70 mm) without any ramification. Their purpose is most likely for anchorage and their role in water uptake is not well documented.

A large fraction of the leaves, almost 75% of the total leaf surface area, were classed as sunlit while the remaining shaded leaves peaked at about 25% (Figure 5.2). The total area of the third and fourth leaf layer represented no more than 8% of the total area of shaded leaves. By the end of the experiment many leaves were affected by powdery mildew (PMD). This fungal disease is one of the main reasons for the decline in leaf area beyond DOY 290. Furthermore, many gaps in the canopy were invaded later in the season by deeply rooted guinea grass and other weeds.

5.3.1 Stomatal conductance

The diurnal pattern of stomatal conductance was measured on four complete days (DOY 262, 281, 290 and 300). The data are presented in Figure 5.3 along with a calculation of g_S obtained from Eq. 5.7. There is a reasonable agreement between measured and modelled conductance for the first three days. However, there was a consistent over-estimation in modelled g_S compared to field measurements on the last day (DOY 300, Figure 5.3) just before harvest. It appears the squash plants were 'stressed' on that day compared to their leaf stomatal functioning earlier in the season. The average leaf-to-air temperature difference exceeded 5 C, while on previous days the

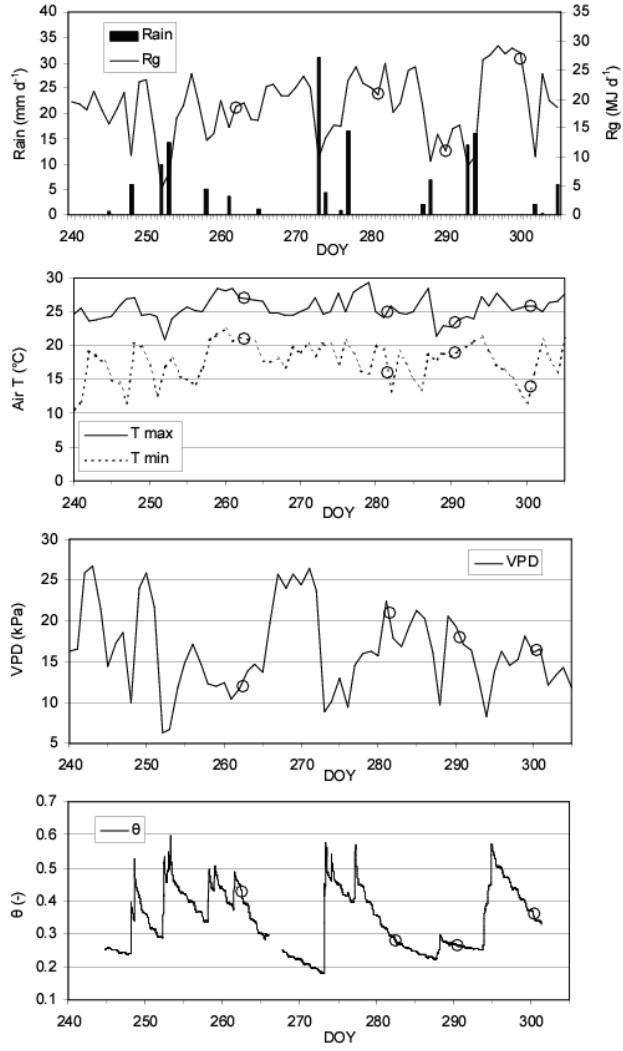

Figure 5.1. Daily rainfall, solar radiation (Rg), minimum (T min) and maximum air temperature (T max), vapour pressured deficit (VPD) and soil moisture content (θ) measured in the top 0.3 m. The circles indicate the days when stomatal conductance measurements were carried out.

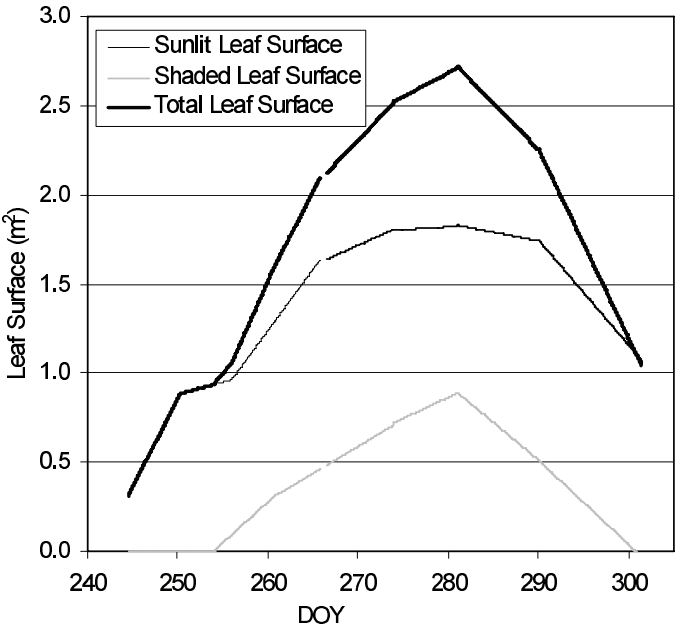

Figure 5.2. Seasonal development of the total leaf surface area of the average squash plant. The fractions of sunlit leaves and the leaves in the shade (grey line) were determined using a point quadrant method (see text for details). The break in the line indicates the time when the heat-pulse equipment was removed from one set of plants and re-installed into another set of plants.

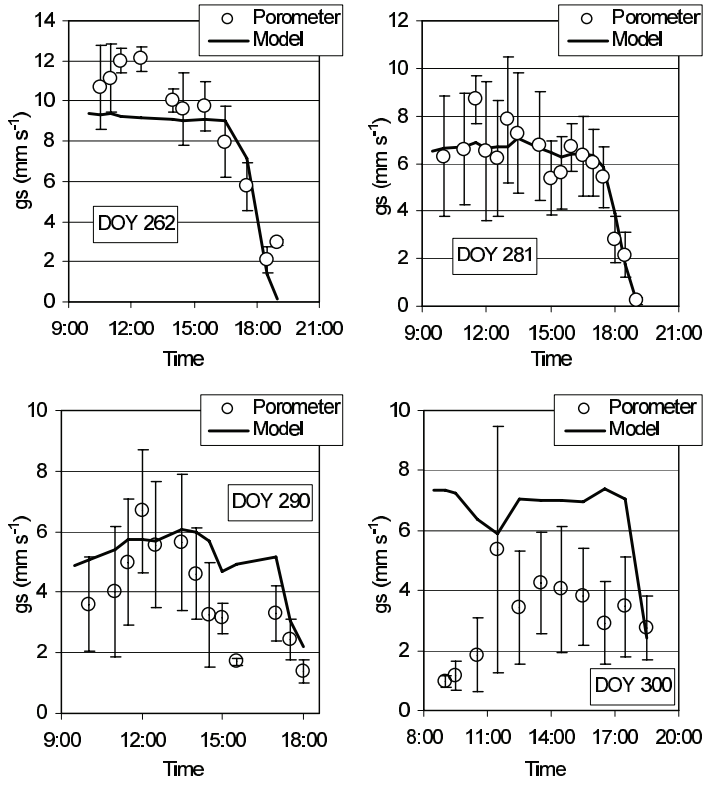

Figure 5.3. The diurnal pattern of stomatal conductance measured on six sunlit leaves (data) and modelled using Eq 5.5. Model parameters are given in Table 5.1. The error bars represent +/- one standard error about the mean.

difference was less than 1.5 C on average, under similar climatic conditions.

Although the leaves were sprayed regularly with conventional fungicides, a large proportion of them had become infected with PMD later in the season. Patches of silver leaf disease and mosaic virus infection were also observed across the field. Aging of the leaves and the occurrence of the fungal diseases clearly changed the leaf stomatal characteristics towards the end of the season. Such changes are not included in the simple model of g_S described by Eq. 5.6. Such a term could be added easily if disease pressure was known *a priori*, or modelled retrospectively.

It should be noted that some wilting of the squash plants was observed many times throughout the growing season. Large leaves on the top layer would become cupped for several hours during the middle part of the day, especially when soil moisture content declined below about 0.3 $m^3\ m^{-3}$. These symptoms of mild water-stress would often be relieved overnight, presumably as the plant tissues were re-hydrated, and would be much less obvious

Table 5.2. K_2 parameter values and moisture content of the top 0.3 m of soil (θ) on days with porometer measurements (see Figure 5.1).

DOY	K_2 (kPa $^{-1}$)	θ (m^3 m^{-3})
262	0.18	0.43
281	0.3	0.28
290	0.34	0.27
300	0.25	0.36

for a number of days following a rainfall event. We are drawn to the conclusion that a water stress probably occurred between DOY 265-273, and maybe at other times too, when the soil got quite dry (Figure 5.1). Unfortunately we have no porometer data to confirm this between DOY 265 to 273. Preliminary modelling with Eq. 5.6 suggested that stomatal conductance was overestimated at those times when the VPD was elevated and the soil moisture content was low. As a result, an additional 'water stress' factor was used to express this stomatal response.

The functional approach used to model g_S assumes leaf stomata to close partially in response to increasing vapour pressure deficit. This is normally modelled by setting the K_2 factor as a constant [*Winkel and Rambal*, 1990]. Here K_2 was modified to enhance the VPD effect, using the following simple adjustment factor that further reduces g_S in response to low soil water contents. The empirical adjustment to K_2 is given by

$$K_2 = \max(K_{2,m}, (\theta_S - \theta)C) \tag{5.9}$$

Here $K_{2,m}$ represents a minimum value of K_2 when soil water is non-limiting, θ represents the average water content of the root-zone soil and θ_S is the corresponding saturated soil water content. C is a constant of 1 with units kPa^{-1}. For the purpose of calculation, θ is defined using the TDR data (0-0.3 m) taken close to the main plant roots (see Figure 5.1); it will also be calculated at a later stage using a soil-plant-atmosphere system model. The value of θ_S is set equal to 0.60, or the highest water content measured and $K_{2,m}$ was set equal to 0.1 kPa^{-1}. K_2 ranges between 0.10 kPa^{-1} at $\theta > 0.5$ and 0.42 kPa^{-1} at the lowest measured water content of $\theta = 0.18$. Table 5.3 gives the values for K_2 on days that the stomatal conductance was measured. So the modelled VPD effect on g_S has a sensitivity that increases from 10 to 42% as the soil dries out. Such a large change in g_S will have a measurable effect on plant water use.

5.3.2 Modelling plant transpiration

Half-hourly averages of the climate variables are used to calculate vine transpiration rates once every 30 minutes. These values are then integrated over the day (midnight to midnight) to calculate a daily total for vine transpiration. The results are shown in Figures 5.4 and 5.5, for the early part of the season, and in Figures 5.6 and 5.7 for the latter part of the season. Calculations of vine transpiration were synchronised with the heat-pulse measurements.

5.3.3 Heat-Pulse measurements of sap flow

Instantaneous rates of sap flow were recorded between the 1^{st} of September (DOY 244) and the 28^{th} of October (DOY 301). Initially the plants were quite small (LAI = 0.5 m^2 m^{-2}) and they had stem diameters of between 13 to 16 mm. However, by the 2^{nd} of October (DOY 275) the plants had grown significantly (LAI = 2.5 m^2 m^{-2}) and the stem diameters had increased to around 22 mm. Stem diameters for three of the plants from the second set of instrumented vines remained fairly constant ($\sim$22 mm diameter) over the measurement period (DOY 266-301). The diameter of the fourth vine grew from 21 to 26 mm over the same period. Changes in stem diameters were measured once a week and any growth was accounted for in the calculation of volumetric sap flow because of the radius-squared relationship between a flux density (i.e. m s^{-1}) and a volume flow (i.e. m^3 s^{-1}).

Generally there was a very good correspondence between measured and modelled transpiration from the developing squash plants during the first set of observations (Figures 5.4 and 5.5). Prior to canopy closure, transpiration rates peaked at about 0.35 l h^{-1}. The vines responded, as expected, to diurnal changes in sunlight, air temperature, humidity, and wind speed. Rainfall during the 18^{th} of September (DOY 261) reduced the sap flow rate from 0.3 down to about 0.1 l h^{-1}. Some nocturnal sap flow was observed during the following night. This probably indicates a recharge of the plant tissue following the small amount of rainfall (i.e. 5 mm) on the previous day. However, we cannot be certain of the magnitude of this nocturnal sap flow. This is because the T–max method has difficulty in resolving such low flows since the solution of Eq. 5.1 becomes non–unique [*Green et al.*, 2003]. For that reason we have only integrated the sap flow between the hours 06:30 and 19:30 in order to calculate total sap flow on a daily basis.

On a daily basis, plant water use increased from about 0.5 l day^{-1} when the plants were small (DOY 245) to about 2.5 l day^{-1} by the time the canopy had closed (DOY 265). Once again, there was a reasonable agreement between measured daily sap flow and the modelled transpiration over this three-week period. Transpiration nearly ceased on the 10^{th} of September (DOY 253) because that was a day with almost continuous rain. On all

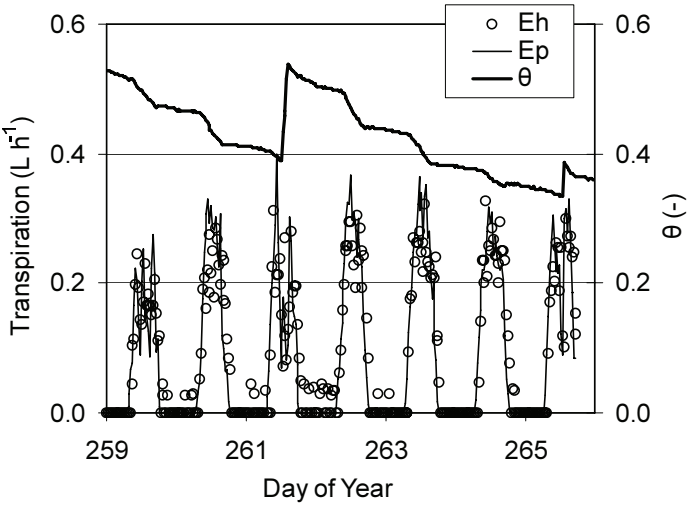

Figure 5.4. The diurnal pattern of crop transpiration as determined from heat-pulse measurements of sap flow, E_h, and calculated using a big-leaf model of plant transpiration, E_p. These measurements are the first set of plants at the start of the growing season. Θ represents the root-zone water content in the top 0.3 m of soil.

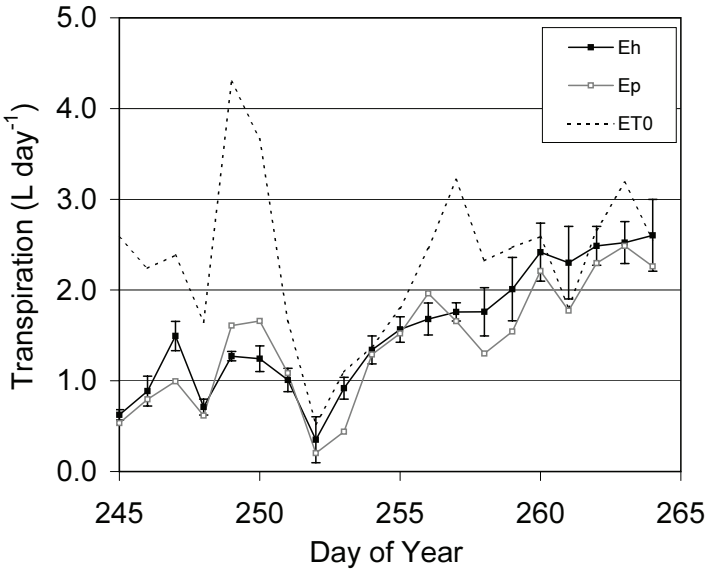

Figure 5.5. The daily pattern of vine water use as determined from heat-pulse measurements of sap flow, E_h, and calculated using a big-leaf model of plant transpiration, E_p. The error bars represent the standard deviation of sap flow in the three plants instrumented with heat-pulse at the start of the season. The FAO reference crop ET is shown by the broken line.

Table 5.3. Stem diameter, leaf surface and percentage of total leaves infected with PMD and the total water use of the second set of squash plants installed with heat pulse (DOY = Day of Year).

	DOY 275		DOY 288		DOY 301				
	Stem Diam. (mm)	Tot. Leaf (m^2)	Tot. Leaf (m^2)	PMD (%)	Tot. Leaf (m^2)	Green Leaf (m^2)	Dead (%)	PMD (%)	Tot. Water Use (l)
P1	21–26	5	3.8	81	5	1	61	20	120
P2	20	2.7	1.7	89	2.1	0.1	87	9	85
P3	22	2.2	3	64	3.3	0.7	58	21	115
P4	20	2.7	2.7	83	4.8	0.6	73	13	60

days the actual crop water use was much less than the potential evaporative demand given by ET_0. However, this difference was progressively reduced as the canopy leaf area increased and a larger fraction of the total evaporative losses was partitioned into transpiration from the squash plants. Soil evaporative losses on a daily basis accounted for between 10 and 30 % of the daily total evaporation and transpiration from the field at full crop cover.

The heat–pulse probes were re-installed into four different plants on the 22^{nd} of September (DOY 265). By that stage the individual vines had become intertwined and the LAI had increased to about 2.0 m^2 m^{-2} (Figure 5.2). Sap flow was monitored every half an hour from the 22^{nd} September until harvest on the 28th of October (DOY 301). The data from this period are shown in Figures 5.6 and 5.7. Individually, these new plants had quite different leaf areas (Table 5.3) and that difference produced a wide range in the measured plant water use. The plant with the largest leaf area (P1) had the largest sap flow. Generally the difference in water use between the plants could be explained by the difference in total leaf area (Table 5.4).

Two of the vines (P2 and P4) were more severely affected by PMD fungal disease. This resulted in a decline in transpiration rate compared to the other plants coinciding with the observed progression of PMD infection (respectively 89% and 83% on DOY 281 for P2 and P4). P1 had a similar percentage of leaves affected but had a larger remaining green leaf surface. By the end of the season P2 and P4 consequently had a greater fraction of dead leaves (respectively 87% and 73%).

Nonetheless, average sap flow in the four heat-pulse plants compared quite favourably with plant transpiration calculated via the big–leaf model. The overall resemblance between measurements and model is generally good for both the diurnal pattern (Figure 5.6) as well as the daily total (Figure 5.7). A linear regression between the daily measured and modelled totals yielded a $r^2 > 0.8$ and 0.6 for respectively the first and second monitoring period. This result gives us added confidence in the modelling procedure as well as the measurement of sap flow by the T–max method.

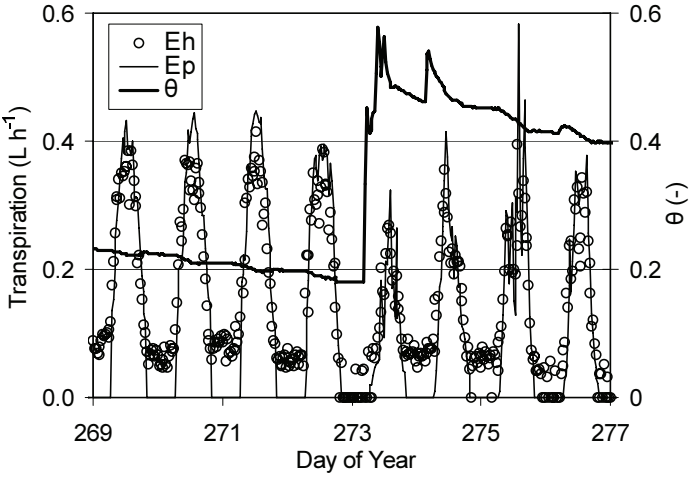

Figure 5.6. The diurnal pattern of crop transpiration as determined from heat-pulse measurements of sap flow, E_h, and calculated using a big-leaf model of plant transpiration, E_p. Measurements are averaged and from the second set of four plants later in the growing season. θ represents the root–zone water content in the top 0.3 m of soil.

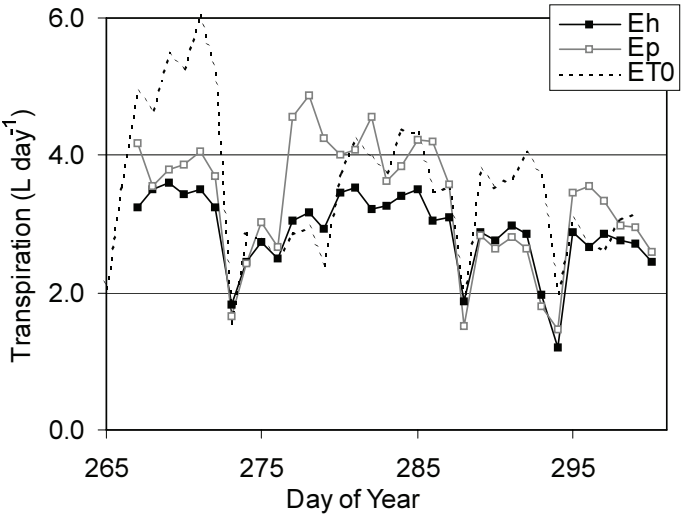

Figure 5.7. The daily pattern of vine water use as determined from heat-pulse measurements of sap flow, Eh, and calculated using a big-leaf model of plant transpiration, Ep. Measurements are averaged and from the second set of plants later in the growing season. The FAO reference crop evapotranspiration is shown by the broken line.

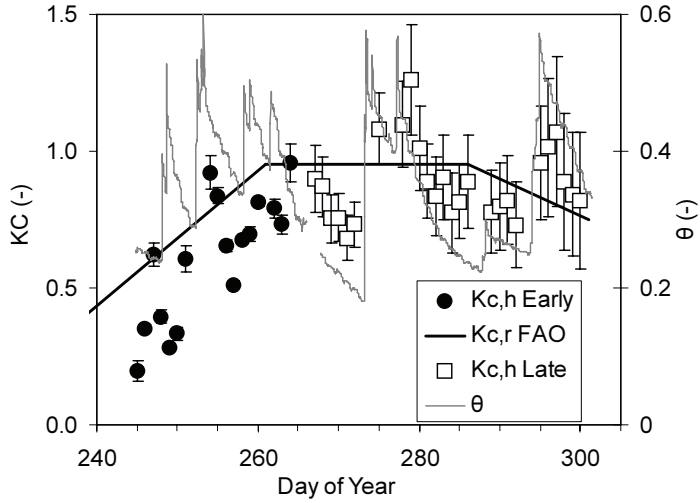

Figure 5.8. The crop factor for transpiration by squash in a tropical maritime climate as determined from heat-pulse measurements of sap flow, $K_{C,H}$. The error bars represent +/- one standard error about the mean. $K_{C,R}$ is the FAO recommended crop factor for squash.

The accuracy of the modelled water use will depend on how good the estimate of leaf area is. Here we obtained good agreement between the average sap flow from the few vines we sampled and the calculation derived for an average plant. Such good agreement is encouraging given the wide range of plant surface areas. With increasing confidence in both measurement and modelling methods, the final task is to calculate a crop factor, K_C, that relates the transpiration to the prevailing microclimate. Integrating the sap flow on rain-free days and dividing the total by the corresponding daily value of ET_0 achieved this task. The results of this calculation are shown in Figure 5.8 and they are compared against the FAO recommended reference crop ET for squash.

During the rapid growth phase of the squash (DOY 244 to 265) the crop factor calculated from sap flow, $K_{C,H}$, followed the expected trend of increasing as the leaf area developed. There was only a small variation (CV $< 15\%$) between the three plants on any single day because of the similar leaf areas of the three plants. However, the temporal pattern of $K_{C,H}$ was quite scattered from day to day. Once the heat-pulse sensors were re-installed into the other four plants there was a big jump in standard error of $K_{C,H}$. This was mainly because of the large difference in leaf surface area of the individual squash plants. The seasonal pattern of $K_{C,H}$ was similar to the FAO recommended crop factor for squash [*Allen et al.*, 1998]. However, the total length of the growing season was a little shorter, being just 95 d in this tropical maritime climate compared to 100 d in the Mediterranean and

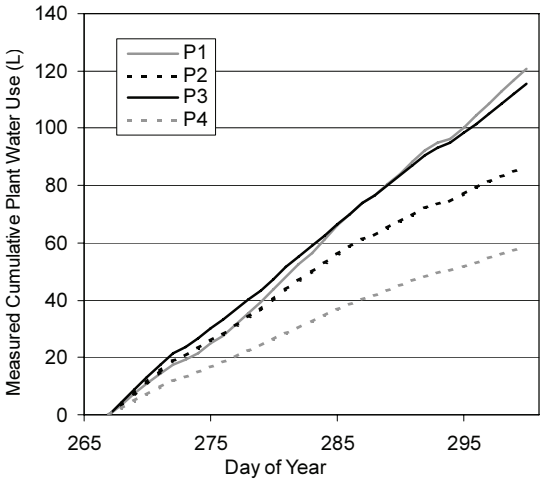

Figure 5.9. Measured cumulative water use (L) of the second set of four plants installed with heat-pulse. P2 and P4 were most severely affected with powdery milldew.

120 d in Europe. The middle growth stage appears to be a little shorter on Tongatapu.

Beyond canopy closure (around DOY 260) there were three distinct periods where $K_{C,H}$ declined. Two of these periods (beginning around DOY 266 and again around 275) are likely related to water stress because the soil had already become quite dry ($\theta < 0.30\%$). The third period of decline, just before harvest, was due to the emergence of PMD and has already been discussed. There were also a few days, e.g., around the 22^{nd} to the 25^{th} of October (DOY 295-297) when $K_{C,H}$ was relatively high. This could be associated with a luxury consumption of water related to the re-hydration of fruits and plant tissue when rain occurred after a long period of drought.

The rainfall distribution of this season was quite favourable and resulted in good yields across the whole island, albeit with low economic returns [*Fonua*, 2003]. Some previous years have returned much lower yields because of prolonged droughts. Water stress and quite variable yields are commonplace in the Kingdom of Tonga where rain-fed agriculture is the norm and where rainfall during the growing season remains unreliable and erratic. Some farmers are considering irrigation to help overcome periods of drought. Information presented here should be beneficial to them in determining crop water needs and in developing sustainable irrigation practices.

5.4 Discussion

Overall, transpiration losses from the squash were satisfactorily quantified using the presented measurement and modelling approach. However, an al-

ternative measurement of transpiration would be needed to provide a full validation of the use of this heat–pulse technique in non-woody species. Yet, there are several possible explanations for observed differences between measured sap flow and modelled plant water use. In addition to a tap–root that joins the main stem, squash also have several weakly developed adventitious roots at stem nodes. These roots have no ramification and are no longer than 70 mm. However, their role in water uptake is not well understood. Any water uptake by adventitious roots would not be measured with the current heat-pulse installation as these roots do not join the main stem where the heat-pulse equipment is installed. It is possible that the adventitious roots do contribute to transpiration, perhaps when the soil surface is re-wet following a rainfall event. While re-hydration of plant tissue and night-time transpiration would be detected by the heat-pulse, such sap flow would not be calculated with the big-leaf model because Eq. 5.7 sets g_S equal to zero at night time. The $g(Q)$ function could easily be changed so that $g_S > 0$ at night (Q=0), but we have not done so here.

Over the course of the season, and during the day, squash leaves change position and orientation. Such changes can alter the distribution of diffuse (scattered) light within the canopy soon after closure. Initially, neighbouring plants on the same mound developed in such a manner that they avoided each other. The vine tendrils and supporting leaves grew into the gaps, generally in opposite directions from their neighbouring vines thereby optimising light interception by randomly arranging their leaves. Competition between plants from different mounds starts as soon as the canopy begins to close. Subtle changes in the leaf light environment could yield a more horizontal distribution of leaf surfaces that would intercept proportionally more light. In contrast, a mid-day cupping of the leaves in response to a mild water-stress would act to reduce the radiant load on the leaves. Such changes in leaf architecture as the canopy closes, or as the leaves subsequently broke down because of PMD infection, have not been taken into account in the model, but they might have been detected by the heat-pulse. This is especially true in the case of the PMD were the plant P2 showed a 50% drop in sap flow and a 50% reduction in green leaf area. On three consecutive days (4^{th} until 6^{th} of October, DOY 277–279) modelled plant water–use was much larger than measured sap flow. It is possible that rain on the preceding day caused a lower than expected sap flow especially if the leaves were either wet or damaged by a fungal problem.

The T–max measurements in small stems are most sensitive to errors in stem radius (error increases as the radius-squared) and at low flows they are also very sensitive to the value of κ. For example, if κ is too big or the measured value of t_M is excessive then non-real values of v can be calculated using Eq. 5.1. Conversely, if either κ or t_M is too small then the calculated value of v could exceed the true value. In that case one would measure an apparent flow that is bigger than the real flow. The good news here is that

providing κ is reasonable in the first place, then it has only a small influence ($< 5\%$) on measured flow rates typical during the daytime (i.e. $J_S > 0.02$ mm s^{-1}). Here, for simplicity, a constant value of κ was assumed throughout the season. This was determined once, at the start of the experiments, when the average night-time value of t_M were consistently around 130 s. This corresponds to a measured value of $\kappa = 1.9$ m^2 s^{-1} and is similar to the theoretical value reported by *Green et al.* [2003] for this probe spacing and stem moisture content. We note that there was a general drift upwards in nocturnal values of t_M as the season progressed. A lower value of κ is consistent with a gradual drying out of the sapwood as the stem material aged. We cannot discount the possibility of nocturnal sap flow and this increases the difficulty of calculating κ using Eq. 5.2.

Indeed the apparent flow at night is a possible indication of either nocturnal transpiration or a re–hydration of plant tissues (Figure 5.6). On a number of occasions the porometer was used to measure g_S close to dusk, but not during the night. Porometer data around sunset suggested reasonable closure of the stomata so transpiration losses were probably quite small. As noted earlier, the T–max has a measurement difficulty in resolving very low flows and so we cannot be too sure of the actual magnitude of the sap flow measured at night. In hindsight, the use of slightly wider probes would have theoretically improved the low-flow resolution [*Green et al.*, 2003]. However, a wider spacing would also have decreased the signal-to-noise ratio because a lower temperature rise would be recorded at a greater distance from the heater, and there would also have been a greater opportunity for temperature drifts because of increased t_M values [*Green et al.*, 2003].

5.5 Conclusion

The aim of this study was to measure and model transpiration of *Cucurbita maxima* under tropical maritime conditions. A specific objective was to measure sapflow using heat-pulse that is novel because successful measurements in non–woody species are still quite rare. Steady state porometry was used to develop a sub–model of stomatal conductance that was included in a two-layer big-leaf model of transpiration. The resemblance of measurements and model adds to our confidence that the T-max method can be used successfully in squash and other non–woody species. Measured sap flow and the derived crop factor revealed periods of short-term water-stress and leaf fungal disease that reduced the actual transpiration losses. They also hinted at a rapid recovery from water stress following rainfall events.

Many factors influence crop transpiration in the field and we are aware that any integration of these factors should be done with caution. The results help reinforce our contention that a measurement and modelling dualism is a good approach to better understand crop–water relations. More practi-

cally, by quantifying the transpiration rates of squash we can provide new information to engineers and farmers who are seeking to develop irrigation practices for squash on Tongatapu. Such information is essential to optimise pumping strategies, a requisite to minimise salt–water intrusion and reduce the environmental impact of emerging irrigation practises on the freshwater aquifer and the fragile soil environment.

Chapter 6

Evaluation of Drainage from Passive Suction and Non-suction Flux Meters in a Volcanic Clay Soil under Tropical Conditions *

Abstract Root zone drainage measurements are needed to improve fertilizer management in areas where agriculture may be impacting groundwater supplies. We present results of field-tests where drainage was measured with two types of suction (resolution of 0.16 mm tip^{-1} and 1.6 mm tip^{-1}) and a non-suction (resolution of 0.22 mm tip^{-1}) water-flux meter (WFM). The soil was a micro-structured weathered volcanic ash located on a coral atoll in the Kingdom of Tonga subject to intense rainfall. The objectives were to evaluate water flux measurements by comparing them with 1) simple water balance estimates of cumulative fluxes; 2) cumulative fluxes deduced from soil moisture content changes and; 3) simulated fluxes using HYDRUS-1D. Soil hydraulic properties were obtained at 5 soil depths. During the 60-day evaluation period rainfall totalled 340 mm. The WFMs were installed in duplicate using disturbed soil. The consistency of the shape of the drainage curves measured with the WFMs, those derived from soil moisture changes, and those obtained with modelling lead us to conclude that soil disturbance during WFM installation did not severely influence measurements. This is attributed to the strong micro-aggregation and disturbance introduced by ploughing. Water balance and HYRDUS model estimates of drainage corresponded well with the measurement by non-suction WFMs. Suction-WFMs overestimated drainage possibly due to flow convergence created by wick and divergence barrier lengths being not properly sized for the observed flow conditions. After the evaluation period some of the WFMs failed to respond. Nevertheless, flux meters are seen as promising tools to provide remote and continuous measurement of root zone drainage.

*Adapted from van der Velde, M., S.R. Green, G.W. Gee, M. Vanclooster and B.E. Clothier, Evaluation of drainage from passive suction and non-suction flux meters in a volcanic clay soil under tropical conditions. *Vadose Zone Journal*, 4, 1201-1209, 2005.

6.1 Introduction

Detailed estimates of the water flux in a field soil are needed to understand the fate of water and solutes in soil. Water fluxes can be estimated using either indirect or direct methods. Indirect methods include the use of water balance calculations based on changes in measured soil water potential or soil water content, and the use of numerical modelling that requires soil physical and hydraulic properties as well as appropriate crop and climate data. Direct methods introduce an obstruction in the soil that is designed to intercept, to measure, and often to sample the drainage water. A distinction can be made between instruments without a suction and those that introduce a suction to the surrounding soil. The greatest advantage of these devices is the possibility of simultaneously measuring the flux of water and solute in the field. Disadvantages include a certain level of disturbance when the instrument is installed and the limited soil volume that is sampled by the device.

The creation of a good contact between the soil and the top of the instrument is critical. Zero–tension lysimeters [*Russel and Ewel*, 1985; *Zhu et al.*, 2002] collect drainage water only when the soil directly above them is saturated. Instruments that apply a tension or suction to the soil have the potential to more accurately simulate matric potentials in the soil. The suction is either controlled by the generation of a vacuum [*Montgomery et al.*, 1987; *van Grinsven et al.*, 1988; *Brye et al.*, 1999; *Barzegar et al.*, 2004; *Kosugi and Katsuyama*, 2004] or it is set by the height of a hanging water-column introduced by a wick in contact with the soil [*Holder et al.*, 1991; *Boll et al.*, 1992; *Knutson and Selker*, 1994; *Brandidohrn et al.*, 1997; *Louie et al.*, 2000; *Gee et al.*, 2002]. *Brye et al.* [1999] developed the 'equilibrium tension lysimeter' where suction was manually adjusted according to the matric potential of adjacent soil directly above the lysimeter. *Masarik et al.* [2004] developed an automated version of the equilibrium tension lysimeter of [*Brye et al.*, 1999]. *Kosugi and Katsuyama* [2004] developed an alternative lysimeter where the period of suction was controlled directly using the difference in matric potential between the natural and the sampled soil profile. Several field studies have been carried out using the above described instruments. *Boll et al.* [1997] for example used grid pan samplers to quantify the spatial distribution of water and solute flux with a temporal resolution dependent on the time of sampling.

The number of field studies reporting the direct measurement of water flux with a high temporal resolution is still quite limited. To our knowledge, no studies have reported the performance of different types of WFMs in micro-structured and weathered volcanic free-draining tropical clay soils. Furthermore, given the practical nature of our research, we sought to test the reliability and robustness of a low cost system that could operate without the need of maintenance and without much human interference. The harsh

tropical conditions and a free-draining clay soil posed specific challenges to the devices. The principal objective was to evaluate the performance of the WFMs and this was achieved by comparing the water flux measurements with 1) potential drainage estimated from a simple water balance, 2) soil moisture content changes derived from calibrated soil moisture measurements and 3) 1D modelling of water movement using measured soil properties.

6.2 Materials and Methods

The experiments were carried out on the island of Tongatapu (175^{o}12'W 21^{o}08'S), the main island of the Kingdom of Tonga, located in the South Pacific Ocean. The island is a flat raised coral atoll with a highest elevation of 60 m above sea level [*Furness and Helu*, 1993]. The limestone base of the island consists of permeable limestone that has a saturated hydraulic conductivity of $\sim$0.015 m s^{-1} [*Hunt*, 1979]. Groundwater is present as freshwater lenses that float on the saltwater in the limestone aquifer. Tongatapu has no surface water. The groundwater is interconnected to a relatively enclosed sea-waree lagoon and a mix of ground and sea water can be seen seeping into the lagoon at low tide. Soil depth on the island generally decreases from 6 m in the west to 0.5 m in the east [*Cowie et al.*, 1991]. The soil sits directly on top of the permeable limestone. Any water and solutes that have passed through the soil, are likely to flow downwards through the limestone towards the freshwater lenses.

6.2.1 Experimental Site

An experimental site was established at the Vaini Agricultural Research Station during the 2002 growing season of squash. A meteorological station was installed at the experimental site to measure global radiation, relative humidity, air temperature, wind speed and rainfall. Incoming global radiation was measured with a silicon-cell pyranometer (Skye, SKS 1110). Air temperature and relative humidity were measured with a Vaisala, HMP45A probe. Wind speed was measured with a sensitive 3-cup anemometer (Vector Instruments, R30), and a tipping-spoon rain gauge (Pronamic, Rain-O-Matic) was used to monitor rainfall. Data were recorded every 15 seconds and half hour averages were stored on a data logger (Campbell Scientific, CR10X). The instruments were mounted on a mast in the middle of the field, at a height of 2 m above the ground. Daily meteorological data were used to calculate the FAO reference crop evaportranspiration, ET_0 following [*Allen et al.*, 1998].

6.2.2 Soil

The soil on the island was classified as typic argiudoll, very-fine, halloysitic and isohyperthermic [*Cowie et al.*, 1991]. Halloysite is the dominant clay mineral ($> 90\%$). Two characteristic layers, each associated with different volcanic deposits can generally be identified on the island. Often a shallow (< 50 mm) buried soil can be found between those layers. Perched water tables may occur at the transition between the young and old ash deposits. The soil at the experimental station is part of the Vaini soil series [*Cowie et al.*, 1991]. Total soil depth was 2.8 m. Groundwater was found at a depth of about 20 meters in the limestone aquifer. The soil surface was flat and no surface ponding or runoff had been observed. The transition between the younger and the older clay layer occurs at around 90 to 100 cm [*Cowie*, 1980]. The soil had a clay content from about 70% at the top of the profile, to 90% at 1 m depth. Soft, weathered lapilli occur throughout the whole soil profile. The dry bulk density of the soil ranged from 0.5 to 1.2 * 10^3 kg m^{-3} and the pH ranged between 6 and 7.2. The organic carbon content in the top 18 cm was about 3.4% and decreased to 0.8% at a depth of 28 to 43 cm [*Cowie et al.*, 1991]. A strong micro-aggregation was observed in the soil and this was explained by interactions of the halloysitic clay minerals, organic components and iron oxides [*Trangmar*, 1992]. A large observation pit was excavated in a representative area of the field. Water retention was determined at 15-, 30- (in triplicate), 60-, 90- and 120- cm depths (in duplicate). Undisturbed cores (20 mm height and 50 mm diameter) were collected to measure water retention at 0.1-, 0.5-, 3.0-, 6.0- kPa using Haines' apparatus and at 113.0 kPa using a pressure plate. Bulk soil obtained at the same depth was used for the determination of water retention at 1513 kPa using a pressure plate. The *van Genuchten* [1980] parameters associated with the soil's water retention properties are presented in Table 6.1.

Table 6.1. *van Genuchten* [1980] parameters and saturated hydraulic conductivity for 5 soil depths.

	van Genuchten [1980] parameters					
Soil Depth (cm)	θ_s (m^3m^{-3})	θ_r (m^3m^{-3})	α (cm^{-1})	m (-)	n (-)	K_s (cm h^{-1})
15	0.58	0.45	0.05	0.31	1.450	28
30	0.53	0.43	0.05	0.33	1.496	2.6
60	0.67	0.60	0.05	0.35	1.538	1.5
90	0.80	0.60	0.04	0.32	1.466	0.9
120	0.61	0.53	0.10	0.37	1.596	0.6

The following strategy was chosen to fit the curves. Saturated and residual water content were set so that they reflect the measured water content at respectively 10^{-1} kPa and 1.5 * 10^3 kPa. The alpha and n parameters were obtained by means of least square regression (m = 1-1/n).

The soil retains a lot of water even at very low soil matric potentials.

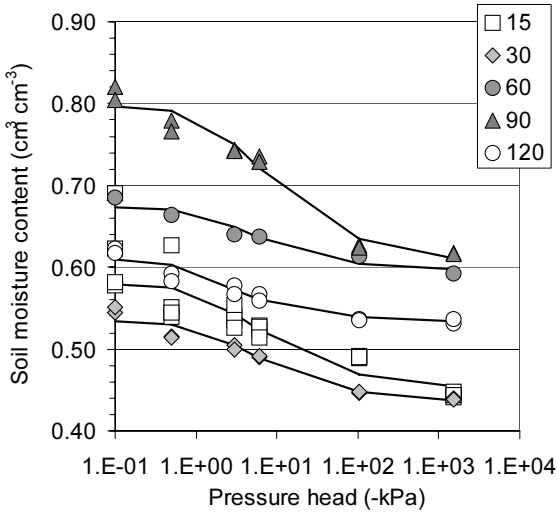

Figure 6.1. Measured water retention characteristics and the corresponding van Genuchten (1980) curves obtained for five soil depths at the field site.

The values of the parameters are similar to the water retention properties determined in three other profiles at the island (data not shown) and as measured by *Cowie* [1980]; *Cowie et al.* [1991]. This lead us to consider that, for this exercise, the values of the parameters determined for five layers were representative for the soil above the WFMs. Hydraulic conductivity (measured at a head of -10 mm) was measured in triplicate using a tension disc infiltrometer at the same depths in the observation pit. These were linearly extrapolated to obtain a value of the soil's saturated hydraulic conductivity (K_{sat}). The values for the K_{sat} indicate that water transport through the structured clay is rapid. Similar soil hydraulic properties have been observed in other soils from volcanic origin. *Dorel et al.* [2000] described a volcanic soil hydrodynamically behaving as a sand at matric potentials $>$ -300 kPa and as clay below -1550 kPa. The micro–aggregation associated with this effect is illustrated by *Miyamoto et al.* [2003]. Micro-aggregated clay soils derived from volcanic ash exhibiting this behavior are commonly referred to as pseudo-silts or pseudo-sands.

6.2.3 Water flux meters design and installation

A schematic figure of the WFMs is shown in Figure 6.2. All WFMs were installed with the top of the funnel at a depth of 1 meter (Figure 6.2, vertical exaggeration of funnel height). We used two types of passive–capillary wick [*Gee et al.*, 2002, 2003] and one type of non–suction WFM. The WFMs were designed to minimize divergence of flow. Measurements were carried out in duplicate. Installation of the WFMs should ideally be done by inserting

the WFMs in the ground and placing an undisturbed soil column on top of the device. Unfortunately the tillage practices and the reworked heavy clay soil did not allow for an easy insertion of the tube into the soil to create an undisturbed core. Therefore the soil above the WFMs was refilled and repacked to a similar bulk density as the surrounding field soil following tillage. Given the micro-aggregation of the soil and the principal objective of the study, the evaluation of the WFMs, the interpretation of the WFM measurements is believed to remain sound in these conditions. Two soil pits close to the observation pit were excavated, and a WFM of each type was installed into each pit. The two pits were repacked and the surface levelled with respect to the surrounding soil surface. The micro-structure of the soil in the flux meter resembled that of the surrounding tilled soil. After the first rain event, a minor depression above one hole was levelled off. The WFMs are equipped with a pipe that extends from the top of the funnel to minimize divergence. *Gee et al.* [2004] showed that a WFM in a clay soil should perform well at high fluxes while at low fluxes divergence may occur. The collection efficiency increased with increasing height of the pipe. The suction WFMs had a collection area of 314 cm^2 and the non-suction WFMs had a collection area of 779 cm^2. Because of the larger collection area the pipe height could be lower [*Gee et al.*, 2004]. Below each instrument a cavity was excavated and re-filled with sand to accommodate drainage water from the devices.

The suction WFMs consisted of the overlying pipe that rested upon a funnel filled with soil. The suction WFMs were each equipped with two prepared [*Knutson et al.*, 1993] inter-twined wicks (Pepperell Braiding Company, no. 1381) each with a diameter of 12.5 mm, to control the suction. The wick has a Ksat of 1168 cm hr^{-1}. The inside area of the funnel cone is occupied by carefully separated and aligned fibreglass wick material of 10 cm length. The remaining 50 cm of the wick goes through the funnel neck downwards where it ends just above the measurement device. The advantage of using a wick instead of a vacuum to create suction is that no additional equipment or energy is used for operation of the measurement. Diatomaceaous earth was placed in the bottom of the funnel, above the wick strands, to prevent soil filtering into the device. Two types of suction WFMs were of similar design but used different techniques to measure the drainage water flux. The first type described by *Gee et al.* [2003] is referred here as the tipping bucket-water flux meter (T-WFM). This device uses a mini-tipping bucket (Rain-O-Matic, Pronamic) to measure the flow out of the bottom of the wick. The tipping bucket was calibrated at 5.0 ml tip^{-1} which equates to a resolution of 0.16 mm tip^{-1}. The second type of suction-WFM is commercially available as a Gee Passive Capillary Lysimeter or Drain Gauge (Decagon Devices). We will refer to this device as being the capacitance-water flux meter (C-WFM). Drainage water is accumulated in a siphon chamber that automatically empties at a volume that is pre-

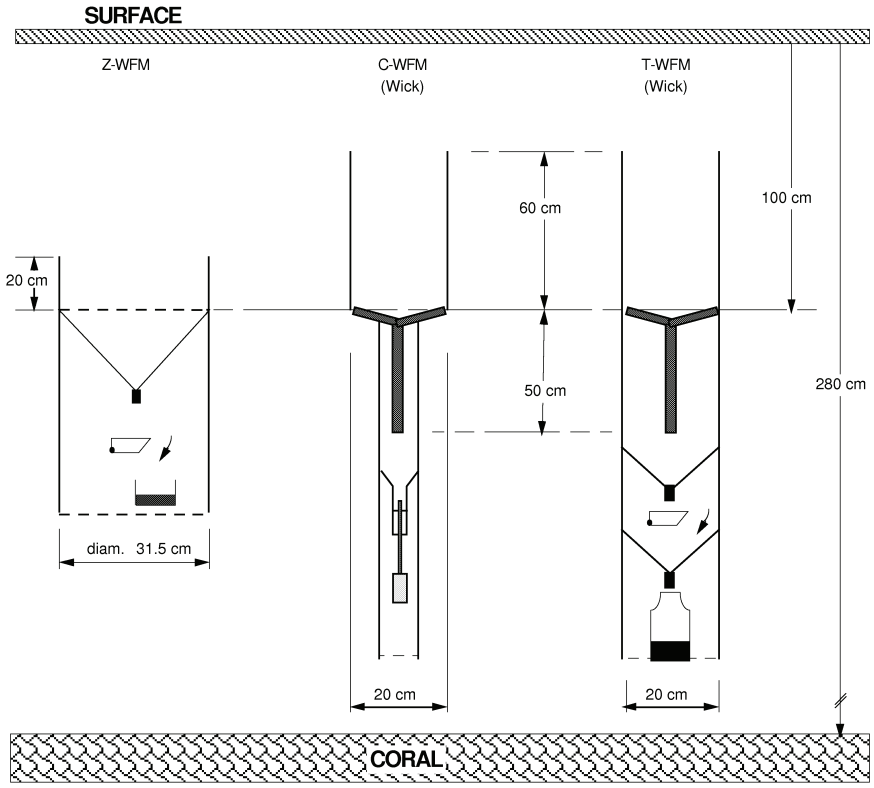

Figure 6.2. Schematic cross section (exaggerated horizontal scale) of the three WFM types installed in the soil. A soil solution sample can be extracted from each device (with Z-WFM, non-suction water flux meter; C-WFM, capacitance water flux meter; and T-WFM, tipping-bucket water flux meter).

determined. An ECHO-type capacitance sensor, similar to that of Masarik et al. (2004) measures the water depth in the siphon chamber. The instrument auto-siphons at approximately 50 mL which equates to a resolution of 1.6 mm tip^{-1}. However, the resolution can be increased if the water level in the instrument is directly measured and recorded. The non-suction WFM with zero-tension will from here be referred to as the 'Z-WFM'. Drainage through the Z-WFM was measured with a tipping bucket that has an accuracy of 17.4 mL tip^{-1} which equates to 0.22 mm tip^{-1}. The Z-WFMs have a 20 μm nylon mesh to filter out soil particles transported with the drainage water and the mesh also prevents deep roots from entering the device. The sum of the tips measured by the WFMs were stored every half hour by the CR10X data logger. Prior to installation, the operation of each WFM was checked with a number of calibration pulses at high intensity. The Z-WFMs and the T-WFMs both functioned well during these simulated events. The

auto-siphoned volume of the C-WFMs was determined to be 43 mL. For this study, only the siphon events of the C-WFMs were recorded since we were not convinced that a higher accuracy would be needed during high-intensity drainage events. A simple edge-detection algorithm was used to determine each time a volume was auto-siphoned from the collection chamber. For the calibration of the C-WFMs Appendix E.1. The performance of the WFMs was evaluated during a two month period between day of year (DOY) 200 and DOY 260.

6.2.4 Soil moisture content measurements

Soil moisture content (SMC) was measured using a number of water content reflectometer probes (CS616, Campbell Scientific). Measurements of SMC were done once every half an hour. Two horizontal sets (30-, 60-, 90- and 120- cm) and two vertical probe sets (0-30, 30-60, 60-90 and 90-120 cm) were installed in the volcanic ash soil during the previous year. CS616 probes are known to exhibit a calibration that is sensitive to the soil's clay content. Because the soil on Tongatapu has such a high clay content ($> 70\%$) which increases with depth, it was felt prudent to check the calibration of the CS616 probes. A field calibration of the CS616 probes was done with soil moisture contents that were gravimetrically determined using rings of a known volume. The SMC was determined by placing all samples into an oven ($> 100\ C$) for 48 hours. Separate calibration curves for the CS616 probes (Figure 3) were determined for the clay soil of the upper part of the profile, and for the deeper clay (70 cm). A good linear relationship (r^2 of 0.94 and 0.79 for respectively the top and the deeper part of the clay soil) was found between measured and actual SMC. However, the calibration for both layers was found to differ markedly from the 1:1 line (Figure 3).

Un-calibrated, the error in SMC would be about 0.15 $cm^3\ cm^{-3}$ at the wet end for the deep clay layer and approximately 0.05 $cm^3\ cm^{-3}$ for the top clay soil. The difference between the two layers is likely related to the lower soil organic mater, higher clay content and other structural properties of the clay [*Miyamoto et al.*, 2003] that become more pronounced deeper in the profile. Similar studies in volcanic soils [*Veldkamp and O'brien*, 2000] had previously shown errors of up to 0.15 $m^3\ m^{-3}$ in SMC using un-calibrated CS615 probes. The highest saturated SMC measured by the calibrated CS616 probes was 0.62 $cm^3\ cm^{-3}$. Compared to the obtained water retention curves at 60 and 90 cm (Figure 1) this is low. The high saturated and residual water content obtained at 60 and 90 cm are not unusual compared with *Cowie* [1980]; *Cowie et al.* [1991], and other water retention data we have obtained for the same soil type elsewhere on the island. We attribute the difference to the natural variability in the soil profile [*Cowie*, 1980].

The total amount of water for soil layers between 30-60, 60-90 and 90-120 cm was summed to provide the average water content between 30 and 120

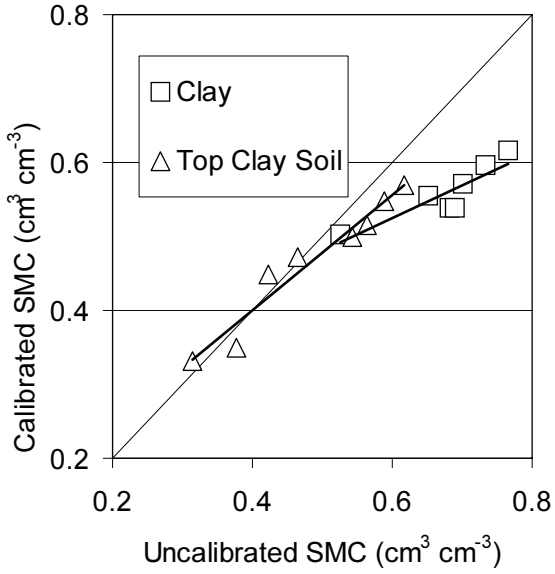

Figure 6.3. Calibration curve for CS616 probes in the weathered volcanic ash soil of Tongatapu (SMC signifies soil moisture content). The calibration had a r^2 of 0.94 for the top clay soil and a r^2 of 0.79 for the deeper clay soil.

cm. Evaporation and plant water uptake were considered to occur only in the top 30 cm, since very few roots were encountered below 30 cm during the evaluation period reported here. This was also confirmed by deeper soil moisture content measurements that registered almost no plant water uptake (<5 mm over evaluation period) deeper than 30 cm. Ignoring the top 30 cm's of soil, changes in stored water were solely attributed to either infiltration or drainage. Thus, infiltration was calculated by simply summing up the positive differences in total stored water. Likewise drainage was calculated by summing the negative differences.

6.2.5 Modelling with HYDRUS

Soil water movement was modelled using the HYDRUS-1D numerical code that solves Richards' equation [*Simunek et al.*, 2003] using the van Genuchten-Mualem model [*van Genuchten*, 1980; *Mualem*, 1976] to describe variably-saturated flow so that:

$$\frac{\delta\theta}{\delta t} = \frac{\delta}{\delta z}\left[K\left(h\right)\left(\frac{\delta h}{\delta z} - 1\right)\right] - S \tag{6.1}$$

where θ [L^3 L^{-3}] is the volumetric water content, t is time [T], z is the distance from the soil surface downward [L], K is the hydraulic conductivity

[L T^{-1}] as a function of h, h is the soil water pressure head [L], and S represents storage changes [L^3T^{-1})].

The soil water retention and hydraulic conductivity characteristic curves are modeled with the van Genuchten-Mualem equations [*Mualem*, 1976; *van Genuchten*, 1980]:

$$S_e = \frac{\theta(h) - \theta_r}{\theta_s - \theta_r} = [1 + \alpha |h|^n]^{-m} \tag{6.2}$$

$$K(\theta) = K_{sat} S_e^l \left[1 - \left(1 - S_e^{1/m}\right)^m\right]^2 \tag{6.3}$$

where θ [L^3 L^{-3}] is the volumetric water content, θ_s is the saturated water content [L^3 L^{-3}], θ_r is the residual water content [L^3 L^{-3}], K_{sat} is the saturated hydraulic conductivity, and α [L^{-1}], n, m (which is set equal to 1-1/n) and l (set equal to 0.5) are curve shape parameters.

We used the soil hydraulic properties listed in Table 6.1 although the soil disturbance likely led to a greater homogeneity of the soil physical and hydraulic properties directly above the WFMs. The upper boundary condition for water flow was prescribed by the rainfall rate measured in mm per half hour. Evapotranspiration was taken as daily ET_0 equally distributed over half hour periods between 7:30 AM and 7:30 PM. The lower boundary condition at 100 cm was set as a seepage face and as a constant matric potential of -50 cm to mimic the capillary suction applied to the soil by the wick material. Initial soil matric potential was set equal for the whole soil profile at -50 cm because the soil was initially quite wet due to recent rainfall.

6.2.6 Land preparation

The experimental plot was prepared by three ploughs. The top 30 cm of the soil was effectively turned over by the ploughing and resulted in a rough soil surface consisting of large clumps of soil and loose aggregates. Thereafter mounds of 15 cm high were prepared manually at a spacing of 1.5 x 1.5 m. Mounds were also made above the two pits where the WFMs were installed. One pit was located in the middle of four mounds while the other pit was located underneath one mound. One replicate of each WFM-type was thus located in the pit underneath the middle of four mounds, and the other replicate was placed in the pit directly beneath one mound. Within each pit, each individual WFM was thus configured differently with respect to the mounds on the surface. Some 120 grams of NPK fertiliser, on average, was added and mixed into each soil mound. Squash seeds were planted on the 25^{th} of July (Day Of Year 206). The soil remained bare until about DOY 220 when the squash started to emerge. After about 6 weeks a further side dressing of 15 grams of Urea was applied to each mound.

6.3 Results

6.3.1 Climatological Measurements

Daily values of rainfall and ET_0 reflect the occurrence of heavy rain events which are typical in this tropical climate (Figure 6.4). Large rainfall events exceeding 100 mm can stretch over several days, with the appearance of almost continuous rain (e.g. DOY 232 - 233).

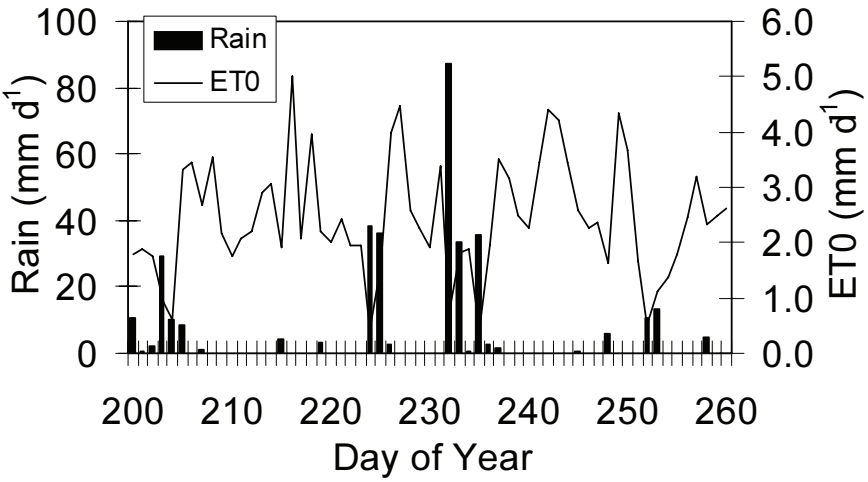

Figure 6.4. Daily rain and FAO crop reference evapotranspiration values for the evaluation period.

During the evaluation period a total of 4 rain events (see Figure 6.4, starting on DOY 203, 224 , 232 and 235) occurred that triggered flow through the non-suction WFMs The non-suction WFMs did not register flow beyond DOY 240 as there were no extreme rainfall events and plant cover became more established. Highest rainfall intensity was measured at 35.6 mm h^{-1} over a 30 minute period. The largest amount of rain during a single storm event was 120.8 mm on DOY 232 and 233 (Figure 6.4). In the rain-free periods between storm events, ET_0 was typical for a tropical climate [*Allen et al.*, 1998] and ranged from 1 to 5 mm d^{-1}. Independent estimates of evaporation and transpiration obtained in the field using a combination of micro-lysimeters and sapflow measurements in the squash (*van der Velde et al.* [2006a], for methodology see *Green and Clothier* [1988]) indicated about losses measured at about 126 mm while cumulative ET_0 amounted to 197 mm. Cumulative rain equalled 343 mm. This does not include the 35.4 mm that fell between the day of installation DOY 192 and DOY 200, it is assumed that this rain brought the soil close to saturation (as indicated by SMC measurements).

6.3.2 WFMs performance

Measured drainage divided by potential drainage is a measure of the collection efficiency of the WFMs (Table 6.2). Potential drainage was calculated with a simplified water balance. It was derived as the difference between measured rain (343 mm) and measured ET (126) between DOY 200 and 260, giving cumulative potential drainage of 217 mm.

Table 6.2. Drainage and collection efficiency of the water-flux meters (WFM). Collection efficiency was calculated with potential drainage estimated from a simple water balance at 217 mm. Each WFM was tested in duplicate. T-WFM 1 was not functioning properly. Acronyms depict a non-suction WFM (Z-WFM), and two types of suction-WFMs using a tipping-bucket (T-WFM) and an ECHO-type capacitance sensor (C-WFM).

	Z-WFM 1	Z-WFM 2	T-WFM 1	T-WFM 2	C-WFM 1	C-WFM 2
Measured Drainage (mm)	280	199	*319*	564	508	546
Collection Efficiency (%)	129	92	*147*	260	234	252

The Z-WFMs collected the lowest drainage amounts. The Z-WFMs collected 92% and 129% of the water balance estimation of drainage. No consistent relation between total drainage and location in one of the two pits was observed. Z-WFM1 collected a higher cumulative drainage compared to Z-WFM2, while C-WFM1 collected a lower cumulative drainage compared to C-WFM2. The surprising result was that the suction-WFMs collected more drainage than rain. We discuss this later.

No technical problems with the WFM measurement components (i.e., tipping bucket, capacitance probe) occurred during the growing season. Some problems related to the installation procedure did occur with one of the T-WFMs as it appeared to have not enough drainable volume below the unit to accommodate excess water passing through the meter. It seems that free water temporarily flooded the instrument at such times. A similar problem occurred once with one of the C-WFMs (DOY 232). Here an alternative explanation may well be that the auto-siphoning chamber could not cope with the high fluxes. The C-WFMs and Z-WFMs had ceased to function after the growing season. In experimental sites in the USA some of the C-WFMs were dug up and it was found that the ends of the siphon tube were rusting and subsequently rusted shut. We suspect that the same has occurred under these humid tropical conditions. We suspect that, similar to our experience with the Z-WFMs during the previous experimental season, the tipping buckets of the Z-WFMs rusted loose and came off, although this season they had been sealed with water-proof glue. Unlike the Z-WFMs, the tipping buckets of the T-WFMs are constructed with plastic and stainless steel materials and are rust resistant.

6.3.3 Timing

The time course of the drainage provides information on the flow velocities through the soil. Here we compare the response of the WFMs for the four large drainage events. Events that began on DOY 203, 224 , 232 and 235. All WFMs showed a fast response soon after the onset of rain. This was corroborated by rises in the soil water content recorded by CS616 probes at 90 and 120 cm. The time difference between the highest rain intensity and the peak drainage flux ranged from 1.5 to 7.5 hours for the different instruments. A similar time delay was observed in the peak in SMC measured with the CS616 probes at 90 cm. Although the CS616 probes always registered the water movement a little earlier than the WFMs. Similarity between WFMs and the passage of the waterfront registered by the CS616 probes at 90 cm, suggests that the saturated hydraulic properties of the repacked soil were similar to that of the natural soil profile. This can be explained by the micro-structuring of the clay soil. Differences in the timing of first drainage are most likely related to the different amounts of water needed to restore the soil moisture content of the repacked soil above the WFMs. Once the soil in the WFMs had obtained similar soil moisture conditions, all WFMs responded in a similar fashion with peaks occurring within 1.5 hours of each other for the three remaining drainage events. There is also good agreement with the timing of the HYDRUS modelled flux. Both the response and the peak of the modelled flux were at the same time, within 30 minutes, of the response of the first responding WFM for the first three events (DOY 203, 223 and 232, see Figure 6.7). The modelled flux for the last event (DOY 335) predicted the first response about an hour earlier than the measured flux, while the predicted peak flux occurred at the same time as that measured.

The temporal pattern of cumulative infiltration and drainage deduced from SMC data between 30 and 120 cm is shown in Figure 6.5. One set of probes measured 163 mm cumulative infiltration and 147 mm cumulative drainage during the period (Figure 6.5). The other set of probes also measured more cumulative infiltration (140 mm) than drainage (115 mm) during the period (data not shown). Storage changes where thus positive and in the order of 20 mm.

None of the measurements done with the CS616 indicated saturated SMC as high as suggested by the water retention curves obtained at 90 cm. We therefore choose to compare SMC measured at 90 cm and modelled SMC at 91 cm depth (Figure 6.6).

The shapes of the curves are similar and they clearly reflect the four largest drainage events. The measured SMCs appear to drain over a smaller range of SMCs. However, the variability in water retention properties in the field, especially introduced at the interface of the younger and older clays [*Cowie*, 1980], leads to uncertainties in the values of the modelled SMC. Additionally, given the uncertainty due to natural variability and the error

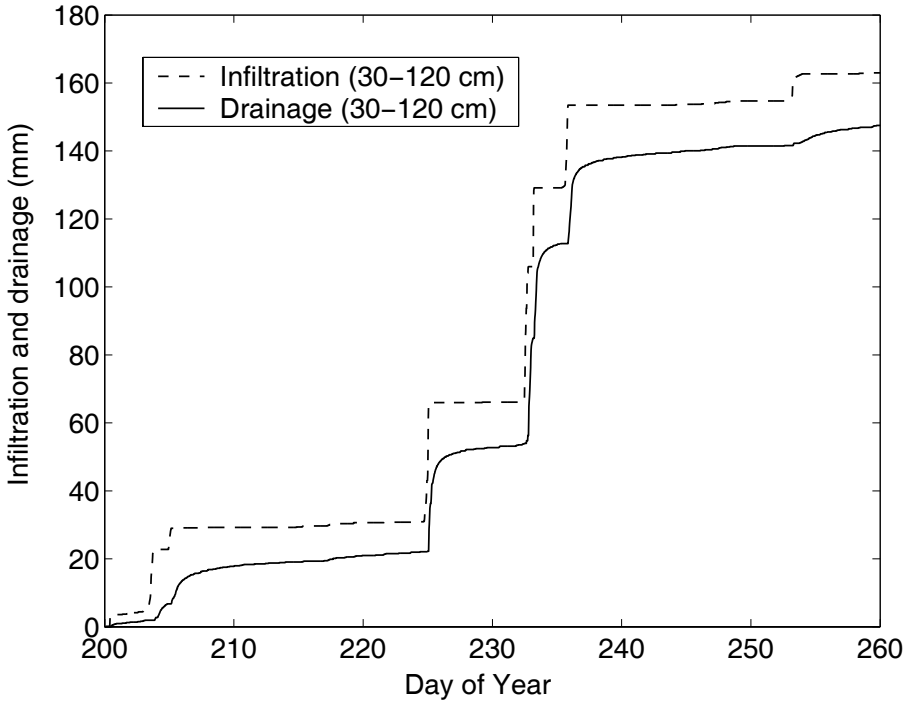

Figure 6.5. Infiltration and drainage estimated from the combined measurement of soil moisture content by one set of calibrated CS616 probes placed vertically at depths of 30-60, 60-90 and 90-120 cm.

introduced by the calibration of the measured SMCs, we can not justifiably compare the modelled and measured SMC values with the current data set.

6.3.4 Water Flux

The drainage flux at 100 cm, measured by two WFMs and modelled with HYDRUS for a snapshot period of three days is shown in Figure 6.7.

There is a good correspondence between measured and modelled drainage events. The rapid drop in the water flux indicates the importance of near–saturated transport in this soil under these tropical conditions. Beyond DOY 240 the Z-WFMs ceased to record any drainage events. During this period, the suction-WFMs continued to measure drainage. The peak water flux ranged between 0.004 mm s^{-1} (14.4 mm h^{-1}) for the model and 0.007 mm s^{-1} (25.4 mm h^{-1}) for the suction WFMs. The peak and the tail of the drainage events are both higher under the suction-WFM compared to the Z-WFM and the model predictions (Figure 6.7). The agreement between the modelled water flux at 100 cm and the Z-WFM is good. The model also confirms that significant water movement occurred during the same time that drainage events were registered by the Z-WFMs. The current

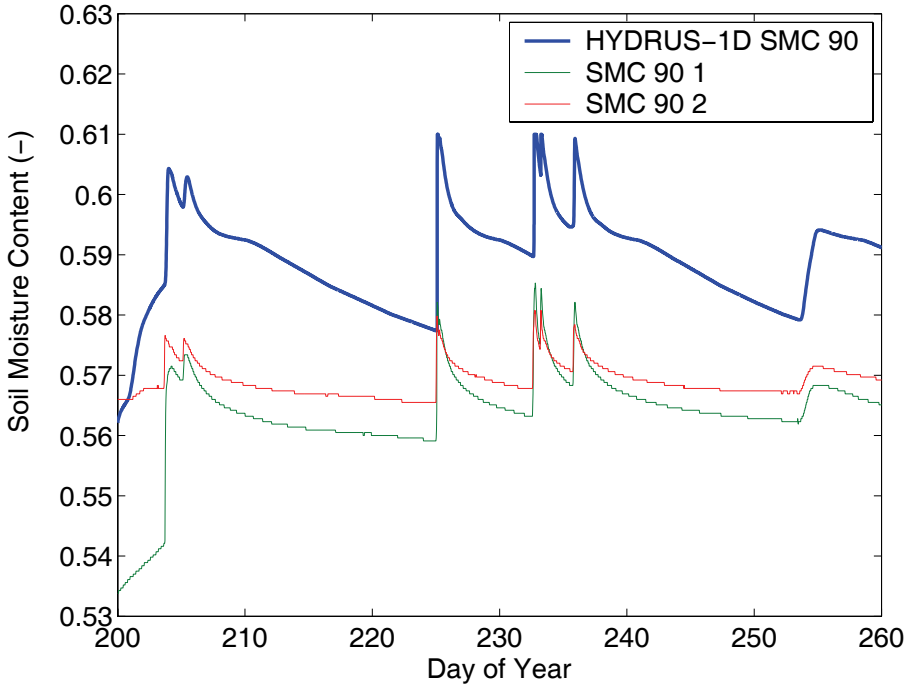

Figure 6.6. Soil moisture contents measured at 90 cm and modelled at 91 cm. Soil moisture contents were measured with 2 calibrated CS616 probes.

divergence-control dimensions of the Z-WFMs seems to be appropriate to measure the large drainage events in this soil under this climate.

6.3.5 Drainage volumes

The temporal pattern of cumulative measured and modelled drainage is presented in Figure 6.8. The model indicates a cumulative drainage of 235 mm. About 20 mm higher than the simple water balance estimate of 217 mm. This difference is attributed to the high intensity of the events and the uncertainty of the hydraulic conductivity near saturation and a mismatch in the initial moisture conditions of the modelled soil profile. Drainage derived from SMC between 30 and 120 cm (147 mm) was considerably lower than both the modelled and simple water balance estimate. This is mainly attributed to the fact that under near-saturated conditions there can be large drainage fluxes of water and yet very little change in SMC. There is a good agreement between the cumulative drainage measured with the Z-WFMs and the modelled drainage. We attribute the improved collection efficiency of the Z-WFMs (92% and 129%) to the use of a divergence pipe and specific climate and soil hydraulic properties during the evaluation period. Reported values are normally found to be about 10 to 58% [*Zhu et al.*, 2002; *Jemison*

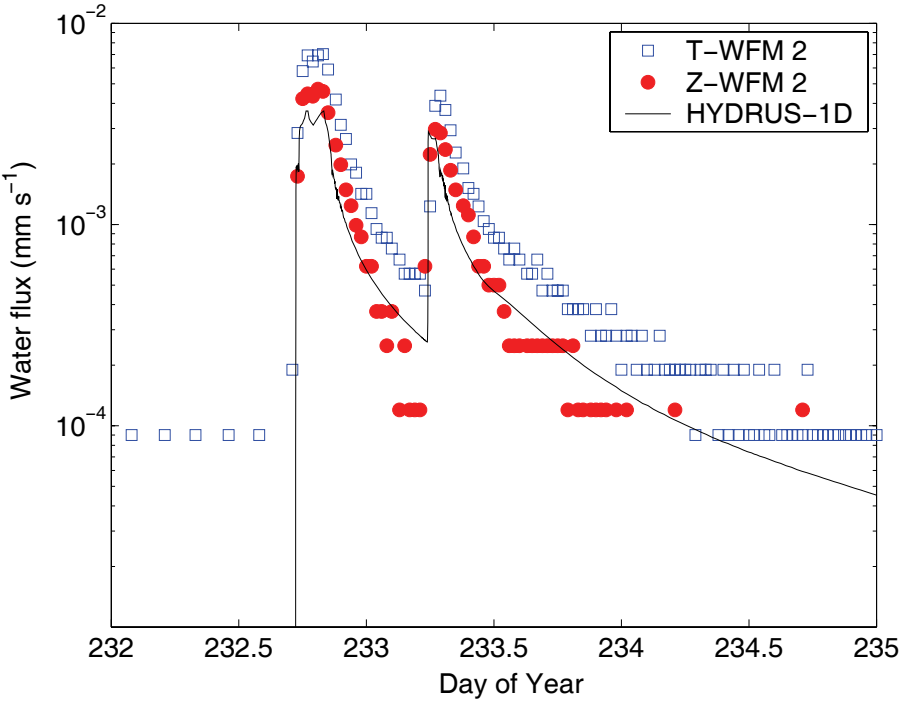

Figure 6.7. Measured and HYDRUS-1D modelled water flux at 100 cm. Measurements are shown of a non-suction water flux meter (Z-WFM 2) and a suction tipping-bucket water flux meter (T-WFM 2).

and Fox, 1992].

6.4 Discussion

The suction-WFMs clearly overestimated drainage because the totals exceeded actual rainfall (Figure 6.8). Periods when the Z-WFMs were responding can be used to calculate cumulative drainage for the suction-WFM when the soil saturated. The suction-WFMs collected about 350-360 mm of drainage during the periods when the soil directly above them saturated. This is comparable to the total amount of rain that fell during the period. An additional 200 mm was captured by the suction-WFMs during unsaturated flow. In contrast in the HYDRUS model about 20 mm of drainage, from a total of 235 mm, occurred under unsaturated conditions. Other authors have had reasonable success with passive capillary samplers in humid climate conditions but also have seen over-sampling of drainage with wick units. In western Oregon, USA, *Louie et al.* [2000] measured an average collection efficiency of 125% comparing recharge estimated by 30 passive capillary samplers to a water-balance estimate of recharge on annual basis.

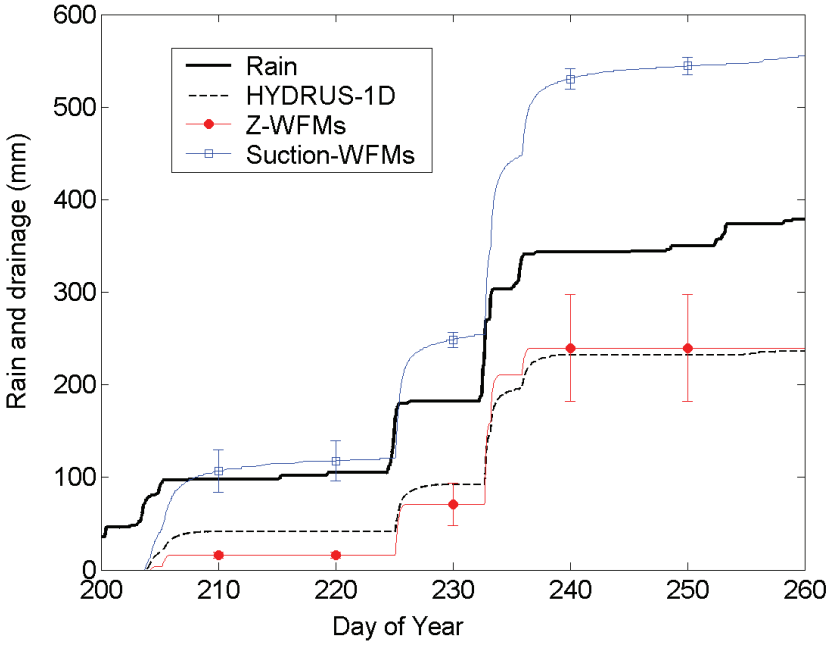

Figure 6.8. Cumulative rain, modelled drainage (HYDRUS-1D), and measured drainage and standard deviations for replicate non-suction water flux meters (Z-WFM 1 and 2) and suction WFMs (T-WFM 2 and C-WFM 1 and 2).

Under the high flow rate conditions experienced here, the height of the divergence barrier appeared to significantly affect measured drainage. For the Z-WFM, which had a 20 cm divergence height, the rainfall regime and high porosity soil combined to provide the tension control needed to achieve a nearly exact match for capturing the correct drainage. It appears that there was significant convergent flow in all of the wick units. *Rimmer et al.* [1995] showed that fine-textured soils require a large sampling area in order to create an undisturbed zone above the sampler. Due to the micro-aggregation of the clay soil studied here fast flow is possible in the near saturated range. We attribute the overestimation of the suction-WFMs to the effect of the continuous suction (h = -50 cm) applied by the wick. We suspect that the matric potentials in the soil were often above -50 cm (less negative) during the measurement period. This was confirmed by the modelled head at depths of 90 and 100 cm (data not shown). The effect of the 60 cm of divergence control needs to be explored by more detailed 2D modelling. Probably, if we had maintained a lower tension on the soil the probability of convergence would have been reduced greatly. Another option would have been to extend the divergence barrier to the surface, completely eliminating any chance for convergence (or divergence for that matter). However, it is also opted that

with very permeable soil, when very wet, the whole extension pipe may act as a hanging-column wick because of gravity flow. Hence the tension at the mouth of the extender pipe would be lower than the wet surrounding soil. If that is the case, then the 60 cm extension pipe for the wick units was apparently too large for the extremely wet conditions and highly permeable soil. However, this could also have been mediated by a shorter wick length. Predicted drainage increased only by about 20 mm when HYDRUS was run with a continuous matric potential of -50 cm as lower boundary condition. The suction seemed to have drawn soil water from a larger area above and around the suction-WFMs and 1D-modelling is not sufficient to explain these measurements. We propose to further investigate reasons for the overestimation of the suction-WFMs found in our study, with more detailed 2D modelling to explore different combinations of wick lenght and height of the divergence control. However there are also other factors that may have influenced the measurement. The occurrence of macropore flow may have contributed to the higher drainage measurement by the suction-WFMs, especially during such high percolation rates. Other possibilities include natural soil variability, some influence of the repacking of the soil above the WFMs and preferential flow triggered by the overlying pipe. The soil surface was quite rough, and even imperceptible local depressions may have triggered funnel flow above the WFMs. The largest differences between the suction-WFMs were observed during saturated drainage events. Interestingly, after this drainage the scatter of observations done by the suction-WFMs decreased. So, it seems that the suction applied to the soil by the wick tends to even out the total drainage collected by the suction-WFMs. This is likely due to different ratio's of macro and micropores in the soil directly above the meters. Different pore sizes will tend to drain under different tensions.

Disturbance caused by installation did not appear to severely influence observations. We deduce this from the consistence of 1) the passage of the water front and the shape of the drainage curve measured with the WFMs and the soil moisture probes and, 2) the agreement between the measurements of the Z-WFMs and the modelling using soil hydraulic properties obtained from undisturbed soil and, 3) the similarity of the shape of the drainage curve obtained with the suction-WFMs and the model. This is probably due to the strong micro-aggregation observed in the soil and the inherent disturbance of the top soil introduced by ploughing. This leads us to conclude that a large fraction of the rain drains through the soil towards the limestone under saturated conditions. The Z-WFMs indicated that $\sim$70% of the precipitation drained under these wet conditions. High drainage volumes have been reported for similar climates with similar soils. *Duwig et al.* [1998] attributed 64% of a 170 mm rainfall event to drainage. *Russel and Ewel* [1985] reported on drainage measurements during big storms in Costa Rica. They found that 84% of the annual drainage was collected during two week storms. The Z-WFM units with a 20 cm extender pipe (acting as

a relatively short divergence barrier) worked better than the wick units in optimizing the drainage collected during the 60 day test. Testing is required for better matching of the divergence-control dimensions for the wet soil conditions in these highly permeable soils. In this case we would expect that it would call for a higher divergence barrier and a shorter wick combination. As shown by *Gee et al.* [2002, 2004] the lower the flow rates the greater the chance for flow divergence.

6.5 Conclusions

Water-flux meters are a useful and low-cost tool for a direct determination of water fluxes in field soils. The performance of the WFMs depends on their design criteria and operational conditions, including the soil and climate conditions. This study envisaged to analyse the performance of three WFM types (Z-WFM, T-WFM and C-WFM) in tropical micro-structured clayey soils. The micro-structuring of this specific soil yields a pseudo–sand type of hydrodynamic behaviour that seemed to allow the use of disturbed soil material in the evaluation analysis. Water-flux meters are relatively easy to install and maintain and are therefore suitable for on-farm use. However, during this study only short-term success was achieved (3–12 months). At other sites with temperate climatic conditions (USA) the instruments have been functioning continuously over several years [*Gee et al.*, 2004]. Soil moisture content storage changes deduced from SMC measurements were positive and accounted for about 10% of the total drained volume. Successful direct measurements of water flux at 100 cm depth were achieved with non-suction WFMs and this was supported via modelling of soil water movement using HYDRUS. Overestimation of drainage flux with suction WFMs was attributed to convergence of the flow paths above the divergence pipe. We speculate that during this evaluation period the soil matric potential was higher than the tension applied by the wick. From an operational point of view, we also recommend to provide sufficient 'drainable' soil volume under the WFMs if they are used under tropical conditions characterised by intensive rainfall events. Disadvantages of the WFMs include the locality of the measurement and the relatively small sampling areas. The discrepancies between suction-WFM measurements and model and alternative WFM designs for these conditions need to be furhter explored. The results presented here will be combined with nitrate and pesticide analyses of the drainage water to develop more sustainable agricultural practices on this Pacific island atoll.

Chapter 7

Measuring and Modelling the Components of the Field Water Balance

7.1 Introduction

The objective of this Chapter is to integrate the previous results from Chapters 5 and 6, and to present and evaluate different components of the water balance at the experimental site at the Vaini Research Station. Besides the measurements presented in the two previous Chapters, this Chapter uses soil–evaporation measurements and deterministic modelling with WAVE [*Vanclooster et al.*, 1996, 1995] for the 2003 growing season. Unfortunately we could not give explicit estimates of uncertainty in the predictions. These uncertainties may arise from conceptual modelling errors, parameter and input uncertainty, and the appropriateness of the chosen model (see for example *Vanclooster et al.* [2005]). Quantifying these uncertainties merits further study. Nevetheless, we aim here to provide an integrated picture of the water balance by comparing measured and modelled totals of soil–evaporation, plant transpiration, soil moisture storage changes, and drainage.

The water balance of a field soil can be generally written:

$$P = E + I + T + R + D + \Delta S/\Delta t \tag{7.1}$$

Total precipitation (P) is partitioned between surface runoff (R) and infiltration. The canopy intercepts a part of the precipitation until it reaches its storage capacity. The water that is intercepted by the leaves (I) may be evaporated later. Water that infiltrates into the soil will flow downwards by gravity and change the soil's water storage (ΔS / Δ t). A part of the infiltrated water will evaporate from the soil surface (E), and another part will be taken up by plants that transpire the water back into the atmosphere (T). Finally, some of the soil's water will drain out of the base of the rootzone towards the groundwater (D). The different components that were measured at the experimental site at Vaini and modelled here, are indicated in Figure 7.1.

Field water–balance studies have been carried out for the estimation of groundwater recharge [*Timlin et al.*, 2003], so as to asses the risk of offsite

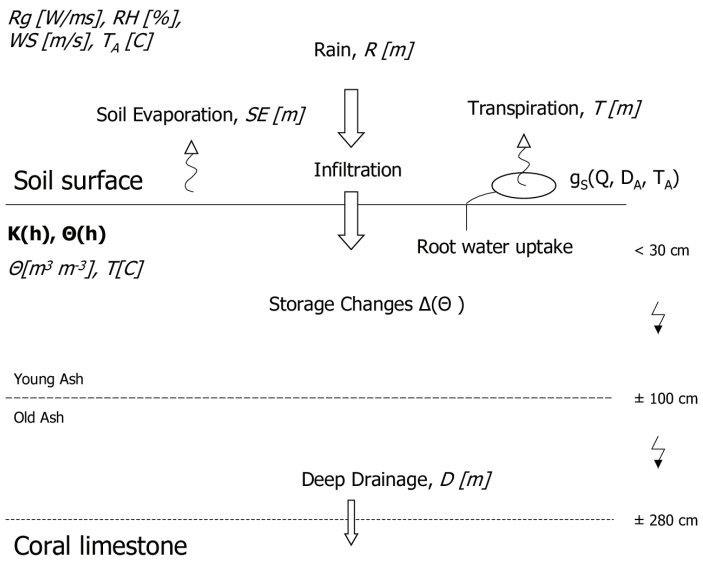

Figure 7.1. Schematic representation of the water balance. The ambient microclimate was characterised by global radiation (Rg), relative humidity (RH), windspeed (WS) and air temperature (T_A).

movement of contaminants from crop production practices or animal manure applications [*Sauer et al.*, 2002] and to couple physiological models of growth and photosynthesis to soil water dynamics [*Lebon et al.*, 2003].

Abenney-Mickson et al. [1997] used the SWAP model to calculate the water balance of a pumpkin field in Japan. Good agreement was obtained for measured and modelled soil moisture contents, however the agreement between model calculations of evapotranspiration and measured evapotranspiration was not satisfactory.

It still remains quite unusual to have complete measurements of transpiration, soil evaporation and drainage in the field. Here we integrate our measurements of these components, and determine if they add up as expected, and to assess if there is a good agreement with our water balance modelling.

7.2 Materials and Methods

The experiment was carried out on the experimental site at the Vaini Agricultural Research Station, Tongatapu. The data presented here are from the 2003 measurement campaign. The weather station that was on–site, measured incoming global radiation, relative humidity, air temperature, wind speed and rainfall. These data were collected for the purpose of modelling the water balance of the site and calculating the potential evapotranspiration

so to have an estimation for potential leaching losses.

Runoff had never been observed on this flat field with high hydraulic conductivity. Transpiration and drainage were measured during the growing season. Modelling could also be used to evaluate management options (e.g. *Vanclooster et al.* [2005]) during both the growing and the non-growing season to minimize leachate losses. However, we have not explicity accounted for leachate losses during the non-growing season.

7.2.1 Evaporation

Soil evaporation was measured on a daily basis with 10 micro–lysimeters, each having a depth of about 8 cm and a diameter of 15.3 cm. In the morning, the micro–lysimeters were inserted into the soil and the soil and micro-lysimeters weighed in the lab. The micro-lysimeters, now containing the soil were put back in the field before 8:00 AM. The next day the weight difference was measured and used to calculate soil evaporation. Occasionally, the samples were left in the field for one or two additional days, to record the total evaporation that was measured over those days.

7.2.2 Transpiration

Transpiration was measured using heat-pulse probes and the T-max method [*van der Velde et al.*, 2006a]. The transpiration was modelled using a 2–layer big–leaf model, along with the measured leaf area development. Stomatal conductance parameters were derived from porometer measurements (for details see Chapter 5 and *van der Velde et al.* [2006a]).

7.2.3 Drainage

The zero-tension drainage flux meters were used to monitor water and nitrate transport through the root–zone soil, and these results are reported on in Chapters 6 and 8 and *van der Velde et al.* [2005].

7.2.4 Modelling

The WAVE model [*Vanclooster et al.*, 1996, 1995] was used to model the water balance components. WAVE is an integrated crop–soil model that is able to describe the transport and transformation of mass and energy in the soil, crop and vadose environment. WAVE is a deterministic one–dimensional model. For our purposes, we only used the water transport module of WAVE. Daily measured rainfall and daily Penman–Montheit reference evapotranspiration (ET_0) were calculated on a daily basis using measured global radiation, wind speed, and minimum and maximum daily temperatures (see Figure 6.4). WAVE uses Richards' equation for the description of water transport. WAVE was run with a coupled van Genuchten–Mualem model

Table 7.1. The *van Genuchten* [1980] water retention parameters used in the WAVE model.

Layer	θ_r (m^3m^{-3})	θ_s (m^3m^{-3})	α (m^{-1})	n (-)	m (-)
1	0.45	0.60	0.005	1450	0.31
2	0.43	0.53	0.005	1496	0.33
3	0.60	0.67	0.005	1538	0.35
4	0.60	0.80	0.004	1466	0.32
5	0.53	0.61	0.010	1596	0.37

Table 7.2. *Mualem* [1976] parameters for the hydraulic conductivity function of each layer.

Layer	K (cm day^{-1})	L (-)
1	672	0.5
2	62.4	0.5
3	36	0.5
4	21.6	0.5
5	14.4	0.5

for the description of water retention and flow in the soil. As in Chapter 5, and *van der Velde et al.* [2005], five soil layers were recognised in the soil: 0-15, 15-30, 30-60, 60-90 and 90-200 cm. Each layer was subdivided into 5 cm compartments. The soil water retention properties used for this simulation, and the hydraulic conductivity functions, are similar to those used in Chapter 5. These are given in Tables 7.1 and 7.2.

The evapotranspiration was calculated using the measured leaf area development, and the K_c derived from heat pulse measurements. This was 1 until the 12^{th} of October (DOY 286), until senescence when the K_c started to drop and reached 0.8 K_c on the 25^{th} of October (DOY 300). The time series of LAI values was measured with the point quadrant method (see Chapter 5). WAVE uses the LAI as a division parameter to split the potential transpiration and evaporation (Equations 7.2 and 7.3), *Vanclooster et al.* [1996]:

$$E_p = fe^{-cLAI} ET_{crop} \tag{7.2}$$

$$T_p = ET_{crop} - E_p - I \tag{7.3}$$

where E_p is the potential soil evaporation (m day^{-1}), T_p is the potential crop transpiration (m day^{-1}), ET_{crop} is the potential evapotranspiration (m day^{-1}). I is the amount of water which has been intercepted and can be 'released from the crop canopy (mm)' [*Vanclooster et al.*, 1993] during 1 day. This also implies that transpiration only starts after all intercepted water has evaporated. In fact, interception is not directly calculated in WAVE, but rather is an input. To determine the amount of intercepted water, we used the approach of *Norman and Campbell* [1983]:

$$I = (1 - \exp(-0.5LAI)) * P \tag{7.4}$$

where I is the interception (mm d^{-1}), LAI is the leaf area index (m^2 m^{-2}), and P (mm $^{-1}$) is daily rainfall. The maximum interception was set as LAI measured at that day. Subsequently in WAVE, the water that is stored in the canopy can either be released or is allowed to evaporate during the following day. The crop specific parameters f (-) and c (-) are fixed in WAVE and set to respectively 1 and 0.6. Equations 7.2, 7.3 and 7.4 imply that the sum of soil evaporation, evaporated interception water and transpiration cannot exceed ET_{crop}. The rooting depth was estimated from field observations to be 5 cm on the 18^{th} of July, 15 cm on the 8^{th} of August, and to be 30 cm on the 6^{th} of September.

7.3 Results and Discussion

Transpiration and drainage have been discussed in Chapters 5 and 6. Here we discuss evaporation separately. All components are then discussed in the water balance subsection following below.

7.3.1 Evaporation

Considering errors of observation and model simplifications, the measurements of evaporation agreed moderately with the modelled evaporation. The order of magnitude, and temporal variation are reasonable (Figure 7.2). The mismatch between measured and modelled soil evaporation may be caused by the tin–can material of the micro–lysimeters (which were in fact old corned–beef cans) that might heat–up differently with respect to the surrounding soil. This can distort the energy balance and so affect the mass balance of the micro–lysimeters. This may also explain the higher measured soil evaporation compared to the modelled soil evaporation. Another factor that may influence the measurement is the shallow depth of the micro–lysimeters. This hydraulic rupture cannot account for the capillary water that moves upward to the surface to evaporate under intense radiation over longer measurement periods (e.g. 3 days). On the other hand, as the water content decreases the hydraulic conductivity will also drastically decrease. Another important factor concerns the crop specific parameters f (-) and c (-), that may very well be different for the squash considered here.

7.3.2 Water balance

The components for the water balance during the growing season of squash are given in Figure 7.3. To calculate the cumulative soil evaporation on days without evaporation measurements, the average measured soil evaporation was used for interpolation.

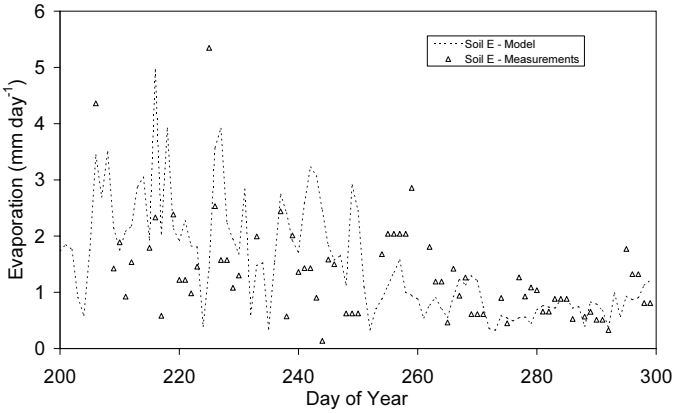

Figure 7.2. Measured and modelled soil evaporation

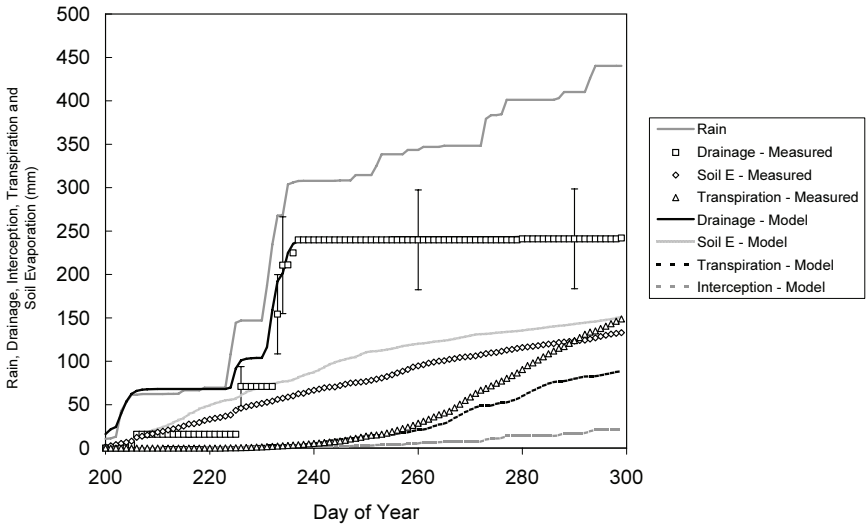

Figure 7.3. The measured and modelled water balance components. Drainage was measured at 1 m with 2 zero–tension lysimeters (see Chapter 5).

Rain totalled 440 mm over the 100–day experimental period. The water balance was dominated by drainage which we measured at a depth of 1 m. Modelled cumulative drainage accounted for 243 mm and measured cumulative drainage equalled 242 mm. This respectively corresponds to about 55% of the total rain that fell. We can compare this to the recharge of the lens that is reported in several sources, and which is based on measurements and models. The estimates or recharge range from 10 to 35 %, with a generally accepted average estimate of 30 % (see Chapter 9 for a further discussion). Repacking of the soil in the fluxmeters may partly explain this high drainage average (n = 2), although it was verified with our modelling that used locally measured soil hydraulic characteristics ([*van der Velde et al.*, 2005] and Chapter 6). Spatial heterogeneity of soil hydraulic properties, and thus of drainage, and a subsequent redistribution occurring in the deeper soil and rock layers, may lower this estimate with respect to the average island recharge estimate. Also, upward capillary flow towards the topsoil may continue to contribute to transpiration and evaporation during subsequent dry periods. So, it remains debatable what the exact drainage percentage is, and given a considerable local heterogeneity, our best estimate at 1 m depth would range between 30 to 60 %.

Total transpiration was measured and modelled respectively at 149 and 89 mm. This is between 34 and 20 % of total rainfall. A considerable difference, also with respect to our calcultion in Chapter 5 and *van der Velde et al.* [2006b]. The mismatch between measured transpiration and modelled transpiration could possibly be attributed to water stress. Water stress in the field did occur, and can vary according to local soil heterogeneity of hydraulic conductivity. In the model, plant water stress relates to the root water uptake parameters used in the model, and the hydraulic conductivity in the model. Potential transpiration modelled in WAVE equalled 124 mm vs. 89 mm for actual transpiration, this would indicate major water stress conditions. During the season, transpiration progressively increased in relation to the growth of the squash plants. Conversely, soil evaporation decreases with increased plant cover and deepening root distribution. Soil evaporation was measured and modelled to be respectively 133 and 151 mm, equalling between 30 and 34 % of the water balance. Modelled interception totalled 21 mm over the period, or 5 % of total rain.

The modelling and measurements estimates od soil evaporation differ by about 5 %, while the modelled transpiration estimate is only half of measured transpiration. The soil moisture storage changes were minimal during the season (cf. Chapter 5). The sum of measured drainage, transpiration, soil evaporation equals 523.66 mm. The sum of modelled transpiration, interception, soil evaporation and drainage equals 503.5 mm. This is respectively some 83 and 63 mm higher then the amount of rainfall which totalled 440.2 mm. This is a water balance error of about 14 to 19%, which is large. Explanations of this mismatch may relate to either inaccurate representations

of the water balance components by both modelling and measurements, or by changes in soil moisture storage that was unaccounted for.

We can evaluate the different water balance components to detemine the estimates that are most likely to be eroneous. It appears that drainage estimates seem reasonable, as this was separately verified by modelling in Chapter 6. Unfortunately, there is no measured estimate of interception.

Soil evaporation estimates are in reasonable agreement. Still, modelled soil evaporation seems too large compared to modelled transpiration, and quite possibly, given the tin-can material of the micro-lysimeters, measured soil evaporation could be too large as well. The model results seems to be greatly dependent on the crop specific parameters c and f. If we examine equation 7.2, we see that a reduction of 5 % in factor f results in a equal reduction of soil evaporation, with a constant value for c. Increasing factor c from 0.6 to 0.65, while keeping f at 1, results in a maximum reduction of soil evaporation of 13.3 % at the maximum LAI. Conversly, reducing factor c from 0.6 to 0.55, while keeping f at 1, results in a maximum increase in soil evaporation of 15.3 %. Simultaneously changing f to 0.95, and c to 0.65 results in a maximum reduction of 17.6 %. This illustrates the sensitivity of soil evaporation to these crop specific parameters.

Transpiration was modelled with reasonable agreement in Chapter 5, but the transpiration modelled by WAVE is only half of the measured transpiration. In WAVE transpiration is determined by substracting the soil evaporation from estimated ET_crop. The only explanation seems that if indeed soil evaporation was too high, a correct, lower, estimate of soil evaporation would result in a higher modelled transpiration. Also, possibly, although a reasonable average behaviour was observed for the 4 plants equiped with heat pulse equipment, these plants might be larger and transpire more then the average squash plant in the field.

We observe that the soil moisture status on DOY 200 was similar to the soil moisture status at DOY 300. Soil moisture storage change was negligible, as indicated by soil moisture measurements ($<$ 7 mm between DOY 200 and 300). In contrast, modelling with WAVE indicates that the soil was acutally drier at the end of the growing season. The cummulative error on the water balance for the whole soil profile modelled with WAVE amounted to -0.6 mm. The mass balance of WAVE thus appears to be correct, and no numerical errors seem to have occured. The initial pressure head in WAVE was set to -50 cm. These relatively wet conditions reflect previous rainfall that may contribute to the modelled transpiration and evaporation. In addition, the measured cumulative soil evaporation was lower than modelled soil evaporation. So, both the measurements and our modelling seem to indicate water balance totals that are too high, but we cannot clearly state the reasons. At this stage it seems that soil moisture storage did change, although this was not indicated by our soil moisture measurements. This discrepancy remains unexplained.

Using WAVE, with the current set of hydraulic parameters, results in a large underestimation of cumulative transpiration, and a higher estimate for cumulative soil evaporation compared to independent measurements. In WAVE, the sum of potential evaporation, potential evaporated interception water, and potential transpiration equals the potential evapotranspiration, ET_{crop}. In WAVE, interception is not derived within the model's framework. Consequently, in the current structure of WAVE, this bears on the estimate of the amount of plant transpiration since transpiration is directly determined by substracting the sum of soil evaporation and plant interception from total evapotranspiration. It is therefore recommended that interception is explicitly incorporated within WAVE's model framework.

No attention is given to the uncertainty of the estimates, and this would merit further study. Another point of interest would include the quantification of the contribution of spatial heterogeneity of soil physical parameters on the water balance estimates, for both field, as well as modelling conditions [*Hupet*, 2003].

7.4 Conclusion

We used measurements of rainfall, transpiration, drainage, and soil moisture storage changes, and an integrated modelling approach to estimate these water balance components. The measured and modelled estimates were of a similar magnitude and in reasonable agreement. However, water balance totals for both model and measurement exceeded actual rainfall during the 100–day period. We have proposed several reasons for this mismatch, but cannot identify what exactly caused the mismatch. It may relate to both modelling errors, related to model simplification and parameter input, as well as measurement errors, relating to spatial variability of soil physical properties and plant physiological conditions.

Chapter 8

Measurements of Nitrogen Fluxes with Flux Meters through a Volcanic Clay Soil under Tropical Conditions *

Abstract The accurate measurement of soil water flux combined with a measurement of solute concentration of the flux in the field has long been a focus of soil science and continues to remain a challenge. Understanding the controls on flux concentration C_f is essential to understand the variability found in field solute transport studies. We used flux meters to measure both water flux (see Chapter 6) as well as flux concentration of NO_3 and NH_4 at 1 m depth. The flux concentration was modelled using the approach of *Steenhuis et al.* [1994] and a temperature response function that represents biotic processes related to N mineralisation and adsorption in the plough layer. The predictions were in agreement with timing of the peak and subsequent drop of the $C_f(NO_3^-)$ observed by the fluxmeters. However the model clearly underestimated the concentrations and temporal pattern of the initial stages of drainage. The model also failed to capture the general pattern in $C_f(NO_3^-)$ observed during the last drainage event. Nevertheless, we can conclude that a part of the variability, and the temporal pattern of $C_f(NO_3^-)$ are determined by biotic processes governed by soil temperature. The effect of soil temperature on mineralisation rate and thus the amount of NO_3^- in soil solution is directly translated in the $C_f(NO_3^-)$ observed at 1 m depth due to the fast flow of water and solutes through the soil.

*Contains parts from van der Velde, M., S.R. Green, G.W. Gee, M. Vanclooster and B.E. Clothier, Using water flux meters as a tool for agricultural water management *Integrated Methods for assessing water quality - COST 629*, Water pollution in natural porous media at different scales: fate, impact and indicators, p 21-27. Université catholique de Louvain, Louvain la Neuve, 2004. To be submitted in modified form.

8.1 Introduction

The accurate measurement of soil water flux combined with a measurement of solute concentration of the flux at a high temporal resolution in the field remains a challenge. This understanding is essential to understanding the variability found in field solute transport studies. Preferential flow (including macropore flow, finger flow, and funnel flow) further challenges our efforts to predict the transport of chemicals. There is an increasing experimental evidence suggesting that preferential flow transport is more the rule than the exception [*Jury and Fluhler*, 1992; *Flury et al.*, 1994; *Flury*, 1996; *Derby and Knighton*, 2001; *Kladivko et al.*, 1991]. This Chapter addresses two related topics that continue to be of interest to the scientific community involved with water and solute transport, 1) preferential flow and, 2) the quantification of resident and flux concentrations of solutes. We will analyse the impact of preferential flow and soil temperature on the nitrogen fluxes measured with the flux meters (see Chapter 5). Data of plant nitrogen and soil nitrogen analysis obtained throughout the growing season will be presented as well.

8.2 Materials and Methods

The field trial that was carried out at the Vaini research centre and followed the agricultural practices recommended by the Ministry of Agriculture [*Manu et al.*, 1998]. The grass that had grown on the field during the Tongan fallow period was slashed several months before the start of the season (in June). Normally, a part of the dried grass is incorporated into the soil when the field is ploughed several weeks before the planting of the squash seeds. This ploughing is then followed by several diskings and ploughings as seems fit by the farmer. At our site, a part of last years dried grass was removed due to fire hazards. Mounds spaced 1.5 x 1.5 m apart were planted with 2 to 3 squash seeds. Each mound contained an application of 120 g NPKS (11.5, 12.8, 18.0, 1.0) that was applied on DOY 205 resulting in 62 kg N ha^{-1}. Urea (N) was applied in a circle around the mound at 45 grams per mound (about 80 kg N ha^{-1}) several weeks after the germination of the seeds on DOY 260. Herbicides were applied at the beginning of the season; manual weeding was done as the squash grew bigger. Fungicides were applied regularly against powdery mildew. When the squash has grown mature its root system consists of a well-developed taproot with a fibrous root system that explored the top 30 cm of the soil.

8.2.1 Drainage Plates

Two sets of three 'drainage plates' obtained from the 'Soil Unit' of the UCL, were installed below the mounds and below the interrow at a depth of about

10 cm to quantify differences in the concentration of NO_3^- and NH_4^+ in the drainage. The drainage plates were installed before the fertilisers were applied on DOY 198. The drainage plates consist of a plastic plate with 0.5 cm grooves. The drainage plates had a surface area of 329 cm^2 and were installed under a slight angle in the soil so that the drainage water flowed through the grooves into a collection flask. The flask was controlled after each rainfall event and if it contained any drainage emptied with a syringe. The drainage volume was determined and the collected drainage was stored in a freezer until further analysis.

8.2.2 Flux Meters

We used water flux meters (WFM) without and with the application of a suction (–50 cm) to the surrounding soil (for more details see Chapter 5). The location of the two sets of three different flux meters with respect to the mounds is shown in Figures 8.1 and 8.2.

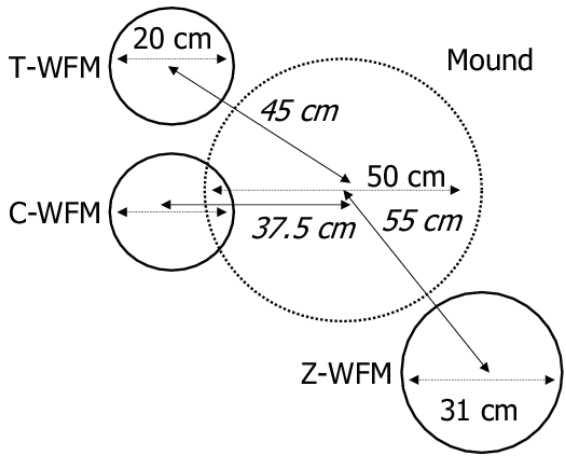

Figure 8.1. Location of the WFMs in pit 1 with respect to the mounds planted with squash seeds and that contained NPK fertiliser

Drainage was collected in a collection chamber that was emptied manually directly after the rain (and sometimes during the rain) with a 50 mL syringe.

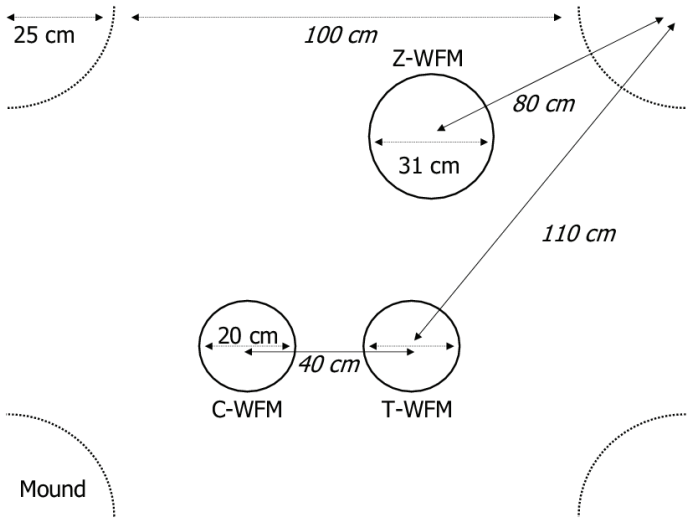

Figure 8.2. Location of the WFMs in pit 2 with respect to the mounds planted with squash seeds and that contained NPK fertiliser

8.2.3 Soil and water N analysis

Soil samples were collected at the site for N analysis and gravimetric water content determination, along with a measurement of soil bulk density. Weights of the samples were determined gravimetrically, as well as volumetrically from the bulk density samples, by putting the samples for 48 hours in an oven at 100 C. We collected soil samples of about 150 g in a plastic bag and began the extraction process on that day. We began the extraction process by mixing up the sample in the plastic bag to homogenise as much as possible. We then added between 10 and 11 g of soil to a clean, empty centrifuge tube. Subsequently we added 30 ml of $2M$ KCl to the tube and shook for 3 hours on an end-over-end shaker. After shaking we let the extracts settle overnight and after centrifugation we filtered the samples and froze the sample until transport to New Zealand. Nitrate and ammonium concentrations in extracts were determined by the methods of *Downes* [1978] and *Technicon* [1976] respectively, using a Technicon auto analyser. Drainage samples were collected and frozen and analysed for nitrate and ammonium using the method of respectively *Downes* [1978] and *Technicon* [1976].

8.2.4 Plant N analysis

Bulk samples of from 10 different squash plants including at least three leaves from each plants, vines, roots and fruits were collected on several days.

They were weighted, dried in an oven (75 C), and their moisture content was determined. Total phosphorus and nitrogen were determined following Kjeldahl digestion by colorimetric autoanalysis methods. The method of *Twine and Williams* [1971] for the determination of phosphorus in Kjeldahl digests of plant material by automatic analysis was used for phosphorus and the method as described in *Technicon* [1973] was used for the determination of nitrogen. The plant and soil analysis was done at the Soil and Fertiliser Laboratory at Massey University, Palmerston North, New Zealand. Results are reported on a dry weight basis.

8.3 Theory

Initially we had used a deterministic model employing Richards' equation to model water movement along with the convection dispersion equation to describe solute transport and calculate $N0_3^-$ flux concentrations ($C_f(NO_3^-)$). The model calculations were not in agreement with measured flux concentrations (data not shown). We attribute this to the preferential flow phenomena that we had observed in this soil, exacerbated by a lack of knowledge on key parameters governing processes related to nitrogen mineralisation and decomposition. A dye tracer experiment with Brilliant Blue carried out in the experimental field showed that preferential flow was triggered at the interface of the plough layer, and the A_h at about 10 to 20 cm (Figure 8.3). We identified macropores resulting from decaying ploughed-in grass material, deep-rooting Guinea grass roots, and worm activity down to a depth of 1 m. In addition, the strong structure of the clay aggregates allows for fast flow around the aggregates, also called 'bypass ' flow.

We therefore chose a simple approach that specifically incorporates the preferential transport of water and solutes [*Steenhuis et al.*, 1994]. This approach distinguishes different zones in a soil exhibiting preferential flow. The topsoil is considered as a distribution zone were water and solutes are funnelled into flow paths that lead into the conveyance zone. The flow paths then continue through the conveyance zone.

Recently, following up on the work of *Steenhuis et al.* [1994], *Kim et al.* [2005] proposed an analytical expression for the description of solute transport under steady-state conditions in field soils with preferential flow paths. They stated that 'the thickness of the distribution zone depends on land use and tillage practises.' For ploughed fields the distribution zone should be equal to the depth of ploughing and for repacked soils it would correspond to the saturated layer near the surface.

The loss of solutes from the distribution zone through preferential flow has been modelled with a simple equation by [*Steenhuis et al.*, 1994]. In case water is added without solutes, the concentration in the water leaving the distribution zone $C_{w,o}$ is described by [*Steenhuis et al.*, 1994]:

Figure 8.3. Visualisation of preferential flow paths by means of a brilliant blue dye tracer experiment using a disc permeameter.

$$C_{w,o} = \left(\frac{M^0 r}{W_a}\right) exp\left(-\frac{\int Rdt}{W_d}\right) \tag{8.1}$$

Here $C_{w,o}$ is the concentration of water flowing out of a column [M L^{-3}], M^0 is the initial mass of solute [M L^{-2}], $\int Rdt$ the integrate of the rainfall rate over $.dt$ [L], and r equals;

$$r = \left[\frac{V_p}{(V_p + V_m)}\right] \tag{8.2}$$

here V_p and V_m respectively are the volume of preferential and matrix flow. The percentage of preferential and matrix flow was determined from the drainage measurements presented in Chapter 5 and set to be equal for V_p to 90 % and for V_m to be 10 %.

W_a and W_d are respectively the apparent water content of the distribution zone during adsorption and desorption. These can be defined as:

$$W_a = h_{mix}\left(\rho k_a + \theta_S\right) \tag{8.3}$$

$$W_d = h_{mix}\,(\rho k_d + \theta_S) \tag{8.4}$$

where h_{mix} is the depth of the distribution zone and equals 0.15 m, θ_S the saturated moisture content taken as 0.4 ($cm^3\ cm^{-3}$), ρ the bulk density taken as 1 kg m^3 and k_a and k_d respectively the adsorption and desorption partition coefficient.

This equation is mathematically similar to Burns' equation [*Scotter et al.*, 1993] in that it uses an exponential dependency on the net rainfall that occurred over a certain time period to determine the fraction of solute initially resident in the topsoil. *Scotter et al.* [1993] noted that 'the leaching pattern implied by this equation involves some preferential flow and it is consistent with the soil behaving as a system of independent flow tubes in which the water and solute moves at varying speeds'. This is compatible with the behaviour expressed by Steenhuis' 1994 equation.

The concentration of the solutes, in our case, NO_3^- and NH_4^+, depend on the amount of fertiliser that was applied to the soil, and the rate at which the nitrogen becomes available in the soil. The nitrogen mineralisation rate Q_m, that corresponds to the release of N from organic matter, is dependent on the soil moisture and soil temperature and is often modelled so that [*Johnsson et al.*, 1987]:

$$Q_m = -\frac{dN_0}{dt} = -k_1 N_0 f_T f_M \tag{8.5}$$

where dN_0/dt represents the change of mineral nitrogen concentration in the soil solution in time, k_1 is a potential rate, f_T and f_M respectively represent the biotic response functions involving soil temperature and moisture content.

The effect of temperature (f_T) at a certain depth z is then modelled as [*Johnsson et al.*, 1987]:

$$f_T(z) = Q_{10}^{\frac{[T(z)-T_s]}{10}} \tag{8.6}$$

where Q_{10} is the factor change in rate due to a 10-degree change in temperature, $T(z)$ is the temperature of the soil layer under consideration, T_s is the base temperature at which f_T is equal to 1.

The effect of soil moisture (f_M) at a certain depth z is modelled as [*Johnsson et al.*, 1987]:

$$f_M(z) = 1 - 0.64\left(1 - \frac{\theta(z)}{\theta_{FC}}\right) \tag{8.7}$$

where θ(z) is the measured water content at depth z, and θ_{FC} is the soil water content at field capacity which we defined at 0.4 $m^3\ m^{-3}$.

To investigate the effect of soil temperature and water content on the nitrogen mineralisation rate and thus on the amount of soil nitrogen available

for plants as well as possibly leaching, and thus the measured flux of nitrate, we defined the product of f_T and f_M to be indicative for the release of N from the topsoil, from both fertiler and organic matter. We consider this product for depth 0-30 cm as it includes the distribution zone and the surface layer where fertiliser was applied. We further consider another zone, the 30-60 cm soil layer as the soil moisture content observations are not as much influenced by plant water uptake. These two soil layers will be most important in absolute terms with respect to supplying the amount of nitrate to preferentially flowing water. Water content was measured from 0-30 and 30-60 cm, while soil temperature was measured at 15 and 45 cm depth.

To include the effect of soil temperature on nitrogen mineralisation we included f_T into equation 8.1 so that:

$$C_{w,o} = \left(\frac{f_T * M^0 r}{W_a} \right) exp \left(- \int \frac{Rdt}{W_d} \right) \tag{8.8}$$

For simplicity we have not taken into account the fertiliser release rate, and have kept M^0 as a constant equal to 70 kg hectare^{-1}. Again, we consider only the temperature effects at depths 0-30 and 30-60 cm.

The degree of preferential flow in a soil relates to the differences observed between resident and flux concentrations. Total resident concentration of the solute can be defined as $C_r = M_s/V_{soil}$ with M_s the total mass of solute and V_{soil} the total volume of soil. Concentration of the solute C_f in the water flux, the flux concentration, is measured at the outlet of the fluxmeters. It can be defined as $J_s(\mathrm{t})/J_w(\mathrm{t})$ where $J_s(\mathrm{t})$ represents the solute flux and $J_w(\mathrm{t})$ the flux of water. *Kim and Feyen* [2000] measured C_r and C_f simultaneously with TDR in a structured soil exhibiting preferential flow. *Kim and Feyen* [2000] concluded that 'for structured soils having preferential flow, the TDR-measured resident concentrations are not representative of solute transport in the soil macropores but are primarily [representative for] the soil matrix region'.

8.4 Results

8.4.1 Plants

The beginning of the growth season was marked by three or four heavy rains (Figure 8.4) around DOY 205, 225, 233 and 235. In Figure 8.4 the time of NPK and urea application are also noted. The leaf area of an average plant was extrapolated from DOY 215 when plants started to emerge to 245 when actual measurements were carried out. Here we will focus on the three periods (DOY 205-206, DOY 225 and DOY 233-235) with heavy rainfall and the leaching of NO_3^- and NH_4^+ associated with these events. During these events (upto DOY 245) plant leaf surface area (for measurement see Chapter 4) and the root system were both still very small.

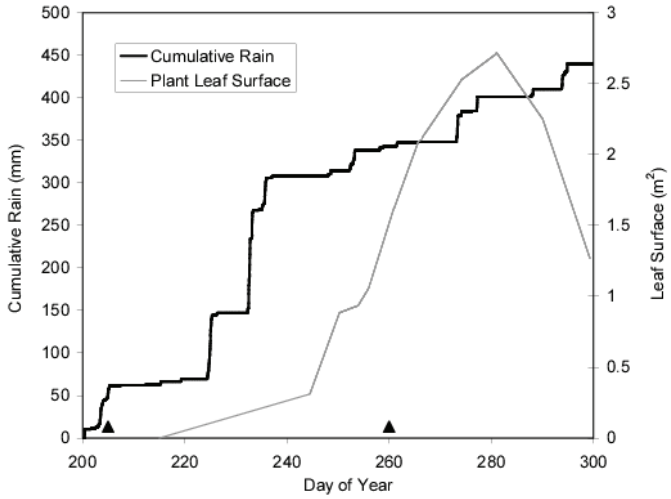

Figure 8.4. Cumulative rain and plant surface area of an average plant in the field. The triangles indicate the times of the application of NPK (DOY 205) and the application of Urea (N, DOY 260)

Table 8.1. Nitrogen and phosphorus concentrations in squash leaves, vines, roots and fruits. At least 10 samples were bulked together and 'n' indicates the number of days the bulk samples were collected

	N (mg kg^{-1})		P (mg kg^{-1})	
	Average	Standard Deviation	Average	Standard Deviation
Leaves (n = 6)	78.1	9.2	6.7	1.8
Vines (n = 5)	50.8	18.0	5.2	2.0
Roots (n = 3)	43.8	10.3	4.8	1.6
Fruits (n = 2)	29.9	4.2	3.7	3.7

Measurements of nitrogen in several plant components during the 2003 season (Table 8.1) showed that roots contain approximately 43.8 N mg kg^{-1}, leaves approximately 78.1 N mg kg^{-1}, and the vines approximately 50.8 N mg kg^{-1}. At the time of harvest, and thus the N content of the squash pumpkin when it is exported to Japan, the fruit contained approximately 29.9 N mg kg^{-1}. Similar N and P contents were found during the 2002 growing season (data not shown).

For the plants equiped with heat-pulse probes we determined the dry weight of these different plant components after we removed the heat probe equipment. The average dry weight for leaves equalled about 100 g, the average dry weight for roots equalled 50 g, for vines 150 g, and the fruits had an average weight of 1500 g.

8.4.2 Soil

The concentration of the solute in the mixing zone depends on the initial applied mass of NPKS fertiliser and the amount initially resident. Mounds spaced 1.5 x 1.5 m apart were planted with 2 to 3 squash seeds. Each mound contained an application of 120 g NPKS (11.5, 12.8, 18.0, 1.0) that was applied on the 24^{th} of July 2003 (DOY 205) resulting in 62 kg of N ha^{-1}. N was in the form of NH_4. Urea was applied in a circle around the mound at 45 grams per mound (about 80 kg N ha^{-1}) several weeks after the germination of the seeds on the 12^{th} of September 2003 (DOY 255).

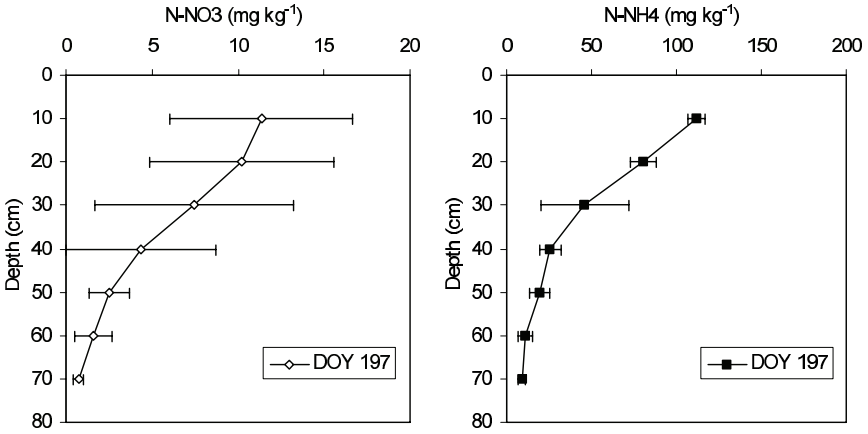

Figure 8.5. Nitrate and ammonium concentrations of the topsoil measured on DOY 197 before fertiliser was applied. Measurements were done at 6 locations in the field with three replicates at each depth (errorbars represent the standard deviation of 27 samples).

The concentration of NO_3^- and NH_4^+ before the fertiliser was applied was measured at 6 locations in the field with three replicates at each depth (10, 20, 30, 40, 50, 60 and 70 cm). These indicate a concentration of NO_3^- and NH_4^+ of respectively 10 and 110 mg kg^{-1} at 10 cm depth that decrease to about 1 and 10 mg kg^{-1} at 70 cm (Figure 8.5). The values for NH_4^+ are high, and would correspond to approximately 100 kg N ha^{-1} for the first 10 cm.

During the growing season the concentrations of NO_3^- and NH_4^+ were measured on an additional 6 days (DOY 210, 227, 248, 272, 283 and 303) under the mounds and in the interrow (Figures 8.6, 8.7, 8.8 and 8.9) . On each of these days, measurements were carried out under three mounds and three interrows with three replicates at each measured depth.

Figures 8.6 and 8.7 show that the concentrations of NO_3^- in the top 10 cm are similar to those obtained before the fertiliser was applied (Figure 8.5). However, on DOY 210 the concentration of NO_3^- at below 10 cm has increased both under the mounds and under the interrow. Until DOY

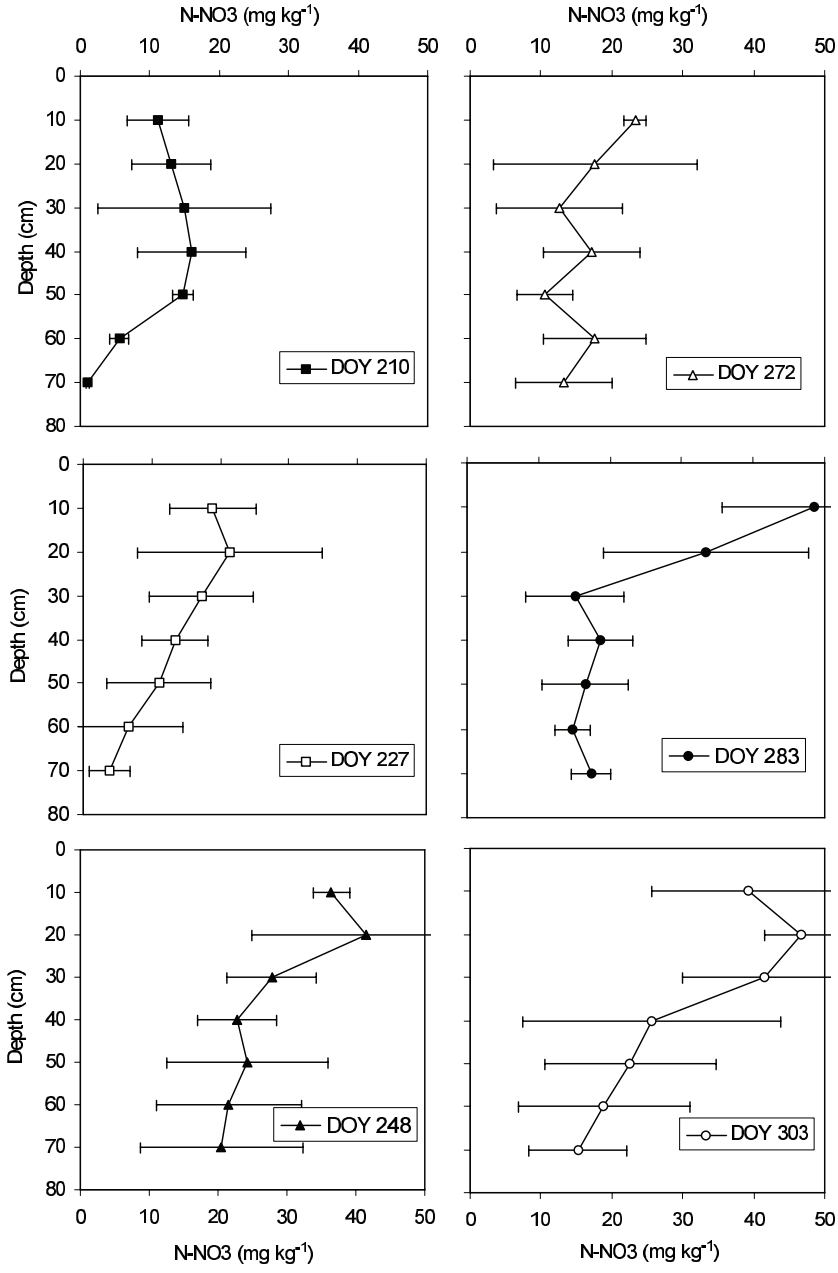

Figure 8.6. Nitrate content of the soil (mg kg^{-1}) measured underneath mounds at 6 days through the growing season. NPK was applied on DOY 205 in the mounda and urea around the mounds on DOY 255.

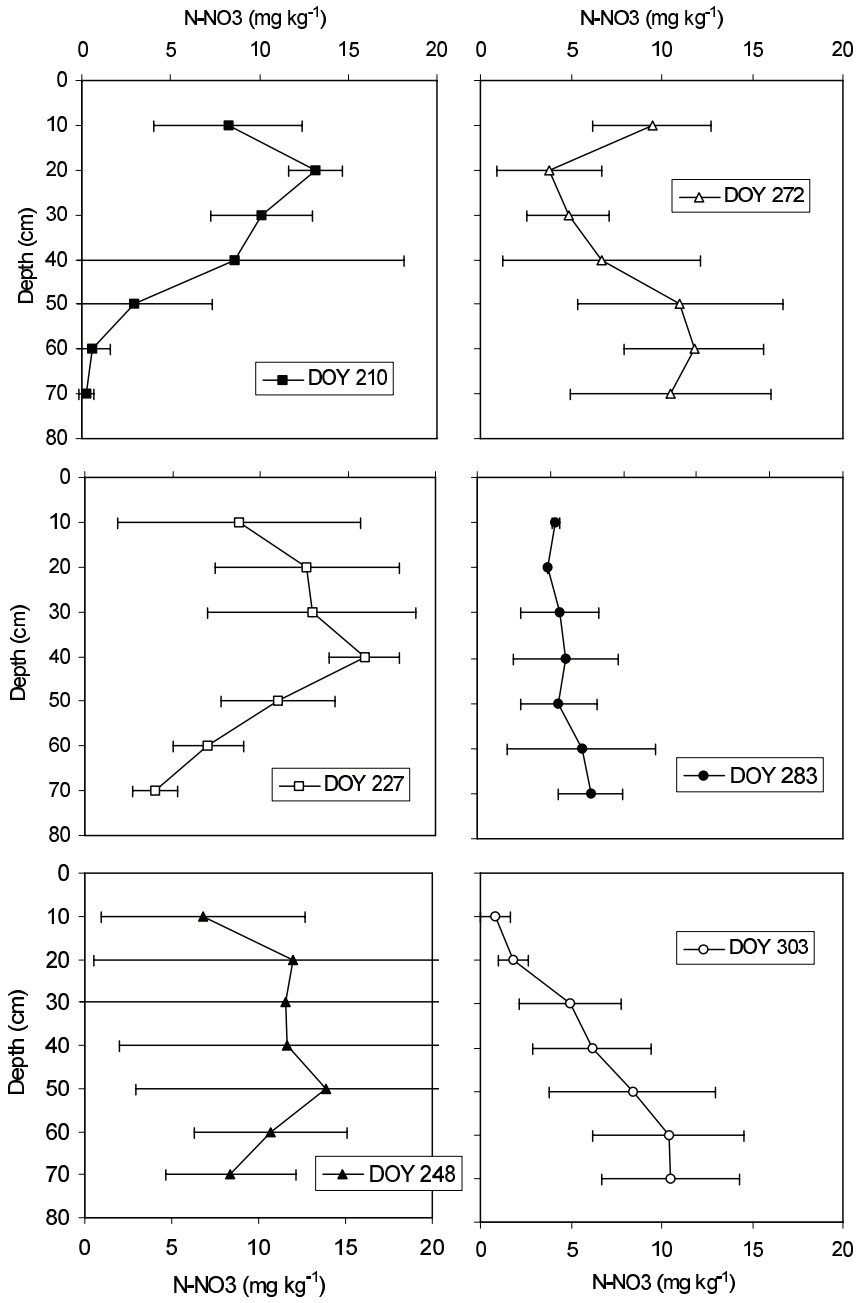

Figure 8.7. Nitrate content of the soil (mg kg^{-1}) measured underneath interrows at 6 days through the growing season. NPK was applied on DOY 205 in the mounda and urea around the mounds on DOY 255.

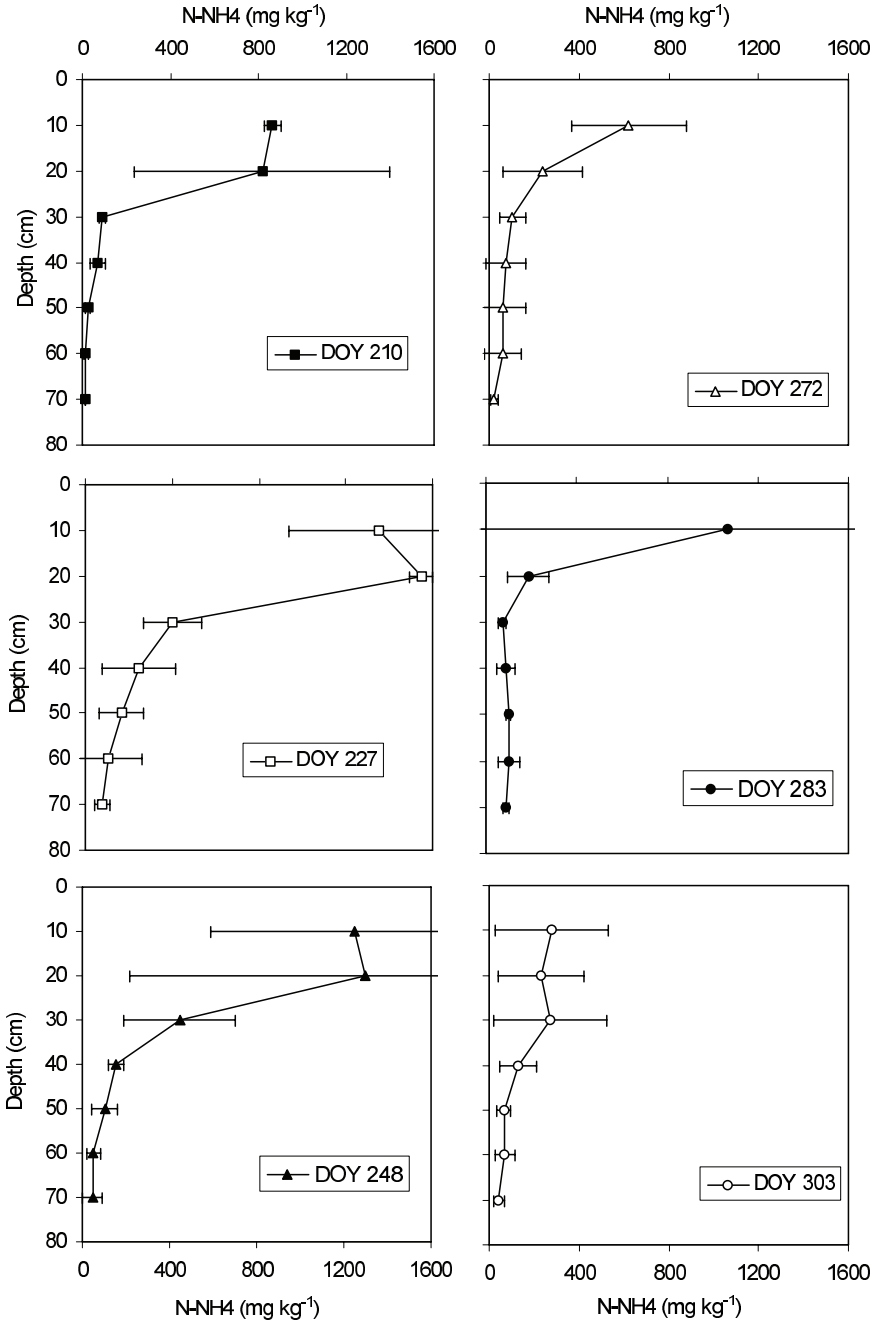

Figure 8.8. Ammonium content of the soil (mg kg^{-1}) measured underneath mounds at 6 days through the growing season. NPK was applied on DOY 205 in the mounda and urea around the mounds on DOY 255.

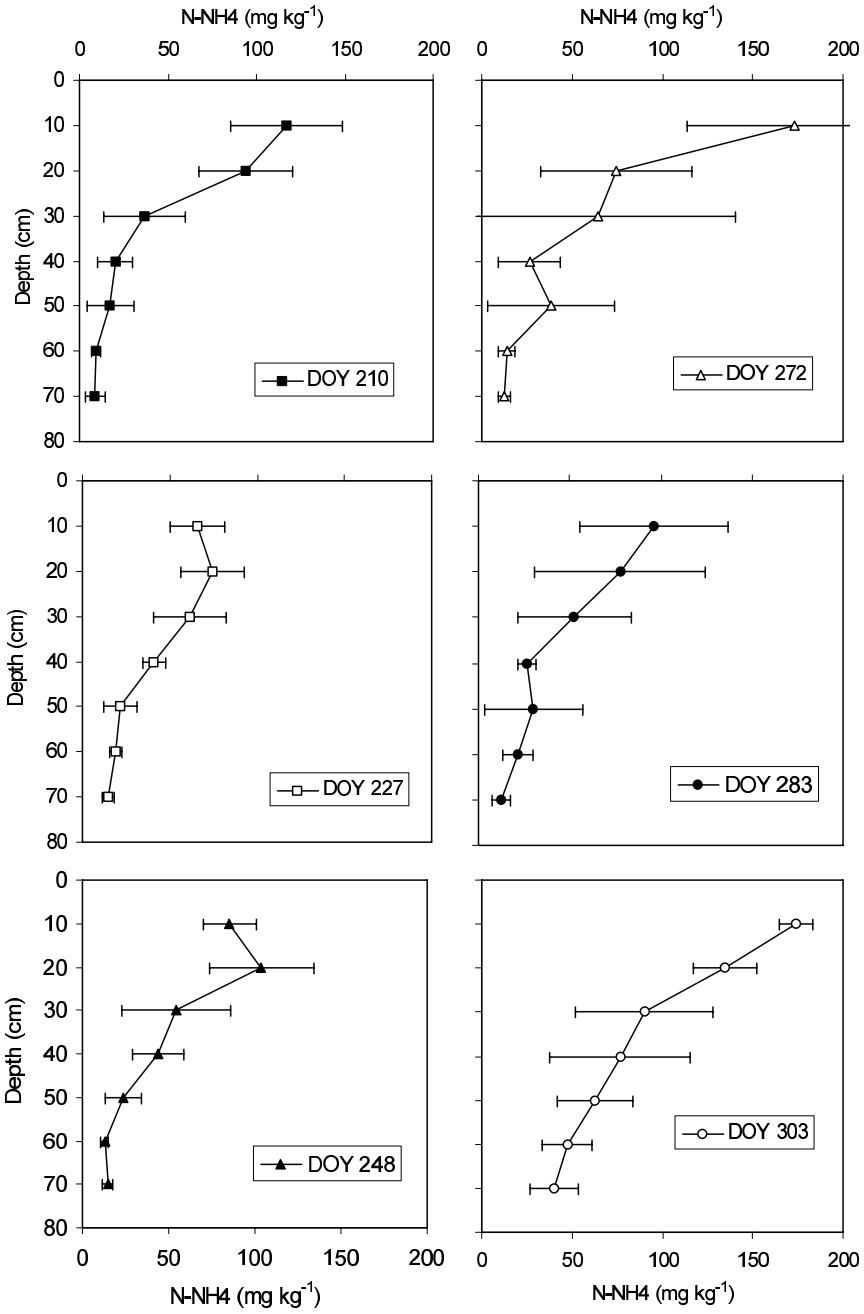

Figure 8.9. Ammonium content of the soil (mg kg^{-1}) measured underneath interrows at 6 days through the growing season. NPK was applied on DOY 205 in the mounda and urea around the mounds on DOY 255.

248 the concentration of nitrate in the profile under mounds increases over the whole profile (Figure 8.6). This relates to the NO_3^- coming available after nitrification of NH_4^+ derived from the fertiliser. On DOY 272 the whole profile has decreased in nitrate content that could be attributed to plant uptake and possible leaching. The effect of hydrolysis and subsequent oxidation of the urea applied on DOY 255 on the concentration of nitrate is not seen on DOY 272, and only on DOY 283 an increase in topsoil nitrate is observed. This may relate to large nitrate plant uptake preivous to and around DOY 272 after which the squash plants got severely infected by powdery milldew. The nitrate subsequently leaches down and gets taken up from the first 10 cm as shown by the profile on nitrate concentration on DOY 303.

Figure 8.7 shows the temporal changes in NO_3^- measured under the interrow. The panels in the figure indicate that the NO_3^- leaches down from DOY 210 to DOY 227, and DOY 248. From DOY 272 and onwards plant uptake of NO_3^- clearly starts to become important as the plant roots increasingly start to explore the interrow area. On DOY 303 the topsoil contains less then 3 mg kg^{-1} NO_3^-.

The initial concentration of NH_4^+ is similar to that measured under the interrow after the fertilizer application (Figure 8.9). On the contrary the concentration of NH_4^+ under mounds (Figure 8.8) shows consistent high concentrations in the top 20 cm soil for DOY 210, 227 and 248. On DOY 272 the concentrations under the mounds have decreased. The measured NH_4^+ is highly variable, with values under the mounds measured at 627, 85 and 2479 mg kg^{-1} NH_4^+, with 2479 the highest value measured during the measurement campaign. Considering this value to be not representative, measured NH_4^+ values of DOY 283 lie in lince with both values measured at DOY 283 and DOY 303. The values of DOY 303 are lowwer then those measured on DOY 272.

The concentration of NH_4^+ under the interrow is much lower and is similar for DOY 210, 227, and 248. In the interrow the application of urea on DOY 255 does show a direct effect on DOY 272 with an increase in NH_4^+, after which it descreases on DOY 283. It normally takes only a couple of days for urea to be hydrolysed to NH_4^+ [*Green and Clothier*, 2002]. On DOY 303 the concentrations NH_4^+ under the interrow is higher again, and this may relate to the destructive harvest on DOY 300.

Overall, we encountered some high values of NH_4^+ in the soil, while the concentrations in the drainage are low (see further). Analysis of NH_4^+ with a KCl extraction, replaces the NH_4^+ with K^+ and thus removes NH_4^+ from the soil's exchanger. The concentrations show that a large fraction of the ammonium is attached to the soil particles. Bacteria only transform ammonium into nitrate using ammonium available in the soil solution. Bacteria are not able to transform ammonium retained on clays. Comparing the measured value of ammonium to the other cations shows that ammonium is a

small proportion of all cations on the soil's exchange complex. High CEC values for this soil were measured [*Pochet et al.*, 2006]. *Pochet et al.* [2006] measured values between 27.0 and 95.5 cmol kg^{-1}, with an average of 60.5 $cmol_c$ kg^{-1}. The determination of the CEC also allows to describe the CEC as to average nearly 10000 mg kg^{-1} [*Pochet et al.*, 2006]. Then, ammonium maximally accounts for about 10% of the total CEC. In separate measurements *Pochet et al.* [2006] measured N_{total} (equalling the sum of NH_4^+ and $N_{organic}$) for the Forest, Low and High site (cf. Chapter 4). *Pochet et al.* [2006] found that at depth (> 80 cm), where N_{total} is largely determined by NH_4^+, minimum and maximum values for N_{total} for the Forest, Low and High soil of respectively 420-537, 459-911 and 891-1075 mg kg^{-1}. In comparison, top soil (0-30 cm) N_{total} ranged between 1700-5990, 1704-2992 and 2000-2389 mg kg^{-1} for Forest, Low and High soil respectively. These values found at depth seem to be in agreement with the values we have found here.

Still, it appears that something is slowing down the nitrification. Soil ammonium accumulation is observed following forest felling and burning on a volcanic soil [*Matson et al.*, 1987], and in both dry and wet heaths after sod cutting [*Dorland et al.*, 2003]. Possibly, similar processes that might affect microbial dynamics occur following the impact of slashing, and partly burning of the Guinea grass, and partly plouging it into the soil. This would merrit further investigation.

Measurements reveal a complex pattern as a result of nitrification and leaching. Leaching can not be inferred from these measurements, this lead us to employ flux meters.

8.4.3 Drainage

Leaching is determined by the water flux and the solute concentration of the flux. To infer leaching of solutes simultaneous measurements of both are required.

8.4.4 Drainage Plates

At the field site, we measured the hydraulic conductivity at 5 depths with at least 3 replicates with tension disc infiltrometers (Chapter 4). At a depth of 15 cm the hydraulic conductivity averaged 260 mm hr^{-1}, albeit with a large variation. At a depth of 120 cm we measured an average hydraulic conductivity of 32 mm hr^{-1}, ranging from 7.6 to 86 mm hr^{-1}. Drainage was thus likely to occur rapidly and to be highly variable. Consequently, the measurements made with the drainage plates were highly variable as well. This may partly be related to the natural variability of the topsoil, but may also relate to the installation procedure. Only one drainage plate responded during all events. The concentration of NO_3^- (mg l^{-1}) was always lower below the interrow compared to the mound (Figure 8.10).

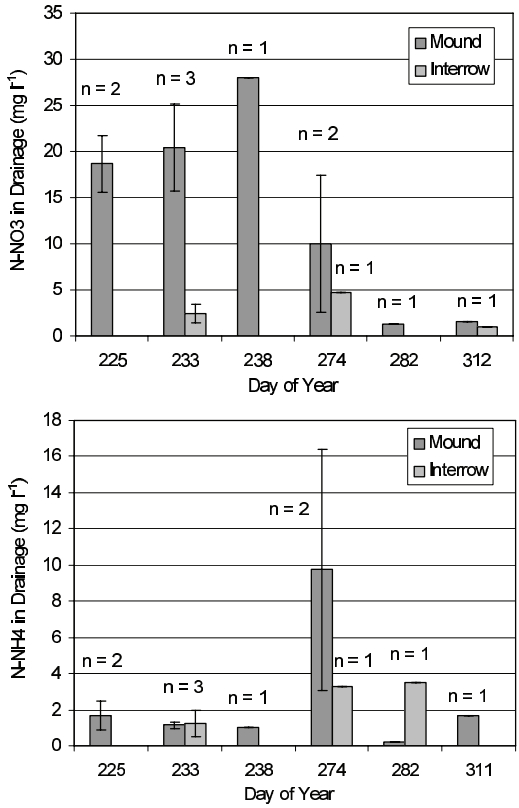

Figure 8.10. Concentration of NO_3^- (mg l^{-1}) and NH_4^+ (mg l^{-1}) with standard deviation in drainage below mounds and below the interrow measured with drainage plates 10 cm below the surface. The number of samples on each date is indicated as well.

The clearest difference in NO_3^- concentrations can be observed on DOY 233 when all drainage plates collected drainage. On DOY 233 the drainage plates below the mound recorded 1, 11 and 12 mm of drainage while the drainage plates below the inter rows recorded 1, 2 and 3 mm of drainage. There was no relation between the volume and the concentration of NO_3^-. The measurements of the drainage plates confirm that leaching of N will predominantly take place below the mounds. The measurements later in the season (DOY 274 and 312) were lowest. Measurements of NO_3^- in the soil under the mounds and under the interrow indicate three times higher concentrations of NO_3^- were found for the topsoil of the mounds compared to the interrow (see Figures 8.6 and 8.7). The NH_4^+ concentration was below 4 mg l^{-1}, except for DOY 272 when an average concentration (2 samples) of nearly 10 mg l^{-1} NH_4^+ was measured.

8.4.5 Fluxmeters

The fluxmeters measured the flux of water (Chapter 5) and from the collected drainage we determined NO_3^- and NH_4^+ concentrations in that flux, C_f. The concentration of NO_3^- showed a similar temporal pattern for the measurements made with the different flux meter types in the two soil pits, but they were higher for the second pit. This is likely related to the location of the flux meters with respect to the mounds at the surface (Figures 8.1 and 8.2). Average concentrations ranged approximately from 30 to 70 NO_3^- (mg l^{-1}). Concentrations of the ZWFMs were affected by the dilution of heavy rains. Leaching of N in the form of NH_4^+ was less then 10% of the N leached in the form of NO_3^-.

We measured very similar $N - NO_3^-$ (mg l^{-1}) and $N - NH_4^+$ (mg l^{-1}) flux concentrations with the ZWFMs and the wick fluxmeters. This is in agreement with *Steenhuis et al.* [1994] who measured similar dye and Br^- concentrations with wick and gravity pan samplers. To evaluate the mean temporal behaviour of NO_3^- and NH_4^+ flux concentrations we averaged the normalised data for each fluxmeter ($z_{average}$) for which we collected a sample on that day, totalling n measurements, and multiplied this by the average standard deviation (σ) and added the average measured NO_3^- (mg l^{-1}) and NH_4^+ concentration (μ). This provides a correct temporal average ($x_{average}$), so that:

$$z = (x - \mu)/\sigma \tag{8.9}$$

$$z_{average} = \sum_{i=1}^{n} z_i \tag{8.10}$$

$$x_{average} = z_{average} * \sigma + \mu \tag{8.11}$$

This was done because on days when samples were obtained, drainage was not always registered by all the different fluxmeters. There are some similarities between the variation in NO_3^- and NH_4^+ flux concentrations (Figure 8.12). We discuss this later.

Resident concentrations (C_r) were obtained from soil sampling while flux concentrations (C_f) where obtained from the drainage collected with the fluxmeters. We plotted the averaged C_r and the averaged C_f against the cumulative outflow registered with T-WFM1. The averaged C_r where generally three times lower than averaged C_f (Figure 8.13).

To investigate the impact of the water flux on the measured concentration we distinguished three periods of drainage (cf Chapter 5). The concentrations of NO_3^- during the three drainage periods show some similarities (Figure 8.14). The flux does not seem to influence the concentrations, but

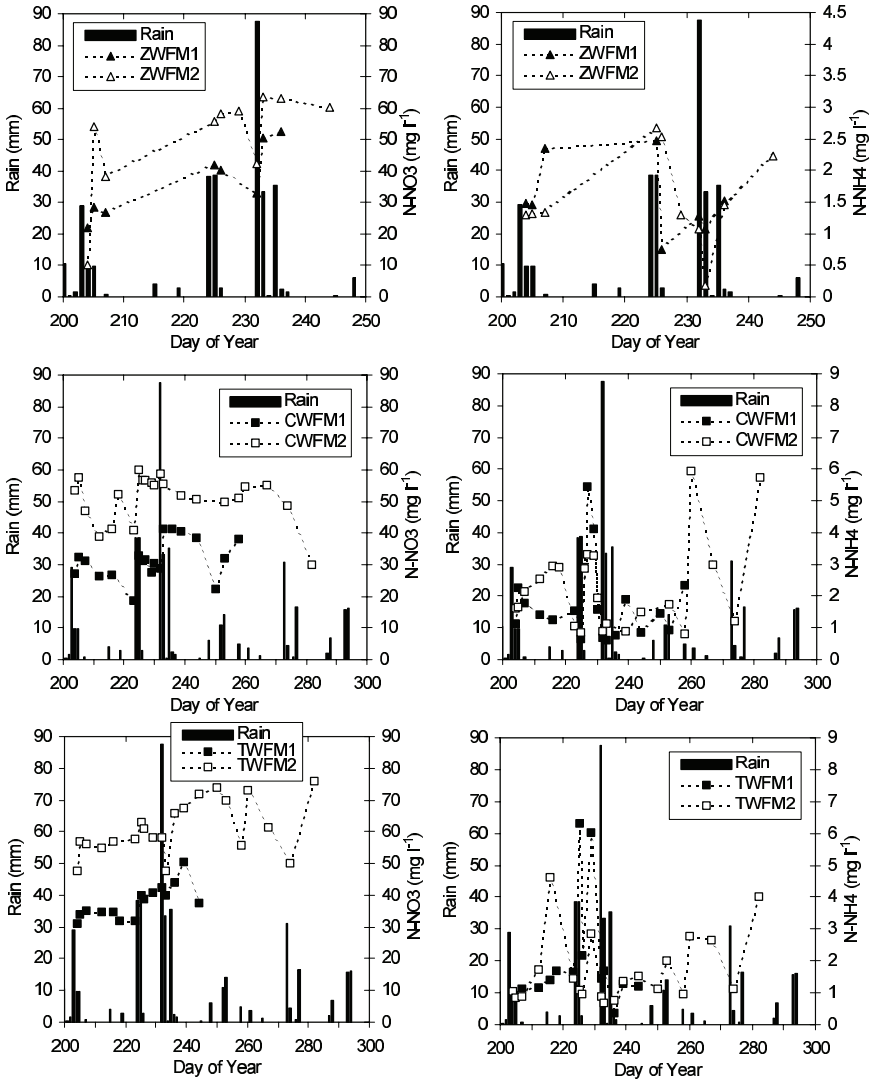

Figure 8.11. Measured $N - NO_3^-$ (mg l^{-1}) and $N - NH_4^+$ (mg l^{-1}) fluxes with the different fluxmeters and daily rainfall (mm). The ZWFM acronym represent the non-suction flux meters, CWFM are suction fluxmeters using a capacitance chamber for the water flux measurement, and TWFM is a suction fluxmeter with a small tipping bucket.

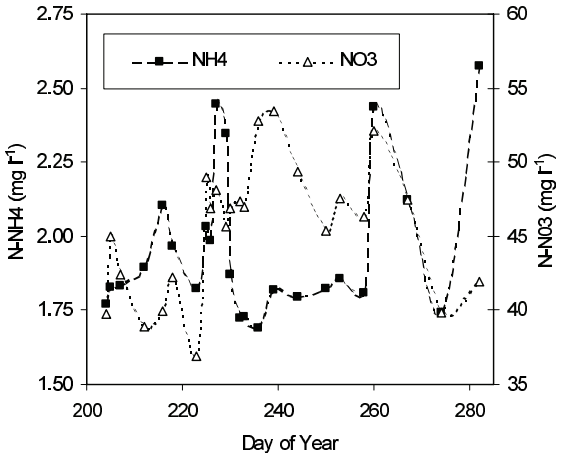

Figure 8.12. NO_3^- (mg l^{-1}) and NH_4^+ (mg l^{-1}) fluxes obtained from averaging the normalised data for each fluxmeter and multiplying by the average standard deviation and adding the average NO_3^- (mg l^{-1}) and NH_4^+ concentration.

each drainage event has a slight increase in concentration as the water flux becomes lower.

Soil temperature and soil moisture content show some similarities with the temporal pattern of measured NO3 concentrations as indicated by the product of f_T and f_M (Figure 8.15). The soil moisture content is directly determined by water flux and this has thus to be interpreted with care. Nevertheless, this bodes well for application of a simple model that uses soil temperature to indicate the amount of nitrogen that is mineralised and thus available either to be taken up by plants, or leach out of the rootzone.

8.4.6 Modelling

Nitrate is generally considered as a nonsorbing solute. However using a k_d and a k_a of zero in equations 8.3 and 8.4 resulted in a mismatch between model predictions and observations. Furthermore in the volcanic soil on Tongatapu that displays both cation, as well as an anion exchange capacity, we choose to determine the apparent water contents from a linear regression of the natural logarithm of the concentration $C_{w,o}$ versus the measured cumulative outflow as suggested by *Steenhuis et al.* [1994] for three distinct episodes of drainage so that W_a and W_d can be found from:

$$W_a = \left[\frac{rM^0}{exp\,(b)}\right] \tag{8.12}$$

$$W_d = \frac{-1}{\alpha} \tag{8.13}$$

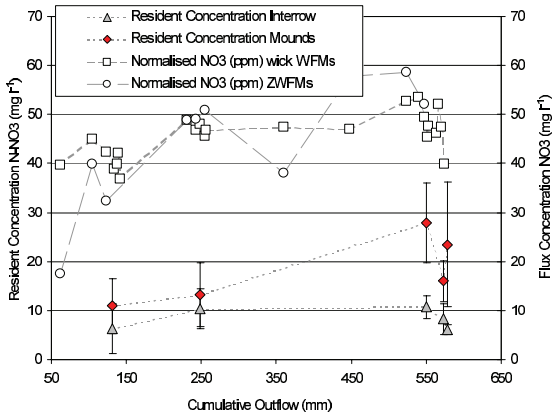

Figure 8.13. Resident and flux NO_3^- concentrations (mg l^{-1})

where b equals the intercept with the y–axis and α the slope of the regression line as shown in Figure 8.16. The values for W_a and W_d are displayed in Table 8.2.

Table 8.2. W_a and W_d obtained from the α and beta coefficients from the linear regression as shown in Figure 8.16

Cumulative Outflow				
100-150	alpha	-0.00403	Wd	248.14 (cm)
100-150	b	4.23	Wa	0.91 (cm)
220-260	alpha	-0.00196	Wd	510.20 (cm)
220-260	b	4.34	Wa	0.82 (cm)
520-580	alpha	-0.00409	Wd	244.50 (cm)
520-580	b	6.14	Wa	0.14 (cm)
Average			Wd	334.28 (cm)
Average			Wa	0.62 (cm)

The empirical values thus obtained for W_d are unrealistic. The slope of the linear regression α is low, as the flux concentrations are quite constant. The NO_3^- flux concentrations seem to be not only dependent on an initial solute concentration in the rootzone (that is hypothised to decrease in time), but also on an amount of NO_3^- available for leaching, that seems to be replenished continuously. This result may be related to the tropical conditions and the wet soils. Nevertheless, for the moment we do not have any means to show otherwise, we use the these values for W_d for further analysis. We caution however, that further investigation on the deriviation of these W_d values is needed.

The fraction of predicted and measured NO_3^- flux concentrations expressed as the fraction of initial solute concentration is given in Figure 8.17 for the three main period of drainage. All panels show a drainage event with a cumulative outflow of 100 mm. This may be an overestimation (see Chapter 5) although most 'surplus' drainage was collected in the intervening

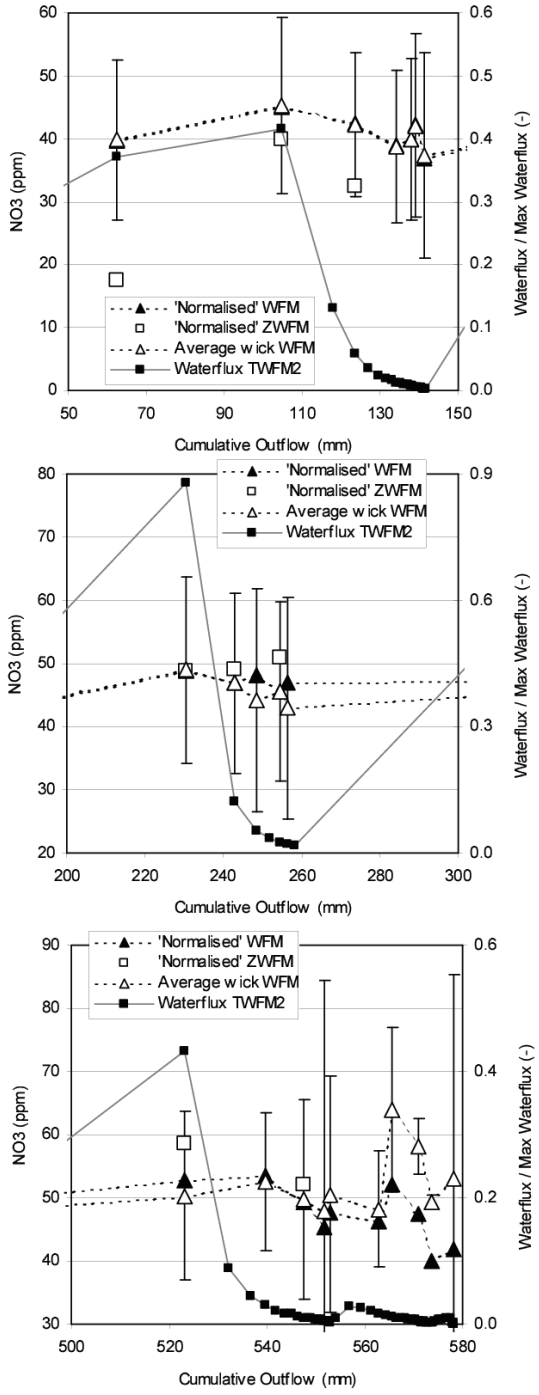

Figure 8.14. Cumulative outflow of TWFM2 plotted against water flux measured with TWFM2 and averaged and 'renormalised' NO_3^- flux concentrations (mg l^{-1}) during three drainage events. The ZWFM acronym represent the non-suction flux meters, CWFM are suction fluxmeters using a capacitance chamber for the water flux measurement, and TWFM is a suction fluxmeter with a small tipping bucket.

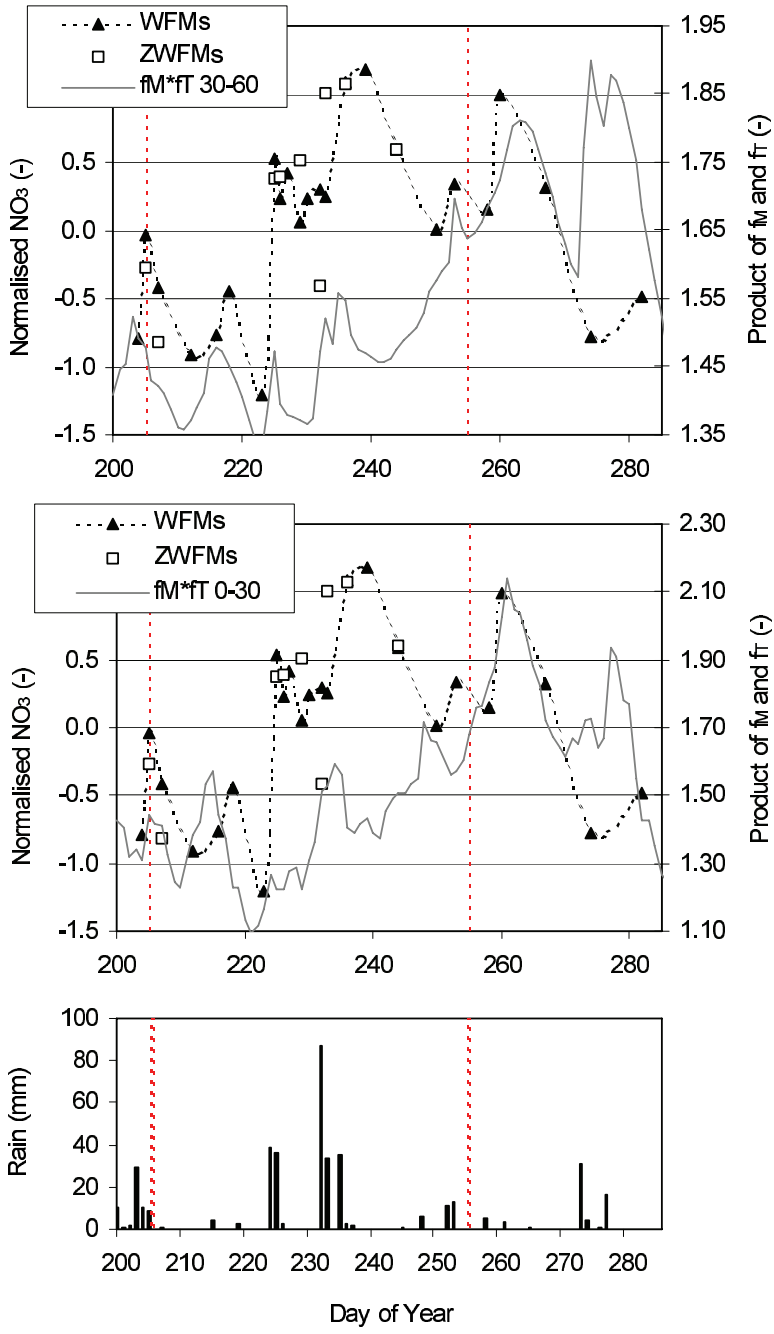

Figure 8.15. Normalised NO_3^- compared to the product of f_M and f_T at 0-30 and 30-60 cm and daily rainfall

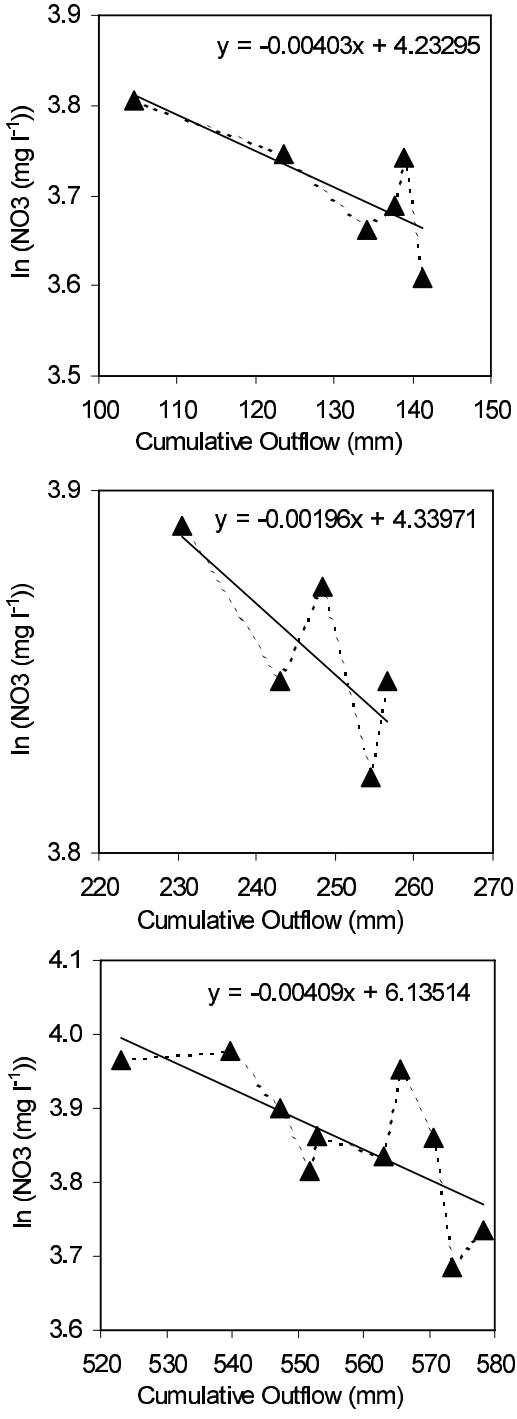

Figure 8.16. Linear regression of the natural logarithm of the NO_3^- flux concentration vs. the cumulative outflow to obtain the slope of the regression line α and the intercept with the y axis b to obtain the apparent water contents during adsorption and desorption

dry periods in between rains due to the suction exerted by the wick. The modelled NO_3^- flux concentrations using the soil temperatures at 15 and 45 centimetres (0-30 and 30-60) show a similar peak as can be observed in the measurements at around 135 mm (top panel). In the middle panel we observe that both the temporal pattern of the measured $C_f(NO_3^-)$ and the $C_f(NO_3^-)$ modelled at 0-30 cm change at around DOY 250. However, it is clear that the measured $C_f(NO_3^-)$ is not in agreement with the modelled $C_f(NO_3^-)$. The lowest panel is characterised by two increases and subsequent drops in $C_f(NO_3^-)$. The predicted increases and drops in $C_f(NO_3^-)$ are in agreement with the measured $C_f(NO_3^-)$. However the initial and pattern of $C_f(NO_3^-)$ is predicted to increase by the model, while the measurements suggest a decrease of $C_f(NO_3^-)$. So while the model seems to capture some of the variability in observed $C_f(NO_3^-)$, especially concerning the peak and drops observed in the measurements, it generally underestimates the $C_f(NO_3^-)$ and its temporal pattern at the initial stages of drainage. In the third panel the general pattern of decrease in $C_f(NO_3^-)$ is not captured by the model.

We note that most of the variation introduced in the modelled $C_f(NO_3^-)$ results from changes in soil temperature. The mismatch between model and measurements at the initial stages may be explained by the concentration of the NO_3^- that is present in the deeper soil layers immediately above the fluxmeters. These layers are not explicitly taken into account in the model. A part of the explanation may be that during a drainage event, the soil solution that was drawn towards the flux meters by the suction exerted by the wick during the preceding dry period, may initially contribute to the observed concentrations when the water potentials decrease. However, since such large quantities of drainage are registered so fast after the rain fell, it may also be expected that the $C_f(NO_3^-)$ would be determined by the drainage directly passing through the soil. It is therefore interesting to note that the $C_f(NO_3^-)$ registered by the Z–WFMs suggest a similar pattern for the first and the third drainage event, while they suggest a general increase in $C_f(NO_3^-)$ for the second event. Nevertheless, we can conclude that a part of the variability, and the temporal pattern of $C_f(NO_3^-)$ are determined by abiotic processes governed by soil temperature.

The effect of soil temperature on mineralisation rate and thus the amount of NO_3^- in soil solution is directly translated in the $C_f(NO_3^-)$ observed at 1 m depth due to the fast flow of water and solutes through the soil.

8.4.7 Fluxmeters and agricultural management

Strategies for agricultural management can be evaluated using modelling of alternative scenarios (for example see *Vanclooster et al.* [2000, 2002]). This becomes problematic in areas with a lack of soil physical measurements needed as input data and where the actual processes are not yet identified. For the management of groundwater in such cases we need (additional)

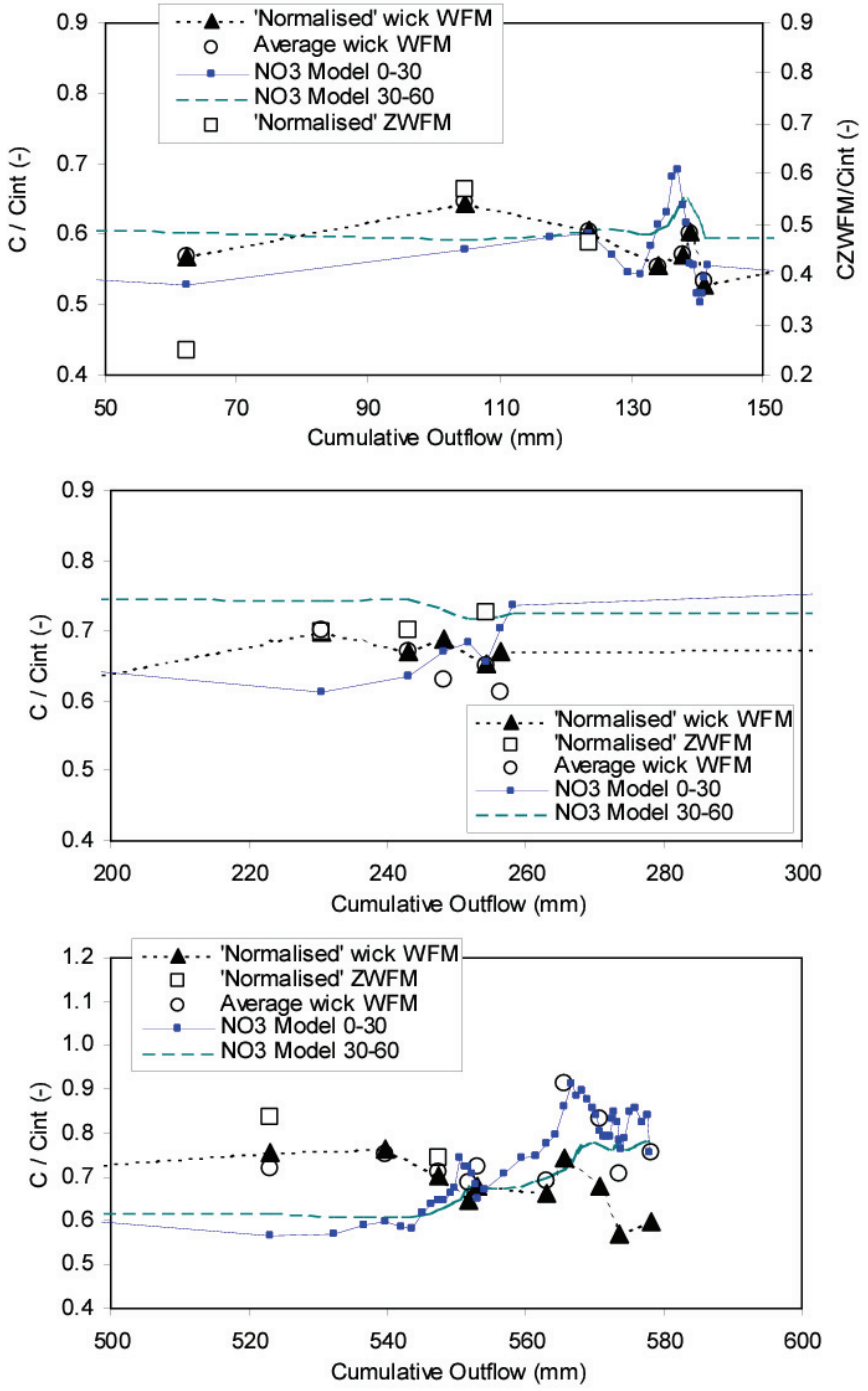

Figure 8.17. Modelled and measured NO_3^- flux concentrations expressed as the fraction of initial solute concentration for the three main periods of drainage

practical tools that allow quantifying the amount and quality of the drainage water that is leaching out of the root zone. This monitoring information can then function as an early warning for groundwater pollution and is essential to avoid possible risks of groundwater pollution. Most important, if these tools are to be used on farms, they have to be reliable, robust and easy to operate. These tools can for example be used on remote sites or farms where irrigation and fertiliser use needs to be optimised. Flux meters [*Gee et al.*, 2003] are such tools.

If we assume that the average concentration during the period up to DOY 250 ranges between 30 and 60 mg l^{-1} NO_3^- we can make a rough calculation of the NO_3^- that has leached out of the root zone before the plants have grown large enough to utilise the fertiliser. A total of 240 mm with a concentration of between 30 and 60 mg l^{-1} NO_3^- yields a total leaching of between 72 to 144 kg NO_3^- per hectare. This is more than the applied amount of 62 kg NO_3^- per hectare by about 45 kg NO_3^- per hectare. A possible explanation is the spatial variability introduced by the mounds, as leaching of fertiliser will predominantly occur beneath the mounds. The mounds (with a diameter of roughly 50 cm) occupy about 6% of the total surface area. Mineralisation of initially available soil nitrogen may have been important as well. For example, if the Guinnea grass that is ploughed in at the start of the season would mineralize over the next year, a large pool N would become available. We measured the dry matter yield of the Guinnea grass in a 4 m^2 plot, and found this to equal 3.3 kg m^2. If we assume an N content of 10 g kg^{-1} of dry matter (compare to *Aganga and Tshewenyane* [2004]), we obtain a pool of 330 kg N ha^{-1} that could be mineralised over the next year. In any case, it is clear that high amounts of N have leached before the plant has developed a root system that is large enough to utilise the nitrogen.

We can conclude that siginficant amounts of nitrates leach out of the rootzone with current agricultural practices. As a management option we therefore suggest to allow for mineralisation in nutrient budgetting, delay inorganic fertilisation in time, and/or avoid the first N application.

8.5 Discussion

We introduced preferential flow phenomena attributed to the macroporous structure of the soil to explain our observations. We had several reasons to use preferential flow concepts to explain our data: specific water retention properties of the soil, the high values for saturated hydraulic conductivity through this heavy clay soil, field evidence of bypass flow from dye tracer experiments, observations and explanations of micro–aggregation [*Pochet et al.*, 2006], shrinkage of the soil, and our inability to describe solute transport with classical convection dispersion equation. We were able to explain, at least

part, of the fluctuations observed in the leaching of NO_3^-. The empirical method of *Steenhuis et al.* [1994] we used yielded unrealistic values for W_d. At present we do not have a satisfactory explanation for this, but it is related to the slope of the linear regression α being low, as the flux concentrations are quite constant. In fact, a straight line to describe the observations of Figure 8.17, would already give, to some extent, a satisfactory description. Our work, however, suggest that the variations around this straight line are goverend by rainfall flux and soil temperature.

Duwig et al. [2003] found that the deterministic model WAVE [*Vanclooster et al.*, 1996] performed better during wetter years than dry years, and that the predictive capability of the model was limited. They concluded that 'under such wet conditions (...) fluxes seemed to be mostly a function of climate'. We may draw a similar conclusion here.

Repacking of the soil above the fluxmeters may have resulted in erroneous measurements of water and N fluxes. Soil disturbance and subsequent repacking of the soil may have stimulated additional mineralisation of soil organic matter resulting in increased nitrification as the soil was wetted. This would have led to increased leaching of nitrogen. This is supported by work of *Bergstrom* [1987] who measured threefold higher nitrate concentrations in drainage water of repacked lysimeters compared to undisturbed monolith lysimeters.

Soils derived from volcanic soils often exhibit an anion as well as a cation exchange capacity. The clay soil derived from volcanic ash studied here has a cation exchange capacity of 50 $\text{cmol}_c{}^*\text{kg}^{-1}$ (see *Pochet et al.* [2006]). Anion adsorption was not measured. The values reported for phosphate retention were reported in Table 5 of *Pochet et al.* [2006]. The values for phoshporus retention equalled $\sim$ 40 %). In young volcanic soils (Ansosols) the phosphate retention reaches 75%. In this more strongly weathered soil, this would suggest that the anion exchange capacity would not be that high either. However, *Maeda et al.* [2003] reported that they did not observe a retardation of NO_3^- leaching at 1 m depth that would have been related to the high anion exchange capacity of the Andosol they were working with. *Maeda et al.* [2003] attributed this to 'uneven water flows caused by the presence of aggregates' so that 'percolating water tends to pass the small intra–aggregate pores'. Similar to [*Maeda et al.*, 2003] we haven not observed a retardation of NO_3^-. The leaching of NH_4^+ shows some similarities to the leaching of NO_3^- (Figure 8.12) and thus also seems to be influenced by the product f_M and f_T at 0-30 and 30-60 cm.

Recent studies have focussed on measuring local soil water–flux under steady-state constant flux infiltration and local solute mass–flux using the change of impedance as measured with TDR probes that allow to measure a change in water content as well as a change in impedance [*Si and Kachanoski*, 2003]. Both TDR and WFMs give measurements at a local scale. For future studies it would be useful to compare the results obtained by these

measurement methods as it may guide in scaling up towards field scale flux concentrations and its variability. Possibly through the installation of more fluxmeters in combination with geophysical tools such as electric ressisivity tomography, or ground penetrating radar.

8.6 Conclusions

We have presented measurements and predictions of the flux concentration of nitrate. The predictions were in agreement with timing of the peak and subsequent drop of the $C_f(NO_3^-)$ observed by the fluxmeters. However the model clearly underestimated the concentrations and temporal pattern of the initial stages of drainage. The model also failed to capture the general pattern in $C_f(NO_3^-)$ observed during the last drainage event. Nevertheless, it appears that a part of the temporal pattern of $C_f(NO_3^-)$ is determined by abiotic processes governed by soil temperature and soil moisture. There is some indication that the effect of soil temperature on the mineralisation rate and thus the amount of NO_3^- in soil solution is directly translated in the $C_f(NO_3^-)$ observed at 1 m depth due to the fast flow of water and solutes through the soil. However, the current description lacks detail since we could not incorporate a good description of the exchange processes between the soil exchange complex and the soil solution, as well as the mineralisation of the Guinnea grass that potentially presented a large pool of organic N available for mineralisation. These processes would need to be included and evaluated to identify the controls that determine the leaching of nitrates observed at depth.

Based on the observations, it seems likely that a split application of fertiliser, preferably after a heavy rain event should improve the effectiveness of the fertiliser. This would mean a lower risk of leaching of $N - NO_3^-$ early on when the plants are small. If properly timed with plant development, a reduction in the amount and thus cost of fertiliser would follow. Economically this could be beneficial to the farmers, especially in this region where fertiliser prices are among the highest in the world [*FADINAP*, 1999]. The farmers win, and the environment benefits. Using direct measurements of the quality and quantity of drainage flux helps to define more sustainable agricultural practices.

One of the most pertinent challenges lies in the incorporation of preferential flow phenomena into models that describe water and nutrient transport in the soil.

Part III

Climatic Impacts - Island Scale

Chapter 9

Hydrogeology, Freshwater Lenses, Recharge, Wells, and Transfer Times

Abstract The main well field on Tongatapu, Mataki'eau, supplies water to the capital of Nuku'alofa. Using data obtained from the Tongan Waterboard, a characterisation of the travel times through the soil, vadose zone, and the mixing of recharge with the lens became possible. The data includes 1) salinity measurements of 21 monitored and pumped wells, 2) several profiles of salinity through the freshwater lens, as measured at monitoring bores located in, or in the vicinity of, the wellfield, and 3) some information on the pumping rates of the different wells. We used the delayed response of the variations in salinity to the variation of rainfall to determine hydrogeologic characteristics of the aquifer with transfer function theory. We defined an objective function to minimize the error between observations and a log-normal transfer function model linking rainfall and salinity variations. The minimisation of the objective function through a simple inverse procedure allowed describing the fluctuations in salinity with the variations in rainfall. The hydrogeologic characteristic is essentially a combination of vertical travel times trough the soil and vadose zone, plus the mixing time of the recharge water with approximately the top 1 meter (the depth of pumping below the water table) of the freshwater lens.

Generally this approach gave a good agreement between model and measurements. The minimum error of the objective function was successfully obtained for most wells with the inverse procedure. For some wells, due to a lack of data, or inconsistent temporal pumping pattern, the optimal parameter ranges were not clearly defined.

Nevertheless, we were able to show that a positive correlation existed between μ and σ indicating the importance of increased spreading with larger travel times. The peak of the probability density function ranged between 8 and 305 days. The depth of the wells was not related to the model parameters, or obtained transfer times. The average salinity of the well–water showed a weak positive correlation with μ, and a weak positive correlation with the absolute value for the scaling factor α. Similar relations could be observed by the location of the wells with respect to the lagoon, suggesting the occurrence of faster horizontal flow rates going towards the lagoon. The error of the objective function was larger for wells closer to the lagoon, possibly indicating the stronger influence of tidal fluctuations on the variation in well–water salinity.

9.1 Introduction

Coastal aquifers around the world suffer from salt water intrusion caused by natural as well as human-induced processes [*Oude Essink*, 2001a]. Human interferences that threaten coastal lowlands include mining for natural resources (water, sand, oil and gas) and land reclamation that leads to subsequent subsidence. Coastal aquifers are affected by mean sea level (MSL). The present best estimate predicts a MSL rise of 0.50 m for the coming century [*Oude Essink*, 2001a]. It is thus expected that the salinisation of coastal aquifers will accelerate. Consequently, the availability of fresh groundwater resources at coastal areas will decrease, putting serious constraints on present populations and future coastal development. It is for this reason that the amount of research work on the intrusion of seawater in coastal or island groundwater systems is increasing.

Sea water intrusion is reported for areas all around the world, including for example, Mexico [*Halvorson et al.*, 2003], Greece [*Lambrakis and Kallergis*, 2001], and Cypress [*Ergil*, 2000]. Salt water intrusion is also a severe problem in several islands located in the Pacific region. Salt water intrusion has been reported for Kiribati, Kingdom of Tonga, Salomon Islands, Fiji, Hawaii, amongst others (see SOPAC website *www.sopac.org*). One of the main reasons for salt water intrusion, or local upconing, is (over) pumping at well sites.

The leaching of chemicals used for agriculture pose another threat to coastal water systems. In the previous Chapters leaching of N out of the rootzone has been studied at the field scale. Deep drainage moves water and solutes towards the freshwater lenses of the island. One of the main aims of this thesis is to elude some of the risks posed by the agricultural practises on the quality of the freshwater resources of the island. If we wish to do so, we need to move up towards the island scale. At this scale we can effectively connect the processes that occur in the soil, the vadose zone, and the limestone aquifer, with the saturated groundwater zone.

So, the purpose of this Chapter is to provide a hydrogeological characterisation of the aquifer medium and the recharge processes which is essential 1) to connect the hydraulic behaviour of the rootzone and the vadose zone with the saturated zone in relation to the leaching of agrichemicals and 2) to mediate and manage effects of salt water intrusion. Flow and transport of water and solutes towards the groundwater occurs through the voids of a heterogeneous medium that encompasses the soil, vadose and saturated zone. The heterogeneity of the medium that is imposed on the flow and transport processes lies at the center of the current research in soil physics [*Vogel and Roth*, 2003]. The discrepancy in the values of hydraulic parameters obtained at different scales was illustrated by *Javaux* [2004]. The near-saturated ends of the hydraulic conductivity curves obtained at the 'Kopeky ring' scale were about a factor 4 lower compared to the hydraulic

conductivity obtained at the monolith scale [*Javaux*, 2004]. However, the water retention curves where relatively comparable at near saturation for both scales (same θ_s). This was explained 'by the fact that the water retention curve is a static property of the porous medium', whereas the 'hydraulic conductivity curve characterises a dynamic process which is tremendously dependent on pore connectivity and continuity' [*Javaux*, 2004]. *Vogel and Roth* [2003] point out that it seems to be the rule 'that soils and aquifers are structured at any scale'. Clearly, this affects solute transport. Earlier, transport experiments under saturated conditions led *Neuman* [1990] to propose a universal power law to scale longitudinal dispertivities of aquifers. *Neuman* [1990] showed that for geological media both the hydraulic conductivity and the dispersivity increase approximately with a power of the observation scale.

Specifically, the scale effect on the hydraulic conductivity in fractured and karstified limestone aquifers was presented by *Kiraly* [2002], who identified the effects of pores and microfractures, macrofractures and the effect of the karst network, going from laboratory, through borehole, to basin scale. *Whitaker and Smart* [1997] showed a log-linear relationship between annual rainfall and the mean island effective hydraulic conductivity for 14 limestone islands distributed through the Bahamian Archipelago. *Whitaker and Smart* [1997] note however, that effective hydraulic conductivity may also be directly related to island size, since larger freshwater lenses, and fresh-saltwater mixing zones, expose more bedrock to dissolution.

9.2 Materials and Methods

9.2.1 Aquifer properties

The water table of Tongatapu's freshwater lens is extremely flat. It is influenced by tides, sea level change, barometric pressure, recharge, pumping and drought. Sea water level is mainly influenced by tidal processes but is also affected by wind that causes build up of water masses of about 0.2 to 0.3 m at one side of the island and in the lagoon [*Falkland*, 1992]. *Furness and Gingerich* [1993] showed that the water level of a well in Tonga show a semi-diurnal response to the tidal constituents. *Furness and Helu* [1993] found that the barometric effect is of larger magnitude than the tidal pattern. *Hunt* [1979] presented 39 measurements of water table height in wells equally distributed over the island. Average water level above MSL was 0.32 $\pm$ 0.11 m.

In Tongatapu the permeable limestone aquifer is overlain by a clay soil derived from volcanic ash with a variable thickness generally declining from 5 m in the west to 0.5 m in the east of the island. The filtering of the water that percolates towards the freshwater lenses depends on the hydraulic conductivity and the water holding holding capacity of the vadose zone. This

in turn, in combination with the soils chemical characteristics, determines the flux of solutes (e.g. agrichemicals) that are transported with the drainage water.

Freshwater lens geometry is affected by recharge, hydrogeological characteristics of the aquifer and pumping well locations. Results from a sensitivity analysis by *Griggs and Peterson* [1993] show that the depth of the 50% salinity contour was most sensitive to permeability, and the transition–zone thickness was most sensitive to dispersivity. The transition–zone thickness increases with increasing dispersivity values, and is most sensitive to changes in the transverse dispersivity. For a given recharge rate, the depth of the 50% salinity countour will decrease with increasing hydraulic conductivity.

Several authors have estimated the recharge towards the freshwater lens on Tongatapu. The percentages of recharge these studies have calculated are listed in Table 9.1. The estimates or recharge range from 5 to 35 % with a generally adapted average estimation of 30 %. *Furness and Helu* [1993] summarized the available recharge estimates (and also reported on the work of *Kafri* [1989]; *Hasan* [1989]). *Furness and Gingerich* [1993] could not estimate the annual recharge due to a lack of rainfall during the measurement period. It was however resolved from the residual fluctuation derived from the subtraction of the smoothed well water level signal with the smoothed tide gauging signal, that an individual recharge event of less than 13 mm may pass undetected using water level data.

Table 9.1. Reports containing previous recharge estimates.

Document	Recharge estimates	Method
Pfeifer and Stach [1972]	5 to 15 %	Previous experience
Lao [1978]	25 %	Water Balance
Hunt [1979]	25 to 30 %	Callibration of sharp interface steady state model
Kafri [1989]	35 %	Chloride ion ratio
Hasan [1989]	20 %	Monthly water balance
Falkland [1992]	30 %	Water balance model 44 years of data
Furness and Helu [1993]	-	Summary of previous estimates
Furness and Gingerich [1993]	no estimate not enough rain	Hydrographs, pluviographs, tide gauging, barometer

Based on a pump test the hydraulic conductivity of the limestone was calculated by *Hunt* [1979] to be 1.5 cm s^{-1} (corresponding to 1296 m day^{-1}). This relatively large value of K related to the extremely porous nature of the coral limestone (especially since K was derived for the horizontal flow direction). *Hunt* [1979] reported this to be in the top end of the hydraulic conductivity range typical for coarse, clean sands, as reported by *Harr* [1962]. However, as a reference, representative values of physical parameters associ-

ated with various types of aquifer materials are presented in Table 9.2 (based on *Timlin et al.* [2003]). We find that the hydraulic conductivity calculated here is above any of the aquifer materials listed in Table 9.2. *Furness and Gingerich* [1993] reported 'from modelling of the aquifer and examination of drill-hole cores and exposures of rock in quarries, caves and cliffs it is apparent that the porosity and specific yield of the aquifer is very high. The latter probably averages as much as 0.4 (40%).' Limestone aggregate samples were obtained by *Harrison* [1993] to determine aggregate properties in relation to quarrying of the limestone for building and civil engineering purposes. Due to the weakness of the aggregates, and the ease by which they abrade, the limestone aggregates failed to meat specifications for concrete and road stone commonly used [*Harrison*, 1993]. *Harrison* [1993] further reports that the limestone is highly porous with a low density and that it contained large amounts of absorbed water. The physical quality (with respect to density, porosity, strength and durability) of the aggregates was also reported to be extremely variable. The limestone was found to be very pure, with percentages of $CaC0_3$ over 98.5%.

Table 9.2. Representative values of physical parameters associated with various types of aquifer materials. Taken from Table 4 in *Timlin et al.* [2003]. ^{v} - indicates vertical measurement of hydraulic conductivities, ^{h} - indicates vertical measurement of hydraulic conductivity, ^{r} - indicates measurement on a repacked sample.

Material	Porosity (%)	Specific Yield (S_y, %)	Hydraulic Conductivity (m day^{-1})
Coarse Gravel	28^r	23	150^r
Medium Gravel	32^r	24	270^r
Fine Gravel	34^r	25	450^r
Coarse Sand	39	27	45^r
Medium Sand	39	28	12^r
Fine Sand	43	23	2.5^r
Silt	46	8	0.08^h
Clay	42	3	0.0002^h
Fine-grained sandstone	33	21	0.2^v
Medium-grained sandstone	37	27	3.1^v
Limestone	30	14	0.94^v

9.2.2 Wellfield Dataset

The present Chapter, and Chapters 10 and 11 use very valuable data, obtained through the diligent monitoring efforts of the Tongan Water Board (TWB) and the Ministry of Lands, Survey and Natural Resources, from the main well field of Mataki'eau. Because of its importance to the water supply for Nuku'alofa, the salinity measurements at the Mataki'eua wellfield have been carried out (although irregular) over a long time period. The data we use here include 1) salinity measurements of 21 monitored and pumped

wells, 2) several profiles of salinity through the freshwater lens, as measured at monitoring bores located in, or in the vicinity of, the wellfield, and 3) some information on the volumes pumped at several wells, as well as some water table heights. We use this information to derive transfer functions through the whole soil-limestone aquifer continuum for the pumped wells.

9.2.3 Wellfield salinity data

On the whole island of Tongatapu about 240 wells are in use. Depth of the wells has been measured for 90 of those and the depth generally increases from northwest to southeast conforming the general tilt of the island's limestone. The wells on the island include village wells with one or more wells in each village, which pump to an elevated watertank, private wells which are mostly hand dug and not equipped with a motorised pump. However, most pumping is done at the main wellfield of Tongatapu, the Mataki'eua wellfield (see Figure 9.1). A typical well design used for the Mataki'eau wellfield is illustrated in Appendix F.1. Some of the wells were reported to be not operational (e.g. well 118, 121 *Steen* [1995]). Wells in Mataki'Eua and Tongamai wellfield are approximately spaced 150 m apart (Figure 9.2). The wells 121 and 129 are not shown as they lie more inland and are part of the Tongamai wellfield. The Tongamai wellfield was reported to be inactive in October 1995 by *Steen* [1995]. The current status of the Tongamai wellfield is not known, but the data from well 121 and 129 are nevertheless used for the present analysis. Pumping is done from approximately 1 m below the average water level. Pumping data from the well site is scarce. Average pumping rates are about 3 L s^{-1}. Groundwater extraction from the Mataki'eau wellfield was approximated by *Falkland* [1992] to be 5.3 * 10^3 m^3 day^{-1}. We obtained production data from *JICA* [1998]. Data from the TWB shows that monthly water production was quite stable, apart from a slight increase in 1998. The water production for 1996, 1997 and 1998 equalled 5.8 * 10^3 m^3 day^{-1}. However, leakage is reported to be high (above 30 %) for the Tongan reticulation system. Also, when the water production is compared with the metered water, we find that roughly 50% of the pumped water is unaccounted for [*JICA*, 1998].

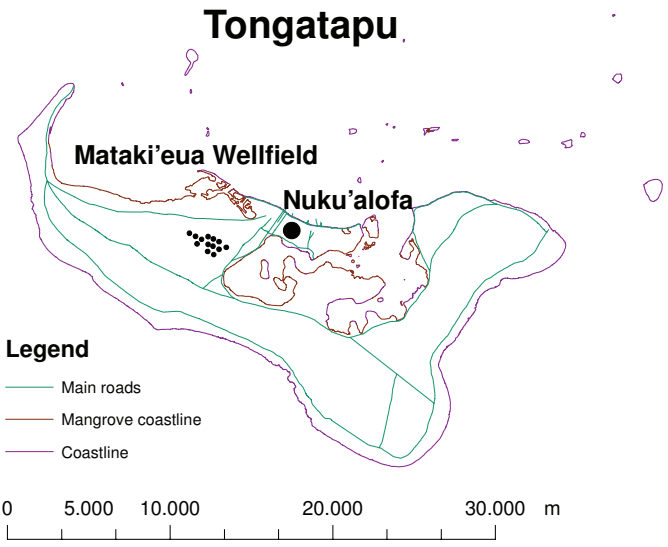

Figure 9.1. The location of the Mataki'eau wellfield on Tongatapu

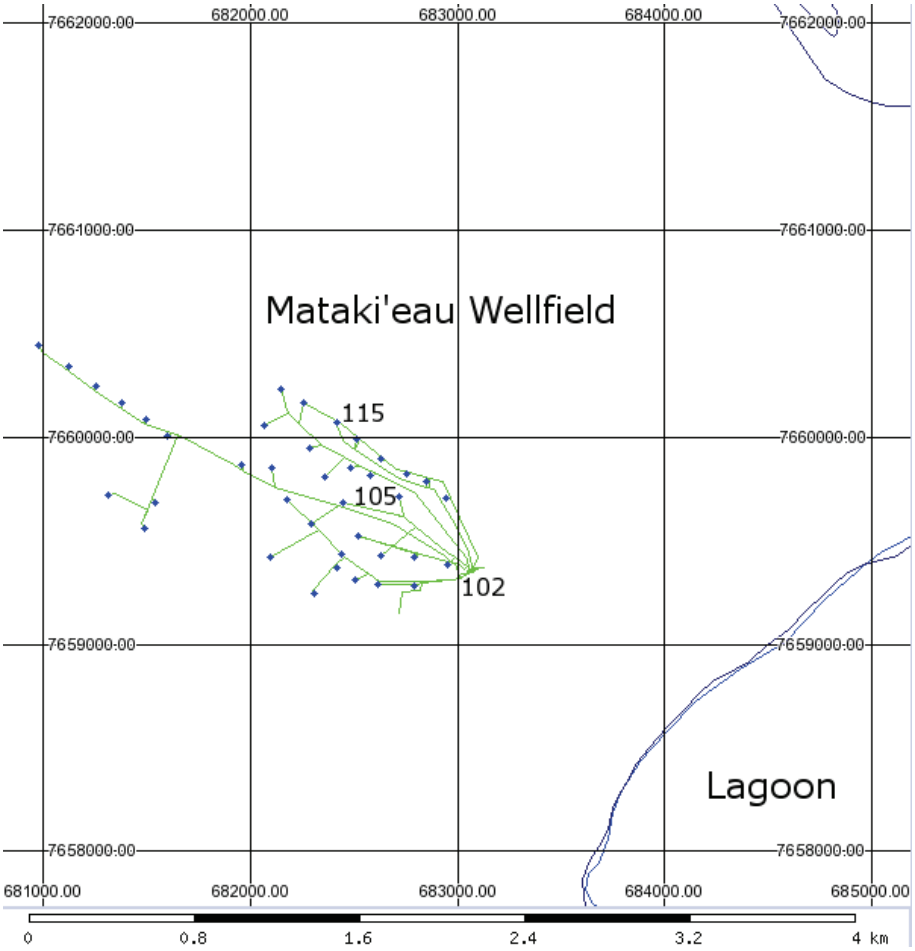

Figure 9.2. The location of the wells in Mataki'eau wellfield and the proximity to the lagoon. Well field spacing is approximately 150 m. The grid represents the Easting and Northing UTM coordinates with a distance of 1 km.

Furness and Gingerich [1993] reported that the pumping at Mataki'Eua has depressed the water table by about 0.25 m in the middle of the well field. According to *Furness and Gingerich* [1993] the water level in one individual well (105) falls about 0.1 meters when the pump is operating. The electric conductivity of the water is inversely proportional to the height of the water table. The relation has a low correlation and conductivity is mostly affected by the time since the last heavy rainfall (see [*Furness and Gingerich*, 1993]). In comparison, *Furness and Gingerich* [1993] noted that 'it was surprising to see on Tongatapu falls of 0.3 m in the fresh water level without a drastic change in the conductivity of the water. Generally a rise of about 10% was noted in monitoring. It was concluded from this evidence that the movement of the transition zone from fresh to salty water is damped'. We suggest that this delay mainly relates to the difference between vertical hydraulic conductivity and horizontal hydraulic conductivity (the latter being much higher in relation to the horizontal deposition of geologic layers). The relation between water table height and salinity was also investigated by *Falkland* [1992] with data taken during three days (6^{th} August, 1990; 11^{th} January, 1991; 1^{st} of March, 1991). As expected, increases in water table elevation were accompanied by expected decreases in salinity of the water at the water table. *Falkland* [1992] also reports on some of the uncertainty associated with the measurements. Most wells at the Mataki'eau wellfield show a decrease in salinity from 1990 to 1991 related to the high recharge during this period. However, it was reported by *Falkland* [1992] that 'some wells (102, 106, 211 and 212) show an increase in salinity during this period. It was noted that wells 102, 211 and 212 all had wind pumps replaced by diesel pumps, which may have caused the increase in salinity. The dates of changeover from wind to diesel power were not determined during this study but could be obtained from the TWB'.

Currently, about 30 wells operate at the wellfield. For this Chapter, the salinity is estimated from electric conductivity (EC, $\mu S.cm^{-1}$) measurements that were carried out sporadically since 1980 and approximately bi-monthly from January 1995 to June 2000. In this study we use measurements made since 1/1/1997 by the TWB. Twenty-one wells were monitored. Maps of the depth to the water table and average salinity in the wells over a 10 year period are presented graphically in Figures 9.3 and 9.4. The maps were obtained from linear interpolation of measurements done in the wells shown in Figure 9.2. The depth of the wells is influenced by the occurrence of relict coral patch reefs at the wellfied. The average salinity shows the occurrence of a salt water wedge extending inland from the lagoon.

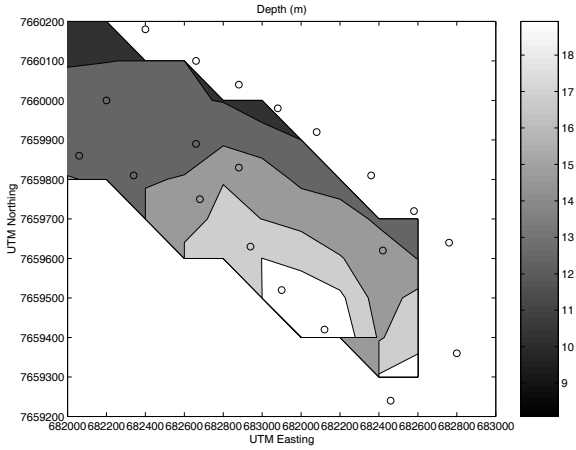

Figure 9.3. Map showing linear interpolation of depth to the water table at the well field. Wells are indicated by circles.

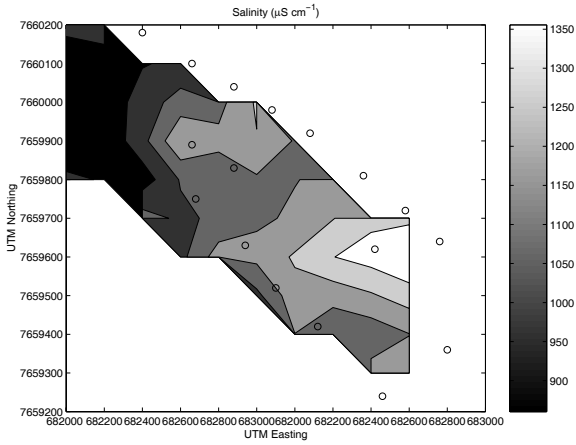

Figure 9.4. Map showing linear interpolation of average salinity at the well field. Wells are indicated by circles.

9.2.4 Monitoring bores and freshwater lens thickness

For a period of three years from 1997 to 2000 with an approximate 3-monthly time step the freshwater lens underneath the island was monitored for electric conductivity and temperature at different depths. Six points and later one additional point were monitored using 5 to 7 bore holes (MBs) at different depths to sample a profile of the freshwater lenses (see Appendix G.1). One point (MB1) was located close to the lagoon. The other points are all located more inland. A polyethylene sampling tube with foot valve was used to

obtain water samples from the monitoring tubes with an internal diameter of 38 mm. When approx. 5 litres had been pumped the electric conductivity of the sample was measured, this was replicated three times, after which the temperature of the water was determined. A dipper was used to measure the depth to the water table. The depth to the base of the tube was determined and compared to the original depth measured after installation. The depth to the water level was also measured [*Falkland*, 1992].

9.2.5 Temporal variations in salinity

From the measurements done in the MBs the depth of the freshwater lens can be inferred. The depth of the freshwater lens can be defined as the depth of potable water defined by the WHO at 2000 μScm^{-1}. From these measurements it can be shown that the thickness of the freshwater lens ranged between 5 to 12 meters and that the lens becomes thinner towards the lagoon (see Chapter 11). The temporal variation in recharge of the lens relates directly to the temporal variations in rainfall. Mixing into the freshwater lens can be derived from the monitoring bores data (not shown). From these data, mixing into the lens can be observed deeper at 5 to 20 m below the water table, while at a certain depth (between 35–40 m) pure sea water is encountered.

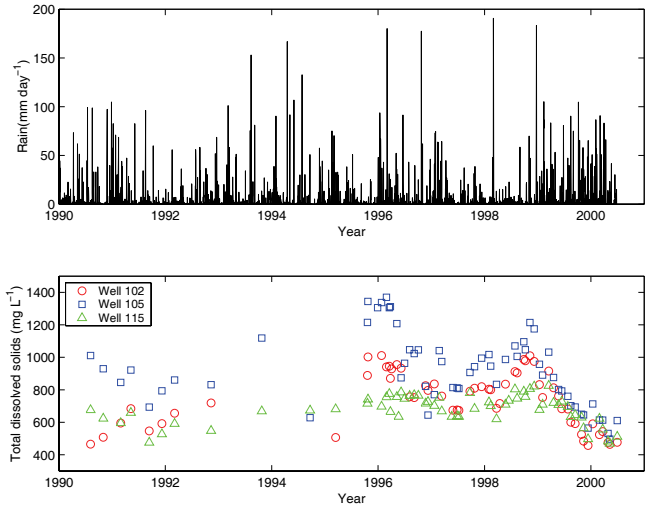

Figure 9.5. Daily precipitation and total dissolved solids measured in 3 (wells 102, 105 and 115) of 21 monitored wells on Tongatapu.

The TDS measurements from wells 102, 105 and 115, indicate a temporal pattern of the variation of TDS that relates to the amount of preceding rainfall. It can be expected, however, that besides hydrogeological factors, pumping rates would also influence the fluctuations in salinity, especially

if the pumps are not continuously operating. Monthly pumping rates of individual wells were reported in *JICA* [1998] for January, February, March, April and June 1999 (data not shown). For these five months, only two wells were reported unoperational for maintenance purposes in the month of June. The average pump rate for this period averaged 2.84 l s^{-1} and ranged between 1.88 l s^{-1} and 4.57 l s^{-1}.

9.3 Modelling

9.3.1 Transfer functions

The TDS of the lens at a certain time is determined by the total mass of solute and the total mass of water in the pumped freshwater layer. If we consider that there exists an equilibrium state for the water lens corresponding to a continuous balance between averaged fresh water input and output and mean sea level, we then expect that every variation in the fresh water input from this equilibrium state will result in a change in the salt concentration. An increase in the rainfall rate would result in a decrease in salinity.

Since the vadose zone between the surface and the aquifer smoothes out the variations of water flux, a transfer-function model can be used to describe the relation between the variation in rainfall and the variations in salinity. Transfer function theory was developed by [*Jury*, 1982; *Jury and Stolzy*, 1982] to simulate solute transport under natural field conditions where substantial variability exists in water transport properties. *Jury* [1982]'s approach derives a distribution function based on the distribution of travel times of solutes from the soils' surface to a reference depth. Here we use the transfer function model in a slightly different setting then originally proposed by *Jury* [1982]; *Jury and Stolzy* [1982]. The transfer-function model describes the convolution of the variations in rain with the variations in the reciprocal of TDS with a daily time step, so that

$$TDS^{-1}(t) - \mu_{TDS^{-1}} = \alpha . \int_{-\infty}^{+\infty} f(t) . \left(P(t-\tau) - \mu_P\right) .dt + Z(t) \qquad (9.1)$$

where:

- $P(t) - \mu_P$ is the variation of rain around μ_P (mm d^{-1});
- α is the scaling factor (mg^{-1});
- $f(t)$ is the transfer function (d^{-1});
- t is time (d) ;

- τ is the lag (d) ;
- TDS^{-1}(t) - $\mu_{TDS^{-1}}$ is the variation of one over TDS around $\mu_{TDS^{-1}}$ ($L.mg^{-1}$);
- $Z(t)$ is white noise (L.mg^{-1});

The integral in 9.1 expresses the convolution between the variations around the mean rainfall ($P(t) - \mu_P$) and the variations around the mean of the inverse of the total dissolved solids (TDS^{-1}(t) - $\mu_{TDS^{-1}}$). For convenience, results are plotted as variations in TDS. Here t is time and t the lag time between rainfall and dilution, α is a scaling factor, f(t; μ, σ) is the transfer function and Z(t) is the residual error.

A log-normal probability density function was chosen for the transfer function $f(t)$ to reflect the transport and mixing of the percolating water as it moves through a porous medium exhibiting a log-normal distribution of pore-water velocities. Hence:

$$f(t;\mu,\sigma) = \frac{1}{\sigma.t.\sqrt{2.\pi}}.\exp\left(-\frac{(\ln(t)-\mu)^2}{2.\sigma^2}\right) \tag{9.2}$$

The model $f(t)$ corresponds to a log normal probability density function where μ and σ respectively correspond to the mean and standard deviation of the log-normal distribution. The peak of the transfer function corresponds to the mode ($\exp[\mu - \sigma^2]$), the median is equal to ($\exp[\mu]$) and the mean to ($\exp[\mu+0.5\sigma^2]$). The use of a transfer function allows us to describe the whole system and the processes occurring in this system in a relatively simple way. Our system is a porous medium through which the infiltrated water moves and it includes the soil, the limestone, and the saturated limestone aquifer to a depth of one meter below water table. The processes in this system include the infiltration of rain water in the soil, the downward movement of this water through the vadose zone, and the subsequent mixing of the drainage water into the freshwater lens to a depth of approximately one meter.

The parameters α, μ, and σ were obtained by minimising the sum of the sum of squared errors of the simulation and each measurement time series of each well. The objective function is obtained by minimizing the sum of squared errors:

$$\phi(\alpha,\mu,\sigma) = \sum_{j=1}^{N}\left(TDS^{-1}_{j,simulated} - TDS^{-1}_{j,observed}\right)^2 \tag{9.3}$$

in which:

- $\phi(\alpha, \mu, \sigma)$ is the objective function ;

- $TDS^{-1}_{i,j,simulated}$ is the inverse of the simulated TDS (Lmg^{-1});

- $TDS^{-1}_{i,j,observed}$ is the inverse of the observed TDS (Lmg^{-1});

- N is the number observations in each well.

The Nelder-Mead multidimensional unconstrained nonlinear minimization algorithm available in MatLabTM was used to minimize the objective function.

9.4 Results and Discussions

9.4.1 Transfer functions

Measured and modelled variations in TDS are given for wells 102, 105 and 115 in Figure 9.6. Differences between the three wells are apparent, but it appears that the transfer function approach used here gives reasonable results. The transfer function model is in good agreement with the variation of the measured TDS. The information contained in the rainfall signal thus seems sufficient to reflect the variation in salinity. The errors of the objective function will be discussed later. The variation in salinity differs between the wells, and the optimal parameters obtained by minimizing the objective function therefore yields different probability density functions (PDF). The PDFs for the individual wells are graphed in Figure 9.7. The thick line represents the PDF that is obtained when all well data is combined and modelled with one transfer function model (see Chapter 10). The occurrence of the peak of the PDF (corresponding to the mode) ranges between 8 and 305 days. The medium and mean lag periods respectively range between 305 and 4912, and 383 and 11572. However we can see that in the histograms of the calculated travel times (Figure 9.8) that the largest part of the wells have a mean travel time below 2000 days, and a medium travel time below 1000 days.

These transfer times are relatively large. Hydrographs of well-level response plotted against daily rainfall by *Jocson et al.* [2002] showed that 'the rate at which water is delivered to the lens is a function of rainfall intensity and the relative saturation of the vadose zone'. This determines the portion of fast flow through preferred flowpaths that bypass the bedrock matrix, with respect to the water that percolates more slowly through the bedrock matrix. *Jocson et al.* [2002] reported significant buffering of recharge to the freshwater lens of Guam, similar processes will influence the recharge here. Nevertheless, *Jones and Banner* [2003a] showed a threshold of rainfall of 190-200 mm month^{-1} before recharge occurs for three different limestone

aquifers, and attributed this to similar climate and geology that produce soils with similar hydraulic properties.

Larger travel times may also be associated with parameters that were obtained from erroneous data, or from wells that are more severely influenced by other processes. Therefore we will now have a closer look at the minimum error obtained for the objective function by the inverse procedure.

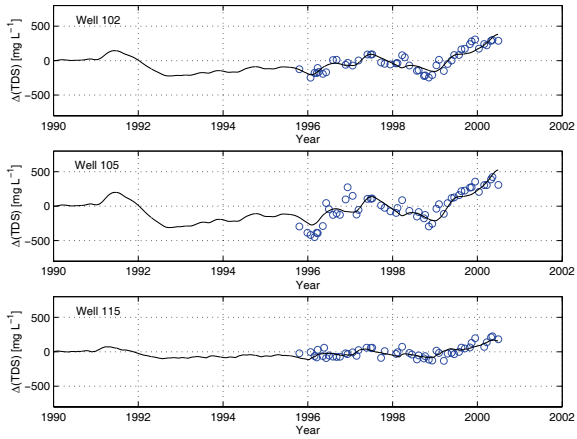

Figure 9.6. Model and measurements of Wells 102, 105 and 115.

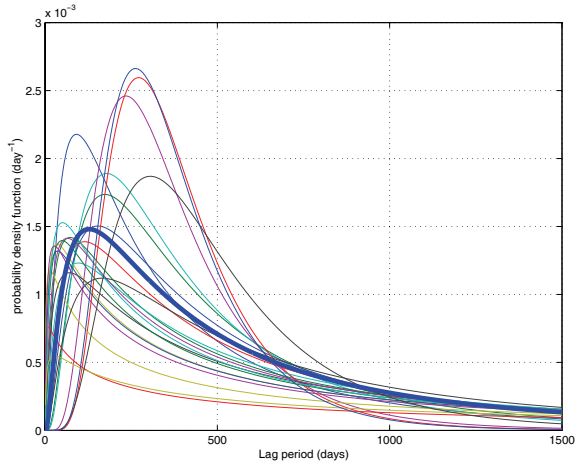

Figure 9.7. The lognormal probability density functions obtained for all the individual wells. The thick line is the probability density function obtained when all well data is combined and modelled with one transfer function model (see Chapter 10).

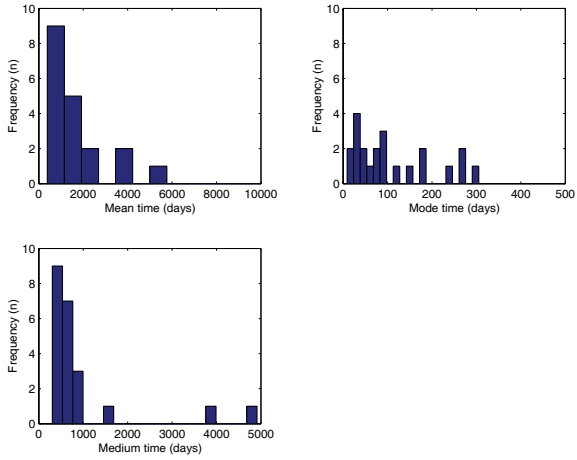

Figure 9.8. The histograms of the obtained mean, mode, and medium travel times for all wells.

9.4.2 Objective function

The uniqueness of the parameters was evaluated by plotting the error surface for a range of parameter value combinations around the minimum error obtained by the inverse procedure. Data were plotted for wells 105 and 115. Values for pairs of parameters and the associated objective function error, as well as the minimum error that was obtained are shown (Figures 9.9 and 9.10). The range of parameter values encompasses a range of probable parameter values. We find no artefacts in the objective function error surfaces. This shows that the minimum error was found by the inverse procedure. The value for μ is most clearly defined as indicated by the short range around the optimal value in both the μ-α as well as the μ-σ. μ relates strongly to the transfer times and corresponds directly to the medium travel time ($\exp[\mu]$). A wider range around the optimal values for σ and α exists. Differences between the error surfaces for both wells, while μ does not constrain α at all at the optimal sigma for well 105, μ does constrain α for well 115.

For most wells the obtained model is in good agreement with the measurements. However, problems of interpretation, and fitting of the parameters give problems for some of the wells. We can choose a threshold value of the objective function beyond which we would dismiss the obtained parameters (compare with Figure 9.12). This could for example correspond to $\tilde{5}\ 10^5$. In that case the data of wells 101, 111 and 105 would be dismissed. Even though the parameter values were well constrained for wells 101 and 105. The well with the biggest error (well 111, see Figure 9.12) did not yield a satisfactory model description of the measurements. Also two wells (118 and 121) have values for μ and σ that are out of the range obtained for the other wells. In fact, both wells 118 and 121 use less data then the other wells for the optimisation (since 1998). Also, the optimal parameters for the wells 118 and 121 were not clearly constrained. It is interesting to note that wells 118 and 121 were reported to be unoperational in October 1995 by *Steen* [1995], in contrast to the other wells reported here. Besides a lack of data, some of these wells were thus possibly not pumped consistently. Nevertheless, presently, we will consider the parameters obtained for all wells.

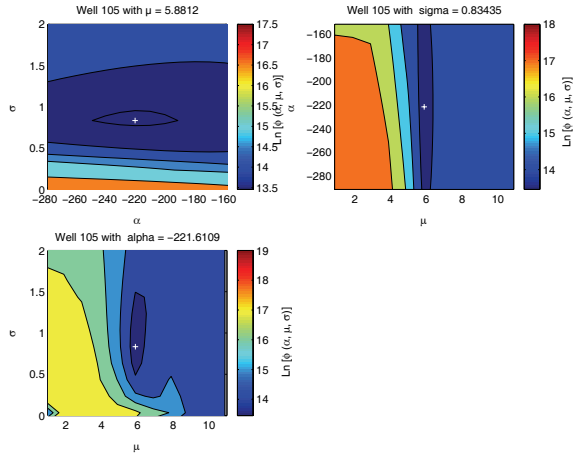

Figure 9.9. Representation of the error surface of the objective function around the minimum error obtained with the parameters for Well 105.

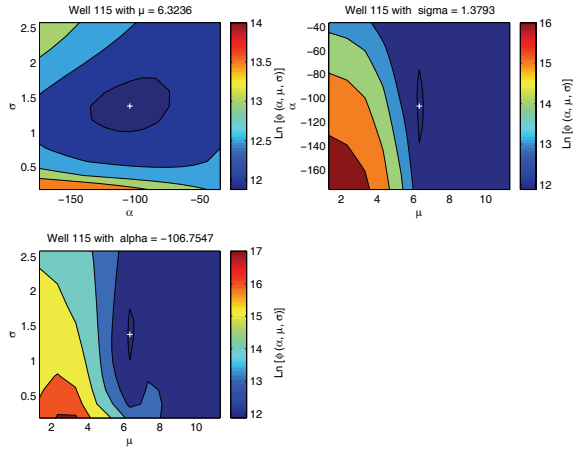

Figure 9.10. Representation of the error surface of the objective function around the minimum error obtained with the parameters for Well 115.

Having found the parameters sets that yield the lowest error of the objective functions, we investigate the relations between the model parameters, and the relation between the model parameters and the minimum error. Figure 9.11 shows that a positive correlation exists between μ and σ. If the travel time is longer (related to a larger μ), and the travel distance is thus longer, this would lead to more spreading, and consequently a larger σ. Consider the following, with a fixed μ, and a σ that increases, the mode of the probability density function will have a slightly higher probability (height of the peak), and will have a shorter lag period. Conversely, with a fixed σ, and an increasing μ, the mode will increasingly have a lower probability of the peak, and a much larger lag period (and be less skewed). So when both μ and σ increase, the mean, medium and mode time associated with the PDF, will change differently (see Appendix H.1. We recall here that the mode is equal to $\exp[\mu - \sigma^2]$, the median to $\exp[\mu]$ and the mean to $\exp[\mu + 0.5\sigma^2]$. The mean of the function increases fastest, while the medium travel time increase exponentially, and the mode increases with $\exp[\mu - \sigma^2]$. So the shape of the function becomes more positively skewed with increasing μ and σ. With higher μ, σ will be larger which relates to a more important spreading associated with longer travel distances. No correlation is found between α and μ and σ.

If we examine Figure 9.12 and compare the relation between the minimal error of the objective function and the obtained parameters, we find that the error appears to be decreasing slightly with increasing μ and with increasing σ. Although, wells 101, 105 and 111 (error larger then $\sim 5\ 10^5$) and 118 and 121, should not be considered here, it appears that for certain wells the inclusion of a longer time period of rainfall decreases the error of the objective function, while this is not the case for others. However, a closer examination is meritted. If the time series are flat without much differentation, no difference will be obtained between large μ's and σ's. No correlation exists between α and the error of the objective function.

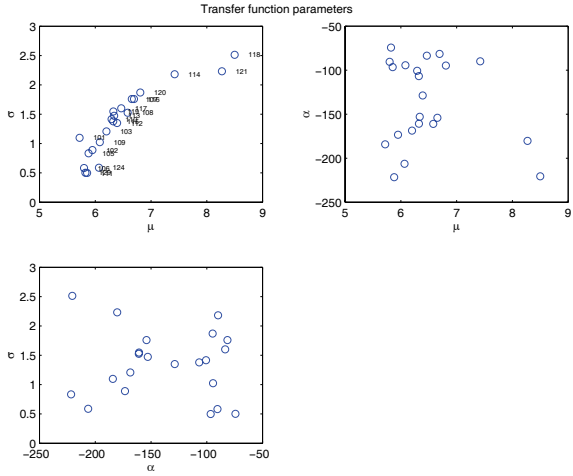

Figure 9.11. Relations between the obtained model parameters μ, σ and α.

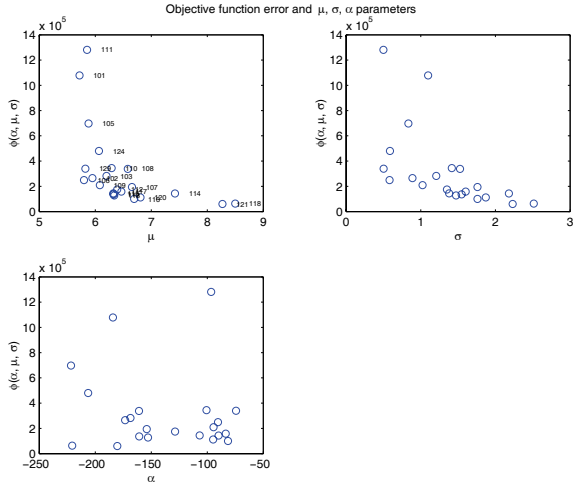

Figure 9.12. Relations between the obtained model parameters μ, σ and α and the objective function error $\phi(\alpha, \mu, \sigma)$.

9.4.3 Spatial relations

The results obtained with the optimal parameter sets obtained for each well can now be investigated more thoroughly in relation to the location of the wells on the island, and the well depth and the average well water salinity.

Each well has a specific capture zone that influences the travel times that are obtained for each well. *Taylor and Person* [1998] showed that the effect of upconing on the size and shape of the capture zone is dependent on the location of the well, related to a 'thinning of the freshwater aquifer thickness and increased groundwater velocities near the coastline' [*Taylor and Person*, 1998]. *Taylor and Person* [1998] also found that near the island center, where the fresh water aquifer is thicker and salt water upconing is less, there was essentially no effect on the capture zone size due to upconing.

In our study, no correlation exists between the depth to the water table in the wells, and the μ and α parameter values (Figure 9.13). So, the vertical conductivity of the soil and vadose zone at the local well does not influence the combined travel and mixing times obtained here. Neither does the redistribution of rainfall induced by the local topography, including the relict reef patches and the lower part of the wellfield, influence the times obtained here. If μ is small, then the travel time is short. If we assume that preferential flow will not occur, this should also mean that the travel time is short. We would then expect a correlation between the depth to the well and μ. This is, however, not the case. So, with no correlation between μ and depth, this could indicate fast flow at large depth and then this could be an index for preferential flow. However, we would then also expect that σ would be small, indicating no spreading but instead flow bypassing the matrix. To investigate this correlaction between μ and σ, we could run the transfer function model of Eq. 9.2 with, instead of $ln(t)$, $ln(t * l/depth)$, where l is a reference depth (e.g. 10 m), and $depth$ the measured well depth.

Interesting relations emerge if we compare the average salinity (μS cm^1) measured in the wells, with the values obtained for μ and α. A weak negative relation seems to exist between μ and average salinity. A clearer relation exist between the scaling factor α and the average measured salinity. Logically, the absolute value of α correlates positively with the average well salinity.

As a proxy for the location of the wells with respect to the lagoon we used the UTM Easting coordinate of each well (Figure 9.14). Average salinity correlates with UTM Easting, but may also reflect differences in pumping, and local hydrogeologic characteristics, while it is expected that UTM Easting coordinate may more clearly reflect the general flow processes towards the lagoon. A weak negative correlation exists between μ and the UTM Easting coordinate. Well 129 lies in the other wellfield, but had a clearly defined minimum error. The water table geometry of the freshwater lens is mound shaped with the highest point above MSL near the center of the island. The potential difference between the height of the freshwater lens at

the middle of the freshwater lens, and the height of the freshwater lens at the lagoon interface, induce faster flow velocities as the lens thins towards the coast [*Taylor and Person*, 1998]. Wells located away from the center will be most strongly affected by the horizontal component of the longitudinal dispersivity. So this may indicate the importance of the increased flow rates where the fresh water wedges into the saltier lagoon water interface. The absolute α scaling factor correlates positively with the UTM Easting coordinate. Also, this suggest that horizontal flow, and thus the horizontal conductivity, in the saturated aquifer more strongly controls the salinity of the water, compared to the vertical travel times through the soil and vadose zone. Similarly, *Ma et al.* [1997] studying a freshwater aquifer overlying a brine aquifer in Kansas concluded that 'mixing of freshwater and saltwater is dominated by horizontal conductivity, however the saltwater upconing is directly controlled by the vertical hydraulic conductivity'.

The error of the objective function increases with increasing UTM easting coordinate. This may be explained by the stronger influence of tidal fluctuations closer to the lagoon edge. These will be more strongly damped going inland.

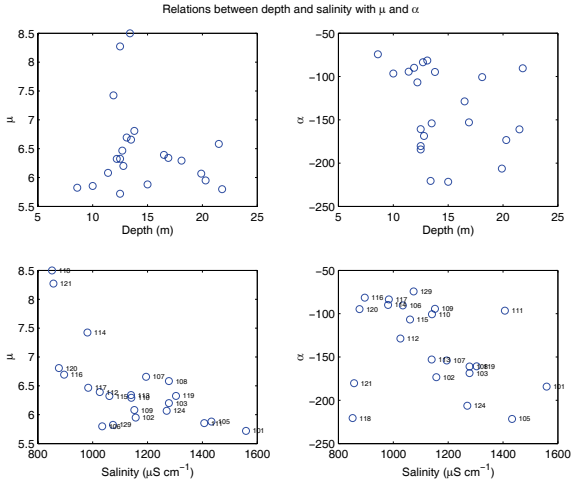

Figure 9.13. Relations between the μ and α and the depth to the water table and the salinity of each well.

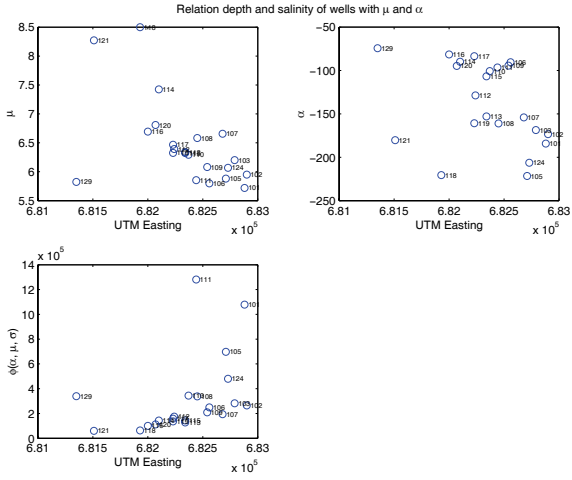

Figure 9.14. Relations the depth to the water table and the salinity of each well and the μ and α parameters.

9.5 Conclusion

We used a simple transfer function model to explain the variations in salinity that was measured for several wells. Generally this approach gave a good agreement between model and measurements. The minimum error of the objective function was successfully obtained for most wells with the inverse procedure. For some wells, due to a lack of data, or inconsistent temporal pumping pattern, the optimal parameter ranges were not clearly defined.

Nevertheless, we were able to show that a positive correlation existed between μ and σ indicating the importance of increased spreading with larger travel times. The peak of the probability density function ranged between 8 and 305 days. The depth of the wells was not related to the model parameters, or obtained transfer times. The average salinity showed a weak positive correlation with μ, and a weak positive correlation with the absolute value for the scaling factor α. Similar relations could be observed by the location of the wells with respect to the lagoon, suggesting the occurrence of faster horizontal flow rates going towards the lagoon. The error of the objective function was larger for wells closer to the lagoon, possibly indicating the stronger influence of tidal fluctuations on the variation in well–water salinity.

On a larger regional scale the effects of interannual climate variability will play a role in the temporal variation in recharge. These processes will be studied in the following Chapter 10.

Chapter 10

El Niño-Southern Oscillation controls the Quality of Freshwater Lenses of Coral Atolls in the Pacific Ocean

Abstract The freshwater resources of coral atolls occur mainly as lenses floating on salt water underneath the islands. The size and shape of these lenses are determined by hydrogeological characteristics, as well as the rainfall recharge rate and its temporal variation, plus abstractions for domestic, industrial or agricultural uses [*Underwood et al.*, 1992; *Jones and Banner*, 2003a, b; *Jocson et al.*, 2002]. In the South Pacific, rainfall exhibits seasonal variability, as well as interannual cycles [*Ropelewski and Halpert*, 1987], which themselves are related to the El Niño-Southern Oscillation (ENSO). We show an ENSO control on the temporal pattern of the salinity of the lenses. We used electric conductivity measurements from pumped wells on Tongatapu to reveal the salinity fluctuations. The salinity dynamics depended on the pattern of low rainfall recharge during dry El Niño periods, or dilution throughout wetter La Niña events. These events determine the quality of the freshwater lenses over the time-scale of several years. We used the Southern Oscillation Index (SOI) [*Troup*, 1965; *Stone et al.*, 1996], to predict the salinity dynamics of the lenses using a lag period of 10 months.

10.1 Introduction

The El Niño-Southern Oscillation (ENSO) is a widely studied quasi-periodic interannual global climatic phenomenon. It influences the location of the South Pacific Convergence Zone (SPCZ) that moves northeast during El Niño and southwest during La Niña events. ENSO variation has been related to several ecosystem processes such as the distribution of global patterns of rainfall and drought [*Ropelewski and Halpert*, 1987], hurricanes [*Bove et al.*, 1998], the development of forest fires [*Siegert et al.*, 2001], the migration of fish in the Pacific Ocean [*Lehodey et al.*, 1997], the epidemics of vector-borne diseases [*Kovats et al.*, 2003] and agricultural production [*Cane et al.*, 1994]. The consequent socio-economic impacts of ENSO are widespread [*Glantz*, 1996].

ENSO impacts the hydrological cycle and it has been related to floods and droughts, river discharge [*Simpson et al.*, 1993], soil moisture [*Poveda et al.*, 2001], coastal water quality [*Lipp et al.*, 2001] and sea surface salinity [*Kilbourne et al.*, 2004]. No quantitative study exists on the impact of ENSO on the quality of the freshwater reserves of Pacific islands. The relations we present here are, to our knowledge, the first description of an interannual climatic control on the groundwater quality of an atoll.

The Pacific Ocean (179.7 million km^2) is the worlds greatest single geographic entity and contains an estimated number of nearly 30,000 islands of which about 1000 are populated [*Mogensen*, 1998]. The population totals 9 million but this varies widely from less than 10.000 inhabitants in Nuie to more than 5 million in Papua New Guinea. Most of these islands are so-called small island developing states (SIDS). Volcanic islands and coral atolls are the two main island types in the Pacific Ocean.

Freshwater lenses underlie islands, coral atolls and coastal areas and sit atop denser salt water underneath. Although the difference in density between fresh (1000 kg m^{-3}) and saline water ($\sim$1025 kg m^{-3}) appears to be small, it has a significant effect on the groundwater system. The size and shape of the freshwater lens are determined by the size of the island, the hydrogeological characteristics of the aquifer, and the average natural groundwater recharge rate, as well as the density difference. A transition zone between the saline sea water and the fresh groundwater exists and the mid-point of this transition zone is commonly approximated as the interface of saline and fresh groundwater using the Ghijben-Herzberg principle [*Ghijben and Drabbe*, 1889; *Herzberg*, 1901]. The mixing of these miscible fluids is a density-driven process largely determined by tidal action and convection and hydrodynamic dispersion [*Underwood et al.*, 1992].

10.2 Materials and Methods

Tongatapu (175^{o}12'W 21^{o}08'S) is the main island of the Kingdom of Tonga and located in the South Pacific Ocean. The island is a flat raised coral atoll with the highest point just 60 m above mean sea level (MSL). The average annual rainfall between 1972 and 2001 was 1670 mm. But it is highly variable (standard deviation of annual rainfall of 450 mm). Rainfall exhibits seasonal and interannual variability linked to variations in ENSO . The groundwater is present as a freshwater lens that floats on the denser salt water in the unconfined limestone aquifer [*Furness and Helu*, 1993]. Tongatapu has no surface water reserves. The limestone base of the island consists of permeable limestone that has a saturated hydraulic conductivity [*Hunt*, 1979] of ∼0.015 m s^{-1}. The groundwater is interconnected to an internal lagoon. Clay soil derived from volcanic ash decreases in depth from ∼6 m in the west to ∼0.5 m in the east [*Cowie*, 1980]. Generally the groundwater level can be found at a depth of about 10 to 20 m with a maximum elevation of 0.5 m above MSL [*Pfeifer and Stach*, 1972].

On Tongatapu the salinity of the groundwater in the pumping wells is monitored using electric conductivity (EC, μS cm^{-1}) measurements. Sparse measurements suggest that salinity levels on the wells around the island have generally increased since 1965 with increasing population pressures. It is likely that pumping demands on the island will continue to increase. Since October 1995 this has been the responsibility of the Tongan Waterboard (TWB) and before it had been carried out by the Ministry of Lands, Survey and Natural Resources (MLSNR). The main well-field of Tongatapu is the Mataki'eua well-field and its water supplies the reticulation system of the capital of Nuku'alofa. Measurements at monitoring bores through the lens at the well-field reveal a thickness approximately corresponding to an EC of 2500 μS cm^{-1} of about 8-12 m. A total of 30 wells currently operate at the field and we use EC measurements made in 21 monitored wells. Due to differing positions in the landscape the depth to the water table in the wells is on average 14.7 m and ranges from 9.2 to 21.8 m. The pumps operate at a depth of approximately one meter below the water table surface and are spaced apart with a distance of about 150 m. Most wells are continuously pumped with a rate of about 2.6 l s^{-1}. The water from the wells is mixed in six distribution tanks. We converted the electric conductivity measurements to total dissolved solids (TDS, mg l^{-1}) using the commonly used factor of 0.6422. The average TDS of the different wells over the 10 year period studied here ranged between 545 and 998 mg l^{-1}. This is mostly related to the relative location with respect to the salt water wedge from the island's central lagoon.

No health based guideline value for TDS has been proposed. The World Health Organisation considers the palatability of drinking-water with a TDS level of less than 600 mg l^{-1} to be good and drinking-water with a TDS level

above 1000 mg L^{-1} to be significantly and increasingly unpalatable [*World Health Organisation*, 2004]. All SIDS rely partly on the freshwater lenses for their water needs, and it is the primary source on several of these islands. Rainfall is the preferred for source for drinking water and it is stored in rainwater tanks. Salinity measurements of the freshwater lens reflect 1) the recharge process and related soil and aquifer characteristics; 2) the climatic conditions that affect this recharge; and 3) variations due to changes in pumping rates. Here we unravel this complexity by analysing the impact of weather patterns on the salinity of the lenses. Long term data on the salinity of the freshwater lenses of coral atolls is scarce as they generally occur in data-poor regions, especially those Pacific islands below the equator.

Rainfall on Tongatapu (data from New Zealand Institute of Meteorology) is variable and frequently intense (with rates often exceeding 100 mm d^{-1}). Here we wish to investigate some of the general recharge patterns. In order to do so all the data obtained by the TWB since the 1^{st} of January 1995 to the 31^{st} of June 2000 for 21 wells was used at the same time. The data of the MNRLS was not used as there were some concerns about its reliability. We used only one transfer function (cf. Chapter 9) to describe all the data of the 21 wells to derive generally applicable transfer times for the aquifer. The objective function is obtained by minimizing the sum of squared errors for all observations within each well:

$$\phi(\alpha, \mu, \sigma) = \sum_{i=1}^{M} \sum_{j=1}^{N} \left(TDS^{-1}_{i,j,simulated} - TDS^{-1}_{i,j,observed} \right)^2 \tag{10.1}$$

in which:

- $\phi(\alpha, \mu, \sigma)$ is the objective function ;
- $TDS^{-1}_{i,j,simulated}$ is the inverse of the simulated TDS (Lmg^{-1});
- $TDS^{-1}_{i,j,observed}$ is the inverse of the observed TDS (Lmg^{-1});
- M is the number of wells
- N is the number of observations in each well.

The Nelder-Mead multidimensional unconstrained nonlinear minimization algorithm available in MatLabTM was used to minimize the objective function.

10.3 Results

Reasonable to good agreement was obtained between the temporal pattern of the simulation and the measured variations in the inverse of TDS, for

convenience graphed as variations in TDS (Figure 4). We averaged the measured variations in TDS and compared this average to the simulated TDS. We obtained a correlation coefficient r of 0.84 for the averaged TWB data and the simulated TDS from June 1995 until June 2000. Overall, for the total 10.5 year period graphed in Figure 10.1, including the averaged MLSNR data, a correlation coefficient of 0.70 was obtained. This indicates that the fluctuations in the salinity levels of the pumped freshwater lens can be explained fairly well by the variations in rainfall. The optimal values for μ and σ (respectively 6.1103 and 1.1208) resulted in a mode of 115 days, and the median and mean were respectively (∼16.7 months) and 1050 days (∼35 months). The results are plotted in Figure 10.1 and for convenience plotted as variations in TDS.

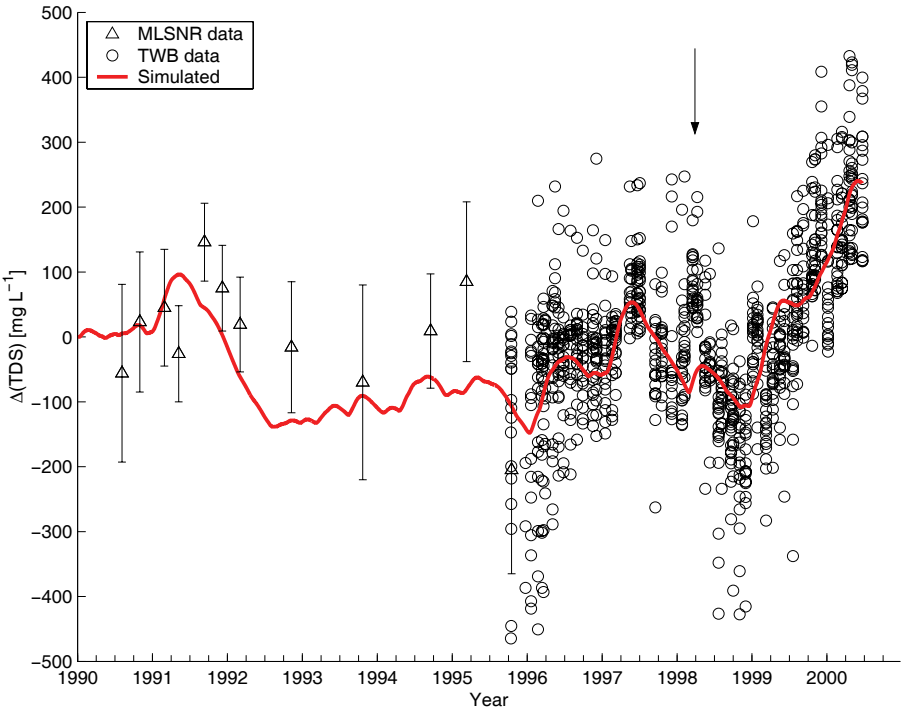

Figure 10.1. Measured and simulated variations of TDS over a 10 year period. Simulations are based on Tongan Waterboard data (circles). The triangles (plus standard deviations) are the averaged data from the Ministry of Lands, Survey and Natural Resources.

The data also shows that recharge after heavy rains is faster than suggested by the simulation. The arrow in Figure 4 indicates a period where the freshwater lens was fresher compared to the modelled TDS concentration. This relates to the 336 mm that fell in just two days associated with the 1997/1998 El Niño that caused flooding on Tongatapu. On the 5th of March

1998 daily rainfall equalled 191 mm day^{-1}, the highest amount of rainfall for the 1990-2001 period, and this was followed by 145 mm day^{-1} on the 6th of March 1998. This rainfall event has triggered rapid flow through the soil and limestone that is not captured by the transfer function model. In fact, this may relate to the occurrence of a fast preferential flow domain, besides the matrix flow domain, as often observed within limestone formations. Additional hydrogeologic information on the triggering of these fast flow needs to be included in a follow-up model.

Other factors will also influence the variability observed in salinity at different wells. This would include the proximity to the lagoon and the interaction of the freshwater lens with the lagoon. As well local variability in the hydrogeological properties of the aquifer that may influence salinity fluctuations around one well site. Another factor relates to the differences in pumping rates between different wells that may also contribute to the variability. On top of that, it is possible that due to cuts in power supply, pumping may also have been interrupted temporarily in the wells that were evaluated. We are however unaware of such cuts in power supply. Further, due to differences in the installation of the wells, it is possible that the pumping depth of the wells in reality fluctuates around the 1 to 2 meter interval as is generally indicated for the depth of the slots. Unfortunately, there is no information available on this. Nevertheless, pumping will make that the water is drawn from a larger aquifer volume.

The measurements done by the MLSNR generally indicate less saline pumped water but show a similar pattern as predicted with the transfer function. It is possible that this is caused by increased pumping over the last decade related to the increased demand for freshwater by Tonga's growing population. We obtain virtually the same simulated variations in salinity if we include the MLSNR data in the optimisation.

10.3.1 Interannual climate variability

Although the climate is seasonal, interestingly, seasonality is not directly recognized in the temporal variations of TDS. We consider the influence of the interannual variability of ENSO using Troup's SOI [*Troup*, 1965]. ENSO (El Niño–Southern Oscillation) conditions are often predicted using indici such as the Southern Oscillation Index (SOI). The Australian Bureau of Meteorology uses the Troup SOI which is defined as 10 times the standardised anomaly of mean sea level atmospheric pressure difference between Tahiti and Darwin (Australia). It is calculated as follows:

$$SOI(-) = 10 * [TD_{MSLP} - \mu_{TD_{MLSP}}] * \sigma(TD_{MLSP}) \tag{10.2}$$

where TD_{MSLP} is the average Tahiti MSLP for the month minus the average Darwin MSLP for the month. $\mu_{TD_{MSLP}}$ is the long term average and $\sigma(TD_{MSLP})$ is the long term standard deviation of TD_{MSLP} for the

month in question. The SOI has been used to predict rainfall three to six months in advance for several regions worldwide [*Stone et al.*, 1996]. The main features of ENSO in Tongatapu are a decreased rainfall in October to July during a mature warm episode (El Niño). There is an increased rainfall from December to April and October to December (ENSO +1 [*Ropelewski and Halpert*, 1987]) during a mature cold episode (La Niña) where the event is defined for the boreal winter (October to February) [*He et al.*, 1998].

Using daily rainfall and our parametric model we extrapolated our predictions backwards for a decade before 1990. Several relations emerge. We calculated the cross-covariance of SOI and TDS^{-1} on a monthly basis so that:

$$c_{12}(u) = cov(X_{1,t}, X_{2,t-u}) \tag{10.3}$$

where $\mathrm{X}_{1,t}$ represents the SOI (-) at time t (months), $\mathrm{X}_{2,t-u}$ represents the modelled variation around the mean of TDS^{-1} at time t with a time lag u (months). We observed the largest cross-covariance at a time lag of off 10 months (based on calculations for the 1972-2001 period). The cross-covariogram is shown in Figure 10.2.

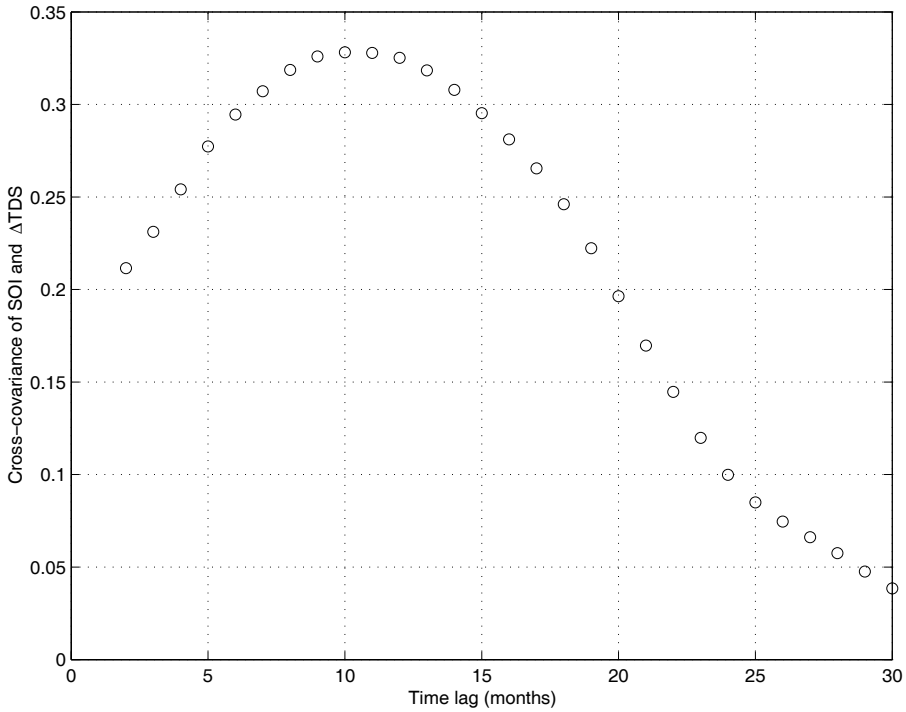

Figure 10.2. The cross-covariogram calculated for SOI and the variations in TDS. The largest cross-covariance was obtained at a time-lag of 10 months.

The correlation coefficient between SOI and modelled Δ TDS^{-1} at the optimal time-lag is 0.52 (in other words the SOI then explains 52% of the variation in modelled TDS^{-1}). El Niño and La Niña thus trigger changes in the salinity of the freshwater lens with a lead time of 10 months (Figure 10.3). With the peak of the transfer function at 115 days (∼4 months) this roughly leaves a maximum lead-time of 6 months between the SOI and rainfall. Although rainfall does not show a simple linear relationship with SOI [*Basher and Zheng*, 1998], this is consistent with a composite analysis (where years were classified according to their ENSO state) that found a sustained temporal correlation of up to 9 months of SOI and the 3 month-running mean rainfall on Tongatapu [*He et al.*, 1998].

In 1984, after the 1983 El Niño event, there is no distinct event until the El Niño of 1987. The oscillatory changes in salinity during this intervening period are simply determined by the rainfall seasonality. Salinity remained above average until the 1989 La Niña event that effectively recharged the freshwater lens of the island.

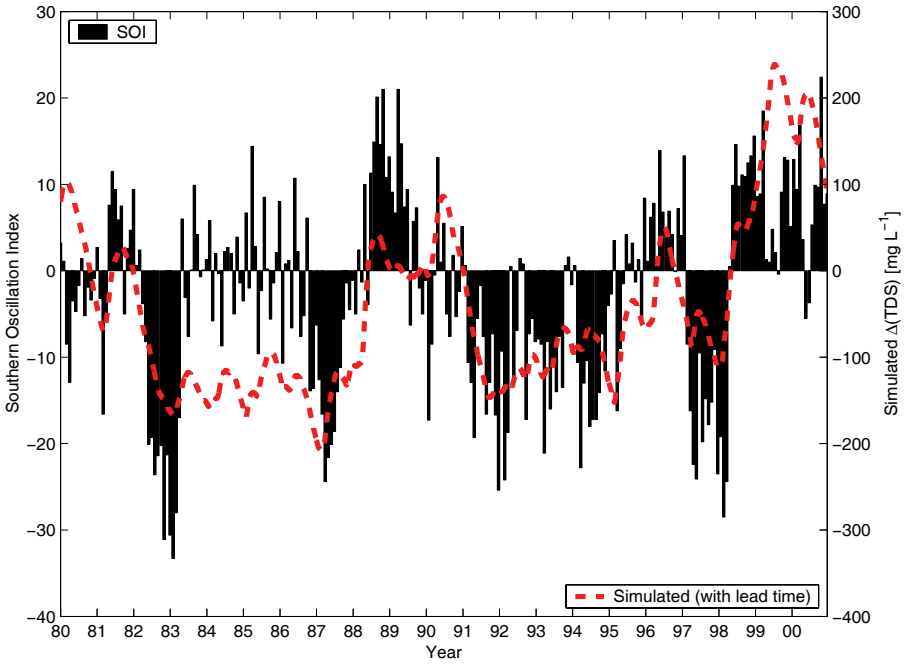

Figure 10.3. Simulated variations of TDS^{-1} (cf. Figure 10.1) and the Southern Oscillation Index with a time-lag of 10 months.

Seasonality is a strong characteristic of Tonga precipitation. Yet our analysis suggest that ENSO events determine the salinity 'state' of the freshwater lens, e.g. the water being either saltier or sweeter than average. This state can than be preserved over a longer period (e.g. 1991-1997), at least

until an opposite ENSO event leads to a change of state. It can be expected that the effects of ENSO are stronger for water quality than for rainfall, as processes in the soil, the vadose zone and the saturated zone effectively filter out the higher frequency effects of rainfall events. This ENSO link may also be assisted by the concomitant effects on soil moisture, evaporation, tides, barometric pressure, plus thermal expansion of the lens and ocean, with a consequent impact on MSL. There was a reported MSL rise of 0.1 m during the 1991-1992 El Niño event [*Furness and Gingerich*, 1993].

Lower rainfall and droughts associated with an El Niño event will likely result in increased pumping of water from the lens, although this is not reflected in the meagre pumping data for this well-field during 1997-1998. This may partly be explained with the refilling of rainwater tanks during sparse but intense rainfall events.

Direct impacts of ENSO on SIDS in the Pacific include cyclones [*Basher and Zheng*, 1995], droughts [*White et al.*, 1999] and floods, fish migration [*Lehodey et al.*, 1997] and disease epidemics [*Hales et al.*, 1996]. Here we show the indirect impact of ENSO on the freshwater quality of the subterranean water resources. These relations are, we consider, the first demonstration of an interannual climatic control on the groundwater quality of a coral atoll. It has direct relevance for SIDS that seek to sustainably manage their water resources and wish to distinguish human-induced changes from underlying climatic patterns. Whereas Tongans were nervous about rises in groundwater salinity from 1997 through 1999, and sought to manage abstractions, this salinisation, and its subsequent dilution by the ensuing La Niña, were just part of an ENSO control. Of course, overpumping will cause local upconing and determine the quality of the water that is pumped up within an individual well.

Similar ENSO links might also be found for islands in the Fiji-New Caledonia (FNC) zone [*Ropelewski and Halpert*, 1987], and other oceanic regions with correlation structures between rainfall and ENSO. Opposite relationships might be found in the central Pacific (CP) zone [*Ropelewski and Halpert*, 1987], or the Pacific islands north of the equator [*Yu et al.*, 1997]. The quality of freshwater lenses of smaller coral atolls such as the Loyalty Islands, will likely be more strongly influenced by interannual ENSO variations.

Recent predictions are that the frequency of El Niño events will increase with global warming [*Timmermann et al.*, 1999; *Tsonis et al.*, 2005]. Sustaining the quality of the freshwater reserves of SIDS would than become even more challenging.

Part IV

Water Management and Sustainable Development

Chapter 11

Managing the Impact of Annual and Interannual Rainfall Fluctuations

*

Abstract In this Chapter, we calculated the return periods of rainfall and droughts and we use these with results from earlier Chapters to illustrate the impact of rainfall variability on both agricultural yield and freshwater availability. From measurements obtained from the Tongan Water Board (TWB), and a simple calculation based on the Ghijben–Herzberg principle, we show that the freshwater lens (with 'fresh' defined with the WHO recommend limit for potable water) has a thickness of about 12 m. In a region that is very much influenced by large–scale trends relating to global warming, such as rising sea water levels and cyclone frequency, it is of paramount importance to manage sustainably this freshwater resource. This can only be done within an appropriate knowledge framework that accounts for the impacts of annual and interannual variations in rainfall on the salinity dynamics of the freshwater lens. Here we present simulations of the salinity dynamics of a freshwater lens with a transfer function that we had derived earlier (see [*van der Velde et al.*, 2006c] and Chapter 10). We generate synthetic rainfall time–series based on the same lognormal distribution as the measured rain, and we increasingly introduce seasonal and interannual (ENSO) components into the synthetic rainfall time series. Here after we use these synthetic rainfall time series as input in the derived transfer function to simulate salinity dynamics. We are then able to show, in a simple way, the influence of annual and interannual variations on the freshwater lens' salinity dynamics. This procedure can be thought as being of similar to a Fourier transform, although we do not derive the strongest signals in the real time series. We reverse the process, and didactically introduce signals we postulate to exist (random, seasonal and ENSO rainfall signals) to generate synthetic rainfall. It is important that well–field managers of coral atolls are aware of these impacts while they judge, for example, their pumping rates on electric conductivity measurements. This procedure can help managers to identify the impact

*Parts of this are submitted in a forthcoming paper 'Aspects of the management of water resources of a low island in the Pacific Ocean.' by M. van der Velde, M. Vakasiuola, S.R. Green, V.T. Manu, V. Minonesi, M. Vanclooster, and B.E. Clothier, for a special issue of *Physics and Chemistry of the Earth* initiated at the Water Management session held at the EGU 2005, in Vienna.

of different climatic rainfall patterns on the salinity dynamics they observe.

11.1 Introduction

The Pacific Ocean contains an estimated 30,000 islands, of which about 1000 are populated with 9 million inhabitants [*Mogensen*, 1998]. Geologically speaking, two types of islands are generally distinguished: low islands and high islands. The low islands mainly consist of coral atolls but also include eroded volcanic islands. The high islands can be classified as either continental or oceanic islands. The oceanic islands consist of volcanic material. Low and high islands experience a lot of similar challenges to their water resources. However, due to the differences in their geomorphic features, the water resources of low and high islands will also be differently affected by the prevailing pattern of land uses and climatic conditions. On low islands, groundwater protection will be critical. While on high islands it will be critical to control the impact of erosion on the quality of surface and connected coastal waters. The freshwater resources of low islands generally consist of freshwater lenses that float underneath the island on top of denser ground (sea) water. As in Tongatapu this groundwater is often connected to an internal lagoon. Surface water occurs seldom on the permeable limestone. High islands are characterised by a network of (intermittent) river systems that drain the higher lands and discharge into the coastal zone. The steepness of the land makes it vulnerable to erosion. Land degradation and erosion associated with intensifying agricultural practices was the focus of the CROPPRO project in Fiji and Samoa. Here we focus on low–island issues.

Agriculture is generally intensifying on the islands located in the Pacific Ocean. Determining the effects of the use of agrichemicals, land degradation and associated erosion, and the spatial distribution of different land uses on the quality and quantity of water resources, will be a key environmental challenge for these islands. Agricultural pollution and increased rates of erosion threaten the island's ecosystems that include surrounding coral reefs [*Zann*, 1994]. The island archipelagos of the South Pacific often contain both types of islands, and each country's administration will thus have to deal with water resource management on both low and high islands. In this paper we will specifically talk about low–lying coral atolls. In a forthcoming study we will combine some of the results from the CROPPRO project and collate these observations in a discussion of water resources challenges that face all the islands of the Pacific Ocean.

11.2 Climate Change Impacts

Climate change will have an important impact on the availability of freshwater resources of low–lying atolls [*Meehl*, 1996]. Land degradation and erosion are likely to intensify if the number of extreme events increases. It

is predicted that an increase in the frequency of El Niño's will occur in a warming global climate [*Timmermann et al.*, 1999; *Tsonis et al.*, 2005]. This may then lead to an increase in the occurrence of dry spells [*Meehl*, 1997]. The effect will be directly noticed in the amount of rainwater that is collected on the islands and stored in rainwater tanks for drinking purposes, and it may indirectly be noticed by a degrading quality of pumped water (Chapter 10, [*van der Velde et al.*, 2006c]). Climate change may also have other indirect impacts on the water quality of the lenses. Small island developing states (SIDS) may suffer for example from sea–level rise. *Mimura* [1999] identified Tongatapu to have, with climate change, an increased risk of inundation and coastal flooding, exacerbation of coastal erosion, saltwater intrusion and changes in sediment deposition patterns. Another threat that is possibly linked to global warming is the increase in the frequency of intense cyclones and associated storm surges. Over a long term, changes in rainfall rate and frequency may impact the hydrogeological characteristics of the permeable limestone aquifer through karst processes. This may lead, for example, to an aquifer with deteriorated storage characteristics, due to solution processes that enhance the formation of fewer and larger conduits involved in the recharge and retention of the freshwater. These processes will be further enhanced with the rising number of cars that may cause increasingly acidic rain, especially during local convective storms. Local convection is induced when moist air is flowing over the heated island during the dry season [*Jones and Banner*, 2003b]. Effects of climate change and variation will often be amplified by human–induced changes resulting from increasing demographic pressures.

Although minimally responsible in a global sense, small islands will be among the first to be struck by climate change. Climate change was the most controversial item on the agenda of the 10–year review of the Barbados Programme of Action (BPOA, *UNEP* [2004]) for the sustainable development (SD) of small island developing states (SIDS), recently held in Mauritius.

In this Chapter we will illustrate some of the impacts of rainfall variations. We will highlight this by summarizing examples from the previous Chapters, as well as by indicating other factors such as hydraulic conductivity and recharge fraction that control the amount of recharge to the freshwater lens. We will then show how the different components of the climatic system create a temporal rainfall pattern that can be used to help local well–field managers to understand the variations they observe in their EC measurements of pumped water.

11.3 Climate of the South Pacific

The South Pacific Convergence Zone (SPCZ) is an important feature of the tropical South Pacific. The climate in the Pacific Ocean is largely determined

by the position of the SPCZ. Long-term rainfall distribution can be directly attributed to the SPCZ (Ropelewski and Halpert, 1987). The SPCZ is a low-level convergence extending from the west Pacific warm pool southeastwards towards French Polynesia. The zone occurs where the low–latitude easterly trade winds and the higher latitude southeasterly trade winds meet. The intensity of the SPCZ can vary considerably and its location is affected by the El Niño-Southern Oscillation and the Interdecedal Pacific Oscillation. Tropical cyclones are a regularly recurring feature of the tropical Pacific climate system and affect the regional climates on the islands.

Precipitation on Pacific islands will result from local convective processes, from tropical cyclones and from rain associated with the cloud sheets of the subtropical jet–stream [*Thompson*, 1986]. Islands with considerable topography will also be influenced by orographic effects on the rainfall distribution [*Jones and Banner*, 2003a].

11.3.1 Tongatapu

Cyclones are also recurring phenomena on the islands of Tonga and attributed to El Niño. From satellite data available since 1969 it is known that Southern Tonga is hit by an average of 1.3 cyclones per year. Tropical cyclones may occur all year around but they are principally confined to the wet season from November to April. Not surprising this is called the cyclone season [*Thompson*, 1986].

The locations of the capital of Nuku'alofa as well as the main well–field for water pumping of Mataki'eau are indicated on the map of Tongatapu (Figure 11.1).

Land use on the island mainly consists of agricultural and urban dwellings and less then 5% of the original tropical forest cover remains [*Wiser et al.*, 2002]. The soil is derived from weathered volcanic ash ranging in a thickness of about 6 m in the west to 0.5 m in the east [*Cowie*, 1980]. Two distinct layers of deposition can be distinguished. We measured the saturated hydraulic conductivities of the soil to range between about 20 and 80 cm hr^{-1} throughout a soil profile with a depth of 1 m.

The sole source of freshwater on the island is the freshwater lens that floats on denser salt water underneath the island. The TWB manages this resource and made measurements of salinity through the freshwater lens between May, 1997 and July, 2000 at 7 monitoring bores (see also Chapter 11). Figure 11.2 shows the salinity (EC in μ S cm^{-1}) profiles obtained at 7 monitoring bores (MB) located near or in the Mata'kieua wellfield (see Chapter 9) as well as the upper limit of consumable drinkable water at an EC of 2500 μ S cm^{-1}. This corresponds to about 1500 mg L^{-1}.

The freshwater lens has a thickness of about 12 m. We also used the Ghijben-Herzberg principle [*Ghijben and Drabbe*, 1889; *Herzberg*, 1901] to estimate the thickness of the freshwater lens with different fractions of the

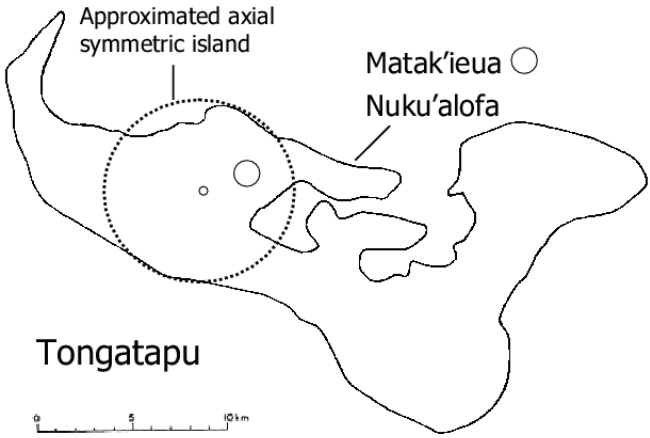

Figure 11.1. The raised coral atoll of Tongatapu (252 km^2). The locations of the main well–field of Mataki'eau, as well as the capital of Nuku'alofa are indicated. The circle represents the approximated axial symmetric 'island' as used with Equation 11.1 (see text) with a radius of 5000 m.

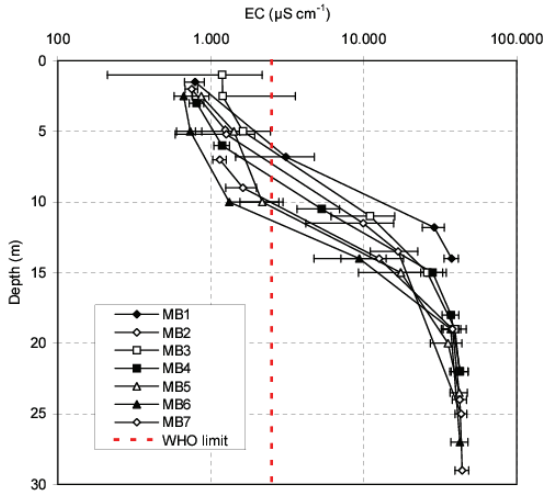

Figure 11.2. Profiles of averaged salinity measurements through the freshwater lens done at the monitoring bores (MB) located near or in the Mataki'eua wellfield, between May, 1997 and July, 2000 by the Tongan Waterboard. The World Health Organisation limit was defined at 2500 μS cm^{-1} (dotted line).

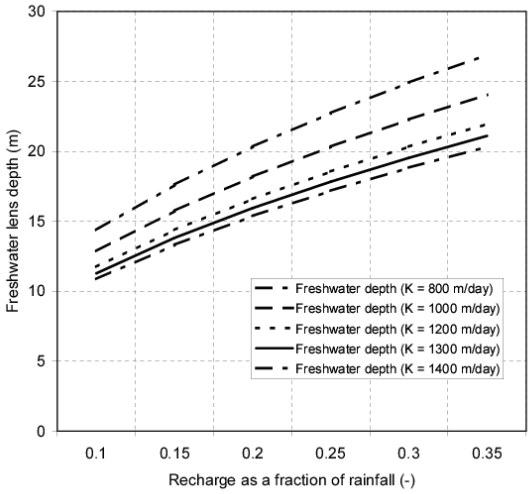

Figure 11.3. The depth of the freshwater lens as a function of recharge fraction of average annual rainfall on Tongatapu and hydraulic conductivity, K (m day^{-1}), approximated by the Ghijben–Herzberg principle

average annual amount of rain (1670 mm) recharging the lens, as well as different values for the aquifers horizontal hydraulic conductivity, K (m day^{-1}). *Hunt* [1979] measured a saturated hydraulic conductivity of 0.015 m s^{-1} (corresponding to 1296 m day^{-1}). For the following calculation we assumed that the west part of Tongatapu could be approximated by an unconfined and axial symmetric island (see Figure 11.1), as earlier suggested by *van der Molen* [1979]. The approximated axial symmetric 'island' has a radius, R, of 5000 m, and the well field occurs at a distance of the centre of the 'circular island', r, of 2500 m. With the relative density difference between salt (ρ_s=1025 kg m^{-3}) and fresh (ρ_f=1000 kg m^{-3}) water, a = 0.025, and natural groundwater recharge f (m day^{-1}) determined by the recharge fraction and the annual average rainfall on Tongatapu, we can calculate the depth of the fresh-salt water interface, H (m), so that [*Oude Essink*, 2001b]:

$$H = \sqrt{\frac{f(0.25R^2 - r^2)}{K(1+\alpha)\alpha}} \tag{11.1}$$

Using this equation, the depth of the freshwater lens as a function of recharge fraction of average annual rainfall on Tongatapu and hydraulic conductivity, K (m day^{-1}), the freshwater lens thickness approximated by the Ghijben–Herzberg principle is given in Figure 11.3. We can see that the profiles obtained from the TWB measurements (Figure 11.2) are best represented by lower recharge fractions and higher hydraulic conductivities.

This approach considers the aquifer as being homogeneous, and hydrodynamic dispersion being negligible. These hypotheses might not fully apply. Nevertheless, although the position of the interface is not completely correct, the use of the equation gives a good approximation of the real situation.

11.4 Rainfall and Droughts

Rainfall distribution directly affects the amount of water that is available for consumption from the lens. The length of a drought determines what part of the freshwater supply will be affected. This ranges from individual rainwater collection tanks to the freshwater lenses of the island [*White et al.*, 1999].

The daily rainfall return periods based on the 30–year daily rainfall records (1972-2002) are plotted in Figure 11.4. Winter was defined starting at Day of Year 92 and ending on DOY 273; while summer was defined as starting at DOY 274 and ending on DOY 91 the following calendar year.

We calculated the return period using the following equation:

$$R_n = \text{frequency}(P < P_n) \tag{11.2}$$

Where R_n is equal to the frequency of an event that fits within a certain 5 mm bin size class P_n, for the rainfall events P, divided over a time period t of 30 years. Similarly the frequency of drought smaller, or equal, to a certain length in days was calculated.

Tongatapu is a flat coral atoll and only occasional runoff and erosion have been observed on the lands gently sloping to the lagoon. However, extreme rainfall events with high intensities can cause movement of sediment and agrichemical residues towards the lagoon. While average annual rainfall is high on Tongatapu, droughts of moderate severity are common for about 2 months, and occasionally for up to 4 months, especially during the period July - November. *Thompson* [1986] defines a dry spell for Tongatapu as 'a period of at least 15 consecutive days with less than 1 mm of rain per day, and a very dry spell (drought) as 15 or more days with no rain.' [*Thompson*, 1986] identified that on Tongatapu, 7 droughts occur per decade with an average length of 18 days. The 1997/1998 El Niño resulted in droughts on Tongatapu and the other islands of Tonga [*Glantz*, 1996]. In Figure 11.5 we have graphed the return period of droughts with a certain length (days) based on the 30-year rainfall record (1972-2002) of Tongatapu. The increase in the slope of Figure 11.5 between 800 and 1000 days is likely related to the characteristic return period of El Niño.

Drought is a deficiency of rain over an extended period. The severity of the drought depends on the activity, group or environmental sector that is affected. This is reflected in the range of definitions of drought that exist. The National Drought Mitigation Center (NDMC) at the University of

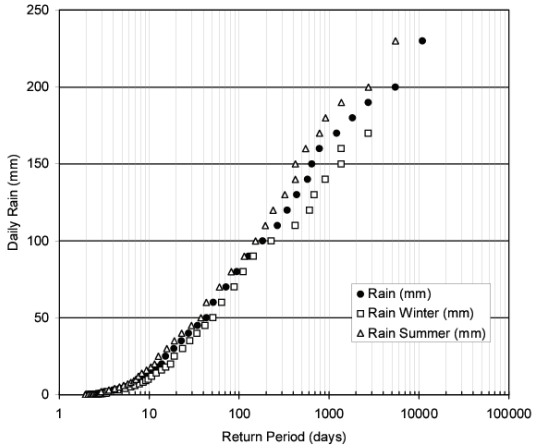

Figure 11.4. Daily rainfall return periods based on the 30–year daily rainfall record (1972-2002) of Tongatapu. The bin size was 5 mm. The return period indicates the return time for daily rainfall to sum up to at least a certain amount of rain. Winter was defined starting at Day of Year 92 and ending on DOY 273 while summer was defined as starting at DOY 274 and ending on DOY 91 the following calendar year.

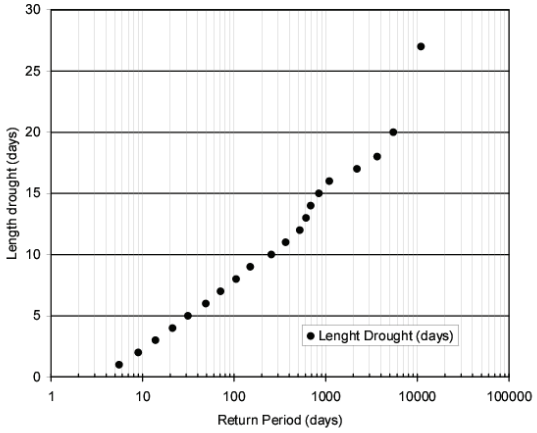

Figure 11.5. Return period of droughts with a certain length (days) based on the 30 year rainfall record (1972-2002) of Tongatapu. The bin size was one day.

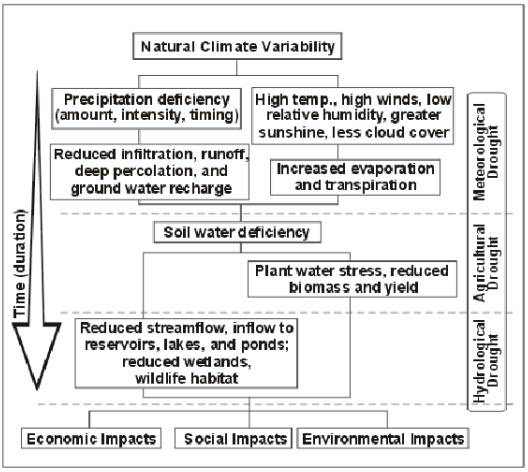

Figure 11.6. Definitions of drought from the National Drought Mitigation Center from the University of Nebraska (*http://www.drought.unl.edu/*)

Nebraska (*http://www.drought.unl.edu*) distinguishes conceptual and operational definitions of drought (see Figure 11.6). Conceptual definitions help people to understand the concept of drought and can be used in drought policies. Several operational definitions can be distinguished. Meteorological drought refers to an expression of precipitation's departure from normal over some period of time. Agricultural drought occurs when there is not enough soil moisture to meet the needs of a particular crop at a particular time. Agricultural drought happens after meteorological drought, but before hydrological drought. Hydrological drought refers to deficiencies in surface and subsurface water supplies.

Agriculture is usually the first economic sector to be affected by drought. We have identified a relation that partly explained the exportable yield of one of Tonga's most exported crops, squash, and the amount of rainfall in the squash growing season (Chapter 12, [*van der Velde et al.*, 2006b]). We have observed water stress occurring in the squash several days after the last rainfall [*van der Velde et al.*, 2006a]. This is related to the shallow rooting depth of the squash which is only about $<$30 cm. So agricultural drought will occur in Tongatapu quite regularly, being droughts of 5 days. These will generally occur every 30 days, cf. Figure 11.5.

11.5 Climatic Variations - Impact on the quality of the freshwater lens

The rainfall distribution affects, in the long term the amount of recharge to the freshwater lens and thus the salinity and quality of the water. Elsewhere (see Chapter 10) we have identified the impact of ENSO related rainfall fluctuations on the quality of the freshwater lens of the island of Tongatapu [*van der Velde et al.*, 2006b]. The climatic conditions affect the amount of recharge to the freshwater lens. *Jones and Banner* [2003a] identified a relationship between El Niño and the amount of recharge towards the freshwater lens. We have used electric conductivity measurements from pumped wells supplied by the Tongan Water Board (TWB) to understand the changes groundwater quality and its relation to interannual climate dynamics. The dynamics of the salinity of the lens depend on the pattern of low rainfall recharge during dry El Niño periods, or dilution throughout wetter La Niña events. These events determine the quality of the freshwater lenses over the time-scale of several years. The Southern Oscillation Index (SOI) was linked with the salinity dynamics of the lenses using a lag period of 10 months. Thus well–field managers should try to minimize pumping 8-12 months after the onset of an El Niño event, and meanwhile urge the public to rely on stored rainwater. We can identify an aspect of hydrological drought that is specific for the freshwater lenses of coral atolls: namely the effect of drought (or precipitation 'deficiency') on the water quality (salinity) of the freshwater lens.

We have also shown that the thickness of the freshwater lens varies with different hydraulic conductivity characteristics of the aquifer, as well as different fractions of rainfall recharging the lens. The salinity of the lenses is largely dependent on the recharge that occurs over a certain time period. Seasonal, as well as interannual variations in precipitation, lead to varying amounts of recharge. The quality of the water that is pumped from the lens thus also depends on these fluctuations. In a region that is strongly influenced by large–scale trends related to global warming, such as rising sea water levels and cyclone frequency, it is of importance to sustainable manage this freshwater resource. This can only be done within an appropriate knowledge framework that accounts for the impacts of annual and interannual variations in precipitation on the salinity dynamics of the freshwater lens. Our following analyses further illustrate the impact of the different climatic components that determine the temporal rainfall pattern.

11.6 Using synthetic rainfall data to simulate salinity fluctuations for didactic purposes

We now provide a 'proof of concept' procedure to simulate salinity fluctuations with synthetically created rainfall series for didactical purposes. We term this 'proof of concept' because only one artificial rainfall series was generated. This could be extended to provide a measure of the variation that is introduced by different climatic components that determine the artificially generated rainfall. The procedure followed here is not that of a true 'weather generator'. Generators take account of the temporal correlations that exist in rainfall by using for example Markov chains. Our approach, for the moment, suits the didactic purpose well.

11.6.1 Synthetic Rainfall

We have calculated the chance of a day being dry (no rain), plus the chance of a day with rain from the daily rainfall data of Tongatapu for a 30 year period (1972-2002, 10951 days). We find that $P_{dry} = 0.5090$ and that $P_{rain} = 0.4910$.

For days that it rained we can describe the rainfall on Tongatapu with a lognormal distribution function f_{rain} (t,σ, μ) with the mean logarithm of the measured daily rainfall measurements, $\mu_{lograin}$ that equals 0.8251 and similarly derived, a $\sigma_{lograin}$ of 1.7885, so that:

$$f_{rain}(x;\mu,\sigma) = \frac{1}{\sigma.x.\sqrt{2.\pi}}.\exp\left(-\frac{(\ln(t)-\mu)^2}{2.\sigma^2}\right) \tag{11.3}$$

- x is the support and equals rainfall classes from 0 to 250 mm d^{-1};
- μ is $\mu_{lograin}$; and
- σ is $\sigma_{lograin}$;

We then created rainfall time–series considering that the rainfall consists of three components, a random component, a seasonal component, and an ENSO–related component. We considered the chance for a day to be dry, or to be wet using P_{dry} and P_{rain}. If it is a rainy day, we sampled a rainfall event from the lognormal distribution of rainfall on days it rained days derived from the measured rains, according to a summation of the random, seasonal and ENSO components. Random rainfall, P_R, was simply obtained by randomly choosing an event from the rainfall distribution for a period of 30 years, or 10951 days. Seasonal rainfall, $Rain_{seas}$, was obtained by multiplying a sine function with a period of 365 days and an amplitude of one, and a mean of one, to an event drawn from the rainfall distribution for a period of 10951 days so that:

$$P_S(t) = 0.5 * (\sin(2\pi \frac{t}{365}) + 0.5) * f_{rain}(x; \sigma, \mu) + Z(t) \tag{11.4}$$

where:

- t ranges from 1 to 10951 days;
- P_S is seasonal rain [mm.d^{-1}]; and
- $Z(t)$ is a random normally distributed error [mm.d^{-1}].

Similarly an rainfall time series, P_{ENSO} was constructed with periodic components of 1200 and 1800 days, reflecting the 'characteristic' return period related to ENSO steered climatic patterns. The final rainfall component time series, P_A, is obtained by adding these components, with several weighting factors.

$$\begin{aligned} P_S(t) &= f_1 * P_R \\ &\quad * (f_2 * P_{ENSO_{1200}} + f_3 * P_{ENSO_{1800}} + f_4 * P_S) \\ &\quad + f_5 * P_R + Z(t), \end{aligned}$$

where:

- $Rain_{ENSO(1200)}$ is the ENSO component with a period of 1200 days;
- $Rain_{ENSO(1800)}$ is the ENSO component with a period of 1800 days;
- $Z(t)$ is a random normally distributed error [mm d^{-1}].

The weighting factors f_1, f_2, f_3, f_4, and f_5 respectively equalled 0.8, 0.2, 0.4, 0.8, and 0.2 and were determined based on the assumption that 20% of the rainfall is completely random (f_5) and that 80% is determined by climatic patterns (f_1). Of these 80%, a fraction of 0.2 f_2 relates to the ENSO component with a periodicity of 1200 days, a fraction of 0.4 f_3 relates to the ENSO component with a periodicity of 1800 days, and a fraction of 0.8 f_4 relates to the seasonal component of rainfall. The values for the weighting factors where determined emperically. Ideally they would be based on literature studies that have shown how much the variation in rainfall can be contributed to ENSO, how much can be attributed to seasonal periodicity, and how much can be attributed to random climatic fluctuations.

By sampling of the lognormal distribution of rain on rainy days, it is possible, due to the long tail of the distribution, to obtain daily rainfall totals that far exceed the maximum rainfall of Tongatapu of 224 mm, observed

during this period. Therefore, to minimize the chance of calculating rainfall distributions with unrealistic daily rainfall extremes, we multiply daily rainfall amounts that exceed 224 mm, with 0.1. We repeat this process twice. If, in any case, daily rainfall amounts surpassing 224 would occur in an artificially generated rainfall time series, we reject this particular series from the dataset.

To evaluate if a realistic time–serie was created we used two criteria. We firstly looked at the total amount of rain generated over a 30-year period, and compared this with the total sum of real rain that fell over the 30–year period. Secondly, we compared the distribution of the synthetic rainfall series with the histogram distribution of the real rainfall, using histograms.

11.6.2 Transfer function

Using the generated rainfall series as the input for the transfer function that we have derived earlier (see [*van der Velde et al.*, 2006c] and Chapter 10), we were now able to illustrate the different climatic components that determine the variations in salinity. We increasingly introduced seasonal and interannual (ENSO) components into the synthetic rainfall time–series. This procedure can be thought of as being similar to a Fourier transform. Although we do not derive the strongest signals in the real time–series, we reverse the process and introduce signals, that we postulate to exist, namely random, seasonal and ENSO rainfall patterns. It is important that water managers of coral atolls are aware of these impacts while they judge, for example, the effect of their pumping rates on electric conductivity measurements. This procedure can help well–field managers to identify the impact of different climatic rainfall patterns on the salinity dynamics they observe.

11.6.3 Results

The real rainfall time series, as well as one example of our three generated components, plus the final synthetic rainfall time–series are plotted in Figure 11.7.

It is striking how well the random rainfall series seems to reflect the real rainfall. The reason is that, at this scale, it is hard to distinguish seasonal or even interannual components in the rainfall series. Not surprisingly, a strong seasonal component can be observed in the third panel. Similarly two interannual components of 1200 (3.3 years) and 1800 (4.9 years) days can be recognised in the fourth panel. Finally, the synthetic rainfall time-series combines all these periodic and random effects. The histograms are shown in Figure 11.8.

The distribution of the artificially generated series is similar to the distribution of the observed amounts. The sum of total rain for the artificial rainfall series for random rain, seasonal rain, ENSO rain, and artificial rain

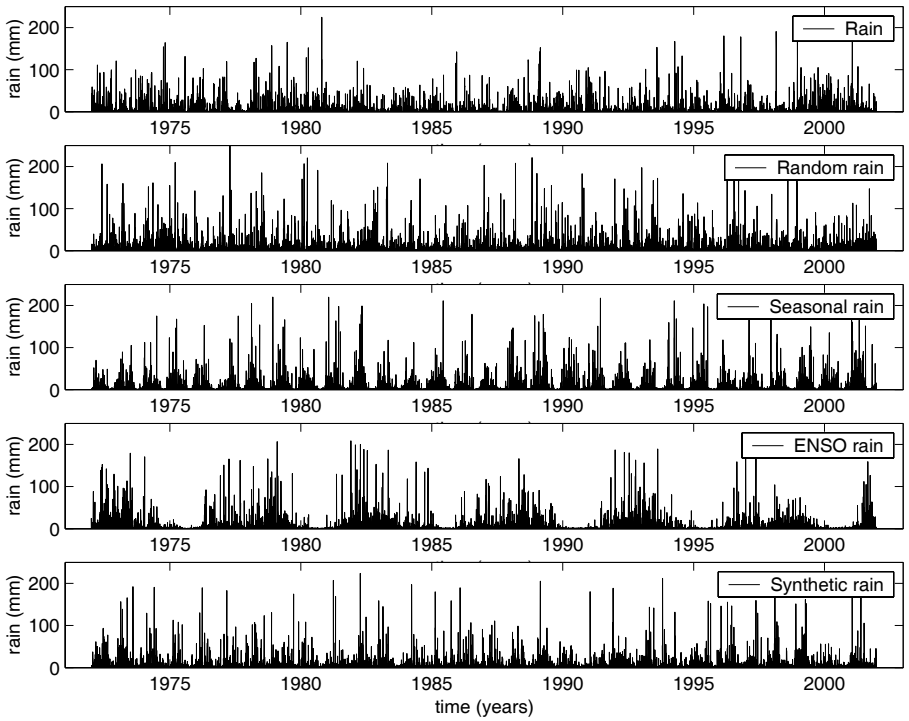

Figure 11.7. Rainfall time series. Daily rainfall measured over a 30 year period (rain), rainfall generated randomly based on lognormal distribution characteristics of the measured rain (random rain), rainfall similarly distributed as before, but based on a seasonal component (seasonal rain), rainfall similarly distributed as before, but based on two ENSO components (1200 and 1800 days), and rainfall similarly distributed, but with a random, a seasonal and two ENSO (1200 and 1800 days) components (rain). These are just one example of the types of rainfall series that can be generated.

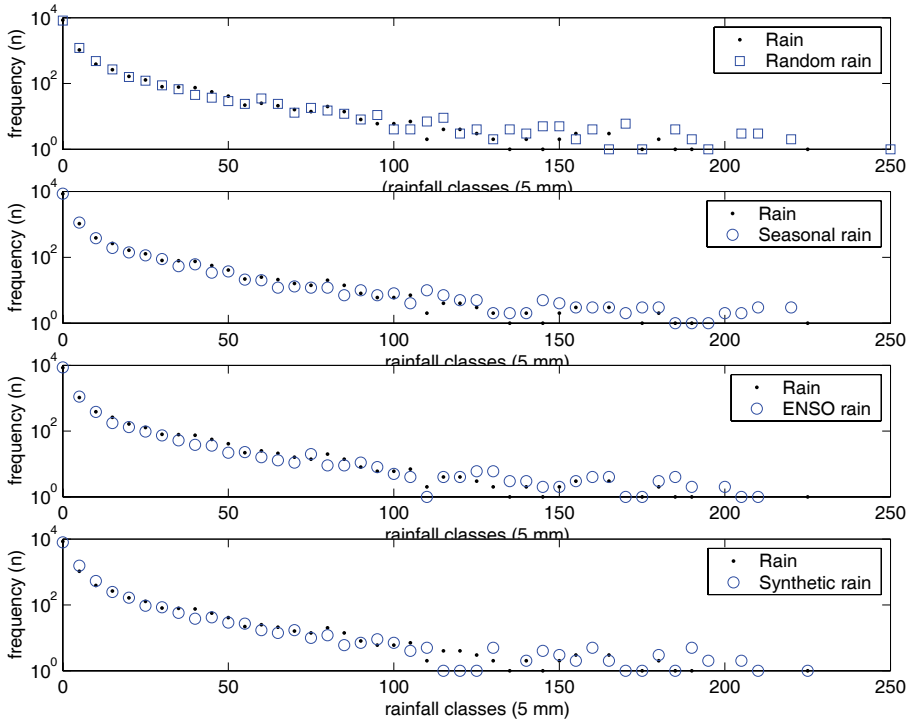

Figure 11.8. Histograms of the generated rainfall series (blue circles and cf. Figure 11.4) compared with the measured daily rainfall (black dots). Histogram bins are 5 mm.

(Figure 11.7 respectively equalled 55402, 50315, 45417 and 50292 mm, compared to the sum of real rain of 50315 mm).

Now, with the transfer function we have derived in Chapter 10, we are able to simulate variations in salinity using the generated rainfall time series. The three components are plotted in Figure 11.9. The different periodic patterns introduced are recognised in the variations of salinity. The magnitude in the variations of salinity is considerably larger for the ENSO component then for the seasonal component.

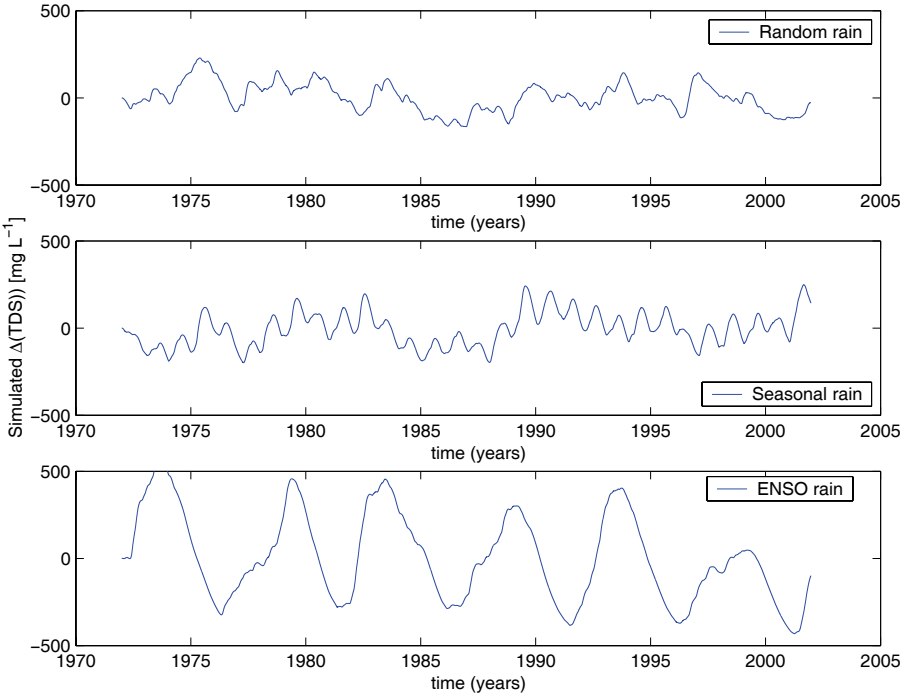

Figure 11.9. Variations in salinity (expressed as TDS in [mg L^{-1}]) simulated with the derived transfer function with input of three generated rainfall distributions (random, seasonal and ENSO, cf Figure 11.4).

If we combine these components we can predict variation in the lens' salinity (Figure 11.10). Comparing these generated variations of salinity with the simulated variations in salinity that are in good agreement with measured variations (cf. Chapter 10), we can recognise similar structures in the created signal. Seasonal components, as well as interannual components can, as expected, be recognised. In the case presented here, judging by the eye, it seems that ENSO variations are not represented strongly enough in the artificial rainfall time–series. ENSO impact is recognised in the upper panel of Figure 11.10, while, in comparison, ENSO is more strongly damped in the variation of salinity derived from the synthetic rain, plotted in the

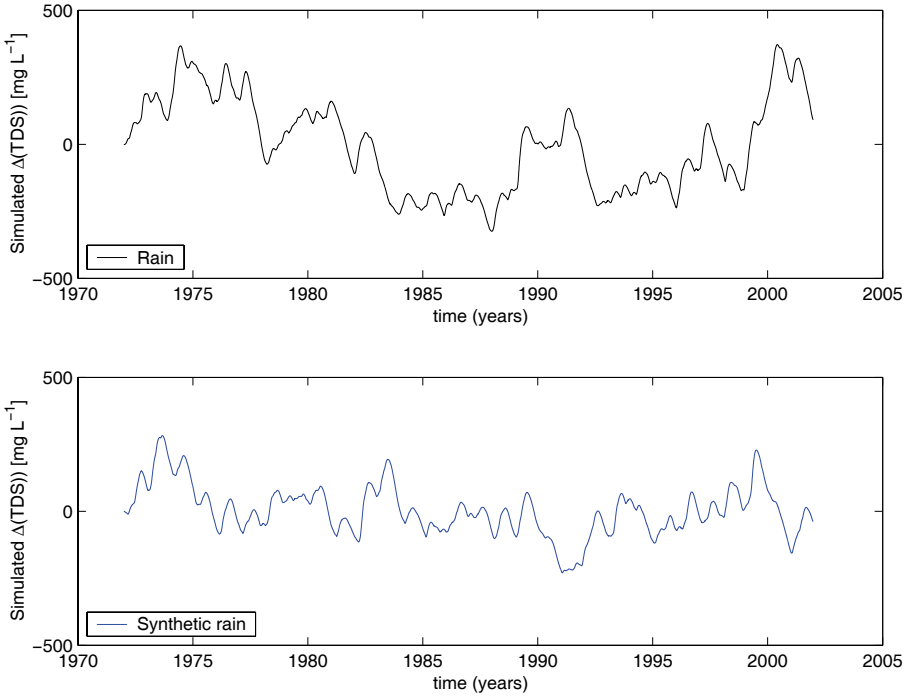

Figure 11.10. Simulated variations in salinity based on measured daily rainfall and measured variations in salinity (upper panel) and simulated with artificial rainfall time series obtained by adding the different artificial rainfall components (lower panel)

lower panel. Of course, a proper determination of the weighting factors, possibly with a larger ENSO component, would yield a more appropriate synthetic rainfall signal. It seems that we are able to simulate realistic variations in salinity by generating a rainfall time–series that consists of random, seasonal and ENSO components. These simulations can help us to evaluate and identify the climatic components that are dominant over a certain time period.

11.7 Conclusion

Well–field managers of coral atolls have to make judgements based on an intrinsically complex tapestry of signals wherein several threads are weaved. Generally speaking, two main weaving directions can be distinguished, the warp and weft. Changes to the quantity and quality of freshwater are affected by the warp, human–induced influences, and the weft, variations in climate.

(1) Human induced influences include:
    (1.1) Increased pumping to supply the countries growing population

and tourism sector (and possibly future irrigation);
(1.2) Pollution of the freshwater lenses by agricultural waste products.

(2)Natural climatic variations would include:
(2.1) Seasonal fluctuations in rainfall and thus recharge;
(2.2) El Niño related droughts and cyclones;
(2.3) La Niña related heavy rainfalls.

In the management of a freshwater lens of a coral atoll it is crucial to be aware of rainfall fluctuations that are related to superimposed climatic patterns. To minimize salt–water intrusion at the well head, pumping rates should always be estimated conservatively. We suggest, however, there should be an increasing awareness of the effects of interannual rainfall fluctuations on the salinity dynamics of the freshwater lens. Our results can be used didactically to illustrate the impact of both human activities and climatic variability on water quality. Pumping strategies for the freshwater lens developed by well–field managers should take interannual climatic variations into account.

Chapter 12

Small Island Developing States and Sustainable Development: a Case Study of Economical Development and Environmental Impact in Tonga

*

Balancing the Earth's accounts...

Abstract Small island developing states (SIDS) are vulnerable due to their small size in both bio-physical and socio-economic senses. They are increasingly confronted with the environmental consequences through utilisation of their fragile natural resources for economic development. Here we illustrate the dilemmas experienced by SIDS associated with sustainable economic development. Our case-study is the main island of the Kingdom of Tonga, Tongatapu, located in the South Pacific Ocean. We analyse the intensification of agriculture and the attendant pressures on the islands freshwater resources. We combine environmental and economic data. Tongatapu (256 km^2) is a raised coral atoll and the freshwater resources exist as lenses that float on top of denser salt water underneath the island. Since 1987 Tonga has exported squash pumpkin solely to Japan. Over the last 10 years, these exports have accounted for more then 40% of total export earnings, and represent 60 to 70% of GDP derived from agricultural export. This increase in exports is matched by an abrupt increase in the import and usage of agricultural chemicals. The island's freshwater lenses are increasingly under pressure from agricultural intensification. In the economic decision process, environmental impacts are not taken into account. This is partly because of overlapping institutional responsibilities of water management, and opaque institutional structures which are highlighted in the paper. The environmental consequences experienced by SIDS in terms of primary production stresses the need of taking ecological and natural capital into account when the benefits from international trade are evaluated. At the same time pollution will

*Adapted from van der Velde, M., S.R. Green, M. Vanclooster and B.E. Clothier. Sustainable development in small island developing states: agricultural intensification, economic development, and freshwater resources management on the coral atoll of Tongatapu. To be published in *Ecological economics*, 2006.

result in irrecoverable losses in terms of tourist potential. Improved agricultural practices have to be implemented through educational tools to ensure continuing economic prosperity derived from agricultural exports. Economic development of SIDS should also focus on the maintenance of kin relationships overseas, securing rent incomes and regional cooperative development efforts.

12.1 Introduction

Protecting natural recources requires a knowledge of both the biophysical and socio-economical domains. Governance at differenent hierarchical levels is needed to implement changes in a society. Although a good understanding of the impact of human activities on the natural world has existed for a long time, degradation of natural resources still continues in many places around the world. Several people have pleaded for a further integration of the 'soft' and 'hard' sciences (see Prof. J. Bouma at the ASSC 2004, and *Bouma* [2006], and others).

One of the challenges small island developing states (SIDS) face is to balance economical benefits with environmental pressures arising from their industrial and agricultural endeavours. The size of SIDS in an socio-economic and biophysical sense makes them extremely vulnerable. The intensity and scale of the issues facing SIDS requires direct attention.

The meeting for the 10-year review of the Barbados Programme of Action (BPOA) for the sustainable development (SD) of small island developing states (SIDS) was recently held in Mauritius. At that meeting the Mauritius Declaration was signed to reaffirm the international commitment to further implement the BPOA (1994). Climate change remained the most controversial item on the agenda. Special attention was given to investigate means to unite and protect SIDS against events similar to the tsunami that struck South-East Asia in December 2004. Since Barbados, the international community has become more aware that traditional concepts of sustainable development (SD) are not applicable to SIDS. This is directly related to the small size of SIDS with their small populations, limited natural resources and undiversified economies. Further, SIDS often have weak institutional capacity in both the public and private sectors. They also suffer from the 'tyranny of distance' and have a limited range in production and exports. They are vulnerable to external economic shocks and are susceptible to natural disasters and climate change as they have fragile land and marine ecosystems. UN Secretary General Mr Kofi Annan remarked that: 'As a result, their economies, including trade, financial flows and agricultural production, show greater volatility than those of other countries'. One of the challenges SIDS face is to balance economic benefits with environmental pressures arising from their industrial and agricultural endeavours. Maintaining resilience is often identified as the main strategy of sustainable management of ecosystems [*Scheffer et al.*, 2001]. Natural resilience on a small island is low, so the environment is vulnerable. The constrained nature of SIDS makes them well suited to illustrate the issues at the biophysical and socio-economic interface. A disadvantage for such an investigation is the lack of basic information available on SIDS. This further hampers policy formulation by SIDS.

A balance between economy and environment underpins sustainable de-

velopment. *UNEP* [2004] stated that: 'Economic development as a measure of human welfare is unsustainable in the presence of persistent deterioration in environmental and natural resource capital'. There is wide variety of definitions of SD and such discussions may be found elsewhere. We adopt *Holling* [2001] 's definition of sustainable development as being 'the goal of fostering adaptive capabilities and creating opportunities'. Sustainable development is also perceived as necessarily being an integrative concept across scales and sectors [*Robinson*, 2004]. We illustrate the issues of sustainable development facing SIDS in the Pacific Ocean. Our case study is the Polynesian Kingdom of Tonga with its exports of a mono-culture crop, and the consequent impact on its freshwater resources. Currently there is a lack of detailed analysis combining economic and environmental data of SIDS in the Pacific Ocean.

12.2 Pacific Islands

An estimated number of 20000 islands are located in the Pacific Ocean (181 million km^2) which cover less then 1% of the total surface area. These islands generally have a limited capacity to buffer against environmental hazards and they posses a low resilience to disturbance. They contain a high number of endemic plants and vertebrates [*Myers et al.*, 2000]. The Pacific islands have made, after sub-Saharan Africa, the least progress among the world's regions towards achieving the 'Millennium Development Goals'. The struggles of these SIDS to become part of the global economy, along with misplaced perceptions of self-reliance [*Bertram*, 1986], often have led them to evolve from functional and traditional practices to less sustainable ones. Traditional subsistence agriculture is being replaced by the production of mono-cultural cash crops for export [*Murray*, 2001]. Utilisation of natural resources for export through agriculture and fisheries are seen, next to tourism, as the main ways of economic development and diversification. Unfortunately these developments lead to environmental impacts on water resources, along with the pollution, degradation, erosion, and loss of biodiversity. One of the main actors to influence water resources is agriculture. Water management in SIDS is influenced by a number of other development issues, including coastal construction works plus solid waste and sewage disposal. Maintaining the quality of water is a necessity for societal well being, the environment and exploitation of the island's tourist potential.

12.3 Island characteristics

Tongatapu (175^o12'W 21^o08'S) is the main island of the Kingdom of Tonga, which is located in the South Pacific. The archipelago consists of about 170 islands, of which 35 are inhabited. The Kingdom of Tonga has a total

population of about 100,000 and of these 60,000 live on Tongatapu. Some 40,000 Tongans live in the country's capital of Nuku'alofa. Tongatapu has a surface area of 256 km^2 which is one third of the total land surface of the Kingdom. To underline the potential impact of agricultural activities on the environment we provide an outline of the island's environmental characteristics. Tongatapu is a raised coral atoll with a layer of soil ranging in a thickness of about 6 m in the west to 0.5 m in the east [*Cowie*, 1980]. The soil is derived from volcanic ash and is naturally quite fertile. The soil rests upon a porous limestone aquifer. The hydraulic conductivity of the limestone is high [*Hunt*, 1979]. Water draining from the soil rapidly joins the groundwater lenses. Fresh surface water resources do not exist on the island. A large amount of about 1780 mm of rain falls each year on Tongatapu [*Thompson*, 1986]. It is estimated that about 30% of the rain flows through the filtering soil to recharge the groundwater (see Chapter 9). The fresh groundwater floats as lenses on the denser salt water at a depth of about 3 to 25 m below the soil surface. The fresh groundwater lenses under the atoll is balanced between episodic rainfall replenishment and continual depletion by evapotranspiration, extraction and outflow to and mixing with the surrounding seawater or internal lagoon. Mixing of freshwater and sea water occurs as tidal heads are transmitted through the aquifer. The groundwater is connected with the relatively enclosed Fanga'uta lagoon with limited ocean exchange [*Zann*, 1994]. The general land gradient is towards the lagoon and groundwater seepage into the lagoon can be observed at several locations during low tide.

12.3.1 Economy

Tonga can be categorised as having a MIRAB (Migration, Aid, Remittances and Bureaucracy) economy consisting of a large public sector with a dependency on aid and remittances [*Bertram and Watters*, 1985; *Storey and Murray*, 2001].

Imports are larger than exports which results in a strongly negative trade balance (Figure 12.1, data from *Cerisola et al.* [2003]). Exports make up about 20% of total imports and mainly of agricultural products. About 40 to 50% of the export revenue over the period from 95/96 to 00/01 was derived from agricultural export to Japan while imports are mainly from New Zealand: about 35 to 40%. Although having a significant trade deficit, Tonga's economy maintains a strong balance of payments [*Bertram*, 1999] mainly due to aid and remittances. Tonga's trade deficit is mainly funded by private remittances. Remittances accounted for, and financed about 50 to 60% of total imports over the 1994-2002 period. Remittances are an integral part of Tonga's economy. It is estimated that as many Tongans live in overseas metropolitan areas as in Tonga. Economic prosperity is based on the familial ties that maintain the flow of remittances. The strength of the

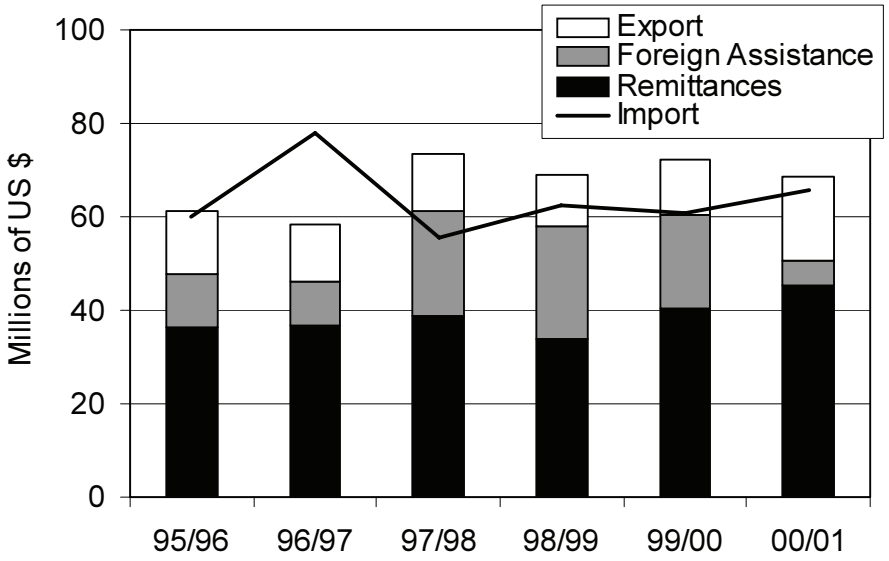

Figure 12.1. Import, export, foreign assistance and remittances in Tonga (data from *Cerisola et al.* [2003]).

international kin relationship has been emphasised [*Bertram*, 1999]. Ways have to be found to develop a 'sense of belonging to the home land' [*Lee*, 2004] to prevent a decline in remittances from the second or third generation of overseas Tongans. This would be disastrous for Tonga's economy. Tonga's major trade partners are Australia, New Zealand, Fiji and Japan and these countries, plus China, are also the main providers of foreign assistance. Foreign assistance is variable and is used as a top up to cover the trade deficit [*Bertram*, 1999]. Pacific economies are 'not driven by productive factor incomes from domestic industries, but by the flows of rent incomes' [*Bertram*, 1993]. *Bertram* [1999] further argues that it does 'not only mean that any increase in aid, remittances or export earnings flows through directly to increased imports, but also that any reduction in external sources of funding places an immediate squeeze on imports and living standards', which is common across several Pacific island economies. Tonga's tourism base is currently small and it is therefore seen as a potential development sector, especially for marine based activities. Recently a memorandum of understanding was signed between Tonga and China that allows Chinese tour operators to bring Chinese tourists to Tonga. This is a first step for Tonga to receive the Approved Destination Status by Chinese authorities (*www.matangi.tonga*). The number of visitors visiting Tonga between 1998 and 2002 ranged between 43,977 and 53,576 [*Tongan National Assessment Commission*, 2003]. Tourism receipts ranged between 11.6 and 16.5 million Tongan Pa'anga (TOP, 1 TOP equates to 0.41 Euro or 0.52 US$, April 2005)

in the period of 1996/1997 to 2000/2001 [*Cerisola et al.*, 2003].

Agriculture is a significant sector in Tonga. The 1996 Population Census recorded that a third of employed people are engaged in agriculture. The majority of the population relies heavily on agriculture for both subsistence and commercial purposes. Nowadays it accounts for more then 50% of the nation's export earnings. Tonga has experienced several temporary successes through exporting cash crops (see *Sturton* [1992]). Unfortunately, the market of these once successful export products has all but collapsed. Coconuts, or copra, was Tonga's first export product at the beginning of the 20th century. Bananas in the late sixties and early seventies were a boom and bust operation. The production of bananas required for 'the first time in three millennia of Tongan agriculture, external inputs in the form of fertiliser, pesticides and extensive mechanical tillage' [*Stevens*, 1999]. Watermelons were exported in the early eighties, and coconuts until the late eighties. Exports of coconuts gradually declined over the period 1985 - 1991 largely because international coconut prices declined (*Sturton* [1992] and see Figure 12.2). Watermelon exports virtually ceased in 1986 with quarantine bans from New Zealand [*Sturton*, 1992]). These were lifted in the early nineties, but the exports have not been able to pick up to levels beforehand. Several explanations exist for discontinuities in the production of export products. Central is the inability of SIDS to buffer against external factors.

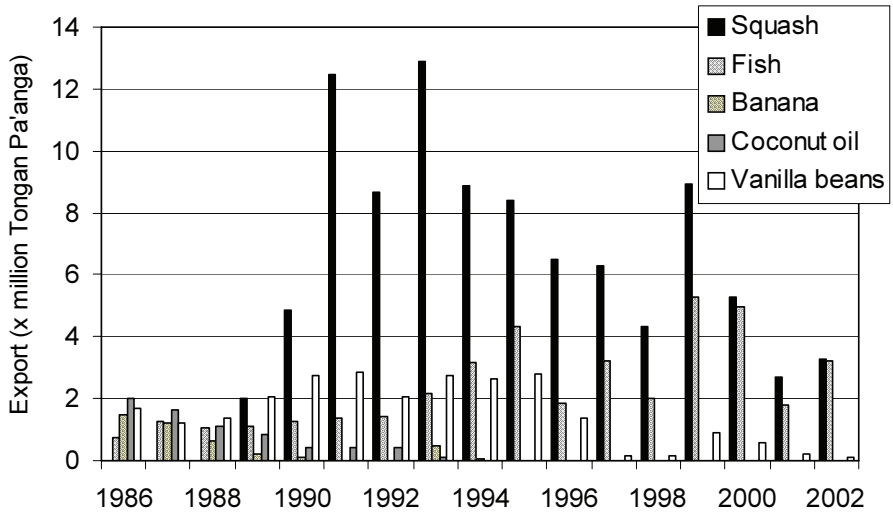

Figure 12.2. Export value of principal export commodities (data from *Bank* [2004]).

Non-traditional agricultural crops such as vanilla and squash have been introduced. Vanilla exports are strongly dependent on the dominance of Madagascar's exports, and have now virtually ceased, accounting for an average of 352,000 TOP in the period of 1997-2002. In 1987 began successful

exporting of *Cucurbita maxima* (squash) to Japan (Figures 12.2 and 12.3). It is likely that the investment in the production of squash will have had a flow-on and negative impact on the investement in the production of other agricultural products [*Sturton*, 1992].

12.3.2 Squash Export

Even though agricultural exports remain relatively unimportant in the overall macroeconomic equation [*Storey and Murray*, 2001], the impact of squash export on Tonga's society is unprecedented. Due to the value of export of squash to Japan, a roughly balanced trade has existed with the value of Japanese imports since 1989. During the period 1994–2000, the squash export industry has accounted for more then 40% on average of Tonga's total export earnings, and more than 60% of the total value of agricultural export. Since the first successful exports in 1990, the squash export has also fluctuated, but it has always dominated total export earnings. The squash industry is often quoted as a market-based economic success story for a SIDS. However, the dependency of such a large percentage of export revenue, on export trade with a single country, is fragile. Tonga utilises a niche period in November and December for the export of squash to Japan. In Tonga about seven local companies have licenses to export squash and many have harmonised the products used for the squash production. The area under cultivation for squash increased from 81 hectares in 1987, to 2,114 hectares in 1994. This yielded a total of 17,000 tonnes for export, with gross earnings of 13 million TOP. In 2000, about 700 farmers grew 4,408 hectares of squash. Forty eight percent of these farms were smaller then 4 acres and only 0.3 percent were larger then 50 acres [*Manu*, 2000]. The export of squash to Japan correlates with the amount of rain that falls in the growing season as the period of squash growth coincides with periods of droughts in Tonga (r^2 of 0.6 for a linear regression between rain in the growing season and export value, in the period 1992-2001).

The export of squash is also influenced by other factors, such as export quotas, fluctuations in the squash price, and storage problems (for example in the 1991 season [*van der Grijp*, 1997]). The export quota system was first operated in 1992 [*van der Grijp*, 1997] to control the market. Quotas were not strictly set, and they are often not met.

12.3.3 Socio–economic impact of the squash industry

The opinions vary about the socio-economic impacts of the squash industry in Tonga. *Felemi* [2001] sees the export of squash as 'undoubtly one of the few success stories of agricultural exporting operations for the South Pacific to developed countries'. *Sturton* [1992] stated that the rapid growth of the squash industry 'indicates the far-reaching consequences for develop-

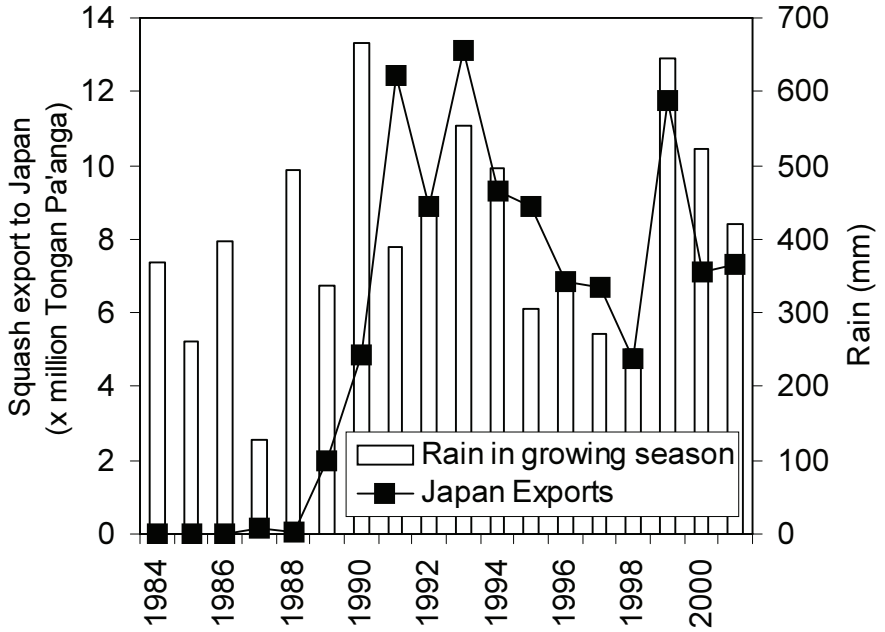

Figure 12.3. Export to Japan and cumulative rain in squash growing season on Tongatapu (Export data from annual reports prepared by Tonga's Statistical Department and meteorological data from NZ meteorological service).

ment if the opportunities and incentives are right'. The World Bank and the IMF also see the squash production in Tonga as an example of an export-orientated economic solution for developing countries to participate in the global economy. Tonga's squash export is, according to *Storey and Murray* [2001] 'a clear indication for the regressive impacts associated with recent policy shifts, particularly in contexts where institutionalised hierarchies allow privileged groups to capture the benefits of export growth'. *Coxon* [1999] described the negative socio-economic effects on small farmers involved in the industry. The success of the squash's export industry for Tonga's economy seems obvious, at first. But recent economic research by *Fleming and Blowes* [2003] suggests that Tonga will struggle to achieve long-term sustained economic development based on squash export. Limited natural capital will hamper primary production industries.

12.3.4 Environmental consequences

The increase in squash production has led to an enormous increase in the import and usage of agricultural chemicals. Reflected in Figure 4 as tons of fertiliser imports per year.

Annual fertiliser use for the whole island of Tongatapu (26000 hectares)

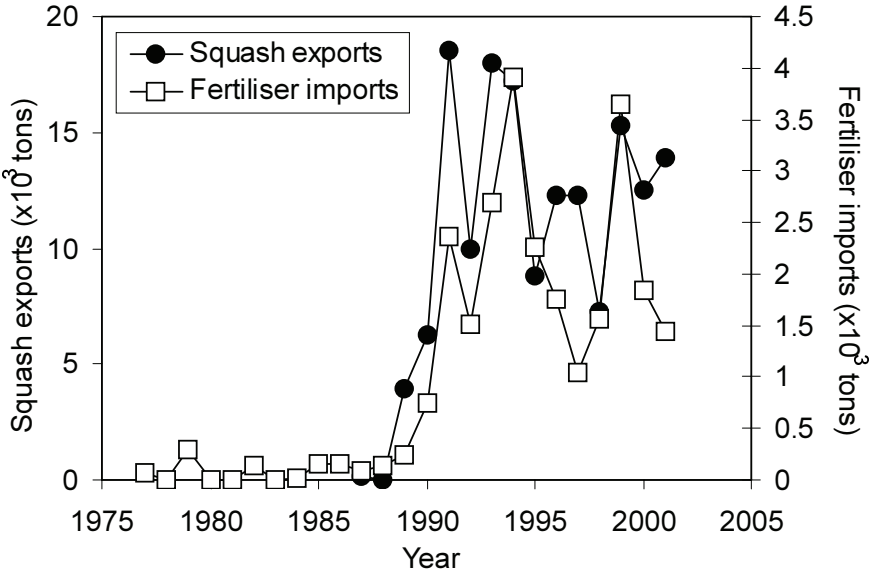

Figure 12.4. Export of squash and import of fertiliser (data from annual reports prepared by Tonga's Statistical Department).

has increased more than an order of magnitude. It has grown from about 5 kg ha^{-1} at the end of the eighties, to 80 kg ha^{-1} at the end of the nineties. This will have led to an increased chemical load on the environment. Fertilisers make up about 60-70% of the value of imported agrichemicals. The total import value of pesticides, that is the fungicides and herbicides used for agricultural purposes, has increased with a factor of about 2.5 since 1987. Pesticide imports were about 0.7 million TOP in the period of 1999-2001, while fertiliser imports were about 1 million TOP in the same period (data from Tonga's Statistical Department).

Squash has thus led to an enormous increase in the usage of agrichemicals. These include fertilisers (Figure 12.4), along with pesticides to control aphid infestations and the spread of viral diseases, as well as and the use of fungicides to prevent powdery mildew. This rise has led to public concern related to health issues, which include risks of spray drift and the lack of protective gear, through to and awareness about the potential contamination of Tongatapu's freshwater resources. Concerns where expressed as early as the early nineties (*www.matangitonga.to*) and anecdotal evidence on Tongatapu suggests a catastrophic eutrophication of the lagoon at points were groundwater seeps into the lagoon. People used to bath at these points only 10-15 years ago. Nowadays algae growth has made this impossible. The source cannot directly be attributed to agriculture, for it may also be due to leaking septic tanks. Although it is yet in detail unclear what impact

the development of squash might have, or has had on the water resources, scientific evidence is mounting about the negative environmental impacts of agriculture. As early as 1984, SPREP [*Chesher*, 1984] prepared a survey of pollution sources on the island and found several pesticides including lindane, heptachlor, aldrin, endosulfan and DDT in well water. Luckily most of these products are now forbidden in international trade. The extent of this legacy is however unknown. Research by *Harrison et al.* [1996] and *Morrison and Brown* [2003] reported that 'some migration of more persistent pesticides residues into Fanga'uta lagoon has occurred'. They found the occurrence of organochlorines in sediment and shellfish of the central Fanga'uta lagoon. The low concentrations found were considered to have a minimal direct impact on human health. Based on studies since 1981, *Kaly et al.* [2000] concluded that a general trend in decreasing water clarity of the lagoon occurred and that generally nutrient concentrations had increased. Degradation of coral communities in the lagoon were attributed in some part to urban nutrient-runoff [*Zann*, 1994].

Concentrations of nitrates in the drainage water leaving the rootzone of the squash measured by *van der Velde et al.* [2004] at approximately five times the WHO limit for drinking water quality of 11.5 ppm N-NO3. During an initial survey of the groundwater quality we identified pesticide traces of dieldrin, diazinon and carbaryl in 3 of 10 groundwater samples taken around the island. Other effects of the agricultural intensification include deforestation. Nowadays less then 4% of the original tropical forest is still intact and that is largely a part of a national park [*Wiser et al.*, 2002]. A recent development is the emergence of irrigation on the island for as we showed, drought can affect the value of squash export (Figure 12.3). The relation presented in Figure 12.3 suggest that soil moisture availability is influencing the exportable squash yield. Farmers have recognised the inadequacy of their dependency on rain, and the influence that droughts can have. The variability of rainfall from season to season is also illustrated in Figure 12.3. Growers are exploring the possibilities of irrigation of squash. Here then, another dilemma is emerging. Increasing irrigational demands will lead to additional pressure on the freshwater lenses that are at some parts already showing signs of saltwater intrusion.

It can be concluded that the abrupt increase in the usage of agrichemicals (Figure 12.4), combined with the general intensification of agricultural practices and increased demographic pressures, is putting the environment of Tongatapu under increasing pressure. A general lack of baseline data in SIDS on the concentration of nutrients and pesticides in the coastal zone has been identified by *Rawlins et al.* [1998] in a review of agricultural pollution of SIDS in the Caribbean. It remains a scientific challenge to pinpoint exactly the contribution of agriculture to environmental degradation, as often there are several contributory effects. The depletion of marine resources in Fanga'uta lagoon and the fringing reef for subsistence purposes has been an

ongoing process and has already resulted in severe loss of stocks, reductions in average catch size and deceased coral reefs [*Malm*, 2001]. This is being aggravated by the effects of agriculture and coastal construction works.

We can summarize that although the export is economically successful, the environmental constraints and production consequences are currently not sufficiently taken into account. Taking fertiliser and pesticide import data as a proxy for environmental pressure would suggest a concomitant rise in their loading on the soil and freshwater resources. This is now being backed up by scientific evidence.

A description of Tonga's institutional arrangements of governance and policy related to environmental issues is presented below in order to understand the current situation and suggest sustainable alternatives. Although our description is specific to Tonga, there are similarities with other SIDS.

12.3.5 Institutional Arrangements

Tonga is a hierarchical society and is governed by a constitutional monarchy. The monarch appoints the Prime Minister and ministers for the Cabinet. The legislature is unicameral and consists of the Cabinet, the Speaker, nine nobles elected by the hereditary nobility, and nine representatives elected by literate taxpayers over the age of 21. Currently the governmental system of Tonga is a topic of discussion (see for example *www.matangitonga.to*). Several developments have occurred in recent years. The Department of Environment became an autonomous government entity in 2001. It is now the central agency for the administration and coordination of national environmental policies, programs and activities. This was a step towards strengthening the institutional basis for the implementation of environmental policies. Recently, Tonga's 7^{th} national strategic development plan (2001-2004) recognized that: 'The central policy guideline is to promote environmentally sustainable development that is consistent with the priority economic and social needs of Tonga'. In 2003, the Environmental Impact Assessment Act (EIAA), the first piece of legislation that states SD as it main objective, was approved [*Tongan National Assessment Commission*, 2003]. The EIAA ensures that all major development projects are supported by an environmental assessment report. The Department of Environment is still limited by a lack of financial resources, a lack of regulations, inadequate capabilities to enforce regulations, and no coordination between the different sectors [*Prescott*, 2003]. Expert local knowledge about the environment is only just becoming available.

12.3.6 Land management

Tonga's land management system incorporates traditional hierarchical values and was created for a predominantly egalitarian subsistence economy

where each male reaching the age of 16 was entitled to 8.25 acres of land. Due to land shortages, this system is currently malfunctioning and has left the government without a means to actively plan the use of land. An analysis may be found in *Crawford* [2001]. Despite the fact that *Crawford* [2001] notes that 'the current land management and tenure systems serve as a barrier to Tonga's incorporation into the global economy' the export success of squash illustrates the strong 'grey market' where land is leased for production purposes in exchange of 'gifts'.

12.3.7 Water management

Water management on the island is carried out by a consortium of government agencies. Public water is vested in the Crown as stipulated in the Public Health Act [*ESCAP*, 1999]. A schematic of the different agencies involved in water management on the island is presented in Figure 12.5. The figure is based on the author's experience and the reports by *Falkland* [1992] and *ESCAP* [1999]. The 'Water Resources Committee (WRC) reviews development proposals related to water resources and makes recommendations that are forwarded to Cabinet. The WRC consists of representatives from government agencies with responsibilities in water resources and it thus has contacts with all agencies presented in Figure 12.5. The Hydrological Section of the Ministry of Lands and Survey and Natural Resources (MNSLR) is the main agency responsible for water resource assessment, development and water management in Tonga. It controls the drilling of wells, assists in the determination of the rate of water pumping from groundwater and is responsible for the prevention of pollution of the freshwater resources for all of Tonga, except for the urban area of Nuku'alofa. The Hydrogeology Unit of the MNSLR provides all the detailed technical know-how concerning water resources development. The Ministry of Health (MoH) is responsible for monitoring and surveying the biological and chemical quality of public water supplies. It also has an Environmental Health Unit concerned with health impacts of environmental hazards and degradation. The WHO representative to Tonga located in the Min. of Health has been involved in water quality monitoring programs. Village Water Committees (VWC) operate and maintain the physical components of the pumping systems of village water supplies. They receive quality information from the MoH and operate under the auspices of the MNSLR. The Tonga Water Board (TWB) was enacted under the Water Board Act (1966), and is responsible for the maintenance of public water-supply systems in the urban area of Nuku'alofa and also for selected urban areas in 'Eua, Ha'apei and Vava'u. The Waterboard used the drilling rig owned by the Ministry of Works to drill new production and monitoring boreholes.

The Ministry of Agriculture (MAF) is currently not directly involved in water management on the island. It does however play an important role

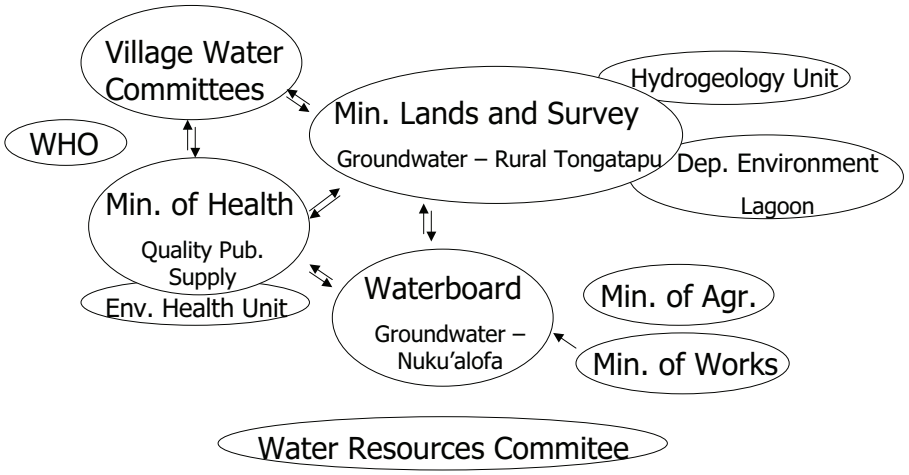

Figure 12.5. The main actors involved in water management on the main island of Tongatapu with main responsibility indicated. Arrows indicate active interaction and intersected ellipses indicate subsidiaries. Arrows connecting Water Resources Committee are not shown.

in regard to the safe use of pesticides and their impact on water supply quality as specified in the Pesticide Act (2000). MAF is also involved in agricultural-practice recommendations for the squash industry, and it promotes integrated pest management. MAF also has an interest in relation to irrigation. However most experimentation with irrigation is done by the larger squash farmers and exporters. There are also other private consumers in the domestic and industrial sectors currently pump large quantities of groundwater. Effective governance of groundwater is hampered by the invisibility of the groundwater resource. *ESCAP* [1999] stated that 'the overlapping of responsibility in the management of this most crucial resource has led to conflicts which have not necessary been satisfactorily resolved'. It should be noted here that the hydrogeological connection of surface, subsurface, lagoon and coastal zone, implies the need of involvement of sectors currently not actively involved in the water management. Sectors that are influenced either directly or indirectly by the quality and quantity of water would include fisheries and tourism.

For drinking, most Tongans rely on and prefer collected rain water. Most rain is collected from rooftops and stored in reinforced concrete, fibre glass or iron tanks maintained by the Village Water Committee's. In the capital of Nuku'alofa groundwater is also used as potable water. In drier periods, groundwater usage and the shipment of bottled fresh water into Tonga has occurred. Groundwater is extracted on Tongatapu via about 250 domestic wells, plus wells for the village water supplies that are equipped with a pumping system. While average annual rainfall is high, droughts of mod-

erate severity are common for about 2 months, and occasionally for up to 4 months, especially during the period July – November. *Fuavao et al.* [1996] tested the water quality in the capitals distribution system and they found some faecal contamination. They emphasized the need for continuous monitoring of water quality. Water quality tests are often carried out independently by the different agencies involved in water management. Several agencies have, for example, an interest in pesticide analysis of groundwater and they have independently carried this out in the past. During a survey agencies which have carried out pesticide analysis of the water resources were identified (see Chapter 3). They included the Hydrogeology Unit (MLSNR), Dep. of Environment (MLSNR), Min. of Health, WHO, the Waterboard, MAF and TongaTrust (a local NGO). Luckily the concentrations that were found were very low. However, currently no consistent protocols exist for regular sampling, and the information that has been gathered is currently not stored centrally, neither is it coordinated. *Prescott* [2003] identified that the Pesticide Act (2000) does not cover storage, sale and distribution of pesticides and the Act lacks enforcement provision. Tonga should revise their regulations related to agrichemical import to minimise health and environmental impacts of agrichemicals. Gramaxone for example, with the active ingredient paraquat, is a non-selective herbicide. It accounts for the highest agrichemical import by value in Tonga. The danger the product poses on human health is well known. It is forbidden in various Scandinavian countries and it's use is restricted in the United States and several other countries.

12.4 Management options

Even though the macro-economic significance of the squash industry may not be as significant as commonly perceived, it is clear that it is extremely important for export earnings, and it is important as an employment provider. Sound water management needs agricultural practices that pose a minimal risk of groundwater pollution. Possibilities to improve the agricultural practices for squash exist [*Petelo*, 2002]. *Petelo* [2002] studied the productive efficiency of the squash export industry in Tonga and concluded that considerable inefficiencies exist. The average economic efficiency for different farm categories was estimated to be only 31% to 46%. One of the issues raised by *Petelo* [2002] was the inefficient use of agrichemicals. Indeed the data (Figure 12.3) suggest that currently soil fertility is not the main limiting factor for squash production, but rather the soil moisture availability in the top soil, which is directly related to the amount of rain in the growing season.

A sustainable scenario would be founded upon community-based initiatives that combine ecologically sound alternatives, which also are economically viable. When James Cook visited Tongatapu in 1780 he wrote in his journal 'Nature, assisted by a little art, no where appears in a more flour-

ishing state than at this isle'. In other words, he observed well-maintained gardens and a productive type of agriculture that had existed for more then 2000 years. By performance, this equates to sustainable! Fertility of the soil was guaranteed by long fallow-periods. Today, part of the solution to the agricultural production for export may thus be the reinvention of, to quote Cook 'the art' of agriculture, albeit now aided by science. Development of sustainable agricultural practices *van der Velde et al.* [2004, 2005] will lower the pressure on the environment. Unfortunately, the adoption of recommended production practices and sustainable agricultural practices is not straightforward. Pragmatic changes are potentially successful on a short time-scale and do not need policy intervention or enforcement. The vulnerability of SIDS demands fast action. Demonstrating the implementation of sustainable practices to the community of interest remains a bottleneck. We believe that educational tools are still the best answer. 'Efficient fertiliser use workshops' have been organised on the island in the past. However, *McGregor* [2002] reports that 'MAF's Policy and Planning Section has found that most squash farmers overuse inputs to the detriment of their profitability, mainly because of advice given by exporters, suggesting an implicit conflict of interest'. Another market option for the squash industry is an organically grown product. However, this has been unsuccessfully explored in the past. Nevertheless, a customer survey [*Ada*, 2000] indicated that specific options to export environmentally friendly grown squash to Japan do exist. In 2003, another development emerged as Japanese importers started to demand the spray diaries for the agrichemical products being used in production. If such Good Agricultural Practices (GAP) protocols as EUREPGAP become international de facto regulations, then such pressures will increase. The Decision Support Tool (DST) we developed, the 'CROPPRO calculator', is an example of an instrument that could provide growers with a means to verify their certification under GAP protocols (Figure 12.6). The 'simple' DST also allows the farmer and the agricultural officer to assess the environmental impact of a range of agrichemical products, quantified by amongst others the 'long term leaching risk', and how that impact is affected by changing for example the number of applications.

The export success of the squash industry in Tonga, and the impact of the agricultural practises on its water resources illustrates the difficulties experienced in sustainable economic development in SIDS. Concerns expressed on the environmental impacts of the agricultural practices currently used in the squash industry were not taken into account in the original economic decision processes. This is partly because of the lack of institutional foresight in the environmental sector and overlapping responsibilities of water management. This is a worldwide problem, not only limited to SIDS (see for example: *Parliamentary Commissioner for the Environment – New Zealand* [2004]). The institutional strength will hopefully continue to increase after the creation of the Department of Environment.

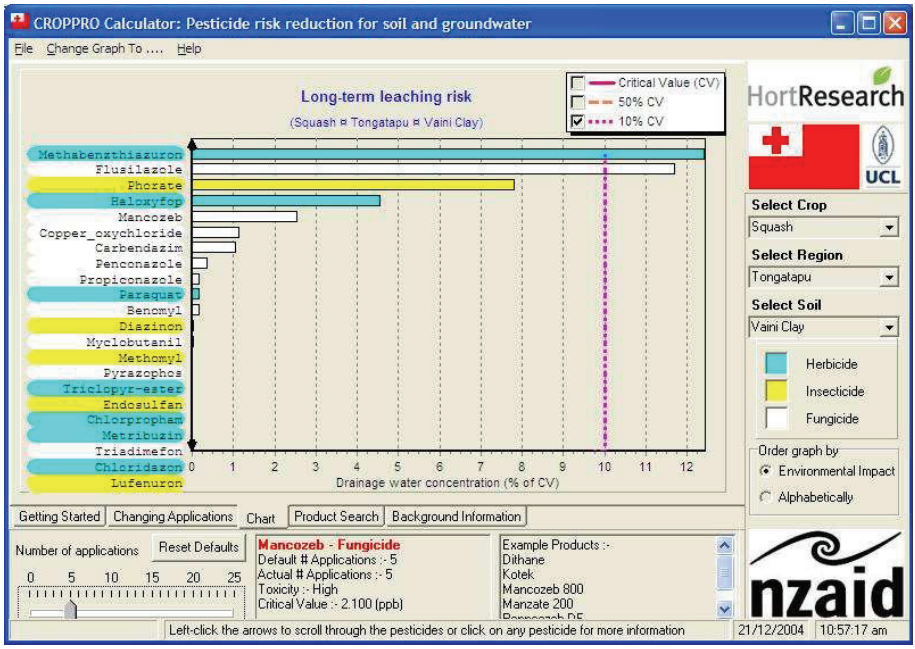

Figure 12.6. Screen dump of a Decision Support Tool that allows farmers evaluate the environmental impact of a range of products. Options include long-term and short-term leaching and soil risk.

12.5 Discussion

The case of the squash industry on Tongatapu clearly falls in the category of unilateral unsustainably exchange described by *Andersson and Lindroth* [2001]. This is reducing the ecological capital of Tongatapu. Currently Tongatapu is exporting its soil quality [*Stevens*, 1999], and water quality to Japan. It is an example of a situation described by *Dietz et al.* [2003] where 'a larger scale economic incentive is not closely aligned with the condition of the local ecosystem'. *ESCAP* [1999] notes 'given the limited resources of the country, the environment will continue to be accorded low priority unless a crisis results from neglect of the environment.' Diversification of products is suggested as a solution to harness the economies of SIDS. This option is constrained by the limitation of the small production capacity of these countries.

Multilateral exploitation of Pacific fish is suggested as one of the few potential sectors for economic development of the region. Currently the Pacific Islanders collect only 5 to 8 % of the US$ 2 billion value of the annual catch of one million tonnes of tuna according to the Pacific Islands Forum Fisheries Agency by the selling their exclusive economic zone (EEZ) fishing rights to distant fishing nations. Individually these SIDS lack the capacity

to sustain a fishing fleet. In Tonga (Figure 12.2) the value of exported fish seems generally to have increased since the eighties. Exploitation of this resource has to be done with care as currently global fish resources are already overexploited [*Pauly et al.*, 2002]. In some Pacific islands Marine Protected Areas have been created in response to overexploitation of fish in the coastal zones and associated damage to the marine environment, this functions at the same time as a useful precautionary approach that allows for the recovery of fish stocks [*South et al.*, 2004]. More thorough analysis of fish and the fishery sector may be found elsewhere (see *Dalzell et al.* [1996]).

Tourism is another sector with potential for development. The Department of Environment is also involved in assisting Tonga in developing it's tourism potential through community clean up campaigns. The Department of Environment in cooperation with the Tonga Tourism Office recognize that compromising environmental quality could put an end to what might, in the future, be a lucrative tourist industry. In the introduction of the paper we spoke about the 'tyranny of distance'. Nowadays the 'death of distance' [*Cairncross*, 1997], which refers to the erosion of distance in a world that is globally connected in cyberspace, may soften some of the aspects of the 'tyranny of distance'. Geographic location loses it's importance as cyberspace provides a frictionless possibility for the transfer of data and information. However, unfortunately, currently most economies of small states (with notable exceptions such as Singapore) are not (yet) data or information intensive. The 'death of distance' may have direct (potential) benefits for tourism, as it allows SIDS to advertise to the global community.

Other economic development routes exist as well, especially those that seek to strengthen and maintain the cultural link of expatriate Tongans to maintain the inflow of money from overseas. *Bertram* [1986] argues that 'the 'development' problem for planners and policymakers is not so much the promotion of modern, capitalist, tradable-goods-producing sectors within the island economies, as the question of how rent incomes should (a) be made more secure and predictable, and (b) be allocated among members of the island society, to determine the 'mix' of economic activities'. Economic development of SIDS should focus on the maintenance of kin relationships that secure transfers of repatriated overseas earnings, private remittances, and official aid. *Bertram* [2004] showed through regression analysis, that SIDS in the Pacific convert to the income levels of their patrons. Those island economies with close political linkages to their former colonial powers were the ones with greatest prosperity in 2000. These common links, primarily with British Commonwealth nations or France also creates options to increase regional economic cooperation for development within the Pacific. A connection of both, through the EU would even be more beneficial to Pacific SIDS.

12.6 Final remarks

DuToit et al. [2004] stated that: 'To expect local people in the tropics to voluntarily forego modern Western living standards for the sake of nature conservation is to naïvely expect them to bear iniquitous costs'. A similar issue can be raised for the Pacific. If we are willing to accept that the responsibility for local environmental resources lies with the global community then an option similar to *Ferraro and Kiss* [2002], the possibility of direct payments for conserving biodiversity, may be proposed.

Proper management and policy formulation requires information. Nowadays indicators are often used to identify trends and make large scale comparisons. In a landmark paper, *Briguglio* [1995] classified SIDS according to their economic vulnerabilities using a composite index representing exposure to foreign economic conditions, remoteness and insularity and disaster proneness. Overall, Tonga ranked second on this economic vulnerability index. Recently the creation of an environmental vulnerability index (EVI) was started by the South Pacific Applied Geoscience Commission (SOPAC, *Kaly et al.* [2003]). Practical use of the EVI has been carried out for the Caribbean island of Tobago [*Gowrie*, 2003]. It was concluded that high scores of individual indicators were mostly due to anthropogenic origin and that 'Tobago's vulnerability could be controlled by vigilant management of the island's resources, coupled with information sharing of agencies governing these resources'. These indices are very useful and they may aid in resolving the main challenge: to evaluate environmental vulnerability along with economic performance. Taking their interdependencies into account is a hard task, as illustrated in Figure 12.4. An option is to take the economic value of water, namely its natural capital, into account. Valuing the ecological, natural and amenity capital value of water remains problematic [*Morris et al.*, 2003]. The use of the 'virtual water' concept in relation to international trade [*Hoekstra and Hung*, 2002] should then be extended to account for the impact that agricultural practices have on the quantity and quality of the water resources of the exporting country. The EVI, and other projects, illustrate the importance and critical role of regional organisations such as SOPAC, and the South Pacific Regional Environment Programme (SPREP, see *Chesher* [1984]). These can provide for effective environmental governance [*Dietz et al.*, 2003] of the Pacific SIDS. These organisations can build long-term relationships to establish trust, exchange local knowledge and even promote a 'Pacific nationhood'. This would be essential for regional economic development, successful introduction of new policies and technologies, and the promotion of environmental awareness in a region that is generally characterised by nations with weak institutional frameworks. It is positive to note however, that these states are increasingly voicing their concerns. Costa Rica's environmental minister was quoted in the *The Economist* [2005] as saying: 'We need to learn the language of finance and economics,

and demonstrate the economic benefits of the environment'.

We argue that effective environmental governance for Tonga should include further commitment to ensure maintenance of ecological and natural capital in the trade balance. This would demand international review of the dependency created by bilateral trade. There is a need to maintain and strengthen the ties of Tongans overseas, and that between Tonga and other SIDS to create international debates on the exploitation of ecological, natural, and economic capital.

12.7 Conclusion

The case study presented here illustrates the fact that SIDS are increasingly confronted with the classic 'contradiction' between economic progress and environmental degradation. We have argued here that this contradiction is more immediate in small states. In Tonga, the export of the cash crop squash, now the main export product, requires additional inputs of agrichemicals on a scale not previously experienced. Even though significance of squash exports in macro-economic terms may not be that large, it is extremely important for export receipts and employment. Alternative and more sustainable agricultural practices need to be implemented. Unfortunately the institutional strength of both environmental measures or obligations and monitoring of the quality of Tonga's water resources is weak. The time it takes for the environmental pressures to be severe, and possibly irreversible, is much shorter in SIDS due to their high vulnerability and fragile ecosystems. The environmental limitations experienced by SIDS in terms of production capacity and the increasing environmental deterioration require taking ecological and natural capital into account when the economic benefits of international trade are evaluated. In not doing so, environmental sustainability and long-term economic development are both at risk. The natural resources of SIDS may represent a comparative advantage if they support tourism, but they represent a comparative disadvantage if they are over-used during land-based development. Compromising environmental quality could put an end to what might, in the future, be a lucrative tourist industry. Governance solutions have to be found to ensure that Tongatapu and other SIDS will continue to reap richness and wealth from their natural resources. At the same time they must regulate the pressures on the environment to ensure the continuing value of their ecological and natural capitals.

Chapter 13

Conclusions, synthesis, and perspectives

13.1 Introduction

The notion of the specific vulnerability, along with observations of the general environmental degradation of SIDS, coupled with an increased awareness of the impacts of climate change on these island environments, has led several international organisations to promote the development of research and management strategies specifically aimed at SIDS. The research presented in this PhD thesis has endeavoured to provide specific understanding of the consequences of agriculture and climate variability on the quality of water resources of SIDS.

The major aim of this thesis was to investigate, in a comprehensive way, the main influences of agricultural intensification and climate variability on the quality of the freshwater resources of the raised coral atoll of Tongatapu. Subsequently, bearing in mind the necessity to manage sustainably the island's freshwater resources, concepts and issues were identified to improve the capacity to manage the freshwater resources. Furthermore, this takes into account the economic benefits of agricultural exports, as well as the need for pumping of the freshwater lens for potable water supply and protecting receiving waters.

This thesis consists of four parts. In the first part the general biophysical characteristics and the current environmental state of Tongatapu are discussed. Thereafter, I continue with three parts which represent three interconnected research areas:

(1) Agricultural impacts on Tongatapu's water resources, as studied at the field scale;
(2) Climatic impacts on Tongatapu's water resources, as studied at the island scale;
(3) Socio–economic considerations for managing these impacts and evaluating economic benefits and consequences on ecosystem services.

We first present a summary of the conclusions of the work presented here, and afterwards we provide a synthesis of the research and outline perspectives for future work.

13.1.1 Agricultural impacts

In the introductory Chapters (1 and 2) we set out the geographical and biophysical background of this study, and showed evidence of the downstream consequences of agricultural intensification on land and water resources of Tongatapu. We specifically provided 1) evidence for the contamination of Tongatapu's ground- and lagoon water resources by fertilisers and pesticides, and 2) the loss of soil structure and associated changes in the soil's hydraulic characteristics which promote runoff and erosion at the field scale. Tongatapu's environment has thus degraded, and continues to degrade. The occurrence of agrichemicals in Tongatapu's environment provides one metric of this overall degradation. Thankfully, the measured quantities of agrichemicals are still very low and options exist for restoration.

Squash pumpkin production is the main reason for agricultural intensification on Tongatapu. To quantify the impacts on the water resources of the agricultural practices used for squash growth, we quantified the components of a field water balance. Specifically, this included plant transpiration (Chapter 4), drainage (Chapter 5), soil evaporation, and a general description of the water balance (Chapter 6).

Transpiration was measured using specifically designed heat–pulse equipment to monitor sapflow. Stomatal conductance was modelled with response functions for light, air temperature, vapour pressure deficit, and soil moisture. Transpiration losses were calculated using a 2–layer, big–leaf model in combination with modelled stomatal response and measured leaf area. A crop factor for squash was derived for this tropical maritime climate. Water use was about 3 to 5 l per plant per day.

Tongatapu's soil exhibits preferential flow phenomena because of the macroporous structure of the soil. Large drainage fluxes were measured using three types of flux meters. However, the measurements with passive capillary fluxmeters overestimated drainage. Drainage fluxes measured with non–suction flux meters were in good agreement with 1D simulations and reached peak rates of 14.4 mm hr^{-1} for both the model and the non–suction flux meters. Overall, summing up the water balance components, a water balance error of about 20% was obtained. However, this approach lacked a detailed sensitivity analysis, and the error may be attributed to local scale heterogeneity in crop and soil properties. The high drainage fluxes highlighted the possibility of fast transport of solutes derived from surface–applied fertilisers. The drainage of NO_3^- and NH_4^+ out of the root zone, was monitored (Chapter 7) using flux meters. Flux concentrations ranged between about 30–60 ppm NO_3^-. This contributes to the nitrate loading on

the receiving waters of Tongatapu's ecosystem, as evidenced by algae blooms at seepage points.

13.1.2 Climate variability impacts

We had thus identified some specific impacts of agricultural intensification on the island's water resources. We then next identified the other important determinant of freshwater quantity and quality of the island: climatic variability. We considered the impact of climatic variations, and the associated changes in the rainfall distribution on Tongatapu's water resources (Chapters 9 and 10). The salinity of local wells is mainly determined by the well–location with respect to the lagoon edge. However, hydrogeological characteristics and variations in pumping rates give rise to differences in variations of well–salinity. Characteristic travel times were derived using transfer function theory. These encompassed drainage through the vadose zone as well as the mixing of the drainage water into the top 1 m of the freshwater lens. The lag period associated with the peaks of the transfer functions ranged between 8 and 305 days. However, it was also apparent that fast flow after heavy rainfall (e.g. 191 mm day^{-1}) was not captured by the model. This indicates the need to incorporate hydrogeological characteristics into the model. At a larger temporal and spatial scale, we discovered a climatic control on the salinity of the freshwater lens of Tongatapu as mediated by the El Niño–Southern Oscillation. We were able to predict the relative salinity state of the island's freshwater lens some 10-months in advance using the Southern Oscillation Index.

13.1.3 Management

We may never be able to control or manage environmental systems so that we are fully protected against the impacts of climatic fluctuations. What we can do, however, is to increase the buffer capacity of the environments to minimize negative impacts. Having identified some of the influences on freshwater quality, related to agriculture and climatic variability, we considered other related water management issues. These include possible alternatives for agricultural export, and options to mitigate climatic variability impacts (Chapters 11 and 12). Agriculture is the main component of economic export in the Kingdom of Tonga. Sustainable development of Tongatapu requires not only a consideration of agriculture's impact on the environment, but it also requires a thorough evaluation of its economic benefits in a socio-economic context. We have established a first step in this analysis (Chapter 12).

More practically, tools are needed to aid the management of Tongatapu's environmental resources. Pesticides have been found in soil, sediments and groundwater. A selection of crop protection products that will not leach is

possible, if a site specific DSS, such as presented in Chapter 12, is adopted by farmers, and especially if used by MAFF extension personnel. We can also conclude that significant amounts of nitrates leach out of the rootzone with the current agricultural practices used for squash growth. As a management option, we have therefore suggested to allow for natural mineralisation in nutrient budgeting plus a delay of inorganic fertilisation in time, or even the avoidance of the first N application.

We have shown that a salt–water wedge exists below the Mataki'eua well–field. Since the freshwater lens is thinner here, pumping rates at wells should reflect the proximity to the lagoon to minimise salt–water intrusion. Also, the Tongamai wellfield could be extended further inland. At a larger temporal and spatial scale, climatic variations control the salinity of the freshwater lens. We suggest that there should be an increasing awareness of the effects of interannual rainfall fluctuations on the salinity dynamics of the freshwater lens. Long–term pumping strategies for the freshwater lens, developed by well–field managers, should take these interannual climatic variations into account. They can be forecasted using the Southern Oscillation Index.

13.2 Uncertainties

Several sources of uncertainties remain. This relates to the lack of a thorough investigation of the error sources in the modelling exercise, as well as errors associated with the measurements. Errors related to the local heterogeneity in soil hydraulic properties, and soil water fluxes, as well as the root water uptake parameters [*Hupet*, 2003]. These remain to be quantified for the field situation. It would be a relatively easy, but a time–consuming task, to perform a sensitivity analysis of the soil hydraulic parameters used in the WAVE model. However, since a robust statistical description of the soil hydraulic parameters at the field site is lacking, it would presently be hard to define ranges of parameter values encountered in the field. The performance of the flux meters was only evaluated using the 1D version of HYDRUS. An evaluation with the 2D HYDRUS scheme might clarify the excess drainage that was recorded by the passive capillary fluxmeters. Besides the empirical approach currently used to model the nitrate leaching, a more physically based approach should be used. Using some predefined probability functions, stochastic analysis may prove additional insight to the nitrate leaching observed by the flux meters.

In Chapter 9 we presented seperate transfer function models to describe the variations in well–water salinity. The errors were visually presented in Chapter 9. The errors need a more explicit consideration. On top of that, a more physically based model, as soon to be discussed in the *Perspectives* section could greatly improve our understanding of the influence of rainfall variations, pumping rates, and hydrogeological characteristics, on the

observed well–water salinity.

Another pertinent question relates to the apparent discrepancy that exists between nitrate concentrations of drainage measured at the bottom of the root zone, and the concentrations of nitrate in the groundwater. Although, the groundwater nitrate concentrations compared to groundwater seepage concentrations, where the algae blooms were observed, seem rather low. *Paerl* [1997] reported that 'groundwater nitrogen inputs [into estuaries and coastal waters] have not been extensively quantified', but that atmospheric deposition and groundwater can 'jointly account from 20 to $>$ 50% of total exogenous nitrogen loading by bypassing estuarine filters of terragenous nitrogen inputs'. *Matson* [1993] concluded that the discharge of nitrates from the aquifer system of Guam can 'enrich the surface seawater by about 20 times the ambient concentration per day.' The sensitivity of these aquatic systems needs to be studied in more detail. Several other questions have also been raised by this research, and these will be discussed in the *Perspectives* section.

13.3 Synthesis

Although SIDS themselves contribute minimally to greenhouse gas emission, and thus climate change, they are among the first countries that are exposed to the impacts of climate change. They also suffer from other climatic related impacts. They have to deal with sea level rise, an increase of the frequency of devastating El Niño episodes in a warming climate, and the damages induced by tropical cyclones that appear to be occurring with increasing intensity. All these events disturb a system that is inherently low in resilience. At the same time, these islands have to survive in a global economy for which they often lack the critical mass. Increasingly some of them are destroying their natural ecosystems irreversibly. This diminishes also their potential revenues from tourism. Effects of climate change and variation will often be amplified by human–induced changes resulting from increasing demographic pressures and demands.

The scope of the PhD research was specifically aimed at Tongatapu, but the research project addresses issues that are relevant to other islands and coastal zones around the world. The Pacific Ocean alone contains over 30,000 islands of which about a 1000 are inhabited with a population of 9 million people. The insights obtained from specifically studying SIDS may also be illustrative to societies of much larger size. Despite having different biophysical characteristics, it will identify key steps in the critical process of building a framework that enables to sustain water resources in a changing climate. The impact of climate change on water resources is one of the main challenges of the 21^{st} Century.

Managing water resources requires an integrated approach. We have at-

tempted to make a small step towards doing so by pointing out the different ecosystem variables, including human activity, that perturbate the natural system of a SIDS. The complexity of the interactions does not allow us to point towards a specific pathway that will lead to sustainability. Sustainability is not a destination it is a journey. Sustainability is intimately related to future risks and uncertainties we cannot know [*Loucks*, 2000]. However, we can influence the future, and, even though, scientifically speaking, uncertainties remain, fundamental choices and adaptations of policies will pave the way towards sustaining water resources of SIDS. The knowledge presented here should serve as building blocks for a decision making strategy. We have quantified the leaching of nitrates out of the root zone, and we have quantified the effect of climate variability on the quality of the groundwater quality of coral atolls. Overall, there is evidence that the environment is degrading. But, we also know that agricultural export is one of the main export earners for SIDS, with few alternatives. It is up to policymakers to make the next step. We have provided a framework to assit the decision making.

13.4 Perspectives for future research

The study of agricultural and climatic impacts on the water resources of SIDS is topical. It is pertinent, because of the rate at which these processes continue to affect small island states.

13.4.1 Agricultural impacts

For harmonious decision making that balances the economic and environmental capital of small islands it first necessary to quantify the contribution of intensifying agriculture to environmental pollution with respect to other possible domestic and industrial causes. We suggest systematic monitoring of water quality of lagoon and ground water in several coral atolls in the Pacific. Subsequent determination could be made of the contribution–ratio of agricultural, domestic and industrial sources to nitrogen pollution by isotopic analysis. Lagoon and groundwater at several atolls around the Pacific Ocean should be sampled. Isotopic analysis should be used to determine the contribution of human activities on water quality degradation. This benchmark is essential for any future studies addressing this issue, as well as for policy making on islands that wish to regulate environmental pollution.

Even if the contribution of agriculture to the N–loading of the environment is known, improved site–specific agricultural strategies are needed. This also holds for high islands in the Pacific ocean as they are increasingly confronted with increased rates of erosion. Ideally, optimal timing of fertilisation and fertiliser rates would result in more efficient and economically viable agriculture. However, providing scientific solutions is only the first step in combating environmental pollution. Therefore, agronomists and

MAFF extension officers should continue their efforts to reduce the amount of nitrogen that is leached from the rootzone so as to minimize the nitrogen load on Tongatapu's ecosystem.

The wide range of influences of larger scale climatic patterns on the well–being of our societies has recently become apparent [*Glantz*, 1996]. Improved understanding of the impacts of climate variability on the economic welfare of SIDS is needed. We propose a link of agricultural production with the El Niño–Southern Oscillation.

13.4.2 Climate variability impacts

Our ability to protect our societies and environments against processes influenced by climate change and variability depends firstly on our ability to understand and predict regional manifestations of the climate system. Secondly we need to translate this knowledge in a workable management strategy. Interannual climatic variations are a characteristic of the coupled global atmosphere and ocean circulation. Significant forecasting improvements can be obtained with an increased usage of information on climate variability to contribute to management of freshwater resources on islands.

This thesis has highlighted the possibility for further studies on the impact of climate variability on the hydrological cycle of SIDS. Currently there is a need for further integration of climatic change models and hydrological models on a regional scale to understand the mutual feedbacks within this system. These feedbacks are related to the changes in evaporation rates, and the changes in the residence times of stored water related to the increased variability in weather. There seems to be a possible 'speeding up' of the hydrological cycle.

Initial groundwater modelling was performed using the model MOCDENS3D [*Oude Essink*, 2001a], which is a modified density–dependent groundwater flow model based on MODFLOW. It is proposed to use this model, and the hydrogeologic characteristics of several coral atolls and islands in combination with 30-year daily rainfall data from Tonga, Fiji, American Samoa, Marshall Islands, Hawaii being areas differently affected by ENSO [*Ropelewski and Halpert*, 1987]. This modelling would show the ENSO related fluctuations in water quality and freshwater lens thickness at these locations (verified with data to be obtained from the water boards at these islands). Also it would quantify the relative influence of hydrogeologic controls (e.g. hydraulic conductivity) and climatic controls (e.g. local climatic variability; different contributions of local, regional and global processes on local rainfall) on the water quality at these locations. Using the 30 year dataset of salinity monitoring on the coral atoll of Tongatapu, and, if similar datasets can be obtained from the other islands (e.g. Hawaii, Marshall Islands, Fiji) these would enable calibration of hydrogeological models coupled with rainfall models. Once the hydrogeologic-groundwater-rainfall response

model is calibrated, IPPC predictions of climate change (e.g. rainfall distributions, predicted sea level rise) can be fed into the model to evaluate impacts. Then possibly through a coupling of advanced global change models for the Pacific region, it could provide an identification of feedbacks between the local hydrological cycle and convective processes will be possible. We could also explore the effect of the loss of an internal water body (e.g. lagoon), because of accelerated erosion due to increased variability in climatic patterns and subsequent infilling of the lagoon, on local convective processes (e.g. the 'oasis' effect).

13.5 Final remarks

This PhD thesis highlights the influence of both agriculture and climate variability on the environments of Tongatapu. The research shows the need for the adoption of agricultural practices that leach less nitrogen, as well as the need to devise pumping strategies that take account of interannual climate variability. This would ensure that the water resources of this tiny dot in the Pacific Ocean will continue to be available for future generations of Tongans.

Appendix A

Soil Map Unit Name

A.1 Soil–map unit names

Table A.1. The soil map unit names belonging to the soil codes as indicated in Figure 2.6, from *Cowie et al.* [1991].

Soil Code	Soil Map Unit Name
Fh	Fahefa soils
FhR	Fahefa soils, rolling phase
Ft	Fatai soils
Ft + Fh	Combination
Island	Islands
La1	Lapaha soils
La1R	Lapaha soils, rolling phase
La1R + La1	Combination
La2 + Va3	Lapaha and Vaini soils, low-lying phase
Mangrove	Mangroves
Na1	Nuku'alofa soils
Na2	Nuku'alofa soils, sandy loam phase
Na2 + F2	Combination
Na2 + So2	Combination
So1	Sopu soils
So1 + Na1	Sopu loam, peaty sandy loam phase
So2	Combination
So2 + So1	Combination
Va1	Vaini soils
Va1 + Va1R	Combination
Va1 + Va2	Combination
Va1R	Vaini soils, rolling phase
Va1R + Va2R	Combination
Va2 + Va1	Vaini soils, shallow phase
Va2 + Va2R	Combination
Va2R + Va1	Vaini soils, shallow rolling phase
Water	Water

Appendix B

Limits of Detection

B.1 Limits of pesticide detection

Table B.1. Limits of detection of neutral insecticides, fungicides and herbicides(μg l^{-1}).

Active ingredient	**LOD's (μg l^{-1})**	**Active ingredient**	**LOD's (μg l^{-1})**
acetochlor	0.03	metribuzine	0.05
alachlor	0.02	oxadiazon	0.02
aldrin	0.01	oxyfluorfen	0.02
atrazine	0.02	pendimethalin	0.01
azinphosmethyl	0.02	pirimiphosmethyl	0.02
bromacil	0.02	ppDDD	0.02
carbaryl	0.02	ppDDE	0.01
chlorpyrifos	0.02	ppDDT	0.01
cyanazine	0.02	procymidone	0.02
cypermethrin	0.05	prometryn	0.05
deltamethrin	0.05	propachlor	0.03
diazinon	0.02	propazine	0.02
dieldrin	0.01	quizalofop-p-methyl	0.04
diuron	0.02	simazine	0.02
fluazifop-butyl	0.02	terbacil	0.02
haloxyfop-methyl	0.03	terbuthylazine	0.01
hexazinone	0.02	terbutryn	0.05
iprodione	0.02	thiabendazole	0.03
lindane	0.01	trifluralin	0.02
linuron	0.03	vinclozolin	0.02
metolachlor	0.03		

Appendix C

Location sampling sites for pesticide analysis

C.1 Location sampling sites for pesticide analysis

Table C.1. The UTM coordinates of the location of wells and fieldsites for water and soil sampling for pesticed analysis.

Groundwater	Site	UTM Easting (m)	UTM Northing (m)	TBU Well nr
1	Kolonga	700019	7661090	48
2	Kolonga (in agricultural field)	699929	7659490	177
3	Lapaha	696350	7656580	35
4	University of Nations	693100	7652500	(238?)
5	Fua'amotu	692990	7647400	180
6	Vaini (field of Kelepi)	689100	7654100	(3?)
7	Veitongo	685680	7656200	22
8	Veitongo	685560	7655800	201
9	Utulau	679839	7655990	161
10	Liahono (Mormon School)	679590	7659000	168
11	Vaini	688910	7655770	29
12	Ha'akame	678200	7656830	192
13	Halaloto	681000	7658100	85
14	Tokomololo (MAF)	682270	7657410	163
15	Sia'toutai College	680950	7661550	93
16	Fatai	678910	7661820	133
17	Ha'avakatolo	672300	7665040	66
18	Vaotu'u	675350	7661820	155
19	Matahau	675420	7661050	147
20	Matatoa	684000	7659000	223
21	Hofoa	684000	7662500	89
22	Tupou	690810	7651500	32
23	Malapo	691890	7653900	55
24	Alakifonua	695580	7654090	53
25	Hoi	696330	7658510	47
26	Talafo'ou	699600	7666125	60
27	Haveluliku	696860	7653960	17
GS1	Groundwater seepage point	694250	7655500	
Soil				
AIR	North of Fua'amotu Airstrip	693000	7650500	
LAF	Field of Lafalafa	692000	7651500	
MAN	Field of Manulatu	683550	7658750	

Appendix D

Soil Description

D.1 Experimental Field Site - Vaini Research Station

A_{p1} 0 - 9 cm ; color : 5YR 3/3 ; friable ; round aggregates (diameter of 3-10 mm) ; a lot of organic matter (worked in dry grass)

A_{p2} 9 - 38 cm ; color : 5YR 3/3 ; friable but plastic when pressed in between fingers ; aggregates become smaller (diameter < 5 mm) ; still a lot of worked in grass ; high root density ; transition towards the next horizon is irregular.

B_1 38 - 89 cm ; color : 5YR 3/4 ; compact ; polyhedric structure ; clayey texture and fine porosity ; sticky ; inclusion of lapilli with a rusty ; thin patchy clay coatings ; low root density (1 mm diameter) ; very hard when dry but breakable. Transition towards the next horizon is clear and regular.

A_2 89 -93 cm ; color : 7.5YR 3/4 ; corresponds to an ancient surface horizon. Directly superposed on top of the old volcanic ash layer ; heavy clay ; compact ; black Mg concretions.

B_2 93 - 120 cm ; color : 7.5YR 4/4 ; heavy clay ; very compact ; sticky ; very fine porosity ; thin patchy clay coating ; no occurence of lapilli ; hard as stone when dry.

Appendix E

Callibration of capacitance flux meters

E.1 Callibration of the capacitance flux meters

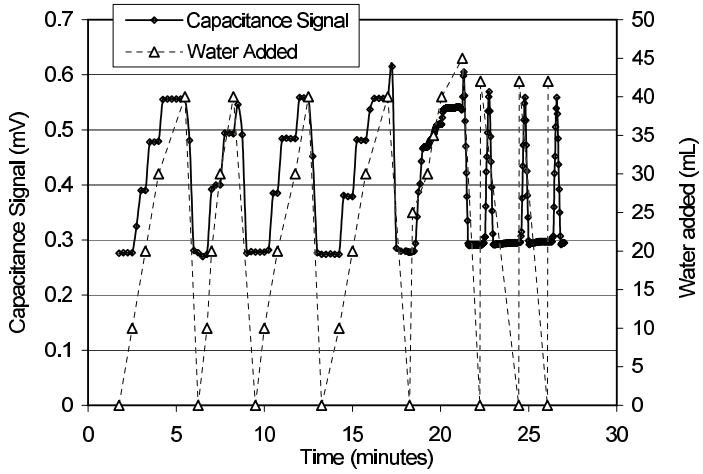

Figure E.1. The callibration for the capacitance flux meters (C-WFM1 and C-WFM2).

Appendix F

Standard Well Design

F.1 The standard well design used for the Mataki'eua wellfield on Tongatapu from *Falkland* [1992].

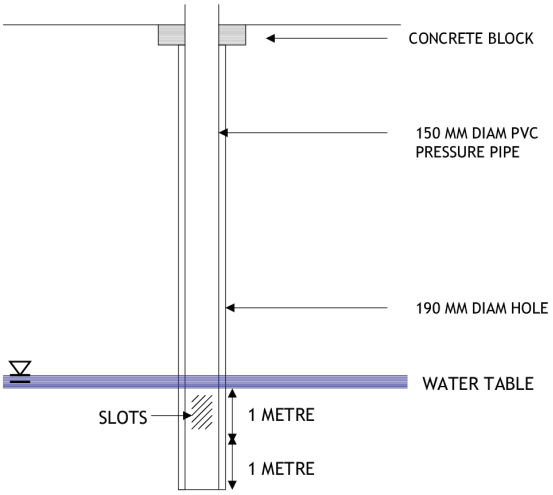

Figure F.1. The typical well design of the wells in the Mataki'eau wellfield.

Appendix G

Monitoring Bores

G.1 The sampling depths of the monitoring bores.

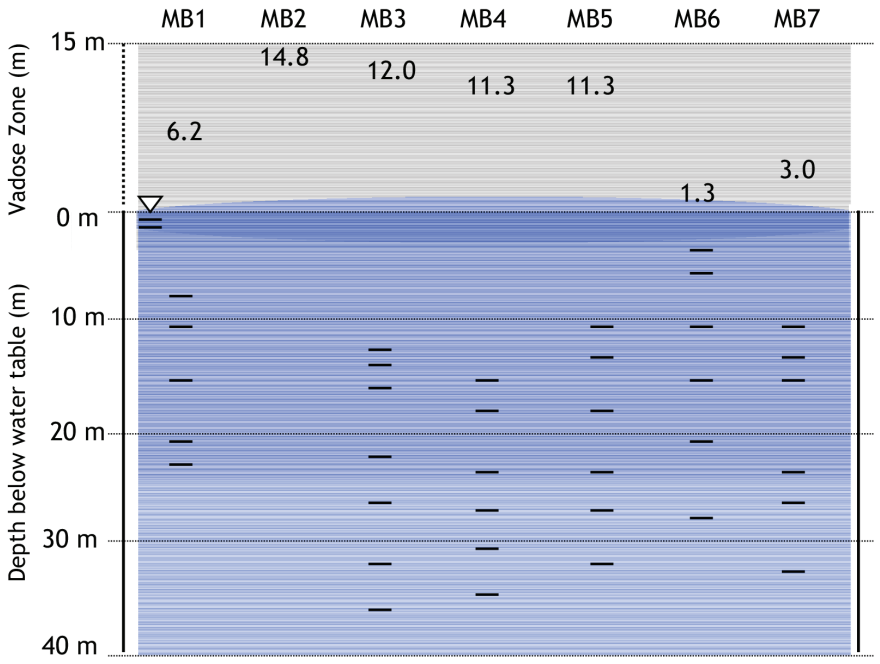

Figure G.1. The monitoring dephts of the monitoring bores below the water table and the thickness of the vadose zone above. The small horizontal lines indicate the depths of the different monitoring tubes.

Appendix H

Travel Times with Increasing μ and σ

H.1 Travel times with increasing μ and σ

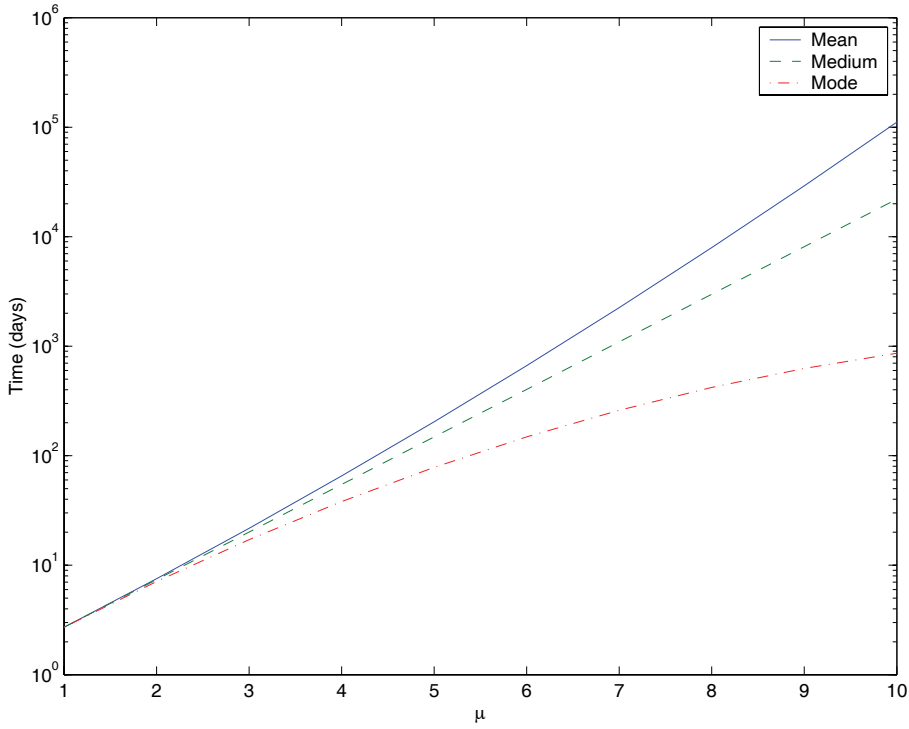

Figure H.1. The mean, medium and mode times associated with the lognormal probability density function with increases of both μ and σ. μ increases from 1 to 10, with steps of 1, while σ increases from 0 to 2 with steps of 0.2.

References

Abenney-Mickson, S., A. Yomota, and T. Miura, Water balance of field plots planted with soybean and pumpkin, *Transactions of the ASAE*, *40 (4)*, 899–909, 1997.

Ada, R., *Japanese Consumer Co-operatives. A market entry strategy for horticultural products. Publication 00/30, 86 pp.*, Rural Industries Research and Development Cooperation, Australia, 2000.

Aganga, A., and S. Tshewenyane, Potentials of guinea grass (panicum maximum) as forage crop in livestock production, *Pakistan Journal of Nutrition*, *3*, 1–4, 2004.

Allen, R., L. Pereira, D. Raes, and M. Smith, *FAO Irrigation and Drainage Paper No. 56 Crop Evaporation (guidelines for computing drop water requirements). 300 pp.*, FAO, Rome, Italy, 1998.

Anderson, G., *The Merchant of the Zeehaen. Isaac Gilsemans and the voyages of Abel Tasman. 162 pp.*, Te Papa Press, Wellington, New Zealand, 2001.

Anderson, J., and J. Bouma, Relationships between hydraulic conductivity and morphometric data of an argillic horizon, *Soil Sci. Soc. Am. Proc.*, *37*, 408–413, 1973.

Andersson, J., and M. Lindroth, Ecologically unsustainable trade, *Ecological Economics*, *37*, 113–122, 2001.

Armas-Espinel, S., J. Hernandez-Moreno, R. Munoz-Carpena, and C. Regalado, Physical properties of 'sorriba'-cultivated volcanic soils srom tenerife in relation to andic diagnostic properties, *Geoderma*, *117*, 297–311, 2003.

Ball, O., *Toloa Rainforest Reserve - a guidebook for visitors. 70 p.*, Tupou College, Toloa, Tonga, 2001.

Bank, A. D., *Key indicators of developing Asian and Pacific countries. Tonga country table. ISSN 0116-3000*, Asian Development Bank, Bangkok, Thailand, 2004.

Barzegar, A., S. Herbert, A. Hashemi, and C. Hu, Passive pan sampler for vadose zone leachate collection, *Soil Science Society of America Journal*, *68*, 744–749, 2004.

Basher, R., and X. Zheng, Tropical cyclones in the Southwest Pacific - spatial patterns and relationships to southern-oscillation and sea-surface temperature, *Journal of Climate*, *8*, 1249–1260, 1995.

Basher, R., and X. Zheng, Mapping rainfall fields and their enso variation in data-sparse tropical south-west pacific ocean region, *International Journal of Climatology*, *18*, 237–251, 1998.

Becker, P., and W. Edwards, Corrected heat capacity of wood for sap flow calculations, *Tree Physiology*, *19*, 767–768, 1999.

Bergstrom, L., Nitrate leaching and drainage from annual and perennial crops in tile-drained plots and lysimeters, *Journal of Environmental Quality*, *16*, 11–18, 1987.

Bertram, G., 'Sustainable development' in Pacific micro-economies., *World Development*, *14*, 809–822, 1986.

Bertram, G., Sustainability, aid, and material welfare in small south-Pacific-island economies, 1900-90, *World Development*, *21*, 247–258, 1993.

Bertram, G., *Economy, 337-352 in:*, Bess Press, Hawaii, USA, 1999.

Bertram, G., On the convergence of small island economies with their metropolitan patrons, *World Development*, *32*, 343–364, 2004.

Bertram, G., and R. Watters, The mirab economy in south pacific microstates, *Pacific Viewpoint*, *26*, 497–519, 1985.

Boll, J., T. Steenhuis, and J. Selker, Fiberglass wicks for sampling of water and solutes in the vadose zone, *Soil Science Society of America Journal*, *56*, 701–707, 1992.

Boll, J., J. Selker, G. Shalit, and T. Steenhuis, Frequency distribution of water and solute transport properties derived from pan sampler data, *Water Resources Research*, *33*,

2655–2664, 1997.

Bouma, J., Hydropedology as a powerful tool for environmental policy research, *Geoderma*, *131 (3-4)*, 275–286, 2006.

Bouwer, H., Integrated water management: Emerging issues and challenges, *Agricultural Water Management*, *45*, 217–228, 2000.

Bove, M., J. Elsner, C. Landsea, X. Niu, and J. O'brien, Effect of El Niño on US landfalling hurricanes, revisited, *Bulletin of the American Meteorological Society*, *79*, 2477–2482, 1998.

Brandidohrn, F., R. Dick, M. Hess, S. Kauffman, D. Hemphill, and J. Selker, Nitrate leaching under a cereal rye cover crop, *Journal of Environmental Quality*, *26*, 181–188, 1997.

Briguglio, L., Small island developing states and their economic vulnerabilities, *World Development*, *23*, 1615–1632, 1995.

Brye, K., J. Norman, L. Bundy, and S. Gower, An equilibrium tension lysimeter for measuring drainage through soil, *Soil Science Society of America Journal*, *63*, 536–543, 1999.

Buytaert, W., J. Deckers, G. Dercon, B. D. Bievre, J. Poesen, and G. Govers, Impact of land use changes on the hydrological properties of volcanic ash soils in south Ecuador, *Soil Use and Management*, *18*, 94–100, 2002.

Cairncross, F., *The death of distance: how the communications revolution will change our lives*, Harvard Business School Press, Boston, USA, 1997.

Campbell, G., and J. Norman, *An introduction to environmental biophysics, 2nd edition. 286 pp.*, Springer-Verlag, New York, USA, 1998.

Cane, M., G. Eshel, and R. Buckland, Forecasting Zimbabwean maize yield using eastern equatorial pacific sea-surface temperature, *Nature*, *370*, 204–205, 1994.

Cerda, A., Aggregate stability against water forces under different climates on agriculture land and scrubland in southern Bolivia, *Soil and Tillage Research*, *57*, 159–166, 2000.

Cerisola, M., R. Baqir, and A. J. de Lucio, *Tonga, selected issues and statistical appendix. 45 pp.*, IMF, IMF Country Report 03/37, 2003.

Chesher, R., *Pollution sources survey of the Kingdom of Tonga. Topic Review 19. 110 pp.*, SPREP, South Pacific Commission, Noumea, New Caledonia, 1984.

Clothier, B., *Infiltration. In: Soil and Environmental Analysis. Physical Methods, 2nd edition (pp. 239-281). Eds. K.A. Smith and C.E. Mullins.*, Marcel Dekker, New York - Basel, 2000.

Clothier, B., and K. Smettem, Combining laboratory and field measurements to define the hydraulic properties of soil, *Soil Science Society of America Journal*, *54*, 299–304, 1990.

Cohen, Y., and Y. Li, Validating sap flow measurement in field-grown sunflower and corn, *Journal of Experimental Botany*, *47*, 1699–1707, 1996.

Cohen, Y., M. Fuchs, and G. Green, Improvement of the heat-pulse method for determining sap flow in trees, *Plant Cell and Environment*, *4*, 391–397, 1981.

Cowie, J., Soils from andesitic tephra and their variability, Tongatapu, kingdom of Tonga, *Australian Journal of Soil Research*, *18*, 273–284, 1980.

Cowie, J., P. Searle, J. Widdowson, and G. Orbell, *Soils of Tongatapu, Kingdom of Tonga. 55 pp.*, DSIR Land Resources, Lower Hutt, New Zealand, 1991.

Coxon, L., *The political economy of contract farming in Tonga. M.A. thesis, 204 pp*, The University of Auckland, Auckland, New Zealand, 1999.

Crawford, C., Tongan land management. putting the breaks on the global economy., *Journal of Pacific History*, *36*, 93–104, 2001.

Cronin, S., *Volcanic ash Tongatapu*, Unpublished Report, Massey University, Palmerston

North, New Zealand, 2005.

Dalzell, P., T. Adams, and N. Polunin, *Coastal fisheries in the Pacific Islands. In: Oceanography and marine biology: an annual review, Ansell, A.D. and Gibson, R.N. and Barnes, M. (editors), 34, 395-531*, UCL Press, London, United Kingdom, 1996.

Darwin, C., *The structure and distribution of coral reefs. Being the first part of the geology of the voyage of the Beagle, under the command of capt. Fitzroy, R.N. during the years 1832 to 1836. (2nd edition) 239 pp.*, Smith, Elder and Co., London, England, 1842.

Derby, N., and R. Knighton, Field-scale preferential transport of water and chloride tracer by depression-focused recharge, *Journal of Environmental Quality*, *30*, 194–199, 2001.

Dickinson, W., D. Burley, and R. Shutler, Holocene paleoshoreline record in tonga: Geomorphic features and archaelogical implications, *Journal of Coastal Research*, *15*, 682–700, 1999.

Dietz, T., E. Ostrom, and P. Stern, The struggle to govern the commons, *Science*, *302*, 1907–1912, 2003.

Dorel, M., J. Roger-Estrade, H. Manichon, and B. Delvaux, Porosity and soil water properties of caribbean volcanic ash soils, *Soil Use and Management*, *16*, 133–140, 2000.

Dorland, E., R. Bobbink, J. Messelink, and J. Verhoeven, Soil ammonium accumulation after sod cutting hampers the restoration of degraded wet heathlands, *Journal of Applied Ecology*, *40*, 804–814, 2003.

Douglas Partners, *Surveillance of groundwater quality in Tonga. Prepared for World Health Organisation, Regional Office for Western Pacific*, Douglas Partners, Bowen Hills, Australia, 1996.

Downes, M., An improved hydrazine reduction method for the automated determination of low nitrate levels in fresh water, *Water Research*, *12*, 673–675, 1978.

DuToit, J., B. Walker, and B. Campbell, Conserving tropical nature: Current challenges for ecologists, *Trends in Ecology and Evolution*, *19*, 12–17, 2004.

Duwig, C., T. Becquer, B. Clothier, and M. Vauclin, Nitrate leaching through oxisols of the Loyalty Islands (New Caledonia) under intensified agricultural practices, *Geoderma*, *84*, 29–43, 1998.

Duwig, C., B. Normand, M. Vauclin, G. Vachaud, S. Green, and T. Becquer, Evalution of the wave model for predicting nitrate leaching for two contrasted soil and climate conditions, *Vadose Zone Journal*, *2*, 76–89, 2003.

Ergil, M., The salination problem of the Guzelyurt aquifer, Cyprus, *Water Research*, *34 (4)*, 1201–1214, 2000.

ESCAP, *Integrating environmental considerations into economic policy making processes, background readings. Vol. I: Institutional arrangements and mechanisms at national level (country studies on Fiji, Nepal, Philippines and Tonga)*, United Nations Environmental Programme, ESCAP, Bangkok, Thailand, 1999.

Espinosa-Gonzalez, J., *Fate and effects of pesticides under tropical field conditions. Implications for and research needs in a developing country. In: Environmental Behaviour of Crop Protection Chemicals, pp 93-107.*, IAEA-SM-343/32, Proc. Int. Symp., 1997.

FADINAP, *Fertilizer Advisory, Development and Information Network for Asia and the Pacific (ESCAP/FAO/UNIDO). Supply, marketing, distribution and use of fertilizer in the Pacific subregion, 17 pp.*, United Nations Publication, Bangkok, Thailand, 1999.

Falkland, A., *Tonga water supply master plan project, water resources report. 116 pp.*, Prepared for PKK Consultants Pty Ltd., Nuku'alofa, Kingdom of Tonga, 1992.

Falkland, T., *Tonga Water Board institutional development project. Technical component progress report*, Hydrolgy Services, ACTEW Corporation, 1995.

FAO, *Environment and Natural Resources in Small Island Developing States. Special Ministerial Conference on Agriculture in Small Island Developing States*, Food and Agri-

cultural Organisation of the United Nations, Rome, Italy, 1999.

Felemi, M., *Constraints, challenges and prospects for development of the squash export industry in Tonga. Proceedings of the regional workshop on the constraints, challenges, and prospects for commodity based development, diversification, and trade in the Pacific island economies, 18-20 September, 2001. 19 pp.*, Fiji, Nadi,, 2001.

Ferraro, P., and A. Kiss, Ecology - direct payments to conserve biodiversity, *Science*, *298*, 1718–1719, 2002.

Fleming, E., and A. Blowes, *Export performance in South Pacific countries marginally endowed with natural resources: Samoa and Tonga, 1960 to 1999. 45 pp.*, University of New Engeland. Working paper series in Agriculture and Resources Economies, No. 8., Armidale, Australia, 2003.

Flury, M., Experimental evidence of transport of pesticides through field soils - a review, *Journal of Environmental Quality*, *25*, 25–45, 1996.

Flury, M., H. Fluhler, W. Jury, and J. Leuenberger, Susceptibility of soils to preferential flow of water – a field-study, *Water Resources Research*, *30*, 1945–1954, 1994.

Fonua, P., Squash pumpkin season, *Matangi Tonga. Vava'u Press Ltd*, *Nuku'alofa, Kingdom of Tonga*, online, 2003.

Foster, S., and P. Chilton, Groundwater: the processes and global significance of aquifer degradation, *Phil. Trans. R. Soc. Lond. B*, *358*, 1957–1972, 2003.

Fuavao, V., S. Tiueti, S. Finau, and S. Moala, How safe is the drinking water in Tonga?, *Pacific Health Dialog*, *3*, 147–152, 1996.

Furness, L., and S. Gingerich, *Estimation of recharge to the freshwater lens of Tongatapu, Kingdom of Tonga. Hydrology of warm humid regions (Proceedings of the Yokohama symposium). IAHS Publ. 216.*, IAHS, Yokohama, Japan, 1993.

Furness, L., and S. Helu, *The hydrogeology and water supply of the Kingdom of Tonga. 143 pp.*, Ministry of Lands, Survey and Natural Resources, Nuku'alofa, Kingdom of Tonga, 1993.

Gee, G., A. Ward, T. Caldwell, and J. Ritter, A vadose zone water fluxmeter with divergence control, *Water Resources Research*, *38*, ISI:000179003000,005, 2002.

Gee, G., Z. Zhang, and A. Ward, A modified vadose zone fluxmeter with solution collection capability., *Vadose Zone Journal*, *2*, 627–632, 2003.

Gee, G. W., Zhang, Z.F., A. L. Ward, and J. M. Keller, Passive-wick water flux meters: theory and practice. Available Online, in *Proceedings of the International 'SuperSoil' Soil Science Conference*, edited by D. B. Singh, p. 5 pages, Sydney, Australia, 2004.

Gerakis, A., and B. Bear, A computer program for soil textural classification, *Soil Science Society of America Journal*, *63*, 807–808, 1999.

Ghijben, W. B., and J. Drabbe, Nota in verband met de voorgenomen putboring nabij Amsterdam (in Dutch)., *Tijdsch. van het Kon. Inst. voor Ing.*, *1888-1889*, 8–22, 1889.

Ginsburg, R., Beachrock in south florida, *Journal of Sedimentary Petrology*, *23*, 85–92, 1953.

Glantz, M., *Currents of change: impacts of El Niño and La Niña on climate and society.*, Cambridge Univ. Press, 2nd ed., 252 pp., Cambridge, UK, 1996.

Gowrie, M., Environmental vulnerability index for the island of Tobago, West Indies, *Conservation Ecology*, *7*, ISI:000189307800,007, 2003.

Green, S., Radiation balance, transpiration and photosynthesis of an isolated tree, *Agricultural and Forest Meteorology*, *64*, 201–221, 1993.

Green, S., and B. Clothier, Water-use of kiwifruit vines and apple-trees by the heat-pulse technique, *Journal of Experimental Botany*, *39*, 115–123, 1988.

Green, S., and B. Clothier, *Modelling the impact of dairy farming on nitrate leaching in the Lake Taupo catchment. Service delivery details (HortResearch to Environment*

Waikato), HortResearch, HortResearch Report no. 2002/383, Palmerston North, New Zealand, 2002.

Green, S., B. Clothier, and B. Jardine, Theory and practical application of heat pulse to measure sap flow, *Agronomy Journal*, *95*, 1371–1379, 2003.

Griggs, J., and F. Peterson, Ground–water flow dynamics and development at the atoll scale, *Ground Water*, *31 (2)*, 209–220, 1993.

Guber, A., W. Rawls, E. Shein, and Y. Pachepsky, Effect of soil aggregate size distribution on water retention, *Soil Science*, *168*, 223–233, 2003.

Haines, W., Studies in the physical properteis of soils. the hysteresis effect in capillary properties and modes of moisture distribution associated therewith, *Journal of Agricultural Sciences*, *20*, 97–116, 1930.

Hales, S., P. Weinstein, and A. Woodward, Dengue fever epidemics in the South Pacific: Driven by El Niño Southern Oscillation?, *Lancet*, *348*, 1664–1665, 1996.

Halvorson, W., A. Castellanos, and J. Murrieta-Saldivar, Sustainable land use requires attention to ecological signals, *Environmental Management*, *32 (5)*, 551–558, 2003.

Harr, M., *Groundwater and seepage. p. 8*, McGraw-Hill, New York, USA, 1962.

Harrison, D., *The limestone resources of Tongatapu and Vava'u, Kingdom of Tonga. 33 pp.*, British Geological Survey, Keyworth, Nottingham, Great Britain, 1993.

Harrison, N., P. Gangaiya, and R. Morrison, Organochlorines in the coastal marine environment of Vanuatu and Tonga, *Marine Pollution Bulletin*, *32*, 575–579, 1996.

Hasan, R., *Preliminary survey on rainwater harvesting*, FAO, United Nations, Rome, Italy, 1989.

Haynes, R., and R. Naidu, Influence of lime, fertilizer and manure applications on soil organic matter conter and soil physical conitions: a review, *Nutrient cycling in agroecosystems*, *51*, 123–137, 1998.

He, Y., A. Barnston, and A. Hilton, *A precipitation climatology for stations in the tropical basin; effects of ENSO, Atlas No. 5*, NCEP/Climate prediciton Center, U.S. Dept. of Commerce, USA, 1998.

Herzberg, A., Die wasserversorgung einiger Nordseebaden (in German), *Zeitung fur Gasbeleuchtung und Wasserversorgung*, *44*, 842–844, 1901.

Hoekstra, A., and P. Hung, *Virtual water trade. A quantification of virtual water flows between nations in relation to international crop trade. Value of water research report series no. 11. 166 pp.*, IHE-UNESCO, Delft, The Netherlands, 2002.

Holder, M., K. Brown, J. Thomas, D. Zabcik, and H. Murray, Capillary-wick unsaturated zone soil pore water sampler, *Soil Science Society of America Journal*, *55*, 1195–1202, 1991.

Holling, C., Understanding the complexity of economic, ecological and social systems, *Ecosystems*, *4*, 390–405, 2001.

Huber, B., Beobachtung und messung pflanzicher saftstrome., *Ber. Dtsch. Bot. Ges.*, *56*, 35–48, 1932.

Hunt, B., An analysis of the groundwater resources of Tongatapu island, kingdom of Tonga., *Journal of Hydrology*, *40*, 185–196, 1979.

Hupet, F., *Estimation of evapotranspiration fluxes at the field scale: parameter estimation, variability and uncertainties. PhD thesis. 273 pp.*, Université catholique de Louvain, Louvain-la-Neuve, Belgium, 2003.

ISSS Working Group Reference Base, *FAO*, Rome, 1998.

Jarvis, P., The interpretation of the variations in leaf water potential and stomatal conductance found in canopies in the field., *Phil. Trans. R. Soc. London Ser. B*, *273*, 593–610, 1976.

Javaux, M., *Solute transport in a heterogeneous unsaturated subsoil. Experiments and*

modelling. 194 pp. PhD thesis., Université catholique de Louvain, Louvain-la-Neuve, Belgium, 2004.

Jemison, J., and R. Fox, Estimation of zero-tension pan lysimeter collection efficiency, *Soil Science*, *154*, 85–94, 1992.

JICA, *Basic design study report on the project for Nuku'alofa water supply system in the Kingdom of Tonga*, TWB, Kingdom of Tonga, 1998.

Jocson, J., J. Jenson, and D. Contractor, Recharge and aquifer response: Northern Guam lens aquifer, Guam, Mariana islands, *Journal of Hydrology*, *260*, 231–254, 2002.

Johnsson, H., L. Bergstrom, and P. Jansson, Simulated nitrogen dynamics and losses in a layered agricultural soil, *Agriculture, Ecosystems and Environment*, *18*, 333–356, 1987.

Jones, I., and J. Banner, Estimating recharge thresholds in tropical karst island aquifers: Barbados, Puerto Rico and Guam, *Journal of Hydrology*, *278*, 131–143, 2003a.

Jones, I., and J. Banner, Hydrogeologic and climatic influences on spatial and interannual variation of recharge to a tropical karst island aquifer, *Water Resources Research*, *39*, 1253, 2003b.

Jury, W., Similation of solute transport using a transfer function model, *Water Resources Research*, *18 (2)*, 363–368, 1982.

Jury, W., and H. Fluhler, Transport of chemicals through the soil: Mechanims, models and field applications, *Advances in Agronomy*, *47*, 141–202, 1992.

Jury, W., and L. Stolzy, A field test of the transfer function model for predicting solute transport, *Water Resources Research*, *18 (2)*, 369–375, 1982.

Kafri, U., *Assessment of the groundwater potential in the island of Tongatapu, Kingdom of Tonga*, Geological Survey of Israel and Ministry of Infrastructure, Tonga, 1989.

Kaly, U., T. Fakatava, S. Lepa, L. Matoto, P. Ngaluafe, A. Palaki, and S. Tupou, *Status of Fanga'uta Lagoon, Tonga: Monitoring of water quality and seagrass communities 1998-2000. Scientific Monitoring Report nr 1.*, Tonga National Monitoring Team, Nuku'alofa, Tonga, 2000.

Kaly, U., C. Prat, J. Mitchell, and R. Howorth, *The demonstration environmental vulnerability index (EVI). Technical Report 356, 136 pp.*, SOPAC, Suva, Fiji, 2003.

Kilbourne, K., T. Quinn, F. Taylor, T. Delcroix, and Y. Gouriou, El Niño-Southern Oscillation-related salinity variations recorded in the skeletal geochemistry of a porites coral from Espiritu Santo, Vanuatu, *Paleoceanography*, *19*, PA4002, 2004.

Kim, D., and J. Feyen, Comparison of flux and resident concentrations in macroporous field soils, *Soil Science*, *165*, 616–623, 2000.

Kim, Y., C. Darnault, N. Bailey, J. Parlange, and T. Steenhuis, Equation for describing solute transport in field soils with preferential flow paths, *Soil Science Society of America Journal*, *69*, 291–300, 2005.

Kiraly, L., Karstification and groundwater flow, *Speleogenesis and evolution of karst aquifers*, *1 (3)*, 1–26, 2002.

Kladivko, E., G. V. Scoyoc, E. Monke, K. Oates, and W. Pask, Pesticide and nutrient movement into subsurface tile drains on a silt loam soil in Indiana, *Journal of Environmental Quality*, *20*, 264–270, 1991.

Knutson, J., and J. Selker, Unsaturated hydraulic conductivities of fiberglass wicks and designing capillary wick pore-water samplers, *Soil Science Society of America Journal*, *58*, 721–729, 1994.

Knutson, J., S. Lee, W. Zhang, and J. Selker, Fiberglass wick preparation for use in passive capillary wick soil pore-water samplers, *Soil Science Society of America Journal*, *57*, 1474–1476, 1993.

Kosugi, K., and M. Katsuyama, Controlled-suction period lysimeter for measuring vertical water flux and convective chemical fluxes, *Soil Science Society of America Journal*, *68*,

371–382, 2004.

Kovats, R., M. Bouma, S. Hajat, E. Worrall, and A. Haines, El Niño and health, *Lancet*, *362*, 1481–1489, 2003.

Lall, U., *Hydromorphology: hydrology in an evolving world. Borland Lecture in Hydrology. Hydrology Days, 2006*, Colorado State University, USA, 2006.

Lambrakis, N., and G. Kallergis, Reaction of subsurface coastal aquifers to climate and land use changes in greece: modelling of groundwater refreshing patterns under natural recharge conditions, *Journal of Hydrology*, *245*, 19–31, 2001.

Landsberg, J., and D. Powell, Surface exchange characteristics of leaves subject to mutual interference, *Agricultural Meteorology*, *12*, 169–184, 1973.

Lao, C., *Assignment report by WHO consultant. Groundwater resources study of Tongatapu. 59 pp.*, UNDP No. - TON/75/004, Regional office for the Western Pacific, 1978.

Lebon, E., V. Dumas, P. Pieri, and H. Schultz, Modelling the seasonal dynamics of the soil water balance of vineyards, *Functional Plant Biology*, *30*, 699–710, 2003.

Lebron, I., D. Suarez, and M. Schaap, Soil pore size and geometry as a result of aggregate size distribution and chemical composition, *Soil Science*, *167 (3)*, 165–172, 2002.

Lee, H., 'second generation' Tongan transnationalism: Hope for the future?, *Asia Pacific Viewpoint*, *45 (2)*, 235–254, 2004.

Lehodey, P., M. Bertignac, J. Hampton, A. Lewis, and J. Picaut, El Niño Southern Oscillation and tuna in the Western Pacific, *Nature*, *389*, 715–718, 1997.

Lipp, E., N. Schmidt, M. Luther, and J. Rose, Determining the effects of El Niño–Southern Oscillation events on coastal water quality, *Estuaries*, *24*, 491–497, 2001.

Loucks, D., Sustainable water resources management, *Water International*, *25 (1)*, 3–10, 2000.

Louie, M., P. Shelby, J. Smesrud, L. Gatchell, and J. Selker, Field evaluation of passive capillary samplers for estimating groundwater recharge, *Water Resources Research*, *36*, 2407–2416, 2000.

Lowe, D., and J. Gunn, Caves and limestones of the islands of Tongatapu and 'Eua, kingdom of Tonga, *Cave Science*, *13 (3)*, 30 pp, 1986.

Ma, S., M. Sophocleous, Y.-S. Yu, and R. Buddemeier, Journal of hydrology, *Journal of Hydrology*, *201*, 120–137, 1997.

Maeda, M., B. Zhao, Y. Ozaki, and T. Yoneyama, Nitrate leaching in an andisol treated with different types of fertilizers, *Environmental Pollution*, *121*, 477–487, 2003.

Malm, T., The tragedy of the commoners: the decline of the customary marine tenure system of Tonga., *SPC Traditional marine resources management and knowledge information. Bulletin*, *13*, 3–13, 2001.

Manu, V., *Effects of cropping on soil C and nutrient availability, and the amelioration practices that enhances optimum and sustainable crop yields in Tonga. 154 pp.*, University of New England, PhD thesis., 2000.

Manu, V., T. Holo, F. Pole, S. Halvatau, S. Kanongata'a, O. Fukofuka, and V. Kami, *Conventional Squash Production. 3 pp.*, Ministry of Agriculture and Forestry, Nuku'alofa, Tonga, 1998.

Marshall, D., Measurement of sap flow in conifers by heat transport., *Plant Physiol.*, *33*, 385–396, 1958.

Masarik, K., J. Norman, K. Brye, and J. Baker, Improvements to measuring water flux in the vadose zone, *Journal of Environmental Quality*, *33*, 1152–1158, 2004.

Matson, E., Nutrient flux through soils and aquifers to the coastal zone of Guam (Mariana Islands), *Limnology and Oceanography*, *38 (2)*, 361–371, 1993.

Matson, P., P. Vitousek, J. Ewel, M. Mazzarino, and G. Robertson, Nitrogen transformations following tropical forest felling and burning on a volcanic soil, *Ecology*, *68 (3)*,

491–502, 1987.

McGregor, A., *The role of farm management in agricultural extension in the Pacific Islands. SAPA discussion paper 1/2002, 65 pp.*, FAO, Suva, Fiji, 2002.

Meehan, H., K. McConckey, and D. Drake, Potential disruptions to seed dispersal mutualisms in Tonga, Western Polynesia, *Journal of Biogeography*, *29*, 695–712, 2002.

Meehl, G., Vulnerability of freshwater resources to climate change in the tropical pacific region, *Water Air and Soil Pollution*, *92*, 203–213, 1996.

Meehl, G., Pacific region climate change, *Ocean and Coastal Management*, *37*, 137–147, 1997.

Mimura, N., Vulnerability of island countries in the south pacific to sea level rise and climate change, *Climate Research*, *12*, 137–143, 1999.

Ministry of Health Tonga, *Results of 18 samples analysed for pesticides*, Government of Tonga - Savingram, Tongatapu, Kingdom of Tonga, 1998.

Mitrovica, J., and W. Peltier, On postglacial geoid subsidence over the equatorical oceans., *Journal of Geophysical Research*, *96*, 20,052–20,071, 1991.

Miyamoto, T., T. Annaka, and J. Chikushi, Soil aggregate structure effects on dielectric permittivity of an andisol measured by time domain relfectometry, *Vadose Zone Journal*, *2*, 90–97, 2003.

Mogensen, U., *Source book of alternative technologies for freshwater augementation in small island developing states. Technical publication series nr. 8.*, Environmental Technology Centre, UNEP, Osaka, Japan, 1998.

Montgomery, B., L. Prunty, and J. Bauder, Vacuum trough extractors for measuring drainage and nitrate flux through sandy soils, *Soil Science Society of America Journal*, *51*, 271–276, 1987.

Morris, B., A. Lawrence, P. Chilton, B. Adams, R. Calow, and B. Klinck, *Groundwater and its Suscesptibility to Degradation: A Global Assessment of the Problems and Options of Management.*, United Nations Environment Programme, Nairobi, Kenya, 2003.

Morrison, R., *Working Paper WP 32. Environmental Chemist Assignment Report. 142 pp.*, Tonga Environmental Planning and Management Strengthening Project (TEMPP), 2000.

Morrison, R., and P. Brown, Trace metals in Fanga'uta lagoon, kingdom of Tonga, *Marine Pollution Bulletin*, *46*, 146–152, 2003.

Motavalli, P., and J. Mcconnell, Land use and soil nitrogen status in a tropical Pacific island environment, *Journal of Environmental Quality*, *27*, 119–123, 1998.

Mualem, Y., A new model for predicting the hydraulic conductivity of unsaturated porous media, *Water Resources Research*, *12*, 513–522, 1976.

Murray, W., The second wave of globalisation and agrarian change in the Pacific islands, *Journal of Rural Studies*, *17*, 135–148, 2001.

Myers, N., R. Mittermeier, C. Mittermeier, G. D. Fonseca, and J. Kent, Biodiversity hotspots for conservation priorities, *Nature*, *403*, 853–858, 2000.

Naidu, R., R. Kookana, and S. Baskaran, *Pesticide Dynamics in the Tropical Soil-Plant Ecosystem: Potential Impacts on Soil and Crop Quality. 171-183 pp.*, Australia, Canberra, 1996.

Nemati, M., J. Caron, and J. Gallichand, Predicting hydraulic conductivity changes from aggregate mean weight diameter, *38*, p. WR000625, 2002.

Neter, J., M. Kutner, C. Nachtsheim, and W. Wasserman, *Applied Linear Statistics. 1418 pp.*, McGraw-Hill, USA, 1996.

Neuman, S., Universal scaling of hydraulic conductivities and dispersivities in geologic media, *Water Resources Research*, *26 (8)*, 1749–1758, 1990.

Norman, J., and G. Campbell, Application of a plant environment model to problems in

the environment, *Advances in Irrigation*, *2*, 155–188, 1983.

Oude Essink, G., Improving fresh groundwater supply–problems and solutions, *Ocean and Coastal Management*, *44*, 429–449, 2001a.

Oude Essink, G., *Lecture notes, density dependent groundwater flow: salt water intrusion and heat transport. 163 pp.*, Utrecht University, Institute of Earth Sciences, Utrecht, the Netherlands, 2001b.

Paerl, H., Coastal eutrophication and harmful algal blooms: importance of atmospheric deposition and groundwater as 'new' nitrogen and other nutrient sources, *Limnology and Oceanography*, *42 (5)*, 1154–1165, 1997.

Park, E.-J., and A. Smucker, Saturated hydraulic conductivity and porosity within macroaggregates modified by tillage, *Soil Science Society of America Journal*, *69*, 38–45, 2005.

Parliamentary Commissioner for the Environment – New Zealand, *Growing for good: intensive farming, sustainability, and New Zealand's environment. 237 pp.*, PCENZ, Wellington, New Zealand, 2004.

Pauly, D., V. Christensen, S. Guenette, T. Pitcher, U. Sumaila, C. Walters, R. Watson, and D. Zeller, Towards sustainability in world fisheries, *Nature*, *418*, 689–695, 2002.

Petelo, H., *Productive efficiency of the squash export industry in Tonga. PhD thesis*, East West Center, University of Hawaii, Honolulu, Hawaii, 2002.

Pfeifer, D., and L. Stach, Hydrogeology of the island of Tongatapu, kingdom of Tonga, *Geol. Jahrbuch*, *C4*, 13 pp., 1972.

Philip, J., *The quasilinear analysis, the scattering analog, and other aspects of infiltration and seepage. In: Infiltration development and application, edited by Y.-S. Fok, pp. 1-27.*, Water Resources Research Center, Honolulu, Hawaii, 1987.

Pochet, G., M. van der Velde, M. Vanclooster, and B. Delvaux, Micro-aggregation in brown halloysitic soils based on soil constitution and hydric properties, *Geoderma*, *X*, submitted, 2006.

Poveda, G., A. Jaramillo, M. Gil, N. Quiceno, and R. Mantilla, Seasonality in Enso-related precipitation, river discharges, soil moisture, and vegetation index in Colombia, *Water Resources Research*, *37*, 2169–2178, 2001.

Prescott, N., *Sustainable environmental and resource management in Tonga, ecological status, community perceptions and a proposed new policy framework. PhD thesis.*, University of Wollongong, NSW, Australia, 2003.

Rawlins, B., A. Ferguson, P. Chilton, R. Arthurtons, and J. Grees, Review of agricultural pollution in the Caribbean with particular emphasis on small island developing states, *Marine Pollution Bulletin*, *36*, 658–668, 1998.

Richards, L., A pressure-membrane extraction apparatus for soil solution, *Soil Science*, *51*, 377–386, 1941.

Rimmer, A., T. Steenhuis, and J. Selker, One-dimensional model to evaluate the performance of wick samplers in soils, *Soil Science Society of America Journal*, *59*, 88–92, 1995.

Robinson, J., Squaring the circle? Some thoughts on the idea of sustainable development, *Ecol. Econ.*, *48*, 369–384, 2004.

Ropelewski, C., and M. Halpert, Global and regional scale precipitation patterns associated with the El-Niño Southern Oscillation, *Monthly Weather Review*, *115*, 1606–1626, 1987.

Roy, P., *The morphology and surface geology of the islands of Tongatapu and Vava'u, Kingdom of Tonga. 51 pp.*, CCOP/SOPAC Technical Report 62, Suva, Fiji, 1990.

Russel, A., and J. Ewel, Leaching from a tropical andept during big storms: a comparison of three methods., *Soil Science*, *139*, 181–189, 1985.

Sakuratani, T., A heat balance method for measuring water flux in the stem of intact plants, *Journal of Agricultural Meteorology*, *37*, 9–17, 1981.

Sampat, O., *Deep Trouble: The Hidden Threat of Groundwater Pollution. Worldwatch Paper 154. 55pp.*, Worldwatch Institute, Washington, USA, 2000.

Sauer, T., P. Moore, J. Ham, W. Bland, J. Prueger, and C. West, Seasonal water balance of an Ozark hillslope, *Agricultural Water Management*, *55*, 71–82, 2002.

Sawkins, J., On the movement of land in the South Sea islands, *Geological Society of London Quarterly Journal*, *12*, 383–384, 1856.

Scheffer, M., S. Carpenter, J. Foley, C. Folke, and B. Walker, Catastrophic shifts in ecosystems, *Nature*, *413*, 591–596, 2001.

Scotter, D., R. White, and J. Dyson, The burns leaching equation, *Journal of Soil Science*, *44*, 25–33, 1993.

Seabergh, W., *Chapter 6. Hydrodynamics of Tidal Inlets. In: Vincent, L., and Dermirbilek, Z. (editors), Coastal Engineering Manual, Part II, Hydrodynamics, Chapter VI-2, Engineering manual 1110-2-1100, US army Corps of Engineers*, US Corps of Engineers, Washington DC, USA, 2006.

Si, B., and R. Kachanoski, Measurement of local soil water flux during field solute transport experiments, *Soil Science Society of America Journal*, *67*, 730–736, 2003.

Siegert, F., G. Ruecker, A. Hinrichs, and A. Hoffmann, Increased damage from fires in logged forests during droughts caused by El Niño, *Nature*, *414*, 437–440, 2001.

Simpson, H., M. Cane, A. Herczeg, S. Zebiak, and J. Simpson, Annual river discharge in southeastern Australia related to El Niño Southern Oscillation forecasts of sea-surface temperatures, *Water Resources Research*, *29*, 3671–3680, 1993.

Simunek, J., K. Huang, M. Sejna, and M. van Genuchten, *HYDRUS-1D version 2.02. Code for simulating the one-dimensional movement of water, heat and multiple solutes in varable saturated porous media/*, US Salinity Laboratory, USDA/ARS, Riverside, California, 2003.

Soil Survey Staff, *Soil taxonomy: a basic systems of soil classification for making and interpretingsoil surveys.*, USDA Natural resources conservation service, Agriculture Handbook 436, US Government printing office, Washinton DC, USA, 1999.

South, G., P. Skelton, J. Veitayaki, A. Resture, C. Carpenter, C. Pratt, and A. Lawedrau, The global international waters assessment for the pacific islands: Aspects of transboundary, water shortage, and coastal fisheries issues, *Ambio*, *33*, 98–106, 2004.

Steen, B., *Tonga Waterboard Project. Report on visit to Tonga, 12-20 October 1995. 10 pp.*, TWB, Nuku'alofa, Tonga, 1995.

Steenhuis, T., J. Boll, G. Shalit, J. Selker, and I. Merwin, A simple equation for predicting preferential flow solute concentrations, *Journal of Environmental Quality*, *23*, 1058–1064, 1994.

Stevens, C., Taking over what belongs to god: the historical ecology of Tonga since European contact, *Pacific Studies*, *22 (3 and 4)*, 182–219, 1999.

Stone, R., G. Hammer, and T. Marcussen, Prediction of global rainfall probabilities using phases of the southern oscillation index, *Nature*, *384*, 252–255, 1996.

Storey, D., and W. Murray, Dilemmas of development in Oceania: the political economy of the Tongan agro-export sector, *Geographical Journal*, *167*, 291–304, 2001.

Sturton, M., *Tonga: development through agricultural exports. 47 pp.*, Pacific Island Develoment Program. East West Center., University of Hawaii Press., Hawaii, USA, 1992.

Summerfield, M., *Global Geomorphology: An introduction to the study of landforms. 537 pp.*, Longman Group, England, 1996.

Swanson, R., and D. Whitfield, A numerical analysis of heat-pulse velocity theory and practice, *Journal of Experimental Botany*, *32*, 221–239, 1981.

Taylor, J., and M. Person, Capture zone delineations on island aquifer systems, *Ground Water*, *36 (5)*, 722–730, 1998.

Technicon, *Industrial Method no. 98/70w.*, Tarrytown, New York, USA, 1973.

Technicon, *Technicon mannual for ammonium analysis*, Tarrytown, New York, USA, 1976.

The Economist, Greening the book - ecosystem services, *The Economist. September 17th 23rd*, *376*, 88, 2005.

Thompson, C., *The Climate and Weather of Tonga. 60 pp.*, New Zealand Meteorological Service, Misc. Publications, Auckland, New Zealand, 1986.

Timlin, D., J. Starr, R. Cady, and T. Nicholson, *Comparing ground-water recharge estimates using advanced monitoring techniques and models. 57 pp.*, U.S. Department of Agriculture. Agricultural Research Service., Beltsville Agricultural Research Center, Beltsvill, U.S.A., 2003.

Timmermann, A., J. Oberhuber, A. Bacher, M. Esch, M. Latif, and E. Roeckner, Increased El Niño frequency in a climate model forced by future greenhouse warming, *Nature*, *398*, 694–697, 1999.

Tongan National Assessment Commission, *Tonga National Assessment Report. 118 pp.*, Government of Tonga, Kingdom of Tonga, 2003.

Trangmar, B., *Proceedings of the soil fertility and land evaluation workshop. 241 pp.*, DSIR Land Resources, Lower Hutt, New Zealand, 1992.

Troup, A., The southern oscillation, *Quart. J. Roy. Meteor. Soc.*, *91*, 490–506, 1965.

Tsonis, A., J. Elsner, A. Hunt, and T. Jagger, Unfolding the relation between global temperature and ENSO, *Geophysical Research Letters*, *32*, L09,701, 2005.

Twine, J., and C. Williams, The determination of phosphorus in Kjeldahl digests of plant material by automatic analysis, *Comm Soil Sci Plant Anal*, *2*, 485–489, 1971.

UNCTAD, *Is a special treatment of small island developing states possible? 110 pp.*, United Nations, New York and Geneva, 2004.

Underwood, M., F. Peterson, and C. Voss, Groundwater lens dynamics of atoll islands, *Water Resources Research*, *28*, 2889–2902, 1992.

UNEP, *UNEP's assistance in the implementation of the Barbados programme of action for the sustainable development of small island developing states. 62 pp.*, United Nations Environmental Programme, New York, USA, 2004.

UNESCO, *Working Group M.IV. Sustainability criteria for water resource systems*, Cambridge University Press, Cambridge, UK, 1999.

United Nations, *Mauritius Declaration. General Assembly Declaration. Declared at the International Meeting to Review the Implementation of the Programme of Action for the Sustainable Development of Small Island Development States. 3 pp.*, United Nations, Port Louis, Mauritius, 2005.

van der Grijp, P., Leaders in squash export: entrepreneurship and the introduction of a new cash crop in Tonga, *Pacific Studies*, *20 (1)*, 29–61, 1997.

van der Molen, W., An analysis of the groudnwater resoruces of tongatapu island, kingdom of tonga – comments. editor's note, *Journal of Hydrology*, *40*, 197–199, 1979.

van der Velde, M., *Agricultural and climatic impacts on the groundwater resources of a small island: measuring and modelling water and solute transport in soil and groundwater on Tongatapu*, University of Louvain (Louvain-la-Neuve), Louvain-la-Neuve, 2006.

van der Velde, M., S. Green, G. Gee, M. Vanclooster, and B. Clothier, *Flux meters as a tool for agricultural water management. COST 629 workshop. Integrated methods for assessing water quality. 21-21 pp*, COST 629, Louvain-la-Neuve, Belgium, 2004.

van der Velde, M., S. Green, G. Gee, M. Vanclooster, and B. Clothier, Evaluation of drainage from passive suction and non-suction flux meters in a volcanic clay soil under tropical conditions, *Vadose Zone Journal*, *4*, 1201–1209, 2005.

van der Velde, M., S. Green, M. Vanclooster, and B. Clothier, Transpiration of squash under a tropical maritime climate, *Plant and Soil*, *280 (1-2)*, 323–337, 2006a.

van der Velde, M., S. Green, M. Vanclooster, and B. Clothier, Sustainable development in small island developing states: agricultural intensification, economical development, and freshwater resources management on the coral atoll of tongatapu., *Ecological Economics*, *X*, xxx, 2006b.

van der Velde, M., M. Javaux, M. Vanclooster, and B. Clothier, El Niño–Southern Oscillation controls the quality of freshwater lenses under coral atolls in the Pacific Ocean, *Environmental Science & Technology*, *X*, xxx, 2006c.

van Genuchten, M., A closed-form equation for predicting the hydraulic conductivity of unsaturated soils, *Soil Science Society of America Journal*, *44*, 892–898, 1980.

van Grinsven, J., H. Booltink, C. Dirksen, N. van Breemen, N. Bongers, and N. Waringa, Automated insitu measurement of unsaturated soil-water flux, *Soil Science Society of America Journal*, *52*, 1215–1218, 1988.

Vanclooster, M., D. Mallants, J. Diels, and J. Feyen, Determining local-scale solute transport parameters using time-domain reflectometry (tdr), *Journal of Hydrology*, *148*, 93–107, 1993.

Vanclooster, M., P. Viaene, J. Diels, and J. Feyen, A deterministic evaluation analysis applied to an integrated soil-crop model, *Ecological Modelling*, *81*, 183–195, 1995.

Vanclooster, M., P. Viaene, J. Diels, and K. Christiaens, *WAVE, a mathematical model for simulating water and agrochemicals in the soil and vadose environment, release 2.1*, Institute for Land and Water Managment, Katholieke Universiteit Leuven, Leuven, Belgium, 1996.

Vanclooster, M., J. Boesten, M. Trevisan, C. Brown, E. Capri, O. Eklo, B. Gottesburen, V. Gouy, and A. V. D. Linden, A european test of pesticide-leaching models: Methodology and major recommendations, *Agricultural Water Management*, *44*, 1–19, 2000.

Vanclooster, M., M. Javaux, F. Hupet, S. Lambot, A. Rochdi, J. D. Pineros-Garcet, and C. L. Bielders, *Effective approaches for modelling chemical transport in soils supporting soil management at the larger scale. In Sustainable land management - environmental protection. A soil physical approach. Chapter 3 in: Advances in Geoecology 35. Eds. Pagliai, M. and Jones R. 598 pp.*, Catena Verlag, International Union of Soil Science (IUSS), 2002.

Vanclooster, M., J. Boesten, A. Tiktat, N. Jarvis, J. Kroes, R. Munoz-Carpena, B. Clothier, and S. Green, *On the use of unsaturated flow and transport models in nutrient and pesticide management. Chapter 11 in Unsaturated–zone Modelling. Eds. Reddes, R.A., de Rooij, G.H. and van Dam, J.C., 331-361 pp.*, Wageningen University Press, Wageningen , The Netherlands, 2005.

Veldkamp, E., and J. O'brien, Calibration of a frequency domain reflectometry sensor for humid tropical soils of volcanic origin, *Soil Science Society of America Journal*, *64*, 1549–1553, 2000.

Vogel, H.-J., and K. Roth, Moving through scales of flow and transport in soil, *Journal of Hydrology*, *272*, 95–106, 2003.

Walkley, A., and I. Black, An examination of the Degiareff method for determining SOM and a proposed modification of chromic acid titration method, *Soil Science*, *37*, 29–38, 1934.

Waring, J., D. Slawinski, and I. Nainar, *Simple estuarian response model II. See www.per.marine.csiro.au*, CSIRO, Perth, Australia, 2003.

Weaver, J., and W. Bruner, *Root development of vegetable crops*, McGraw-Hill Book Company, Inc., New York, USA, 1927.

Whitaker, F., and P. Smart, Climatic control of hydraulic conductivity of Bahamian limestones, *Groundwater*, *35 (5)*, 859–868, 1997.

White, I., and M. Sully, Macroscopic and microscopic capillary length and time scales from field infiltration, *Water Resources Research*, *23*, 1514–1522, 1987.

White, I., T. Falkland, and D. Scott, *Droughts in small coral islands: case study, South Tarawa, Kiribati. IHP-V, Technical Documents in Hydrology 26. 55 pp.*, UNESCO, Paris, France, 1999.

Winkel, T., and S. Rambal, Stomatal conductance of some grapevines growing in the field under a mediterranean environment, *Agricultural and Forest Meteorology*, *51*, 107–121, 1990.

Wiser, S., D. Drake, L. Burrows, and W. Sykes, The potential for long-term persistence of forest fragments on Tongatapu, a large island in Western Polynesia, *Journal of Biogeography*, *29*, 767–787, 2002.

Wittmuss, H., Physical and chemical properties of aggregates in a brunizem soil., *Soil Science Society of America Proceedings*, *22*, 1–5, 1958.

Woodroffe, C., The impact of cyclone Isaac on the coast of Tonga, *Pacific Science*, *37 (3)*, 181–210, 1983.

World Health Organisation, *Guidelines for drinking water quality, 3rd edition. 115 pp.*, WHO, Geneva, Switzerland, 2004.

Yu, Z., P. Chu, and T. Schroeder, Predictive skills of seasonal to annual rainfall variations in the us affiliated pacific islands: Canonical correlation analysis and multivariate principal component regression approaches, *Journal of Climate*, *10*, 2586–2599, 1997.

Zann, L., The status of coral-reefs in southwesternPacific islands, *Marine Pollution Bulletin*, *29*, 52–61, 1994.

Zann, L., W. Kimmerer, and R. Brock, *The ecology of Fanga'uta Lagoon, Tongatapu, Tonga. 99 pp.*, Sea Grant Cooperative Report, UNIHI-SEAGRANT-CR-84-04, Sponsored by Institute of Marine Resources University of the South Pacific, Suva, Fiji. International Sea Grant Program, University of Hawaii, Honolulu, Hawaii, 1982.

Zhu, Y., R. Fox, and J. Toth, Leachate collection efficiency of zero-tension pan and passive capillary fiberglass wick lysimeters, *Soil Science Society of America Journal*, *66*, 37–43, 2002.

List of Publications

1. B.E. Clothier, S.R. Green, B.H. Robinson, T. Thayalakumaran, D.R. Scotter, I. Vogeler, T.M. Mills, M. Deurer, ***M. van der Velde*** and Th. Granel **2001**. Contaminants in the Rootzone: Bioavailability, Uptake and Transport, and their Implications for Remediation. 30 pp. In: Chemical Bioavailability in the Terrestrial Environment. Ed. R. Naidu. CSIRO Publishing, Collingwood, Australia.

2. B. Robinson, S. Green, T. Mills, B. Clothier, ***M. van der Velde***, R. Laplane, L. Fung, M. Deurer, S. Hurst, T. Thayalakumaran, and C. van den Dijssel. **2003**. Phytoremediation: using plants as biopumps to improve degraded environments. *Australian Journal of Soil Research* 41(3), 599-611.

3. ***M. van der Velde***, S.R. Green, G.W. Gee, M. Vanclooster and B.E. Clothier **2005**. Evaluation of drainage and water flux measurements with passive suction and non-suction water flux meters in a volcanic clay soil under tropical conditions. *Vadoze Zone Journal* 4, 1201-1209.

4. ***M. van der Velde***, S.R. Green, M. Vanclooster and B.E. Clothier **2006**. Measuring and modelling transpiration of squash (Cucurbita maxima) under tropical maritime climate. *Plant and Soil* 280 (1-2), 323-337.

5. ***M. van der Velde***, S.R. Green, M. Vanclooster and B.E. Clothier. Sustainable development in small island developing states: agricultural intensification, economical development, and freshwater resources management on the coral atoll of Tongatapu. *Ecological Economics*, accepted.

6. ***M. van der Velde***, M. Javaux, M. Vanclooster and B.E. Clothier. El Niño-Southern Oscillation controls the quality of freshwater lenses under coral atolls in the Pacific Ocean. *Environmental Science and Technology*, in review.

7. Pochet G., ***M. Van der Velde***, M. Vanclooster and B. Delvaux. Evidence of micro-aggregation in Brown halloysitic soils through soil constitution and hydric properties. *Geoderma*, in review.

8. ***M van der Velde***, M. Vakasiuola, S.R. Green, V.T. Manu, V. Minonesi, M. Vanclooster, and B.E. Clothier. Aspects of the management of water resources of a low island in the Pacific Ocean. To be published in a special issue of *Physics and Chemistry of the Earth* devoted to a session on integrative water management held at the EGU, 2005.

9. ***M van der Velde***, S.R. Green, G.W. Gee, M. Vanclooster and B.E. Clothier. Measuring and modelling the leaching of fertilsers through a volcanic soil. In preparation, to be submitted.

10. ***M. van der Velde***, M. Vanclooster and B.E. Clothier. Climatic and hydrogeologic controls on the quality of freshwater lenses under coral atolls. In preparation.

International Conferences

A. Oral and paper presentations

1. Brett Robinson, Steve Green, Brent Clothier, ***Marijn van der Velde***, Lindsay Fung, Thabo Thayalakumaran, Valerie Snow, José-Enrique Fernández, Paula Madejón, Teodoro Marañón and José M. Murillo **2002**. Modelling plant - metal uptake from contaminated soils. NZ Land Treatment Collective: Proceedings of the Technical Session 23. Small community and on-site wastewater treatment systems. Whangamata, 17 -19 April 2002. Compiled by Hailong Wang and John Lavery.

2. ***Marijn van der Velde***, Marnik Vanclooster, Val Snow, Steve Green, Viliami Manu, Brent Clothier, Vunivesi Minoneti, Gregoire Pochet and Carlo van den Dijssel **2003**. Fertilisers and the contamination risk to groundwater and the lagoon on Tongatapu island, kingdom of Tonga. Paper published in the 16th Annual Workshop of the Fertiliser and Lime Research Institute 'Environmental Management using Soil-Plant Systems' 12 - 15 February 2003. Edited by L. Currie, P. Logonathan and B. Simmons. Massey University, Palmerston North.

3. B. Robinson, T. Mills, R. Laplane, ***M. van der Velde***, F. Moreno, S. Green, B. Clothier, C. Anderson, T. Thayalakumaran, L. Fung, S. Hurst, C. van den Dijssel, V. Snow **2003**. Continuing development of phytoremediation: from conception to working technology. Oral Presentation at Annual New Zealand Soil Science Society Golden Jubilee Conference 2003.

4. ***M. van der Velde***, S.R. Green, G.W. Gee, M. Vanclooster and B.E. Clothier. 2004. Measurements and modeling of water flux through volcanic soil on the island of Tongatapu. Eurosoil **2004**, September 4th to 12th, Freiburg, Germany.

5. ***Marijn van der Velde***, Steve Green, Glendon W. Gee, Brent Clothier, Valerie Snow, Viliami Manu and Marnik Vanclooster. Flux meters for quantifying the leaching of agri-chemicals on the island of Tongatapu, The Kingdom of Tonga. SuperSoil. International Soil Science Conference, 5 - 9 December **2004**, Sydney, Australia.

6. ***M. van der Velde***, S.R. Green, G.W. Gee, M. Vanclooster and B.E. Clothier **2004**. Using water flux meters as a tool for agricultural water management. In: COST–629, Integrated methods for assessing water quality. Louvain-la-Neuve, Belgium, (p. 21-27).

B. Poster presentations

1. ***Marijn van der Velde***, Marnik Vanclooster, Val Snow, Steve Green, Viliami Manu, Brent Clothier, Vunivesi Minoneti, Gregoire Pochet and Carlo van den Dijssel **2003**. Fertilisers and the contamination risk to groundwater and the lagoon on Tongatapu island, Kingdom of Tonga. Paper and poster presented at the 16th Annual Workshop of the Fertiliser and Lime Research Institute on 'Environmental Management using Soil-Plant Systems' 12 - 15 February 2003. Edited by L. Currie, P. Logonathan and B. Simmons. Massey University, Palmerston North.
2. ***M. van der Velde***, G.W. Gee, S.R. Green, V.O. Snow, M. Vanclooster and B.E. Clothier. Measurements of water and solute flux with flux meters in a volcanic soil in the tropical environment of Tongatapu. Kingdom of Tonga. In: Unsaturated zone modelling: processes, applications and challenges. Poster abstracts. Wageningen, October, **2004**, p. 87.
3. ***M. van der Velde***, S.R. Green, M. Vanclooster and B. Clothier. Measuring and modelling plant transpiration under tropical conditions. In: Unsaturated zone modelling: processes, applications and challenges. Poster abstracts. Wageningen, October, **2004**, p. 88.
4. ***M. van der Velde***, S.R. Green, G.W. Gee, V. Snow, B.E. Clothier, V.T., Manu, V. Minoneti, and M. Vanclooster. Fluxmeters for quantifying the leaching of agrichemicals on the island of Tongatapu, the Kingdom of Tonga. SuperSoil Conference, Sydney, Australia, **2004**.
5. G. Pochet, ***M. van der Velde***, Vanclooster, M. and Delvaux, B. Water properteis of volcanic ash soils rich in high charge halloysite. Final Joint-Meeting COST–622 (June 2004). Volcanic soil resource in Europe, Akureyri-Egilsstadir, Iceland, **2004**.
6. ***M. van der Velde***, S.R. Green, M. Vanclooster, V.T. Manu, V. Minonesi, B.E. Clothier. Sustainable development and SIDS: protecting freshwater resources from agriculture on Tongatapu. International conference: 'Integrated assessment of water resources and global change: a north-south perspective.', Bonn, Germany, February **2005**.
7. ***M. van der Velde***, M. Vanclooster, S.R. Green, V.T. Manu, V. Minoneti, B.E. Clothier. Integrative water management in the Pacific: protecting freshwater resources from agricultural intensification on the coral atoll of Tongatapu. European Geophysical Union, General Assembly, Vienna, April 25-29, **2005**. EGU05-A-07833. CD.
8. Clothier, B.E., ***M. van der Velde***, S.R. Green, G.W. Gee, V. Manu, V. Minoneti, and M. Vanclooster. Measuring and modelling solute transport in the rootzone: protecting the receiving water environments of the coral atolls of Tonga. American Geophyscial Union, Spring Assembly, New Orleans, USA, **2005**.

C. Tools and popular publications

1. GROWSAFE-TONGA ©. Decision Support Tool for the transfer of technology. A tool to help farmers choose the optimal agrichemical products. In collaboration with S.R. Green and B.E. Clothier (HortResearch, New Zealand),

V.T. Manu and V. Minoneti (MAF, Kingdom of Tonga) and M. Vanclooster (UCL, Belgium).

2. ***M. van der Velde***, Gee, G.W. and Green, S.R. After fire comes rain. *WISPAS* 86, 1-2.
3. ***M. van der Velde***, and Green S.R. Pumping Pumpkins. *WISPAS* 88, 1-2.

About the Author

Marijn van der Velde was born on the 16^{th} of June 1978 in Amsterdam, the Netherlands. After completing secondary school in Wageningen in 1996, Marijn returned to Amsterdam to study Physical Geography and Soil Science at the University of Amsterdam. His MSc research dealt with the mutual relations between vegetation patterning, runoff and micro–topography in a semi–arid area in the south of Spain. At the end of his studies he had the possibility to do an internship in New Zealand on the phytoremediation of a contaminated sawdust pile that leaked boron to local water ways.

Marijn then started on the 15^{th} of March 2002 with his PhD research within the *CROPPRO* project at the Université catholique de Louvain, Belgium. He spent two times half a year in the Kingdom of Tonga at the research station of the Ministry of Agriculture, and two times half a year in New Zealand at HortResearch for his research.

The thesis that resulted from this work is presently lying before you.